HEAT SHOCK RESPONSE IN *THERMOPLASMA VOLCANIUM*: CLONING AND DIFFERENTIAL EXPRESSION OF MOLECULAR CHAPERONIN (THERMOSOME) GENES

A THESIS SUBMITTED TO
THE GRADUATE SCHOOL OF NATURAL AND APPLIED SCIENCES
OF
MIDDLE EAST TECHNICAL UNIVERSITY

BY

FÜSUN DOLDUR

IN PARTIAL FULFILLMENT OF THE REQIREMENTS
FOR
THE DEGREE OF MASTER OF SCIENCE
IN
BIOLOGY

DECEMBER 2008

Approval of the thesis:

HEAT SHOCK RESPONSE IN *THERMOPLASMA VOLCANIUM*: CLONING AND DIFFERENTIAL EXPRESSION OF MOLECULAR CHAPERONIN (THERMOSOME) GENES

submitted by **FÜSUN DOLDUR** in partial fulfillment of the requirements for the degree of **Master of Science in Biology Department, Middle East Technical University** by,

Prof. Dr. Canan Özgen _____
Dean, Graduate School of **Natural and Applied Sciences**

Prof. Dr. Zeki Kaya _____
Head of Department, **Biology**

Prof. Dr. Semra Kocabıyık _____
Supervisor, **Biology Dept., METU**

Examining Committee Members:

Prof. Dr. Mahinur Akkaya _____
Chemistry Dept., METU

Prof. Dr. Semra Kocabıyık _____
Biology Dept., METU

Prof. Dr. Fatih İzgü _____
Biology Dept., METU

Assist. Prof. Dr. Sreeparna Banerjee _____
Biology Dept., METU

Dr. Tülin Yanık _____
Biology Dept., METU

Date: 02.12.2008

I hereby declare that all information in this document has been obtained and presented in accordance with academic rules and ethical conduct. I also declare that, as required by these rules and conduct, I have fully cited and referenced all material and results that are not original to this work.

Name, Last name : Füsun DOLDUR

Signature :

ABSTRACT

HEAT SHOCK RESPONSE IN *THERMOPLASMA VOLCANIUM*: CLONING AND DIFFERENTIAL EXPRESSION OF MOLECULAR CHAPERONIN (THERMOSOME) GENES

Doldur, Füsun

M.Sc., Department of Biology

Supervisor: Prof. Dr. Semra Kocabıyık

December 2008, 239 pages

Chaperonins (Hsp60 chaperones) comprise a class of oligomeric, high-molecular-weight chaperones that have the unique ability to fold some proteins that cannot be folded by simpler chaperone systems. The term "thermosome" is used for molecular chaperonins from Archaeal organisms since they accumulate to high levels upon heat-shock. In this study first time, we have cloned and sequenced two Hsp60 subunit genes (α and β) from a thermoacidophilic archaeon *Thermoplasma volcanium*. For cloning we have followed a PCR based strategy. Amplification of Hsp60 α gene from chromosomal DNA of *T. volcanium* yielded a product of 1939 bp amplicon and that of Hsp60 β gene yielded a product of 1921 bp amplicon. After ligation of the PCR fragments to pDrive vector, recombinant plasmids were transferred into *E. coli* TG-1 competent cells and recombinant colonies were selected by blue/white screening. The cloning of two subunit genes were confirmed by restriction mapping and by sequencing. Both subunit genes were then subcloned to pUC18 vector consequtively to construct a co-expression vector. Both subunit genes were expressed under control of their own

promoters leading to production of active Hsp60 chaperonin (thermosome). Chaperone activity of the recombinant thermosome was shown by using pig citrate synthase enzyme as substrate. Thermosome induced refolding was observed when renaturation was carried out at 50°C for 2,5 h. Under this condition, citrate synthase activities associated with control and test were ΔmA_{412}/min:19.0 and ΔmA_{412}/min:24.0 respectively. Clustal W Version 1.82 was used for multiple sequence alignments of Hsp60 α and Hsp60 β proteins of *T. volcanium* and other Hsp60 proteins from various eukaryotes, bacteria and archaea. The highest sequence similarity was found between α subunit proteins of *T. volcanium* and *T. acidophilum* (94%) and β subunit proteins of *T. volcanium* and *T. acidophilum* (93%). Clusters of orthologous groups and conserved domain database searches revealed the phylogenetic relationships between Hsp60 α and Hsp60 β subunits of *T. volcanium* thermosome and other Hsp60 proteins from various eukaryotes, bacteria and archaea. Induction of both subunit genes under heat shock (65°C, 70°C and 75°C for 2h) and under oxidative stress (imposed by 0,008 mM, 0,01 mM, 0,02 mM, 0,03 mM and 0,05 mM H_2O_2) conditions was studied by Real-Time PCR technique and amplified cDNA band density analysis.

Keywords: Thermosome, Chaperonin, Hsp60, *Thermoplasma volcanium*, heat shock, oxidative stress

ÖZ

THERMOPLASMA VOLCANIUM' UN ISI ŞOKU YANITI: MOLEKÜLER ŞAPERONİN (TERMOZOM) GENLERİNİN KLONLANMASI VE DEĞİŞİMSEL ANLATIMI

Doldur, Füsun

Yüksek Lisans, Biyoloji Bölümü

Tez Yöneticisi: Prof. Dr. Semra Kocabıyık

Aralık 2008, 239 sayfa

Moleküler şaperonlar hücrede proteinlerin katlanması, taşınması ve agregasyonlarının önlenmesi gibi protein yapısını doğrudan etkileyen temel görevleri üstlenmiştir. Şaperoninler (Hsp60 şaperonları) oligomerik, yüksek moleküler ağırlıklı şaperonlar olup diğer şaperon sistemleri tarafından katlanamayan proteinleri katlama özelliğine sahiptirler. Isı şoku sırasında yüksek düzeyde sentezlendikleri için arkea moleküler şaperoninleri termozom olarak da anılır. Bu çalışmada ilk kez, termoasidofilik bir arkeon olan *Thermoplasma volcanium'* un Hsp60 altbirim genlerini (α ve β) klonladık ve nükleik asit dizilerini belirledik. Klonlama için PCR temelli bir yöntem izledik. *T. volcanium*' un kromozomal DNA' sından Hsp60 α geninin çoğaltılması ile 1939 bç büyüklüğünde, Hsp60 β geni için ise 1921 bç büyüklüğünde PZR ürünü elde edilmiştir. PZR amplikonlarının pDrive vektörüne bağlanmasının ardından rekombinant plazmidler *E-coli* TG-1 kompetan hücelerine aktarılmıştır ve rekombinant klonlar mavi/beyaz tarama yolu ile seçilmişlerdir. İki altbirim geninin klonlanması restriksiyon enzim haritalaması ve dizi analizi ile doğrulanmıştır. Daha sonra her iki altbirim geni, ardarda bir ko-ekspresyon

vektörü oluşturmak üzere pUC18 vektörüne klonlanmıştır. Her iki altbirim geninin, kendi promotörlerinin kontrolü altında anlatımları gerçekleşmiş ve bunun sonucunda etkin Hsp60 şaperon (termozom) gerçeklemiştir. Rekombinant termozomun şaperon aktivitesi domuz sitrat sentaz enzimi substrat olarak kullanılarak gösterilmiştir. 50°C' de 2,5 saat inkübasyon sonunda termozomun yeniden katlanma sağladığı gözlenmiştir. Bu koşullar altında sitrat sentazın etkinliği kontrol ve test için sırasıyla ΔmA_{412}/min:19.0 and ΔmA_{412}/min:24.0 olarak bulunmuştur. Clustal W Versiyon 1.82 programı kullanılarak *T. volcanium*' un Hsp60 α ve Hsp60 β proteinleri ile farklı ökaryot, bakteri ve arkea Hsp60 proteinlerinin çoklu dizi hizalaması yapılmıştır. En fazla dizi benzerliği *T. volcanium* ve *T. acidophilum*'un α (%94) ve β proteinleri (%93) arasında saptanmıştır. Veritabanlarında ortolog grupların ve korunmuş bölgelerin karşılaştırması, *T. volcanium*' un Hsp60 α ve Hsp60 β genlerinin çeşitli ökaryot, bakteri ve arkea Hsp60 proteinleriyle filogenetik ilişkisini ortaya koymuştur. Her iki altbirim geninin ısı şoku (65°C, 70°C ve 75°C sıcaklıklarda) ve oksidatif stres (0,008 mM, 0,01 mM, 0,02 mM, 0,03 mM ve 0,05 mM H_2O_2 ile oluşturulan) ile uyarılmaları gerçek zamanlı PZR ve çoğaltılmış cDNA bant yoğunluk analizi ile incelenmiştir.

Anahtar kelimeler: Termozom, Şaperonin, Hsp60, *Thermoplasma volcanium*, ısı şoku, oksidatif stres

To my family,

ACKNOWLEDGEMENTS

I would like to express my sincere appreciations to my supervisor Prof. Dr. Semra Kocabıyık for her guidance, support, criticism, patience, encouragements and insight throughout science.

I would like to thank The Scientific and Technological Research Council of Turkey (TUBITAK) and Graduate School of Natural and Applied Sciences METU for the financial support regarding this thesis project (Project Numbers: 105S071 (SBAG-3104) and 2006-07-02-00-1).

I express my deepest gratitude to my parents, Elif and Kemal Doldur, for their endless love, encouragements and support during my whole education.

I would like to thank to my labmates Burçak Demirok and Sema Aygar for their help and technical support.

I am deeply grateful to Utku Doldur, Mevlüt Ballı and Ayşe Mergenci for their endless moral support during period of my study.

TABLE OF CONTENTS

LIST OF FIGURES

FIGURES

LIST OF TABLES

TABLES

CHAPTER 1

INTRODUCTION

1.1 Molecular Chaperones and Protein Folding

Proteins and multiprotein complexes are necessary for all biological activities and functions (Zhang, *et al*, 2002). Polypeptide chain is the product of protein synthesis and it has to possess the unique three-dimensional structure in order to function in the cell (Walter and Buchner, 2002). Amino-acid sequence of a polypeptide chain keeps the information which leads to the unique three-dimensional conformation of the functionally active protein. Protein folding process utilizes this linear information to form well-defined three-dimensional conformation (Anfinsen, 1973). Christian Anfinsen, who showed that this process is autonomous in that it does not need any additional components or input of energy, was awarded the Nobel Prize for Chemistry in 1972 (Walter and Buchner, 2002). Although Christian Anfinsen' s dogma that is "the amino acid sequence of a polypeptide chain is sufficient to fold to the native state" still holds, it has become clear that assistance of molecular chaperones is essential for protein folding *in vivo* (Hartl, 1996, Klumpp and Baumeister, 1998). In addition, many proteins are partially or completely denatured under stress conditions. These proteins, then need molecular chaperones to prevent aggregation and regain their native structure (Hartl, 1996).

Molecular chaperones constitute a complex and sophisticated machinery (Walter and Buchner, 2002). This machinery of proteins assists polypeptides in folding, to maintain this functional state or folding-competent state under circumstances in which they would unfold and aggregate (Ruepp, *et al*, 2001, Walter and Buchner, 2002). Molecular chaperones also help polypeptides to migrate to their destinations (cytosol, organelle, membrane, extracellular space) in the cell, where they function, and to translocate through membranes.

They participate in dissolving protein aggregates and in delivering damaged proteins toward proteolytic machines for degradation (Maeder, *et al*, 2005 and Macario and Conway de Macario, 2007). Correct assembly of other proteins is mediated by molecular chaperones, but they are not components of these oligomeric assemblies (Ellis, 1993 and Hartl, 1996). Molecular chaperones carry out these diverse functions by the help of their affinity for the exposed hydrophobic residues of substrate proteins (Proctor, *et al*, 2005 and Nixon, *et al*, 2005). Interactions of molecular chaperones with exposed hydrophobic residues of substrate proteins prevent aggregation or incorrect or unwanted interactions within and between non-native polypeptides (Walter and Buchner, 2002 and Proctor, *et al*, 2005). That act of molecular chaperones increases the yield but do not increase the rate of folding reactions. Thus molecular chaperones are distinguished from the so-called folding catalysts (Hartl, 1996). Reactions of molecular chaperones are catalysed by ATP hydrolysis. While chaperones are functioning, they often bind and release their substrate protein with each cycle of ATP hydrolysis (Proctor, *et al*, 2005 and Nixon, *et al*, 2005). Molecular chaperones are present in the cytosol, mitochondria, endoplasmic reticulum and nucleus (Proctor, *et al*, 2005). They interact with other molecular chaperones since teams of chaperones constitute the chaperoning mechanism (Macario and Conway de Macario, 2007).

Nucleoplasmin is the first protein to be called as a molecular chaperone. It is a nuclear protein. Nucleosome assembly is mediated by nucleoplasmin. It prevents incorrect interactions between histones. It is not a part of the assembled nucleosomes, neither. The term “molecular chaperone” was chosen to indicate these features of nucleoplasmin (Laskey, *et al*, 1978).

Recently, a link between the superficial expression of tyrosine phosphorylated molecular chaperones and the ability of spermatozoa to bind to the zona pellucida has been determined. Nixon *et al.* hypothesized that the activation of chaperones, including Hsp60 and endoplasmin, by the tyrosine phosphorylation events associated with sperm capacitation, triggers proteins to assemble and

form a zona pellucida recognition complex on the cell surface before fertilization (Nixon, *et al*, 2005). This research on molecular chaperones and chaperone associated proteins in spermatozoa may clarify the potential importance of these molecules in the assembly and expression of receptor complexes on the surface of different cell types.

Molecular chaperones also have roles in apoptosis, and take part in modulating signals for immune and inflammatory responses (Proctor, *et al*, 2005). Molecular chaperones usually inhibit apoptosis (Sóti, *et al*, 2003). Accumulation of sHsps, Hsp60/Hsp10 or Hsp70 and many other heat shock proteins after mild heat shock or due to cell transfection can overcome both caspase-dependent and caspase-independent apoptotic stimuli and provide immortality in several human cell types (Nylansted, *et al*, 2000 and Verbeke, *et al*, 2001b). However, in nerve and immune cells, overexpression of HSF1, Hsp70, as well as Hsp90, generates no anti-apoptotic or pro-apoptotic effects (Galea-Lauri, *et al*, 1996). As a general anti-apoptotic effect, small heat shock proteins (sHsps) and Hsp70 inhibit a significant initiation factor of apoptotic processes (Arrigo, 2001 and Su, *et al*, 1999). Possible mechanisms for the attenuation of apoptosis by Hsps are the inhibition of apoptosome formation, modulation of stress kinase activation and apoptotic signalling molecules, increase in glutathione levels and/or decrease of protein aggregation. Hsp70 and Hsp90 inhibit apoptosis downstream of mitochondrial cytochrome-c release by forming a complex with apoptotic protease activating factor (Apaf-1). This leads to inhibition of association of Apaf-1 with procaspase 9 to form the apoptosome activating caspase 3 (Bree, *et al*, 2002). Hsp70 inhibits NPε ß, members of stress kinase pathways involved in apoptosis such as SAPK/JNK and p38 kinase (Gabai, *et al*, 1997). On the other side, there are examples for the positive participation of stress proteins in apoptotic signalling. The capacity of stress proteins may be exhausted due to a strong stress response resulting in protein misfolding and aggregation. Chaperone overload initiates either cell cycle arrest or apoptosis by 2 mechanisms: by proteasomal inhibiton and by induction of the JNK-dependent pathway (Sóti, *et al*, 2003 and Gabai, *et al*,

2002). Cytoplasmic translocation of mitochondrial Hsp60 is one of the pro-apoptotic signals, which (together with that of cytochrome c) promotes the activation of cytoplasmic caspases, in Jurkat T lymphocytes (Samali, *et al*, 1999 and Xanthoudakis, *et al*, 1999).

Many of molecular chaperones are also called heat shock proteins (Hsps) because expressions of them were found to be induced under increased temperatures (Ruepp *et al,* 2001). Molecular masses of the principal heat shock proteins are between ~15 and 110 kDa and they are divided into families according to both size and function (Kregel, 2002). According to Winter and Jakob, major molecular chaperone families include Hsp100/Clp, Hsp90, Hsp70/Hsp40, Hsp60/Hsp10, small heat shock proteins (sHsps) and Hsp33 (Winter and Jakob, 2004). However, all molecular chaperones are not heat-shock proteins (Ellis, 1993).

1.2 Chaperones and Disease

Fulfilling diverse functions and existing in the three phylogenetic domains, in Bacteria, Archaea and Eukarya, indicate that chaperones are essential cellular components. Chaperone failure will result in serious malfunction (Maeder, *et al*, 2005, Macario and Conway de Macario, 2007). When abnormal chaperones cause a disorder, that condition can be termed chaperonopathy. Williams syndrome, Charcot-Marie-Tooth disease, certain retinal and eye-lens pathologies, and several hereditary neuromuscular disorders, progressive motor neuronophathy, hereditary spastic paraplexia, Kenny-Caffey syndrome, and distal motor neuropathy are some disorders which are accompanied by abnormal chaperones or chaperone-like molecules. The chaperones including Hsp70, Hsp60, Grp75, Grp94 and alpha-B-crystallin have been found increased or decreased in some neurodegenerative disorders (e.g. Alzheimer's and Huntington's diseases), in certain cardiopathies and in aging (Macario and Conway de Macario, 2004).

Impairment of the induction of heat shock proteins and a decrease in chaperone function occur with age. Age-related accumulation of abnormal/damaged proteins has been implicated in several significant, pathological conditions (e.g. Alzheimer's disease, Parkinson's disease, and cataract) (Proctor, *et al*, 2005). This is mostly observed in the nervous system because of the very limited proliferation potential of neurons (Sóti and Csermely, 2003). Aggregate of damaged protein may become resistant to degradation, in neurons. This condition causes neurodegeneration (Proctor, *et al*, 2005). Other age-related diseases, such as atherosclerosis and cancer have also been found to be related to chaperone action (Sóti and Csermely, 2003).

The missing or reduced chaperone activity may be the cause of a disease. In other cases the action of chaperones may be the cause of a disease. Bovine spongiform encephalopathy or Creutzfeld-Jakob syndrome are examples for this condition, both are characterized by deposition of fibrillous aggregates of the prion protein (PrP) in the brain. Involvement of chaperones in mammalian prion diseases has not been clarified yet. However, in yeast, prion formation was shown to be critically dependent on the activity of Hsp104. The size and the number of seeds that are required for fiber polymerization and propagation seem to be regulated by Hsp104. In this case, inactivation of Hsp104 chaperone can be a means for treatment (Walter and Buchner, 2002). In addition, chaperones may be targets for therapeutic agents to control stress-related disorders and protein-misfolding diseases (Macario and Conway de Macario, 2007). Inhibition or stimulation of chaperone activity may be required for therapy, depending on their respective participation (Walter and Buchner, 2002). The development of methods that use chaperone genes and their products in order to prevent and treat disease has recently been called chaperonotherapy.

The term chaperonology includes the study of normal and abnormal chaperones in all aspects of structure and function. The study of chaperone genes in genomes, in other words, chaperonomics; the identification and

characterization of deficient, pathologic chaperones, namely the chaperonopathies; and chaperonotherapy are also covered by chaperonology (Brocchieri, *et al*, 2007).

1.3 Chaperones in Applied Fields

Formation of inclusion bodies often impair the production of recombinant proteins in bacteria. Inclusion bodies are large aggregates that is mainly composed of inactive forms of the overexpressed protein. In some cases, this problem could be relieved by the simultaneous overproduction of molecular chaperones. Therefore, molecular chaperones may be employed to optimize biotechnological processes and to increase the efficiency of production of recombinant proteins (Walter and Buchner, 2002).

It is expected from several lines of evidence reported in the last few years, that chaperones and anti-chaperone antibodies will most likely be found useful as biomarkers of disease (diagnosis), disease progression (or regression), and as prognostic indicators.

Fields of applied chaperonology-chaperonotherapy and anti-chaperone agents in industrial organizations, such as those aiming at improving plant and animal health and growth, are promising. Cultivation of water products (e.g., fish and shellfish) is one example of industry that can benefit from chaperonotherapy. It has become necessary to keep and improve the chaperoning systems of the organisms so they can deal better with stressors (e.g., pollutants) in natural habitats and in man-made environments such as aquaculture installations. At the same time, it would be appropriate to deactivate the chaperoning systems of the parasites that plague the useful species using anti-chaperone agents. Thus, the development of anti-chaperone agents for downregulating chaperone genes, or for preventing chaperone functions can be predicted to become an active field in the next few years (Macario and Conway de Macario, 2007).

1.4 Major Molecular Chaperone Families

The term molecular chaperone defines members of several structurally and genetically unrelated protein families which share the ability to recognize non-native conformations of other proteins and interact with them, without being a part of the final functional structure (Braig, 1998). Co-chaperones together with Hsp70, form the 'molecular chaperone machine'. The folding activity of Hsp70s requires ATP binding and hydrolysis, that are regulated by two co-chaperones, Hsp40 and GrpE. (Laksanalamai, *et al*, 2004). The chaperonins form a class of oligomeric, high-molecular-weight chaperones that have the unique ability to fold some proteins that cannot be folded by simpler chaperone systems. Chaperonins are made up of two-ring assemblies which contain a central cavity. Unfolded polypeptides bind to this cavity and they reach the folded state in it. Based on the ability to bind to non-native polypeptides in their ring cavities, chaperonins promote productive protein folding to the native state in a highly cooperative, ATP-dependent manner (Spiess, *et al*, 2004).

The Hsp100/Clp chaperone family: Hsp100/Clp chaperones operate with other cellular chaperones and proteases to control the quality and quantity of many intracellular proteins. Hsp100/Clp family, whose members act in an ATP-dependent manner, can be divided into two subfamilies: ClpB/Hsp104 subfamily and ClpA subfamily (Maurizi and Xia, 2004). ClpB from *E. coli* and Hsp104 from yeast have been reported to dissolve protein aggregates. These two chaperones need assistance from the Hsp70 system for their function (Walter and Buchner, 2002). Members of the ClpA subfamily, that contains ClpA, ClpC, ClpX, and HsIU, have protein unfolding activities. They perform mainly in conjuction with proteases, such as ClpP and HsIV (ClpQ), to catalyze ATP-dependent proteolysis (Maurizi and Xia, 2004). The archael species, which have been sequenced thus far, lack Hsp100 family (Laksanalamai, *et al*, 2004).

The Hsp90 chaperone family: Hsp90 chaperones were found in prokaryotic and eukaryotic organisms, but do not exist in Archaea (Ruepp*, et al,* 2001). Hsp90 family proteins are constitutively expressed in the cells, and their synthesis increases during stress (Brown, *et al*, 2007). Representatives of the highly conserved Hsp90 chaperone family are Hsp90 α and β in humans (corresponding to a major and minor isoform), Hsp86 and Hsp84 in mice, Hsp83 in *Drosophila*, Hsc82 and Hsp82 in yeast, HtpG in the bacterial cytosol, Grp94/gp96 in the endoplasmic reticulum of eukaryotes, and Hsp75/TRAP1 in the mitochondrial matrix (Young, *et al*, 2001). Experiments with mouse L-cells and cultured rat liver cells suggested that their heat-shock protein is a phosphoprotein of 90-92 kDa, which functions as a glucocorticoid receptor (Housley, *et al*, 1985). Hsp90 functions as a homodimer and associates with co-chaperones. It facilitates the maturation and/or activation of over 100 substrate proteins. These substrate proteins, which are involved in cell regulatory pathways, contain protein kinases, nuclear hormone receptors, transcription factors, and other essential proteins (Brown, *et al*, 2007). Most of known substrates of Hsp90 are signal transduction proteins and it is distinguished from other chaperones in that feature. Hsp90 binds to substrates, that are at a late stage of folding. It acts as part of a multichaperone machinery in the cytosol, which includes Hsp70, peptidyl-prolyl isomerases and other co-chaperones (Young, *et al*, 2001). Much is known about the ATPase-driven conformational cycling of Hsp90, but the precise physical effects of this chaperone that provide activating its substrate proteins are still poorly understood (Brown, *et al*, 2007).

The Hsp70 chaperone family: All bacterial and eukaryotic genomes, which have been sequenced to date, possess the genes for the Hsp70 chaperone family but most archaea lack these genes. Archaea which possess Hsp70 system appear to acquire it in independent lateral transfer events into different archaeal lineages (Ruepp*, et al,* 2001). DnaK from *E. coli*, Hsp72 and Hsp73 from eukaryotic cytosol, mHsp70 from mitochondria, and BiP from endoplasmic reticulum are representatives of the Hsp70 chaperone family (Evstigneeva, *et*

al, 2001). The Hsp70 chaperone family, which is the most highly conserved molecular chaperone family, acts on nascent chains during *de novo* protein folding, participates in the prevention of protein aggregation in a variety of post-translational processes, including protein targeting and membrane translocation, protein degradation and cellular apoptosis (Barral, *et al*, 2004). It is involved in the protection of stress-denatured proteins from aggregation and in the disassembly of protein complexes (Ruepp*, et al,* 2001). Moreover, Hsp70 chaperones arrange signal transduction pathways by controlling the stability and activities of protein kinases and transcription factors. They refold even aggregated proteins, in co-operation with Hsp100 proteins, as part of their protein quality control function (Erbse, *et al*, 2004). Binding and release of short hydrophobic stretches in partially folded polypeptides seems to be the common function of Hsp70 chaperones in the above mentioned chaperoning processes (Walter and Buchner, 2002). This interaction is controlled by ATP and by different co-chaperones. Co-chaperones regulate the ATPase cycle (Erbse, *et al*, 2004). The most extensively studied member of this chaperone family is the DnaK protein from *E. coli* (Walter and Buchner, 2002). The Hsp70 chaperone family is composed of Hsp70 (DnaK), Hsp40 (DnaJ), and Hsp23 (GrpE). These components do not form a stable high-molecular-weight complex, they interact transiently (Ruepp*, et al,* 2001). The action mechanism of *E.coli* DnaK chaperone system is explained in the Figure 1.1.

Hsp60 chaperone family: Members of the Hsp60 chaperone family are also called chaperonins and they are found in almost all organisms (Laksanalamai, *et al*, 2004). The only exceptions, which do not possess genes for Hsp60 chaperones, are two mycoplasma species known to date (Lund, *et al*, 2003). The chaperonin family of molecular chaperones was identified by Hemmingsen *et al* (1988) (Hemmingsen, *et al*, 1988). The chaperonins promote the ATP-dependent folding of proteins, both under normal growth conditions and under stress (Hartl, 1996). Hsp60 chaperones do not directly interact with nascent chains at the ribosome level. Hsp70 and Hsp60 chaperone systems have been suggested to form a lateral network of cooperating proteins

(Braig, 1998). Until recently GroEL of *Escherichia coli* has been the focus of most structural studies on chaperonins. However, the results achieved from this particular system can not be generalized to all chaperonins (Klumpp and Baumeister, 1998).

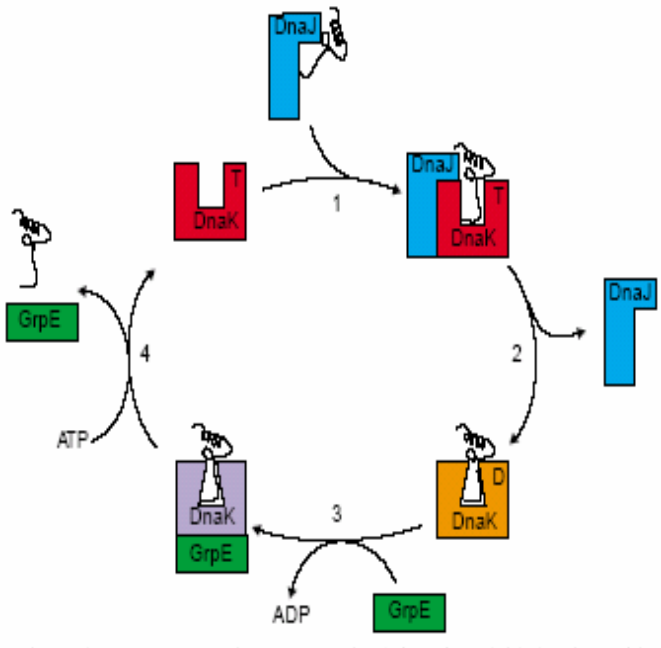

Figure 1.1 *E.coli* DnaK chaperone cycle. A largely unfolded polypeptide substrate (black ribbon) is captured by the co-chaperone DnaJ (blue). Upon complex formation with DnaK (red), the substrate is transferred from DnaJ to the peptide-binding site of DnaK (step 1). DnaJ-stimulated hydrolysis of ATP (T) closes the binding site (orange conformation of DnaK) and locks in the substrate, therefore forming a stable protein/DnaK complex (step 2). After the dissociation of DnaJ, the bound ADP (D) is displaced by the nucleotide exchange factor GrpE, depicted in green (3). Subsequent binding of ATP to DnaK releases GrpE and induces a conformational change that opens the peptide binding site (4). Thus, the polypeptide can dissociate (from Walter and Buchner, 2002).

Members of Hsp60 chaperone family can be divided into two groups based on both function and homology: Group I chaperonins and Group II chaperonins. Group I chaperonins, such as GroEL of *E.coli*, need to cooperate with a co-chaperone such as GroES (Walter and Buchner, 2002). They are found in bacteria (GroEL), in the mitochondria (hsp60 in mitochondrial matrix) and the chloroplasts (Rubisco-subunit-binding protein, RBP) of eukaryotic cells (Carrascosa, *et al*, 2001). *Methanosarcina* species, as an exception in archaea, also possess GroEL/GroES chaperoning system (Conway de Macario, *et al*, 2003). Group II chaperonins do not require a co-chaperone. They are found in the cytosol of archaea and eukaryotes (Walter and Buchner, 2002). Although group I and group II chaperonins share only 20-25 % amino acid sequence identity, they are very similar in basic architecture. Both group I and group II chaperonins assemble to form multisubunit oligomers. These oligomers possess double-ring quaternary structures (Archibald, *et al*, 2001). Group I chaperonins, such as GroEL consists of two seven-membered rings (Braig, 1998), while Group II chaperonin complexes consist of eight- or nine-membered rings (Klumpp and Baumeister, 1998). All chaperonins provide large seperate cavities for incompletely folded proteins. Thus, these proteins are protected from harmful interactions in the crowded milieu of the cytosol (Klumpp, *et al*, 1997).

Small Heat Shock Protein Family: Small heat shock proteins (sHsps) are the most widespread but also the most poorly conserved family of molecular chaperones (Haslbeck, *et al*, 2005 and Winter and Jakop, 2004). Members of the sHsp family exist in all kingdoms except in some pathogenic bacteria such as *Mycoplasma genitalium* and *Helicobacter pylori* (Haslbeck, *et al*, 2005). Hsp16.9 from wheat, Hsp26 from *Saccharomyces cerevisia*, and Hsp 16.5 from methanogenic archaeon *Methanococcus jannaschii* are some representative members of sHsp family and they are temperature regulated (van Montfort, *et al*, 2001, Haslbeck, *et al*, 1999 and Bova, *et al*, 2002). Members of the sHsp superfamily are diverse in sequence and size, however most of them share characteristic features. These features include a conserved α-crystallin domain

of ~90 residues, a small molecular mass of subunits ranging between 12 kDa and 43 kDa, formation of large oligomers, a dynamic quaternary structure and induction by stress conditions and chaperone activity in preventing protein aggregation (Winter and Jakop, 2004 and Haslbeck, *et al*, 2005). One sHsp-complex can bind and stabilize several non-native substrates and Hsp70 and/or chaperonin is thought to perform in following refolding process (Barral, *et al*, 2004). Despite reports of ATP-binding by α-crystallin, the regulation of sHsp chaperone activity seems to be independent of ATP (Winter and Jakop, 2004 and Haslbeck, *et al*, 2005).

Hsp33 chaperone family: Hsp33 protects bacterial cells against oxidative stress. It represents a group of proteins which are regulated by cellular redox status. Cellular functions, like transcription, apoptosis and cellular signaling, are affected by the intracellular redox status. Over 20 homologs of Hsp33 were identified from several bacterial species. These proteins do not show sequence homology to known heat shock protein families (Kim, *et al*, 2001). All members of this family are highly conserved. They include four cysteine residues rapidly respond to shifts in the redox environment in the mechanism of function (Evstigneeva, *et al*, 2001). Hsp33, which prevents aggregation of partially denatured proteins during oxidative stress, possesses a unique chaperone activity among heat shock proteins since its activity is reversibly regulated by cellular redox status. The chaperone activity of Hsp33 is induced by oxidizing agents, whereas Hsp33 is turned off by reducing agents *in vitro*. When reducing agents turn off Hsp33, it results in a regeneration of the dormant protein (Kim, *et al*, 2001). Hsp33 exists in more than 120 prokaryotic organisms. It has also been found in two eukaryotic organisms, *Chlamydomonas reinhardtii* and *Dictyostelium discoideum*. Hsp33 seems to be the only known molecular chaperone in *E. coli*, which is specifically induced under combined oxidative and heat stress (Winter and Jakop, 2004).

Extracellular Chaperones: Molecular chaperones have traditionally been considered to exist only inside cells. However, there is accumulating evidence showing that chaperones also exist on the cell surface, the extracellular space, and in serum and cerebrospinal fluid. Based on the information from studies on importance and functions of extracellular chaperones it is noteworthy to mention that circulating chaperones can bring out production of anti-chaperone antibodies as an autoimmune response. Anti-chaperone antibodies have been determined to exist in patients with some type of cancers, diabetes, and HIV infection. It is not obvious yet what role the anti-chaperone antibodies play. They may take part either in pathogenesis or in protection of the body against disease initiation and progression (Macario and Conway de Macario, 2007).

Prefoldins: Prefoldin, a ~90k-Da complex, also known as the Gim complex (genes involved in microtubule biogenesis, GimC), is a hexameric molecular chaperone complex and is present in all eukaryotes and archaea (Siegert, *et al*, 2000). Prefoldin subunits are subdivided into two classes, namely α and β. Archaea possess one member of each class (PFDα and PFDβ), and eukaryotes have 2 different but related subunits of the α class and four related subunits of the β class (Hartl, *et al*, 2002 and Leroux, *et al*, 1999) (Figure 1.2). The crystal structure of prefoldin displays a unique quaternary structure that is different from other chaperones and it therefore forms a novel class (Zhang, *et al*, 2002). The structure of prefoldin resembles that of a jellyfish, with six α-helical coiled-coil tentacles protruding from a β-barrel body. The distal regions of the coiled coils expose hydrophobic regions for the binding of nonnative protein (Siegert, *et al*, 2000). Unlike Hsp70 and the chaperonins, prefoldin is a novel class of chaperone that is ATP independent. For at least some substrates, group II chaperonins seem to employ prefoldin as a delivery agent, in both archaea and the eukaryotic cytosol. It makes direct physical interaction with the chaperonin to deliver substrate, and it uses multiple interaction sites for substrate binding to protect non-native polypeptide from aggregation before transferring it to other chaperones for completion of folding (Zhang, *et al*,

2002). In eukaryotes, prefoldin appears to enhance the efficiency of the overall folding of its preferred substrates, actin and tubulin, presumably by providing efficient delivery (Siegers, *et al*, 1999). Prefoldin is suggested to fulfill an ATP independent, Hsp70-like function in archaeal *de novo* protein folding, since Hsp70 chaperones are absent in many archaea (Leroux, *et al*, 1999).

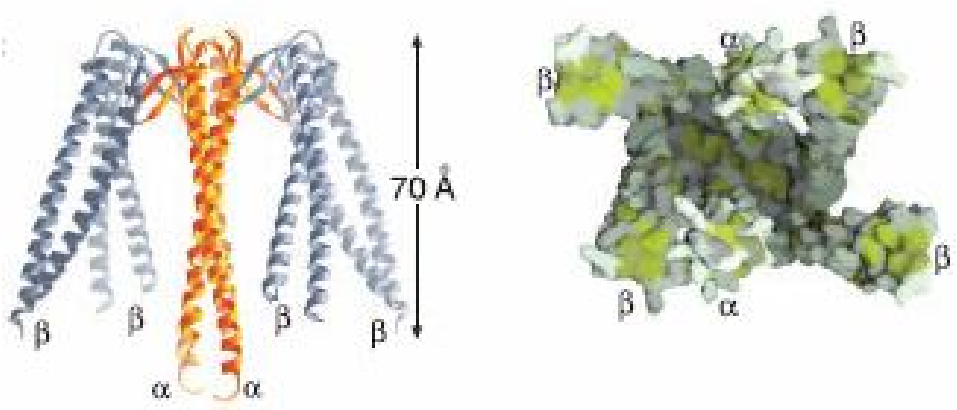

Figure 1.2: (Left) Side view and dimension of the structure of archaeal prefoldin with the two α subunits displayed in gold and the four β subunits in gray. (Right) Bottom view of the prefoldin complex showing the central space enclosed by the six coiled-coil segments. Surface representation is shown with hydrophobic patches in yellow and hydrophilic regions in gray (from Hartl, *et al*, 2002).

1.5 Structural and Functional Comparison Between Group I and Group II Chaperonins

All chaperonins are large oligomers which are comprised of protein subunits with molecular masses of about 60 kDa. These oligomers are built up in the shape of a toroid and usually consist of two rings placed back-to-back. Each oligomer subunit in every chaperonin has a similar structure, arranged into three domains: the equatorial domain, the intermediate domain and the apical domain (Figure 1.3).

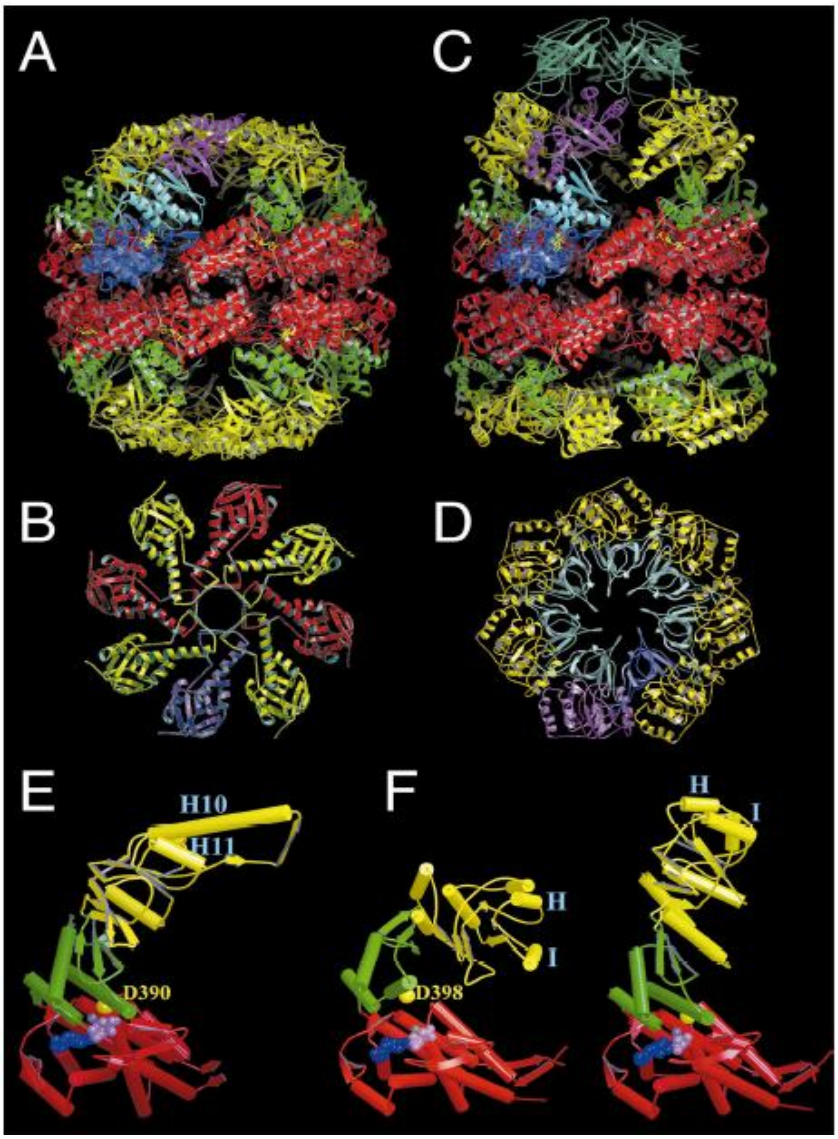

Figure 1.3 Architecture of chaperonins. (A) Side view of the *T. acidophilum* thermosome (Ditzel, *et al.,* 1998). Equatorial domains are shown in red, intermediate domains are in green, and apical domains are in yellow. (B) Top view showing only the apical domains. (C) Side view of the asymmetric GroEL–GroES complex (Xu, *et al.,* 1997), colors as in (A). (D) View of the *cis*-ring with apical domains in yellow and GroES in gray. (E) Domain arrangement in the thermosome; Asp390 contributes to the active site. (F) Domain arrangements in GroEL: (left) substrate binding *trans*-ring; Asp398 is far away from the active site; (right) ATPase active *cis*-ring with Asp398 at the active site. Nucleotides are depicted as ball model (from Steinbacher and Ditzel, 2001).

The equatorial domain keeps the nucleotide binding site and most of the interactions between the subunits of the same ring and those of the opposing ring. The intermediate domain functions as a transmitter of the conformational changes produced upon nucleotide binding between the equatorial domain and the apical domain. Substrate binding takes place in the apical domain (Gómez-Puertas, *et al*, 2004). Firstly, nonnative substrate protein is caught by way of hydrophobic contacts with multiple chaperonin subunits. It is then moved into the central ring cavity. It folds and is protected from aggregating with other nonnative proteins in the central cavity (Hartl, *et al*, 2002).

Group I chaperonins are found in bacteria, some eukaryotic organelles and only one archaea i.e. *Methanosarcina* and they are known as GroEL proteins (Laksanalamai, *et al*, 2004). GroEL is composed of two seven-membered rings which are stacked back-to-back (Braig, 1998). In GroEL, subunits are identical. Each subunit is 57 kDa and is composed of three domains, as mentioned. GroES is a homoheptameric ring of ~10 kD subunits. Substrate proteins up to ~60 kDa can be encapsulated and they are free to fold in the GroEL-GroES cage. The GroEL-GroES cage is also termed "Anfinsen cage" (Hartl, *et al*, 2002). The ATPase cycle of GroEL controls cycles of alternate binding and release of both substrate polypeptide and GroES. Kinetic studies have shown positive cooperativity of ATP binding and hydrolysis within the rings and negative cooperativity between the rings. EM and biochemical studies reveal negative cooperativity of substrate and GroES binding; once one ring is occupied, the second one has a much lower affinity for the same ligand (Roseman, *et al*, 1996). They do not exist in the same nucleotide-bound state. Thus, GroEL is functionally asymmetrical (Hartl, *et al*, 2002).

The chaperonin reaction starts with the binding of substrate polypeptide to the free end (i.e., the trans ring) of a GroEL-GroES complex (Hartl, *et al*, 2002) (Figure 1.4). Within a ring there is cooperative binding of ATP by the seven equatorial sites, with an obvious K_M of ~10 μM. ATP binding triggers small rigid body movements of the intermediate and apical domains in the ring to

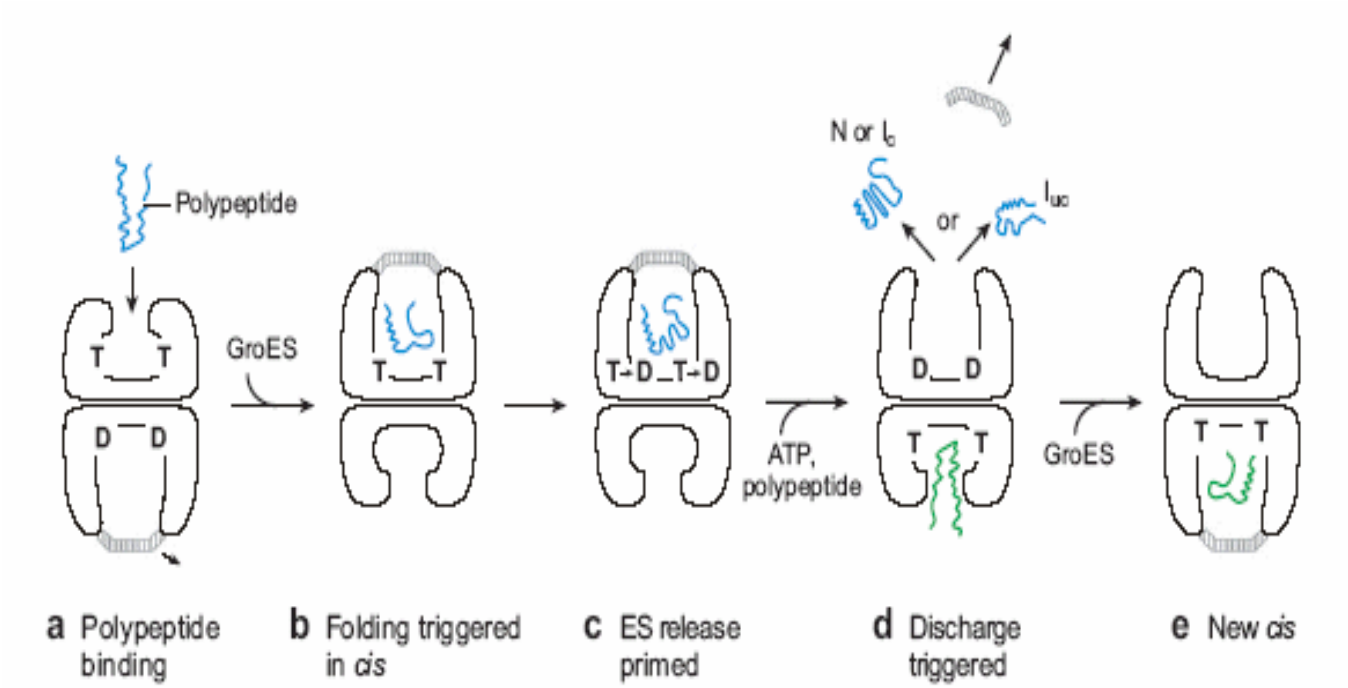

Figure 1.4: GroEL-GroES ATP-directed reaction cycle. Asymmetric behavior of the GroEL machine is directed by the positive cooperativity of ATP binding within a ring but by negative cooperativity between rings; because GroES can bind rapidly and efficiently only to an ATP-occupied ring. T stands for ATP, and D denotes ADP. (N, native; Ic, intermediate committed to fold to the native state; Iuc, intermediate in an uncommitted or kinetically trapped state) (from Horwich, *et al*, 2007).

which it binds. This allows GroES association, which is followed within a second by much larger rigid body movements of the GroEL intermediate and apical domains, and this step results in the end-state GroEL-GroES complex. The GroEL apical domains are elevated by 60 degrees and twisted 90 degrees clockwise, in order to remove the hydrophobic binding surface from facing the cavity. Associated with these large movements, a substrate protein, initially captured on the hydrophobic cavity wall of an open GroEL ring, is rapidly transferred into the central cavity of the now hydrophilic GroEL-GroES cis cavity, where it begins to fold (Horwich, *et al*, 2006). These changes after GroES binding cause an enlargement of the cavity and a shift in its surface properties from hydrophobic to hydrophilic ones (Hartl, *et al*, 2002). The hydrophilic nature of the walls of the cavity may facilitate the folding of the substrate protein. Being surrounded by hydrophilic walls of the cavity may hasten the burying of hydrophobic residues. Completion of this step lowers the tendency of proteins to aggregate (Lund, *et al*, 2003). Folding proceeds until the hydrolysis of the seven ATP molecules in the *cis* ring is completed, for nearly 10 seconds. At the end of this period, completion of ATP hydrolysis serves to weaken the association of GroES with GroEL, and GroES, substrate polypeptide and ADP are released. Both folded and nonnative proteins are released at this point (Figure 1.4). The physiological trigger to such release is the binding of ATP in the opposite ring. Moreover, the additional binding of non-native polypeptide to the opposite ring accelerates release (Hartl, *et al*, 2002 and Horwich, *et al*, 2006).

In summary, the GroEL protein operates as a two-stroke engine (Lund, *et al*, 2003). Folding cycles are repeated till the substrate protein acquires its native state (Hartl, *et al*, 2002). ATP hydrolysis in one ring is essential to promote ATP binding to the opposite ring. ATP binding to the opposite ring triggers GroES and substrate release. Thus, negative cooperativity between the two rings of GroEL enables the system turn over (Gutsche, *et al*, 2001).

GroEL interacts with a wide variety of newly synthesized proteins *in vivo* (Carrascosa, *et al*, 2001). Substrates for the GroEL protein in *E. coli* contain several metabolic enzymes, RNA polymerase subunits, and other proteins involved in transcription and translation. However, all the substrates for GroEL have not been fully defined yet (Lund, *et al*, 2003). It has recently been suggested that most of the substrates which interact *in vivo* with GroEL possess a common structural motif: two or more domains with α–β folds with extended hydrophobic surfaces (Carrascosa, *et al*, 2001). Heat-shock strongly induces expression of the GroEL protein. The signal for this induction is the presence of unfolded proteins in the cell (Lund, *et al*, 2003).

Group II chaperonins are found in Eukaryotes and in all of the Archaea that have been sequenced so far (Laksanalamai, *et al*, 2004). Eukaryotic representative for group II chaperonins is TriC/CCT. In thermophilic or hyperthermophilic archaea, such as *Thermoplasma* spp., *Sulfolobus* spp., or *Pyrococcus* spp., group II chaperonin complexes are also known as thermosomes, archaeosomes or rosettasomes (Quaite-Randall, *et al*, 1995, Phipps, *et al*, 1993 and Laksanalamai, *et al*, 2004). Group II chaperonins, such as TriC/CCT in eukaryotic cells and the thermosome in archaea, consist of eight- or nine-membered rings (Archibald, *et al*, 2001 and Spiess, *et al*, 2004). Group I chaperonins require cooperation with co-chaperones of the GroES or Hsp10 family, as mentioned before. GroES functions as a lid which closes the cavity of the ring it is bound to (Walter and Buchner, 2002 and Hartl, *et al*, 2002). No such co-chaperone exists in the group II chaperonins. Instead, group II chaperonins contain a built-in lid. It is an extension of the apical domain which is called the helical protrusion (Archibald, *et al*, 2001) (Figure 1.5). Recent evidence reveals that the function of this group II chaperonin's 'built-in lid' is controlled by ATP binding and hydrolysis (Iizuka, *et al*, 2003). In addition, this region contains conserved hydrophobic residues, which indicates that it might serve as an initial substrate-binding domain (Ditzel, *et al*, 1998 and Laksanalamai, *et al*, 2004). Protein cofactors which have no evident

homologs in the bacterial system are known to interact with group II chaperonins (Archibald, *et al*, 2001).

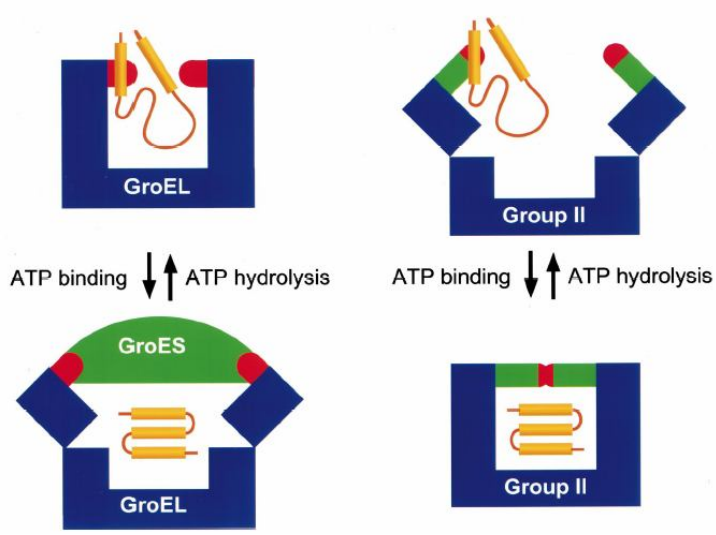

Figure 1.5: Comparison of the basic conformations of group I (GroEL/GroES) and group II chaperonins about the functional cycle. For simplicity the figures of the chaperonin-substrate complexes show only single rings (from Klumpp and Baumeister, 1998).

The functional results of ATP binding and hydrolysis for folding of substrate protein seem to have been conserved between the catalytic cycles of group I and group II chaperonins. However, the influences of nucleotides on the overall structure of the two chaperonin groups are obviously different. The substrate binding ground state of the thermosome learned from cyro-EM observations is open and contracts upon ATP binding to generate the closed conformation. Opposingly, GroEL binds its substrates in a compact conformation, and ATP causes its apical domains to move toward the outside to provide binding of GroES and hence closure of the cavity (Klumpp and Baumeister, 1998).

1.6 Group II Chaperonins in Archaea and Eukaryotes

Archaea include between one and three chaperonin genes as shown by genome analysis. *Methanosarcina acetovirans*, as an exception, possesses five chaperonin genes (Lund, *et al*, 2003). Subunits of archaeal chaperonin are arranged in eight- or nine-membered rings (Hartl, *et al*, 2002). Thermophilic factor 55 (TF55) from *Sulfolobus shibatae* and the thermosome from *Pyrodictium occultum* are the first characterized group II chaperonins in Archaea (Andrä, *et al*, 1996). Thermosomes in many archaea, for example in *Pyrodictium occultum*, *Thermoplasma acidophilum* and *Thermococcus* are made up of two subunits (Phipps, *et al*, 1991, Ditzel, *et al*, 1998 and Yoshida, *et al*, 1997). In hyperthermophiles, at most of three distinct, but sequence-related, hsp60 chaperonin-encoding genes were reported in the archaeon *Sulfolobus shibatae*, as in *Sulfolobus solfataricus* and *Sulfolobus tokodaii* (Kagawa, *et al*, 2003 and Laksanalamai, *et al*, 2004). Since the majority of group II chaperonins in Archaea have eight subunits per ring and are generally referred to as 'thermosomes', chaperonins in Sulfolobales are referred to as 'rosettasomes' by Kagawa *et al* to distinguish them from thermosomes. Rosettasomes are two nine-membered rings made up of three different 60 kDa subunits (TF55α, TF55β and TF55γ) in the Sulfolobales family (Kagawa, *et al*, 2003). However, *Methanococcus jannaschii* possesses only one thermosome gene. The thermosomes from *Methanopyrus kandleri* and *Desulfurococcus* sp. also seem to be homooligomers (Andrä, *et al*, 1996, Klumpp and Baumeister, 1998). Regulation of chaperonins by heat shock was revealed in *Pyrodictium occultum* and *S. shibatae* (Phipps, *et al*, 1991 and Trent, *et al*, 1994).

The *in vitro* chaperone activities of several archaeal chaperonins have been demonstrated using model substrates. Furutani *et al.* (1998) reported that the recombinant *Methanococcus thermolithotrophicus* thermosome (the MTTS) complex assisted the refolding of chemically denatured thermophilic archaeal citrate synthase and glucose dehydrogenase at 50°C in an ATP-dependent manner (Furutani, *et al*, 1998). Yan *et al.* (1997) reported that the recombinant

chaperonin β subunit of *Pyrococcus* sp. strain KOD1 (CpkB) represses the thermal denaturation and increases thermostability of *Saccharomyces cerevisiae* alcohol dehydrogenase (Yan, *et al*, 1997).

The term "thermosome" has been chosen because of its accumulation to high levels upon heat-shock and the extreme temperature profile of this ATPase (Phipps, *et al*, 1993, Klumpp and Baumeister, 1998). This term was first used to define the chaperonin from *Pyrodictium occultum* (Phipps, *et al*, 1993, Klumpp and Baumeister, 1998).

Group I and group II chaperonin subunits share a similar basic structure that are composed of three domains: an equatorial ATP-binding domain; an apical domain which is involved in substrate binding; and a central hinge domain that provides communication between the equatorial domain and the apical domain. The equatorial domain is relatively conserved among the paralog subunits. Most sequence divergence exists in the apical domains, which are thought to possess the substrate binding sites (Spiess, *et al*, 2004). The crystal structure of the thermosome, a group II chaperonin from *Thermoplasma acidophilum*, serves a clue to the absence of a GroES cofactor because the complex appears to contain a 'built-in' lid (Ditzel, *et al*, 1998). Each subunit of the thermosome complex can be superimposed onto a GroEL subunit, with the exception of an additional loop protruding from the tip of the thermosome apical domain. In the crystal, the apical protrusions form an iris-like lid structure which restricts access to the cavity. This crystal structure also indicates that the central chamber could encapsulate a polypeptide of up to 50 kDa in the closed state (Ditzel, *et al*, 1998). The apical protrusions have also been shown to possess a GroES-like function, acting as a built-in lid that opens and closes during the ATPase cycle of TRiC (Meyer, *et al*, 2003).

Group II chaperonin of the eukaryotic cytosol is called TriC (TCP-1 ring complex) or CCT (chaperonin-containing TCP-1) (Klumpp and Baumeister, 1998). TCP-1 (tail-less complex polypeptide-1) is one of the eukaryotic

cytosolic chaperonin with eight different but related subunits (Zhang, *et al*, 2002, Klumpp and Baumeister, 1998). Subunits differ in their apical, substrate-binding domains. Each subunit has an additional α-helical protrusion. The mechanism of group II chaperonins is less well understood than that of group I chaperonins. It is proposed that after binding to substrate, an ATP-driven folding cycle similar to that of GroEL induces encapsulation of the substrate. Encapsulation of the substrate is achieved by rearrangements of the apical domain protrusions (Barral, *et al*, 2004). The binding of ATP to CCT causes apparent structural changes as observed in electron microscopy studies. Structural changes include the equatorial and apical domains of the *cis* ring. These changes lead to an asymmetric particle. The change in the equatorial domain has not been observed as in GroEL, and it could be associated with differences in the inter-ring communication between both chaperonin types.

The apical domain rotates and the equatorial domain moves upward towards the axis of the particle. That shift is distinct in magnitude regarding the small change undergone by the corresponding GroEL domain upon ATP binding (Carrascosa, *et al*, 2001).

TRiC/CCT may also participate co-translationally in the folding of distinct protein domains. The cytoskeletal proteins, actin and tubulin, are the main substrates for TRiC/CCT. A wider set of newly synthesized proteins comprising WD40 β-propeller proteins from the yeast cytosol, the von Hippel-Lindau tumor suppressor protein, luciferase, Gα-transducin and cyclin E have recently been shown to interact with TriC/CCT (Barral, *et al*, 2004). Certain sequences of the substrate protein for TriC/CCT interact with specific domains of a particular subunit of the chaperonin. This type of interaction restricts the function of TriC/CCT to much more specific substrates (Carrascosa, *et al*, 2001). Some reports suggest that TriC/CCT functions in recovery after heat-shock and related chemical stress. The upregulation of TriC/CCT is proposed to be mediated by the HSE (heat-shock element)-HSF (heat shock transcription

factor) system. However, some reports suggested TriC/CCT not to be upregulated by heat-shock. It is concluded that induction of TriC/CCT by stress may be dependent on the type of stress, cells, organisms or other environmental conditions (Kubota, *et al*, 1999).

Group II chaperonins exist at low levels in eukaryotic cytosol. All eight of the subunits are encoded by a seperate gene and each type of subunit holds a distinct position (Lund, *et al*, 2003, Klumpp and Baumeister, 1998).

1.7 Structures and Functions of Hsp60 Chaperones in Archaea

The chaperonin complex is the most plentiful protein in heat-shocked cells in the thermophilic archaeon *Sulfolobus shibatae*, including up to 40% of the total cellular protein (Trent, *et al*, 1991).

The mechanisms of action of several archaeal chaperonin complexes, including those from *Sulfolobus shibatae* and *Thermoplasma acidophilum* have been investigated. The chaperonin complex from *S. shibatae* has a bitoroidal structure (Laksanalamai, *et al*, 2004). As mentioned before, this chaperonin complex is made up of three subunits and it is also called "rosettasome" or "TF55". Kagawa, *et al* (2003) reported that *in vivo* rosettasomes were hetero-oligomeric with an average subunit ratio of 1α:1β:0,1γ in cultures grown at 75°C, a ratio of 1α:3β:1γ in cultures grown at 60°C and a ratio of 2α:3β:0γ after 86°C heat shock. Authors also reported about rosettasome that alpha and beta gene expression was induced by heat shock and decreased by cold shock. Expression of the gamma gene was reported to be undetectable at heat shock temperatures and low at normal growth temperatures, but it was increased by cold shock (Kagawa, *et al*, 2003). Presumably, variants of this thermosome that contain the third subunit (γ) are specialized to cope with protein-folding problems which occur in suboptimal growth temperatures (Laksanalamai, *et al*, 2004). It is proposed that, *in vivo*, the rosettasome structure is determined by the relative abundance of subunits. Therefore, it can not be determined by a

fixed geometry (Kagawa, *et al*, 2003). The chaperonin complex from *S. shibatae* resembles the eukaryotic Hsp60, and alternates between a closed and an open complex. Closed complexes open after ATP binding, and the subunits dissociate when the bound ATP is hydrolysed (Laksanalamai, *et al*, 2004). The thermosome protein from *S. shibatae* also forms interesting filamentous structures *in vitro,* and possibly *in vivo*. Detection of these filamentous structures has led to suggestions that thermosomes have other functions in addition to assisting protein folding. The filaments have been proposed to constitute part of the prokaryotic cytoskeleton (Trent, *et al*, 1997). Furthermore, it was reported that, the chaperonins from *S. shibatae* are membrane associated, and might act in minimizing membrane permeability at lethal temperatures (Trent, *et al*, 2003). Nakamura, *et al.* (1997) reported molecular cloning of the gene for and purification of the group II chaperonin from the thermoacidophilic archaeon *Sulfolobus* sp. strain 7. Although the chaperonin complex seemed to be a homooligomer, the authors afterwards found that it is composed of two kinds of subunits with almost the same molecular weights. The purified *Sulfolobus* chaperonin displayed weak ATPase activity. In the same study, the effect of Sulfolobus chaperonin on the refolding of the chemically denatured lactate dehydrogenase (LDH) was studied. The recovery of LDH activity was found significantly lower than that of spontaneous refolding in the presence of the *Sulfolobus* chaperonin (Nakamura, *et al.*,1997).

The thermosome of *T. acidophilum* is made up of two subunits, namely α and β subunits. Alpha and β subunits of *Thermoplasma acidophilum* thermosome exhibit approximately 60% sequence identity (Nitsch, *et al*, 1997). The arrangement of the two subunits in the thermosome from *T. acidophilum* was identified by cryo-electron microscopy (Klumpp and Baumeister, 1998). A four-fold symmetry was revealed in the native hetero-oligomeric α+β thermosome from *T. acidophilum*. However, in the recombinant, homooligomeric α-only thermosome, expressed in *E.coli*, displayed eight-fold

symmetry. These findings proved that α and β-subunits alternate within two identical rings of the *Thermoplasma* thermosome (Nitsch et al., 1997). The subunit arrangement was similar to the one revealed in the eukaryotic cytosolic chaperonin TriC/CCT. In TriC/CCT both rings include all eight subunits and the subunits hold distinct positions (Liou and Willison, 1997). Recent data shows that ATP binding to α- and αβ thermosomes is adequate to induce their closure at physiologically relevant temperatures (Gutsche, *et al.,* 2001). Like all other thermosomes, both α- and αβ-thermosomes from *T. acidophilum* show a significant temperature dependence for their ATPase activity. The upper limit is achieved close to 60°C, which is the optimum growth temperature of the organism. The native thermosome hydrolyzes ATP about threefold faster than the homo-oligomeric thermosome and the rate limiting step seems to differ in the two cases. The rate-limiting step in the ATP hydrolysis cycle of the α-only thermosomes from *T. acidophilum* and of group I chaperonins is the cleavage of the γ-phosphate bond, however for the native αβ-thermosomes from *T. acidophilum*, the slowest step is the post-hydrolysis isomerisation into a "closed" ADP*Pi species (Gutsche, *et al.,* 2000b). A recent cryoEM analysis of the α-thermosome determined a mixture of three conformations: open (43%), closed (30%), and asymmetric (20%), with one ring open and the other closed (Figure 1.6). Nucleotide binding pockets are closed by the intermediate domains in the closed rings, but the pocket is accessible in the open rings (Schoehn, *et al.,* 2000). Waldmann, *et al.* (1995) reported that co-expression of the two genes which encode the α and β subunits of the *T. acidophilum* thermosome in *E. coli* produced wholly assembled hetero-oligomeric (α+β) complexes. Separate expression of both genes brought about formation of hexadecameric complexes in the bacterial cytoplasm. The native thermosome and the recombinant α-complex were dissociated and observed to reassemble *in vitro* in the presence of Mg-ATP (Waldmann, *et al.*, 1995).

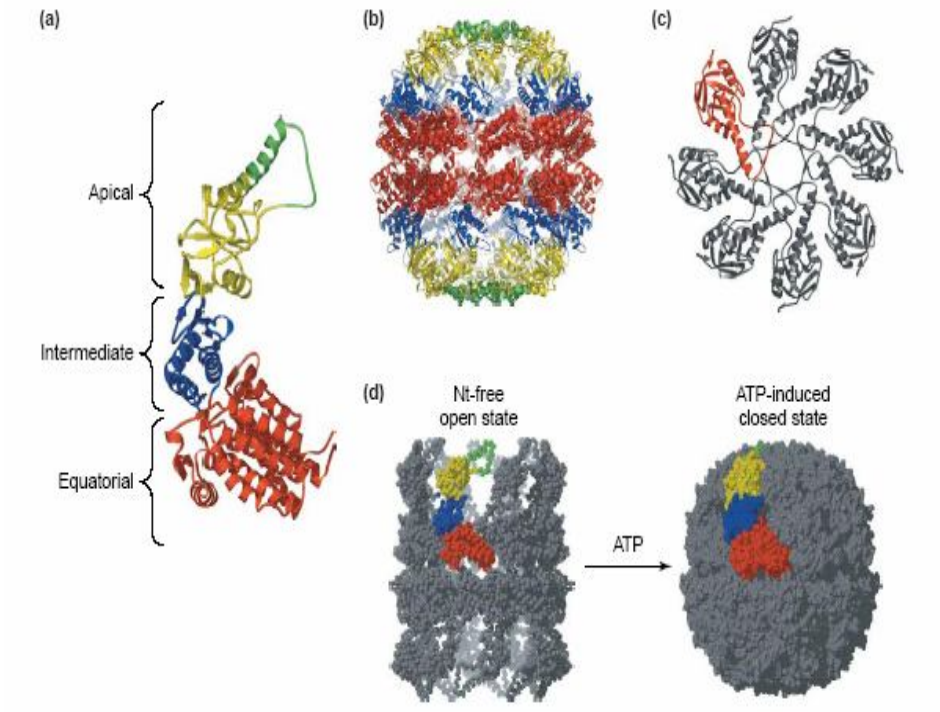

Figure 1.6: General architecture of group II chaperonins. a) Ribbon diagram of an α subunit of the thermosome from *Thermoplasma acidophilum*. The equatorial ATPase domain (red) is linked to the substrate-binding apical domain (yellow) by a flexible hinge or intermediate domain (blue). The helical protrusion, which is unique to group II chaperonins, is in green. b) Side view of the closed conformation observed in the X-ray structure of the thermosome, with subunit domains coloured as in (a) (Ditzel, *et al*, 1998). Viewed from the side, the oligomeric structure is formed by two octomeric rings. In TCP-1 ring complex (TriC), each ring is composed of eight subunits. c) Top view of the closed thermosome structure that emphasizes how the apical protrusions close into an iris-like lid (Ditzel, *et al*, 1998). For clarity, only apical domains are shown, with one domain in red. d) Bead models of the ATP-induced transition from the open to closed state for group II chaperonins. The model of the nucleotide-free, open state (left) is based on electron tomographic studies on the thermosome. The closed state is from the X-ray structure of the thermosome and supposedly reflects the ATP-induced state (from Spiess, *et al*, 2004).

Kawashima, *et al.* (2005) reported identification of proteins present in the archaeon *Thermoplasma volcanium* cultured in aerobic and anaerobic conditions. *T. volcanium* is one of a small number of archaea able to live in both aerobic and anaerobic environments. Under the aerobic condition, proteins expressed in larger quantities were identified as types of proteins reducing active oxygens and the archaeal chaperonin (Kawashima, *et al.*, 2005).

Andrä *et al.* (1996) have isolated the thermosome from the hyperthermophilic methanogen *Methanopyrus kandleri*. They suggested that the thermosome of the *M. kandleri* seems to be a homo-oligomer comprised of two 8-fold symmetric rings. Trial of authors to determine a second subunit in the thermosome complex have failed (Andrä, *et al*, 1996). This is in contrast to the chaperonins from *Pyrodictium occultum* and *Thermoplasma acidophilum* which have two subunits in 1:1 subunit stoichiometry (Yoshida, *et al*, 1997).

The thermosome of *Pyrodictium occultum* is an abundant component of the cytoplasm. It is composed of two subunits, α and β, which constitute a hexadecameric double ring complex. Minuth, *et al*, (1998) produced the two subunits jointly and separately in *E. coli*. They have isolated soluble, high-molecular-mass double-ring complexes of recombinant chaperonins from *E. coli* in all three cases. All three recombinant complex species, namely recombinant all-α, recombinant all-β, and recombinant αβ, exhibited ATPase activity. Furthermore, they could demonstrate that the recombinant complexes slow down the aggregation of citrate synthase, alcohol dehydrogenase, and insulin. Therefore, it was concluded that the recombinant protein complexes possess a chaperone-like activity, interacting with non-native proteins. They exhibit this chaperone-like activity at temperatures below the lower physiological limit of growth (Minuth, *et al*, 1998). Phipps, *et al.* (1991) reported that double rings are composed of eight subunits each and the rings surround a central channel. Thermosome purified from the hyperthermophile *P. occultum* consists of equal amounts of two subunits. Molecular weights of

the two subunits are 56 kd and 59 kd. The complex was found to be a very thermostable ATPase. It accumulates as a consequence of heat shock. Using antiserum, raised against the *P. occultum* ATPase complex, presence of immunologically related proteins in a wide variety of thermophilic, hyperthermophilic Archaea and in *E. coli* has been displayed. Immunoblotting results indicated a positive cross-reaction with the most thermosome antibodies of the extremely thermophilic archaea tested and a strong cross-reaction with *Archaeoglobus fulgidus* and *T. acidophilum* antibodies. Little or no signal was detected with the antibody of the extremely halophilic or methanogenic archaea, *Methanothennus fervidus* being an exception. Chaperonins of the thermophilic eubacterium *Thermotoga maritima* and yeast cells did not react with the antiserum. Immunoblotting results also reveal that a related protein exists in *Escherichia coli* (Phipps, *et al*, 1991).

Archaeal chaperonins have been reported to bind to several denatured proteins *in vitro* and to possess weak ATPase activity (Yoshida, *et al*., 1997). However, Andrä *et al* (1996) have reported that they failed to measure significant enzymatic ATP hydrolysis of *Methanopyrus* thermosome (Andrä, *et al*, 1996). The chaperonin of *S. solfataricus* was reported to possess protein refolding activity. The proteins, chicken egg white lysozyme (one 14.4-kDa chain), yeast α-glucosidase (one 68.5-kDa chain), chicken liver malic enzyme (four 65-kDa subunits), and yeast alcohol dehydrogenase (four 37.5-kDa subunits), were heated in the presence of an equimolar amount of chaperonin. It was observed that the protein aggregation was prevented in all solutions. The inactivation profiles of the single-chain enzymes were comparable with those identified in the absence of the chaperonin, and enzyme activities were recovered in the solutions heated in the presence of the chaperonin upon ATP hydrolysis. The inactivation of the tetrameric enzymes was completely prevented, but the activities decreased in the absence of the chaperonin (Guagliardi, *et al.*, 1995). Yan, *et al.* (1997) reported that the recombinant β subunit of the chaperonin from *Pyrococcus* sp. strain KOD1 prevents thermal denaturation and enhances thermostability of *Saccharomyces cerevisiae* alcohol dehydrogenase. They

found out that it functions without ATP when it exists at a high concentration. However, it was reported to require ATP for its chaperonin function when it exists at a low concentration (Yan, *et al*, 1997). Yoshida, *et al* (1997) reported the cloning and sequencing of two genes coding chaperonin subunits from the hyperthermophilic archaeum *Thermococcus* strain KS-1. This strain possesses two independent genes which encode α and β subunits. Both recombinant α and β subunits assemble to generate homo-oligomeric double-ring complexes. These complexes are found to arrest the spontaneous refolding of a chemically denatured thermophilic enzyme when ATP does not exist. The refolding of arrested IPMDH was continued upon addition of ATP to the reaction mixtures. The yield of spontaneous refolding of the chemically denatured isopropylmalate dehydrogenase (IPMDH) was nearly 16,7 % in this study. The yield of the refolding of IPMDH by assistance of aggregate of the β subunit complexes was about 19,0 %. However, the recovery ratio with assistance of the α subunit single complex was 3,6 % (Yoshida, *et al,* 1997).

The chaperonin from *Methanococcus maripaludis* (Mm-cpn) was reported by Kusmierczyk, *et al*. (2003). The single gene was cloned and expressed in *E. coli*. Mm-cpn was found to be fully functional in all aspects under physiological conditions of 37°C. The complex possess $Mg2^{+}$ dependent ATPase activity and it can prevent the aggregation of citrate synthase. It assists refolding of guanidinium-chloride-denatured rhodanese in a nucleotide-dependent manner. ATP binding is adequate to effect folding, but ATP hydrolysis is not necessary (Kusmierczyk, *et al.* 2003).

Bergeron, *et al.* (2008) reported that the secondary structure of the thermosome (rTHS) from *Methanocaldococcus jannaschii*, which is recombinantly expressed, was not affected by one-hour exposures to various co-solvents including 30% v/v acetonitrile (ACN) and 50% methanol. However, the secondary structure of a mesophilic homologue, GroEL/GroES, was considerably disrupted. rTHS reduced the aggregation of ovalbumin and citrate

synthase in 30% ACN, to assist refolding of citrate synthase upon solvent inactivation, and stabilized citrate synthase and glutamate dehydrogenase in the direct presence of co-solvents (Bergeron, *et al.,* 2008).

Yan, *et al.* (1997) investigated the effect of the recombinant chaperonin β subunit of *Pyrococcus* sp. strain KOD1 (CpkB) on foreign protein solubilization. The *cobQ* gene of KOD1, that encodes cobyric acid synthase, forms an insoluble inclusion complex when it is overexpressed in *E. coli*. However, when CpkB and CobQ were co-expressed, a significant amount of protein was found in a soluble fraction. According to authors, this result indicates that the β subunit is functional as a molecular chaperonin without the α subunit *in vivo* (Yan, *et al*, 1997). Izumi, *et al.* (1999) reported that they cloned and sequenced the *cpkA* gene encoding a second (α) subunit of archaeal chaperonin from *Pyrococcus kodakaraensis* KOD1. They also expressed the subunit protein in *E. coli*. Recombinant CpkA was investigated for chaperonin functions in comparison with CpkB (β subunit). The results indicated that both CpkA and CpkB efficiently decrease the amount of the insoluble form of CobQ in *E. coli*. Both CpkA and CpkB exhibited the same ATPase activity as other bacterial and eukaryal chaperonins. The ATPase-deficient mutant proteins CpkA-D95K and CpkB-D95K were obtained by changing conserved Asp95 to Lys. Effect of the mutation on the ATPase activity and CobQ solubilization was investigated. None of the mutants exhibited ATPase activity *in vitro*. However, they decreased the amount of the insoluble form of CobQ by coexpression as wild-type CpkA and CpkB did. These results suggested that both CpkA and CpkB could assist protein folding in *E. coli* without requiring energy from ATP hydrolysis (Izumi, *et al*, 1999).

The chaperonin complex from the halophilic archaeon, *Haloferax volcanii*, has eightfold symmetry. Kapatai, *et al* (2006) investigated if all three genes (*cct-1*, *cct-2* and *cct-3*) encoding group II chaperonin in *H. volcanii* are individually dispensable. They found out that one of either *cct1* or *cct2* must exist to allow

growth of the organism. CCT3 protein could not support growth on its own (Kapatai, *et al.*, 2006).

Prevention of thermal aggregation of the denatured protein by the group II chaperonin α from the aerobic hyperthermophilic crenarchaeon *Aeropyrum pernix* K1 (*Ap*cpnA) was examined by Jang, *et al.* (2007). The complete genome sequence of *Aeropyrum pernix* K1, revealed that this strain has two kinds of putative thermosome subunit genes (α and β). *Ap*cpnA alone is not adequate for chaperonin activity, but the chaperonin activity increases in the presence of manganese ion and ATP. *Ap*cpnA protects the aggregation-prone unfolded state of the denatured rhodanese from thermal aggregation. Binding of ATP is sufficient for *Ap*cpnA to exhibit the chaperonin function *in vitro*, but hydrolysis of ATP is not necessarily required. It is proposed that utilization of Mn^{2+} and ATP regardless of ATP hydrolysis may be one of peculiar properties of archaeal chaperonins (Jang, *et al*, 2007).

The group II chaperonin from the hyperthermophilic archaeum *Pyrococcus horikoshii* OT3 (PhCPN) and its functional cooperation with the cognate prefoldin were examined by Okochi, *et al.* (2005). They have expressed, purified, and characterized the group II chaperonin from *P. horikoshii* OT3. PhCPN existed as a homooligomer in a double-ring structure. It protected the citrate synthase of a porcine heart from thermal aggregation at 45°C. It also prevented thermal aggregation of isopropylmalate dehydrogenase (IPMDH) of a thermophilic bacterium, *Thermus thermophilus* HB8, at 90°C. PhCPN was shown to enhance the refolding of green fluorescent protein (GFP), which had been unfolded by low pH, in an ATP-dependent manner. Unexpectedly, functional cooperation between PhCPN and *Pyrococcus* prefoldin (PhPFD) in the refolding of GFP was not determined. Instead, cooperation between PhCPN and PhPFD was observed in the refolding of IPMDH which was unfolded with guanidine hydrochloride. Although PhCPN alone was not efficient in the refolding of IPMDH, the refolding efficiency was increased by the cooperation of PhCPN with PhPFD (Okochi, *et al*, 2005).

Emmerhoff, *et al.* (1998) reported that they cloned and sequenced the genes encoding two chaperonin subunits (Cpn-α and Cpn-β), from *Archaeoglobus fulgidus*, a sulfate-reducing hyperthermophilic archaeon. The chaperonin genes seem to be under heat shock regulation, as both proteins accumulate following temperature shift-up. This observation indicates a role of the chaperonin in thermoadaptation. Canonical Box A and Box B archaeal promoter sequences, as well as additional conserved putative signal sequences, are reported to be located upstream of the start codons. A phylogenetic analysis using all the available archaeal chaperonin sequences, proposes that the α and β subunits are the results of late gene duplications. These duplications might have taken place well after the establishment of the main archaeal evolutionary lines (Emmerhoff, *et al*, 1998).

Group I chaperonins are thought to be restricted to the cytosol of bacteria and to mitochondria and chloroplasts, whereas the group II chaperonins exist in the archaeal and eukaryotic cytosol. Klunker, *et al.* (2003) showed that members of the archaeal genus *Methanosarcina* co-express both the complete group I and group II chaperonin systems in their cytosol. These mesophilic archaea have gained between 20 and 35% of their genes by lateral gene transfer from bacteria. In *Methanosarcina mazei* Gö1, both chaperonins are similarly abundant and they are moderately induced under heat stress. The *M. mazei* GroEL/GroES proteins have the same structural characteristics as their bacterial counterparts. The thermosome contains three subunits, α, β, and γ. They assemble preferentially at a molar ratio of 2:1:1. As demonstrated *in vitro*, the assembly reaction is dependent on ATP/Mg^{2+} or ADP/Mg^{2+} and the regulatory role of the β subunit. The co-existence of both chaperonin systems in the same cellular compartment serves the *Methanosarcina* species as useful model systems in studying the differential substrate specificity of the group I and II chaperonins (Klunker, *et al*, 2003).

1.8 Heat-Shock Response in Archaea

How gene expression is effected by heat shock was verified at the mRNA level by Rittosa in 1962 and heat-shock proteins (HSPs) were identified by Tissieres, *et al.* (1974)12 years later (reviewed in Maeder, *et al.*, 2005).

Heat shock response is ubiquitous in both the *Eucarya* and *Bacteria* (Rohlin, *et al.*, 2005). Like other organisms, archaea respond to heat stress or other types of stresses by increasing the synthesis of a number of proteins originally termed heat-shock proteins (HSPs) and accumulating these proteins to higher steady state levels (Becker, *et al.*, 1994, Phipps, *et al.*, 1991). They stop synthesizing a variety of normal proteins and focus on synthesizing HSPs (Trent, 1996). The heat shock response provides assistance for the growth and survival of cells at temperatures higher than their normal growth temperatures (Phipps, *et al.*, 1991). HSPs participate in numerous cellular processes, including membrane transport and stability, protein folding, and cell signaling (Rohlin, *et al*, 2005). These proteins induced by enviromental stress include molecular chaperones, ATPases, proteases and DNA-repair proteins (Walter and Buchner, 2002 and Sőti and Csermely, 2003) (Table 1.1).

Table 1.1: Chaperones present in archaeal genomes (from Laksanalamai, *et al.*, 2004)

Protein	Hyperthermophiles	Thermophiles	Mesophiles
Clp homologues (Hsp100s)	No	No	Yes
Cdc48 and NSF homologues (AAA)	Yes	Yes	Yes
Hsp90	No	No	No
DnaK (Hsp70)	No*	Yes	Yes
DnaJ	No	Yes	Yes
GrpE	No	Yes	Yes
Chaperonin (Hsp60)	Yes[†]	Yes	Yes
Hsp33	No	No	No
sHsp	Yes	Yes	Yes
Prefoldin	Yes[§]	Yes	Yes
NAC	α-subunit only	α-subunit only	α-subunit only
Hsp10	No	No	Some[‖]
PAN	Some[¶]	Some[¶]	Yes

The increased survival of organisms at lethal temperatures after an exposure to near-lethal temperatures which lasts a short time is described as acquired thermotolerance. Two principles that may be developed from studies on acquired thermotolerance are that (i) HSPs do certainly play an important role in acquired thermotolerance and (ii) different species employ different methods (different combinations of HSPs and/or other macromolecules) in order to acquire thermotolerance (Trent, *et al*, 1994). Changes in internal pH, ionic strength, or the structure or composition of membranes are physiological changes that have been proposed to participate in acquired thermotolerance (Trent, *et al*, 1990).

Shockley, *et al*. (2003) performed a research on the heat shock response of the hyperthermophilic archaeon *Pyrococcus furiosus* by employing Northern analyses in conjunction with a targeted cDNA microarray. Cells were grown until mid-exponential phase at 90°C on sea salts-based medium (SSM) and temperature was elevated to 105°C for 1 h; control cultures were provided to continue growing at 90°C for the same period of time. The effects of thermal stress on growth and the induction of known and putative stress genes existing in *P. furiosus* was obvious. The genes which encode the major Hsp60-like chaperonin (thermosome) in *P. furiosus,* the Hsp20-like small heat shock protein and two other molecular chaperones (VAT) belonging to the CDC48/p97 branch of the AAA^{+} family were found to be strongly induced (Shockley, *et al.*, 2003).

Rohlin, *et al*. (2005) investigated the heat shock response of the hyperthermophilic archaeon *Archaeoglobus fulgidus* strain VC-16 by employing whole-genome microarrays. Heat shock treatment was performed by shifting temperature from 78°C to 89°C, and samples were removed at 5, 10, 15, 30 and 60 min after the temperature shift. They removed samples from each flask, before heat shock treatment, to use as the reference and control. In this study, using a whole-genome microarray, changes in mRNA levels for approximately 10% of the 2,410 genes when cells were elevated from 78°C to

89°C by 5 minutes were monitored. It has been clarified, with the development of gene arrays, that a great number of genes in addition to HSPs are affected by heat. Generally, the *A. fulgidus* genes that were strongly induced at 5 minutes stayed induced during the 60 minutes duration of the heat shock exposure. Of the 11 genes that were strongly induced at 5 minutes (5- to 10-fold), 5 were previously explained as heat shock genes. Two were not known to be induced by heat shock (AF1813 and AF1323), and four encode hypothetical proteins (AF1298, AF0172, AF1526, and AF1835). Of the remaining annotated HSPs in *A. fulgidus*, genes for the Hsp60s (thermosomes) and the genes for the small heat shock protein (sHSP20) (AF1296 and AF1971) were also monitored to be induced by heat. In *A. fulgidus* the authors observed that heat induced or repressed the expression of genes associated with energy production, amino acid metabolism, and lipid metabolism. This observation indicates the significance of metabolic adaptation to heat stress. It is known that membrane composition, especially the composition of isoprenoids in *Archaea*, may go through important changes during heat shock (Rohlin, *et al*, 2005).

1.9 Oxidative Stress

In aerobic organisms O_2 is reduced to H_2O_2 with generation of energy rich compounds, in the mitochondria. Also, small amounts of toxic forms of oxygen, are generated: O_2^- (superoxide), and OH^+ (hydroxyl radical). In the normal cell, toxic oxygen species do not accumulate because there are mechanisms for their removal. However, imbalances between the reactive oxygen species (ROS) (or poisonous forms of oxygen), production and ROS removal may result in ROS accumulation. Accumulation of ROS can bring about oxidative stress which damages proteins, lipids, and nucleic acids. ROS cause oxidative stress, by which some stress genes are activated. ROS also, repress many genes, as other stressors do (Morel and Barouki, 1999). Oxidative stress is one of the principal mechanisms of aging and cell death. Mitochondria produce energy from O_2 on one hand, they have the potential for producing

dangerous levels of toxic oxygen derivatives on the other hand. Therefore mitochondria, are the main players in the life of cell (Conway de Macario and Macario, 2000).

Free radicals possess an unpaired electron in an outer orbit. The energy produced by this unstable atomic state is released via reactions with neighbouring molecules, which causes molecular damage. There are various mechanisms available to the cell for coping with the effects of ROS. Antioxidants (*e.g.*, the lipidsoluble vitamins A and E, ascorbic acid, and glutathione), metals in storage and transport proteins (*e.g.,* transferrin, ferritin, and ceruloplasmin), enzymes that breakdown H_2O_2, and O_2^- (*e.g.,* catalase, glutathione peroxidase, and superoxide dismutase, SOD) are some examples for these mechanisms.

There are several SOD subfamilies in three phylogenetic domains which are classified by considering their metal cofactors, Cu/Zn, Fe, Mn or Ni. Fe, and Mn SODs exist in hyperthermophilic and halophilic archaea, but SODs in the halophilic species differ from other Fe and Mn enzymes known. Interestingly, Fe SODs have been discovered in methanogenic archaea which are strict anaerobes. It is interesting why these anaerobes, that are supposed to be evolved in ecosystems lacking oxygen, possess SODs. The physiological role of SODs in anaerobic organisms has been suggested to be the reduction of superoxide with generation of hydrogen peroxide, but this proposal remains to be proven (Conway de Macario and Macario, 2000).

Two archaeal peroxiredoxin from *A. pernix* and *P. horikoshii* which is a new family of thiol-specific anti-oxidant protein, have been characterized. They perform their protective role in cells by reducing and detoxifying H_2O_2. Recently, Limauro, *et al.* also investigated participation of the peroxiredoxin Bcp2 in oxidative stress in the hyperthermophilic aerobic archaeon *Sulfolobus solfataricus* by transcriptional analysis of RNA isolated from cultures which had been stressed with several oxidant agents (Limauro, *et al.*, 2006). Bcp2

was determined as a putative peroxiredoxin (Prx) in the genome database of *S. solfataricus*. A considerable increase in the *bcp2* transcript upon induction with H_2O_2 was observed. They cloned and expressed Bcp2 gene in *E. coli.* Bcp-2 is reported to be the first archaeal 1-Cysteine peroxiredoxin (1-Cys Prx) identified up to now (Limauro, *et al.*, 2006).

1.10 *Thermoplasma volcanium* as a Model Organism

The model organism in this study is a moderately thermophilic archaeon *Thermoplasma volcanium* which grows best at 60ºC and pH 2.0. Temperature range and pH range for growth of the organism are between 33ºC and 67ºC and between 1.0 and 4.0, respectively (Segerer, *et al.*, 1988). Archaeal membranes are comprised of ether-linked lipids bonded to glycerol, and hence differ considerably from bacterial membranes. Archaeal cell walls, like the eukaryotes, do not include peptidoglycan, once more differing them from bacteria. The *Thermoplasma* differ from the other Archaea to some extent: they do not possess cell wall, and their cell membranes include tetraether lipids with mannose and glucose subunits (Gaasterland, 1999). Two *Thermoplasma* species, i.e. *T. acidophilum* and *T. volcanium*, can grow under both aerobic and anaerobic conditions (Reysenbach, *et al.*, 2006). They can grow under anaerobic conditions if they are in contact with elemental sulfur particles as electron acceptors (Margulis, 1996). Recently, by sequencing the proteins from 2-D gels, proteins expressed in *T. volcanium* under two conditions were identified (Kawashima, *et al.*, 2005). *T. volcanium* is a heterotrophic archaeon which was isolated from submarine and continental solfataras at Vulcano Island, Italy, continental solfataras and a tropical swamp in Java and continental solfataras in Iceland and the Yellowstone National Park (Schäfer, *et al*., 1999 and Segerer *et al*., 1988). The complete genome of the organism is comprised of 1,584,799 bases and G-C content is 38% (Kawashima, *et al*, 2000).

1.11 Scope and Aim of This Study

In this study, we have aimed at cloning, expression, and sequencing of two genes, encoding α and β subunits of Hsp60 chaperonin of *Thermoplasma volcanium*.

Co-expression of the two subunit genes was achieved in *E.coli* by combining them in the same plasmid vector.

The chaperone activity of the recombinant *T. volcanium* (Tpv) Hsp60 chaperonin was discussed referring to its refolding capacity of chemically denatured citrate synthase from pig heart.

In silico, sequence, structural and comparative phylogenetic analyses of Tpv Hsp60 subunit proteins were performed by using multiple-sequence alignment, (ClustalW,1.83). BLAST and Conserved Domain Search Programs in NCBI Data Bases. Also, response of *T. volcanium* to heat shock and oxidative stress was studied by time-course monitoring the cell growth (OD_{540}) after heat-shock (65 to 78°C) or H_2O_2 exposure (0,008 mM to 0,05 Mm).

In addition, differential expressions of two Hsp60 genes under specified heat-shock and oxidative stress conditions were investigated by using Real-time PCR and cDNA band densitometry approaches.

CHAPTER 2

MATERIALS AND METHODS

2.1. Materials

2.1.1. Chemicals, Enzymes and Kits

Agarose (low melting point gel), ampicillin, calcium chloride ($CaCl_2$ $2H_2O$), ammonium sulphade ($(NH_4)_2SO_4$), ethidium bromide (Et-Br), glycerol, 3-morpholinopropanesulfonic acid, formamide, 5-5'-bis-nitrobenzoate (DTNB), oxaloacetate (OAA), co-enzyme A, citrate synthase, guanidinium chloride (GdmCl) and glycerol were purchased from Sigma Chemical Co., St. Louis, Missouri, USA.

α-D-glucose, yeast extract, potassium dihydrogen phosphate (KH_2PO_4), magnesium sulphate heptahydrate ($MgSO_4$), sodium chloride (NaCl), ethylenediaminetetraacetic acid (EDTA), chloroform, tryptone, isoamyl alcohol, magnesium chloride ($MgCl_2$), sodium acetate anhydrous, sodium hydroxide (NaOH), tris-base, bromophenol blue, ethylenedinitrilo tetraacetic acid disodium salt dihydrate (disodium EDTA), ß-mercaptaethanol and formaldehyde solution (min 37 %) were purchased from Merck; Darmstadt, Germany.

pUC18 vector, Taq DNA Polymerase, T4 DNA ligase and T4 DNA ligase buffer, restriction endonucleases *Bam*HI, *Eco*RI, *Hin*dIII, *Pst*I, *Sac*I, and their buffers Tango™ Yellow were from MBI Fermentas AB, Vilnius, Lithuania.

QIAGEN PCR Cloning Kit, Qiaprep Spin Miniprep Kit and RNeasy Mini Kit were purchased from QIAGEN Inc. Valencia, USA. Wizard® Plus SV

Minipreps DNA Purification System Kit was purchased from Promega Corporation, Madison, WI, USA. DNA Extraction Kit was from BIO 101.

Agar was purchased from Acumedia, Baltimore, USA. Agarose was from Applichem, Darmstadt, Germany. Hydrogen peroxide (H_2O_2) was purchased from Applichem, Darmstadt, Germany. Ethanol was from Reidel de Häen.

M-MULV reverse transcriptase, M-MULV buffer and SYBR Green Plus Kit were purchased from Roche Diagnostics, Switzerland.

2.1.2. Buffers and Solutions

Compositions of buffers and solutions used in the experiments are listed in Appendix A.

2.1.3. Plasmid Vectors, Molecular Size Markers

The maps of cloning vectors (pDrive and pUC18) are illustrated in the Appendix B. DNA molecular size markers (Lambda DNA/*EcoRI*+HindIII Marker and O'GeneRuler, Fermentas) is given in Appendix C.

2.2 Strain and Medium

2.2.1 Archaeal and Bacterial Strains

Thermophilic archaea *Thermoplasma volcanium* GSS1 (strain type 4299) purchased from DSM (Deutsche Summlung von Microorganismen und Zellkulturen, GmbH, Braunschweig, Germany) was used as source organism throughout the study.

Escherichia coli TG1 strain from our laboratory collection was employed as the recipient in transformation experiments.

2.2.2. Growth and Culture Conditions

T. volcanium was grown in Volcanium medium (pH 2.7) that was supplemented with glucose (Merck) and yeast extract (Oxoid) to final concentrations of 0,5 % and 0,1 %, respectively, at 60 °C (Robb, 1995). Cultures were renewed by weekly subculturing.

E. coli TG1 cells were grown on LB agar plates. Recombinant *E. coli* TG1 strains were cultured on LB agar plates. The cultures were incubated at 37°C overnight. The cultures were renewed by subculturing with 30 days intervals.

2.3. Gene Manipulation Methods

2.3.1. Genomic DNA Isolation from *Thermoplasma volcanium*

Genomic DNA of *Thermoplasma volcanium* following the method of Sutherland, *et al.*, (1990). For the experiments in this study, the stock preparation was used.

2.3.2. PCR Amplification of Gene Fragments of Hsp60 α subunit and Hsp60 β subunit

2.3.2.1. Design of PCR Amplification Primers

For amplification of the gene (1638 bp) encoding Hsp60 α subunit (TVN1128) , forward and reverse amplification primers (FP1 and RP1) were so designed that 216 bp upstream, 100 bp downstream sequences to be included into amplification product (Table 2.1). For amplification of the gene (1635 bp) encoding Hsp60 β subunit (TVN0507), forward and reverse amplification primers (FP2 and RP2) were designed so that 192 bp upstream and 94 bp downstream sequences to be included into amplification fragment. These gene fragments of Hsp60 α subunit and Hsp60 β genes were expected to be amplified from *T. volcanium* genomic DNA as 1939 bp and 1921 bp amplicons, respectively.

2.3.2.2. Amplification of Hsp60 α subunit and Hsp60 ß subunit Genes

T. volcanium genomic DNA was used as template DNA for PCR amplifications. Each PCR reaction mixture with a total volume of 100µl contained: lx PCR buffer [750 mM Tris-HCl pH 8.8 at 25°C, 200 mM $(NH4)_2SO_4$, 0.1 % Tween 20], 50-500 ng of the template DNA, 200 µM of each deoxyribonucleoside triphosphate (dNTP), 1.5 mM $MgCl_2$, 100 pmoles each of primers and 2.5 U of Taq DNA polymerase (MBI Fermentas AB, Vilnius, Lithuania). Total volumes of the reaction mixtures were completed to 100 µl by using sterile ddH_2O.

Table 2.1 : Primers designed for Hsp60 α subunit and Hsp60 β subunit genes of *Thermoplasma volcanium*.

PRIMER	SEQUENCE OF THE PRIMER
FP1 Forward Primer for Hsp60 α Subunit Gene	**5' GTCTCTGTCTTTTTCGTCCAC 3'**
RP1 Reverse Primer for Hsp60 α Subunit Gene	**5' CTAAGGTTAAATTCCATGCCCC 3'**
FP2 Forward Primer for Hsp60 β Subunit Gene	**5' GCGGCTATAGCATAGATGGCA TC 3'**
RP2 Reverse Primer for Hsp60 β Subunit Gene	**5' GTCAGCGTAGAGGTTATTCACGG 3'**

The samples were pre-incubated at 94°C for 5 minutes, before the addition of Taq DNA polymerase. The reactions were carried out with 30 cycles of amplifications in a thermal cycler (Techgene, Techne Inc. NJ. USA). The programme for each cycle was as follows: Denaturation at 94°C for 1min,

annealing at 60°C for 2 min, extension at 72°C for 3 min and final extension at 72°C for 10 min.

PCR products (15 µl samples) were observed by agarose gel electrophoresis (1% agarose gel). Lambda DNA/*EcoRI+HindIII* Marker (Fermentas) was used for length calibration.

2.3.3 Agarose Gel Electrophoresis

PCR amplicons, DNA fragments produced by restriction digestions, real-time PCR products and DNA samples following any manipulation were analyzed by agarose gel elecrophoresis on 1% (w/v) agarose gel (Applichem, Darmstadt, Germany) in 1X TAE buffer. Submarine agarose gel apparatus (Mini Sub™ DNA Cell, Bio Rad, Richmond, CA, U.S.A) was used in these experiments. DNA samples of 10-20 µl, mixed with 1/10 vol of 4x tracking dye, were loaded to gel which was supplemented by ethidium bromide (0,5 µg/ml). Electrophoresis was carried out at 70 volts (Fotodyne Power Supply, Foto/Force™ 300, USA).

After electrophoresis, the bands were visualized with a UV transilluminator (Vilber Lourmat TFP-M/WL, Marne La Vallee Cedex 1, France and Vilber Lourmat, CN 3000, EU) and gel photographs were taken using a gel imaging and documentation system (Vilber Lourmat Gel Imaging and Analysis System, Marne La Vallee Cedex 1, France). The molecular sizes of DNA fragments were determined by referring to *Eco*RI/*Hin*dIII cut Lambda DNA (MBI Fermentas AB, Vilnius, Lithuania) bands (Appendix C).

2.3.4 Cloning of PCR Amplified Hsp60 α subunit and Hsp60 β subunit Gene Fragments

PCR amplified Hsp60 α subunit and Hsp60 β subunit gene fragments were cloned using the QIAGEN PCR Cloning Kit (QIAGEN Inc., Valencia, USA)

following the manufacturer's instructions. The PCR fragment was ligated to the pDrive Cloning Vector, which was provided with the Kit. This kit uses the single A overhang at each end of PCR products generated using Taq and other nonproofreading DNA polymerases and supplies the vector in a linear form with a U overhang at each end, to hybridize them with high specifity. The diagram of the pDrive Cloning Vector and the restriction enzyme cut sites in multiple cloning site (MCS) are given in the Appendix B. The ligation reaction was carried out using T4 ligase (Fermentas, Vilnius, Lithuania) enzyme, as described in the manufacturer's manual.

2.3.4.1 Introduction of Recombinant Plasmids into Competent Cells

2.3.4.1.1 Preparation of Competent *E. coli* Cells

Competent *E.coli* TG1 cells were prepared according to the modified method of Chung, *et al,* (1989). The *E.coli* TG1 cells were grown in 20 ml of LB medium through vigorous shaking (Heidolph Unimax1010 Shaking Incubator, Heidolph Instruments GmbH, Kelheim, Germany). The growth was followed by measuring the optical absorbance of cell culture at 600 nm using the Hitachi U-2800 double beam spectrophotometer (Hitachi High Technologies Corporation, Tokyo, Japan). When the cells reached to early log phase (about 10^8 cell/ml), they were collected by centrifuging at 4000 rpm for 10 min. After discarding the supernatant, the pellet was dissolved in 1/10 TSS solution and distributed into eppendorf tubes as aliquots (100 µl). Competent cells were stored at -80°C until use (Thermo Forma -86ºC ULT Freezer, Thermo Electron Corp., USA).

2.3.4.1.2 Transformation

Competent *E. coli* TG1 cells were taken from -80°C deep freezer and thawed on ice to be used in transformation. A 1/10 (v/v) volume of ligation mixture was added and mixed by gentle tabbing. After a 30 min. incubation on ice, cells were transferred to glass tubes containing 0.16 mM glucose in LB. The

cells were incubated at 37°C for 1,5 hr with vigorous shaking at 230 rpm (Heidolph Unimax 1010 Shaking Incubator, Heidolph Instruments GmbH, Kelheim, Germany). Then, appropriate dilutions of competent cells were spread onto selective LB agar plates containing Ampicillin, IPTG and X-Gal and grown at 37°C for 24 hours.

2.3.5 Isolation of Plasmid DNA from Recombinant Colonies

Putative recombinant colonies were collected depending on blue/white colony selection. Cells from the white colonies were inoculated into 10 ml LB culture containing ampicillin and incubated at 37 °C overnight. Plasmid isolation was performed by using Wizard® Plus SV Minipreps DNA Purification System (Promega Corporation, Madison, WI, USA) according to the procedure provided by the manufacturer. The bacterial cells were pelleted by centrifugation at 4000 rpm for 15 min (IEC Clinical Centrifuge, Damon/IEC Division, U.S.A). The pellet was thoroughly resuspended in 250 µl Cell Resuspension Solution. The cells were lysed by adding 250 µl Cell Lysis Solution and proteins were digested by addition of 10 µl Alkaline Protease Solution. After incubation at room temperature for 4 min., then, 350 µl neutralization solution was added; tubes were inverted gently to mix the ingredients and incubated on ice for 1 min. The cell debris was pelleted by centrifuging at 13 000 rpm for 10 minutes in microfuge (Biofuge 15 Centrifuge, Heraeus Sepatech, Germany). The supernatant was transferred into Spin Column which was provided with kit and centrifuged at 13 000 rpm for 1 min to bind the DNA to the column. The bound DNA was washed twice with the Washing Solution and eluted with 100 µl Nuclease Free Water. After centrifuging at 13 000 rpm for 1 min., 100 µl of plasmid sample, at a concentration of 1.5 µg/ml, was obtained from the starting material. Approximately 15 µl of the sample was run on agarose gel to check the efficiency of purification and the remaining sample was stored at -20°C for further use.

2.3.6 Restriction Enzyme Digestion Analysis of Putative Recombinant Plasmids

Recombinant pDrive plasmid DNAs isolated from the transformed colonies were cut in several single and double digestion reactions by using *EcoRI*, *Bam*HI, *Hin*dIII, *Sac*I and *Pst*I restriction endonucleases (MBI Fermentas Co, Lithuania). Recombinant pUC18 plasmid DNAs isolated from the transformed colonies were cut in single digestion reactions by using *Eco*RI and *Kpn*I restriction endonucleases (MBI Fermentas Co, Lithuania). Digestions were carried out following the instructions of the manufacturer.

2.3.7 Sequence Determination of Hsp60 α subunit and Hsp60 β subunit Genes

The sequence of inserted PCR products containing Hsp60 α subunit and Hsp60 β subunit genes was determined by automated DNA sequencing by Microsynth, Switzerland using the reverse and forward PCR primers.

2.3.8 Construction of Co-Expression Vector

For co-expression of Hsp60 α subunit and Hsp60 β subunit genes, the cloned genes from recombinant plasmids were subcloned into pUC 18 vector, successively. Firstly, Hsp60 α subunit gene fragment was inserted in pUC18 vector, then Hsp60 β subunit gene fragment was ligated into the same vector, to upstream of Hsp60 α subunit gene, at *Kpn*I and *Hind*III sites. The diagram of pUC18 vector is given in Appendix B.

2.3.8.1 Isolation of DNA Fragments from Agarose Gel

BIO 101 GeneClean® Kit (QBioGene, Carlsbad, CA, USA) was used for the isolation of DNA fragments from the gel. The DNA fragments were run on the 1% low melting point agarose (Sigma-Ag414-105, Sigma Chemical Co., St. Louis, Missouri, USA) gel. Isolation was performed according to the recommendations of the manufacturer. The gel slices containing the fragments were removed, weighed and solubilized in NaI (at volume of x3 weight of gel slices). After 5 min. incubation at 55°C, glass milk was added into each mix. Mixtures were incubated for 10 min. at room temperature by intermitent mixing to obtain a complete gel dissolution. Desired DNA-bound silica resins were obtained by centrifugation at 13 000 rpm for 45 seconds (Eppendorf Mini Spin Centrifuge, Hamburg, Germany). Pellets were washed two times with BIO101 wash solution and then, the silica resin was air dried. Pellets were dissolved in minimal volumes sddH_2O and incubated at 55°C for 5 min**.** After centrifugation at 13 000 rpm for 60 secs at room temperature, supernatant was transferred into sterile eppendorf tube and kept at -20°C, until use.

2.3.8.2 Subcloning of Hsp60 α subunit Gene Fragment from pDrive α_4 into pUC18 Vector

Hsp60 α subunit gene fragments were excised from recombinant pDrive α_4 plasmid by digestion with *Eco*RI restriction endonuclease (MBI Fermentas, Lithuania). Also, the expression vector pUC18 (MBI Fermentas, Lithuania) was digested with the same enzymes. Gene and vector fragments were run on 1% low melting agarose gel (Sigma-Ag414-105, Sigma Chemical Co., St. Louis, Missouri, USA) by electrophoresis (Mini Sub™ DNA Cell, Bio Rad, Richmond, CA, U.S.A) in 1X TAE (Tris-acetate-EDTA) running buffer. Low melting agarose gel was supplemented with ethidium bromide at a final concentration of 1,25 μg/ml before it solidified. Hsp60 α subunit gene fragments were mixed with 1/10 volume of 4X tracking dye before loading the

completely solidified gel. Electrophoresis was carried out at 50 volts (Fotodyne Power Supply, Foto/Force™ 300, U.S.A).

The ligation of the Hsp60 α-subunit gene fragment extracted from the gel, to the pUC18 vector which was cut with *Eco*RI restriction enzyme was carried out using T4 DNA ligase under, standard conditions (MBI Fermentas, Lithuania). Ligation mixtures contained variable volumes (12-13 µl, depending on fragment concentration) of gene fragments and pUC18 vector (1-2 µl, depending on vector fragment concentration), 5 weiss unit/µl T4 DNA ligase (MBI Fermentas, Lithuania), 1/10 (v/v) of 10X T4 DNA ligase buffer (MBI Fermentas, Lithuania) and variable amounts of sterile double distilled water in order to complete the final volume to 20 µl. Ligation mixtures were incubated at +4ºC overnight.

Ligation samples were transferred into *E. coli* TG1 competent cells by transformation as described before. The recombinant colonies were selected on LB agar plates containing ampicillin, X-gal and IPTG, after incubation at 37ºC, 16 h.

2.3.8.3 Isolation of Plasmid DNA from Recombinant Colonies

Putative recombinant plasmids from white colonies were isolated as explained in section 2.3.7. Plasmid DNAs were cut with several restriction enzymes, to confirm the cloning of the insert.

2.3.8.4 Sub-cloning of Hsp60 β-subunit Gene Fragment from pDrive β_3 into pUC18 Vector

The recombinant pDrive plasmid (Qiagen) which carries Hsp60 β subunit gene and the recombinant pUC18 plasmid (Fermentas) which carry Hsp60 α subunit gene were both double digested with *Kpn*I and *Hin*dIII restriction endonucleases. These reaction mixes were run on low melting gels and isolated

from the gels as described in the Section 2.3.9. Ligation of Hsp60 β subunit gene fragment to recombinant pUC18 plasmid which carries Hsp60 α subunit gene was performed as described in the Section 2.3.9.3. *E.coli* TG1 cells were transformed with the putative recombinant plasmids as described before. Putative recombinant plasmid DNAs were isolated from colonies, and the insert was characterized by cutting with the restriction enzymes *EcoRI*, *Kpn*I and *Hin*dIII (MBI Fermentas Co, Lithuania).

2.4 Biochemical Methods

2.4.1 Preparation of Cell Free Extract

Overnight cultures (50 ml) of recombinant *E.coli* Puc1-α/β 19 cells were grown at 37ºC by vigorous shaking at 251 rpm (Heidolph Unimax 1010, Germany) and then, cells were harvested by centrifugation at 4000 g (Sigma 3K30 Centrifuge, Germany) for 20 min. at +4°C. Supernatant was discarded and the cell pellet was washed in 20 mM Tris, 5 mM $MgCl_2$ and 2 mM NaN_3 (pH:7,38) buffer solution. The pellet was dissolved in 1/5 volume of the wash Buffer solution. The cells were disrupted by sonication (Sonicator VC 100, Sonics and Materials, CT, U.S.A) for 1 minute durations with 30 second intervals. The cell free extract (CFE) was obtained by centrifugation (Sigma 3K30 Centrifuge, Germany) at 14000 g at 4 °C for 30 min. A 1.5 ml of each sample was heat treated at 65 ºC for 15 min in waterbath and then centrifuged (Micromax 230 RF Centrifuge, Thermo IEC, USA) at 14000 g at 4 °C for 30 min to remove denatured proteins. The supernatant called cell free extract, was stored at -20°C until use.

2.4.2 Determination of Chaperone Activity of Hsp60 Protein From *Thermoplasma volcanium*

The chaperone activity of recombinant Hsp60 protein from *T. volcanium* was determined by measuring the activity of denatured (with 6M guanidinium chloride) citrate synthase. This activity is expected to be regained as a result of refolding of the denatured citrate synthase by the help of chaperonin. The citrate synthase activity was determined as described by Srere *et al.* (1963). This method is based on measurement of the formation rate of 5-thio-2-nitrobenzoate (TNB) as a result of the reaction between 5-5'-dithio-bisnitrobenzoate (DTNB) and free –SH group of AcetylS-CoA formed after the citrate synthase reaction. Absorbance was measured at 412 nm using UV-visible double-beam spectrophotometer with a temperature controlled cell holder (Shimadzu 1601 UV/Visible Spectrophotometer, Shimadzu Analytical Co., Kyoto, Japan). Standard reaction mixture (1ml total volume) contained 0.2 mM OAA, 0.15 mM acetyl-CoA, 0.2 mM DTNB and appropriate volume of enzyme solution in 20 mM Tris-HCl-1mM EDTA buffer (pH: 7.0). For the assay, mixture was preincubated at 50°C for 5 min. and reaction was initiated by the addition of OAA and acetyl-CoA. Absorbance at 412 nm was measured continuously at 35°C.

2.5 Stress Response of *T. volcanium* Cells

2.5.1 Heat Shock Response of *T. volcanium* Cells

T. volcanium was grown in liquid Volcanium Medium (pH: 2.7) supplemented with glucose and yeast extract. The cells were grown until mid-exponential phase at 60°C and then, in three different experiments, the temperature was shifted to 65°C, 70°C, 75°C and 78°C for 2h for heat-shock. After heat shock incubation of the test culture was continued by decreasing the temperature to 60°C. Control cultures were allowed to continue growing at 60°C. The cell growth was monitored through OD measurement of the culture at 540 nm, in a

time dependent manner. Growth curves for control and heat-shocked cultures were obtained by plotting OD_{540} values versus time.

Control and heat-shocked culture samples were removed at regular time intervals to isolate total RNA to be used in the Real Time PCR experiments to study differential expressions of genes encoding Hsp60 α and Hsp60 β subunits as a response to heat shock. The complementary DNAs (cDNA) were synthesized by reverse transcription of the RNA template using MULV Reverse Transcriptase (Roche Diagnostics, Switzerland).

2.5.2 Oxidative Stress Response of *T. volcanium* Cells

T. volcanium was grown in Volcanium Medium (pH: 2.7) supplemented with glucose and yeast extract. The cells were grown until mid-exponential phase at 60°C and then, in five different experiments, H_2O_2 was added to obtain final concentrations of 0,05 mM, 0,008 mM, 0,02 mM, 0,01 mM and 0,03 mM in order to set oxidative stress conditions. Control cultures were grown in Volcanium medium without H_2O_2 supplementation under the same conditions. The cell growth was monitored through OD measurements of the cultures at 540 nm, in a time dependent manner. Growth curves for control and H_2O_2 stressed cultures were drawn by plotting OD_{540} values versus time.

Samples were removed from control and H_2O_2 stressed cultures at regular time intervals (during 1 h or 2h) and total RNA was isolated to be used as template in reverse transcription PCR experiments. The complementary DNAs (cDNA) were synthesized using MULV reverse transcriptase enzymes (Roche Diagnostics, Switzerland) and were used in Real-Time PCR experiments to study effect of oxidative stress on differential expressions of Hsp60 α and Hsp60 β subunit genes of *T. volcanium*.

2.5.3 RNA Isolation

RNA isolation from control and test cultures was performed by using Qiagen RNeasy Mini Kit (50) 74140 (QIAGEN Inc. Valencia, USA) following the manufacturer's instructions. After RNA isolation, OD values of diluted RNA samples were measured at 260 nm and 280 nm. by using UV-visible double-beam spectrophotometer (Shimadzu 1601 UV/Visible Spectrophotometer, Shimadzu Analytical Co., Kyoto, Japan) in order to calculate the purity of samples. The purified RNA samples were kept at -80°C deep freezer, until use.

2.5.4 Agarose Gel Electrophoresis of RNA Samples

RNA isolated from control and test cultures were observed by electrophoresis using 1,2 % FA (formaldehyde) agarose (Applichem, Darmstadt, Germany) gel. Submarine agarose gel apparatus (Mini Sub™ DNA Cell, Bio Rad, Richmond, CA, U.S.A) was used in these experiments. RNA samples of 10-15 µl, mixed with 1/4 vol of loading buffer, were loaded to gel containing ethidium bromide (10 mg/ml) and 37% formaldehyde. Electrophoresis was carried out at 70 volts (Fotodyne Power Supply, Foto/Force™ 300, USA).

After electrophoresis, the bands were visualized with a UV transilluminator (Vilber Lourmat TFP-M/WL, Marne La Vallee Cedex 1, France and Vilber Lourmat, CN 3000, EU) and gel photographs were taken using a gel imaging and documentation system (Vilber Lourmat Gel Imaging and Analysis System, Marne La Vallee Cedex 1, France).

2.5.5. Reverse Transcription PCR (RT-PCR)

2.5.5.1 Design of RT-PCR Amplification Primers

The forward and reverse amplification primers (FP3 and RP3) for synthesis and amplification of cDNAs of the genes encoding HSP60 α subunit (TVN1128) and HSP60 β subunit (TVN0507) are given in the Table 2.2. The cDNAs of HSP60 α subunit and HSP60 β genes were expected to be amplified as 399 bp and 581 bp amplicons, respectively, in RT PCR.

Table 2.2: Forward (FP) and Reverse Primers (RP) for reverse transcription of Hsp60 α subunit and Hsp60 β subunit specific mRNAs and for Real Time PCR experiments.

PRIMER	SEQUENCE OF THE PRIMER
HSP60 α / FP3	**5' GCA AAT TCT TAT GGG GTG GA 3'**
HSP60 α / RP3	**5' CTC CTT GGC CTG GCT GGT TAG 3'**
HSP60 β / FP4	**5' AAGTTGGAGACGACTACATGACC 3'**
HSP60 β / RP4	**5' GTC CTC ACC TGA TGA GGA CTC AG 3'**

2.5.5.2 **Synthesis of cDNAs of Hsp60 α subunit and Hsp60 β subunit Genes From Total RNA**

Total RNA isolated from heat-shocked, H_2O_2 treated or control *T. volcanium* cells were used as template for reverse transcription. For reverse transcription, PCR reaction mixture in a total volume of 20µl contained; 1,25 µM reverse primer, 0,8 µg RNA, 0,5 mM of each deoxyribonucleoside triphosphate (dNTP), 5 µl 5xM-MULV Buffer and 2.5 U of M-MULV reverse transcriptase (Roche). The PCR for cDNA synthesis was performed in the Techgene thermal cycler (Techgene, Techne Inc. NJ, USA). The conditions for PCR are; preheating at 70°C for 10 min, addition of MULV reverse transcriptase, amplification at 42°C for 1 h., heating at 94 °C for 3 min and hold at 4°C.

RT-PCR products (20 µl cDNA samples) were observed by agarose gel electrophoresis (1% agarose gel), using Lambda DNA/*EcoRI+HindIII* Marker (Fermentas) as size standart. Agarose gel electrophoresis was performed as described in Section 2.3.4.

2.5.6 Real-time PCR

Real-time PCR technique was used to analyze differential expression profiles of Hsp60 α and Hsp60 β subunit genes under oxidative stress and heat-shock conditions. The reactions were carried out in Lightcycler 1.5 (Roche Diagnostics, Roche Instrument Center AG, Switzerland). Figure 2.1 shows a schematic representation of the Lightcycler design. Its software provides quantitative and kinetic analysis of the real time amplification reactions. PCR experiments were performed by using the SYBR Green Plus kit (Roche Diagnostics, Switzerland) following the instruction of the Manual.

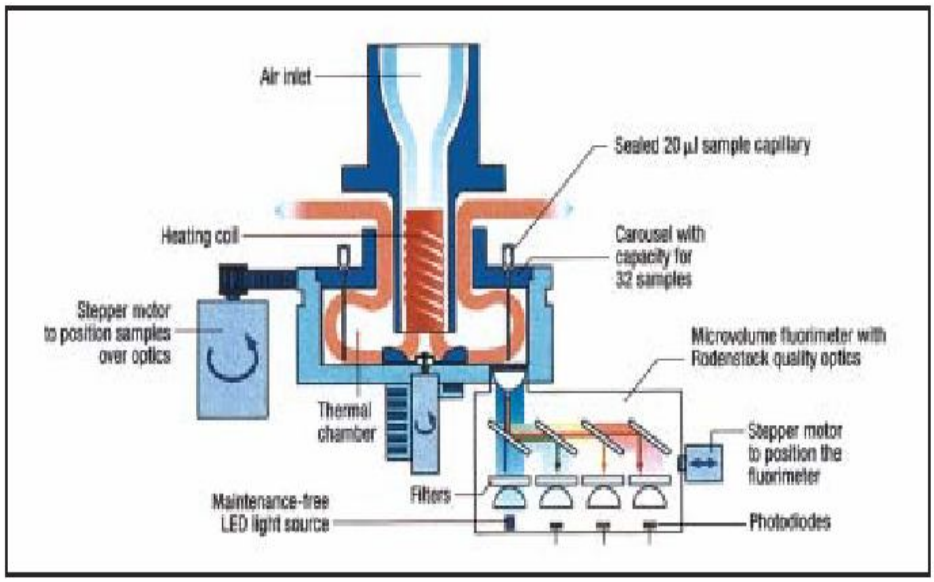

Figure 2.1: Schematic presentation of the LightCycler. Temperature cycling is achieved by alternating heated air provided by the heating coil and ambient air provided by the air inlet and fan. Composite plastic-glass capillary tubes provide a sealed vessel with a high surface-to-volume ratio, which, along with rapid air movement provided by the fan, allows rapid thermal exchange within the reaction fluid in the capillary tube. Fluorescence of polymerase chain reaction product is detected by photodiodes coupled with fluorimeters. Capillary tubes, positioned in a carousel, are periodically rotated over fluorimeters for fluorescent determinations. LED = light emitting diode (Uhl, *et al*, 2002).

The basic principles of the real-time assay with SYBR green dye are explained in the Figure 2.2.

Of the three fluorescence detection channels that measure fluorescence at 530, 640, and 710 nm, fluorescence detection channel which measures fluorescence at 530 nm. was employed since SYBR Green I and Fluorescein was detected at 530 nm . Products of reactions were visiualized by agarose gel electrophoresis as described in Section 2.3.4. The denisites of the DNA bands observed on the gels were analysed by using Scion Image programme.

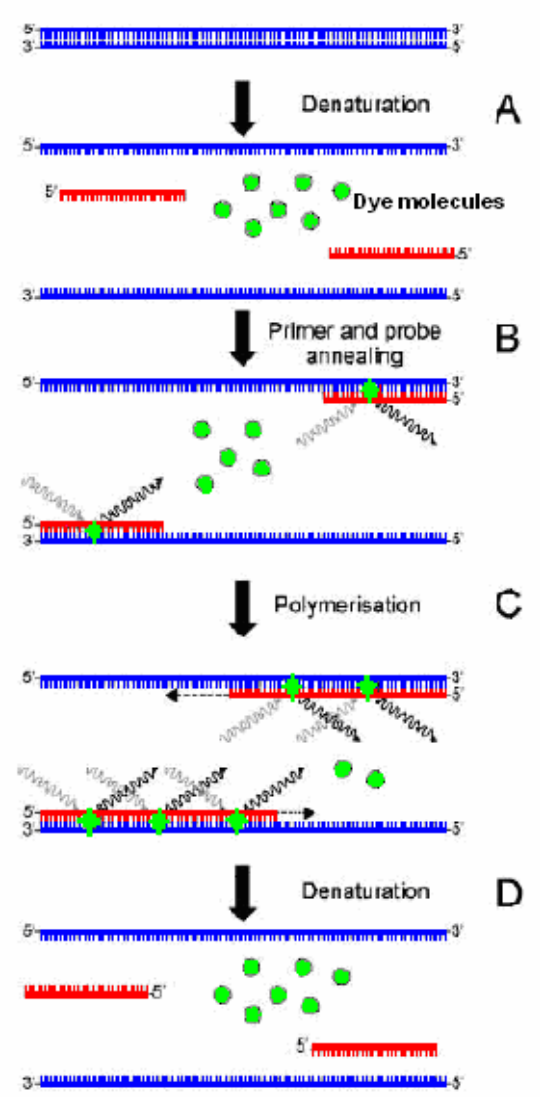

Figure 2.2: Schematic presentation of the lightcycler assay with SYBR green dye. (A) During denaturation, unbound SYBR Green I dye exhibits little fluorescence. (B) At the annealing temperature, a few dye molecules bind to the double-stranded primer/target, resulting in light emission upon excitation. (C) During the polymerisation step, more and more dye molecules bind to the newly synthesised DNA, and the increase in fluorescence can be monitored in real-time. (D) On denaturation, the dye molecules are released and the fluorescence signal returns to background (Bustin, 2000).

2.6 Gene and Protein Structure Analyses

Total genome sequence of *Thermoplasma volcanium* was derived from NCBI genomic database (National Center for Biotechnology Information, US).

Nucleotide and protein sequences of Hsp60 α subunit and Hsp60 β subunit were derived from the online-database of NCBI.

Restriction Mapper Version 3 was used to map the sites for restriction endonucleases in Hsp60 α subunit and Hsp60 β subunit nucleotide sequences.

To search for the highly conserved motifs in the proteins, COG (Clusters of orthologous group) and CDD (Conserved Domain Database) analyses were carried out by referring to the online-database of NCBI.

Multiple alignments of aminoacid sequences of Hsp60 α and β subunit proteins from various Archaea, Eukarya and Bacteria were performed by using ClustalW 1.83 program (European Bioinformatics Institute server). Also, phylograms based on ClustalW (1.83) multiple sequence alignment of Hsp60 α subunit and Hsp60 β subunit aminoacid sequences were derived to estimate their phylogenetic relationships.

CHAPTER 3

RESULTS

3.1 Gene Manipulation

3.1.1 PCR Amplifications of Hsp60 α Subunit and Hsp60 β Subunit Gene Fragments

PCRs were carried out by using the FP1/RP1 and FP2/RP2 primer sets which were given in Table 2.1 to amplify the gene fragments of Hsp60 α subunit and Hsp60 β subunit from genomic DNA of *T. volcanium*. Hsp60 α subunit gene (1638 bp) and Hsp60 β subunit gene (1635 bp) were amplified with additional flanking sequences, as unique 1939 bp and 1921 bp amplicons, respectively, as visualized by agarose gel electrophoresis (Figure 3.1).

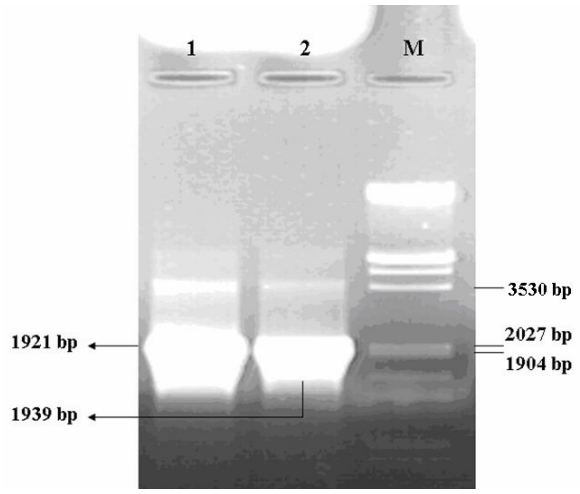

Figure 3.1: PCR amplifications of Hsp60 β subunit (Lane 1) and Hsp60 α subunit (Lane 2) gene fragments at annealing temperature of 60ºC. Marker: *EcoRI/HindIII* cut Lambda DNA (MBI Fermentas, Lithuania).

3.1.2. Cloning of PCR Amplified Gene Fragments

PCR amplicons obtained at 60ºC annealing temperatures by using *Taq* DNA polymerase were used for cloning of Hsp60 α subunit and Hsp60 β subunit genes, respectively. These amplicons were ligated by a UA-based hybridization into pDrive cloning vector which is supplied in linear form with the QIAGEN PCR Cloning Kit (QIAGEN Inc., Valencia, USA). The pDrive cloning vector not only provides the high performance through UA-based ligation, but also enables blue/white colony screening and it allows to select for ampicillin and kanamycin resistance. In addition, the vector carries several unique restriction endonuclease recognition sites within the multiple cloning site, providing alternative sites for excision and easy restriction analysis of cloned fragments.

The cloning schemes for the PCR amplified Hsp60 α subunit and Hsp60 β subunit gene fragments using pDrive cloning vector are shown in Figure 3.2 and Figure 3.3, respectively.

E. coli TG1 competent cells which were capable of efficient transformation (Transformation frequency: $8x10^6$ transformant/µg DNA) were used as recipients in transformation experiments.

For Hsp60 α gene cloning, transformation efficiency was same as the recombination frequency (i.e. $45x10^3$ transformant/µg DNA) since only white colonies grew on the selective agar medium.

Transformation efficiency was $18x10^3$ transformants/µg DNA and recombination frequency was $5x10^3$ recombinants/µg DNA for Hsp60 β gene cloning.

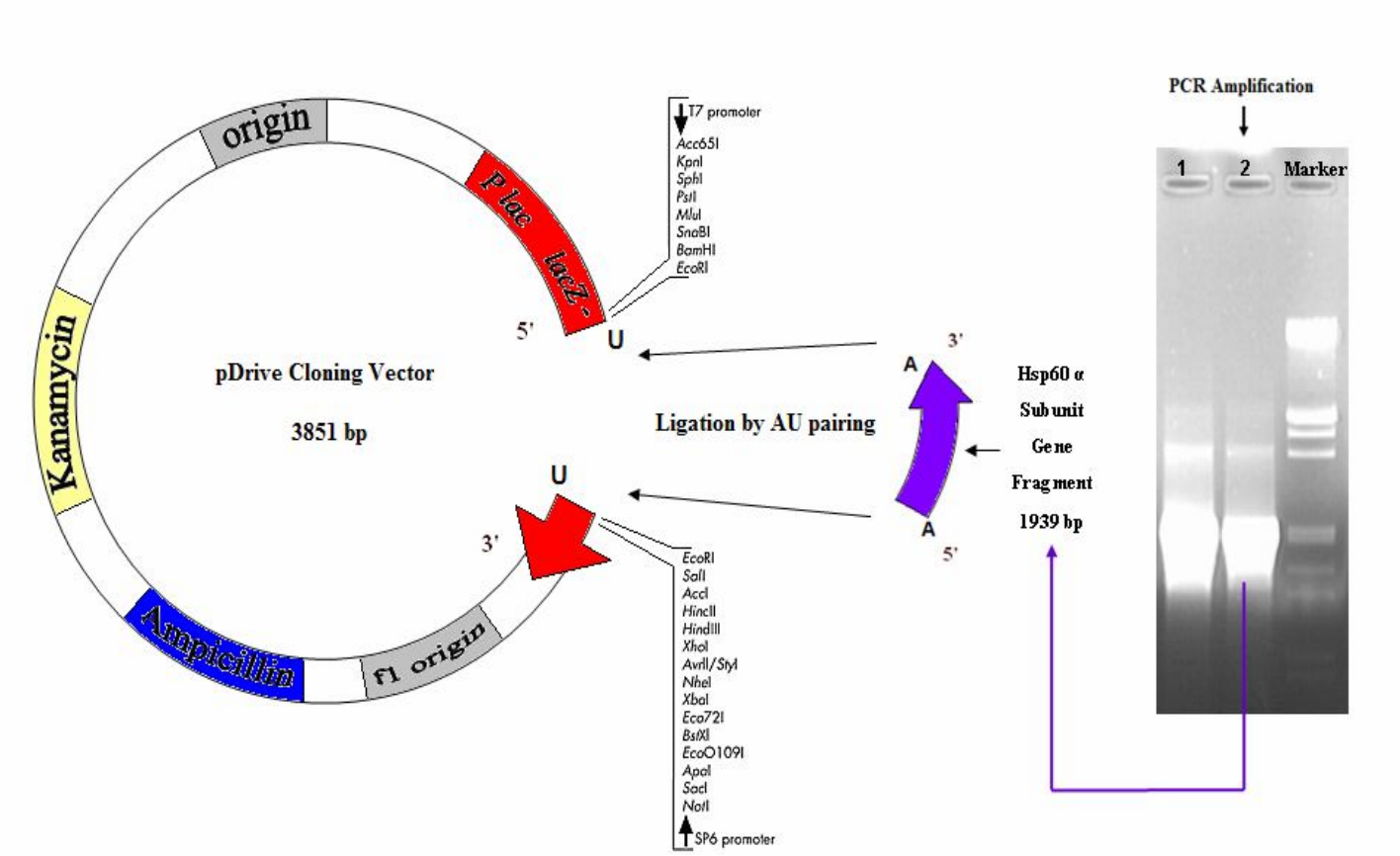

Figure 3.2 : Schematic representation of cloning of PCR amplified 1939 bp Hsp60 α subunit gene fragment by using pDrive cloning vector (QIAGEN Inc. Valencia, USA). Marker: Lamda DNA *EcoRI/HindIII* Cut Molecular Weight Marker (MBI Fermentas, AB, Vilnuis)

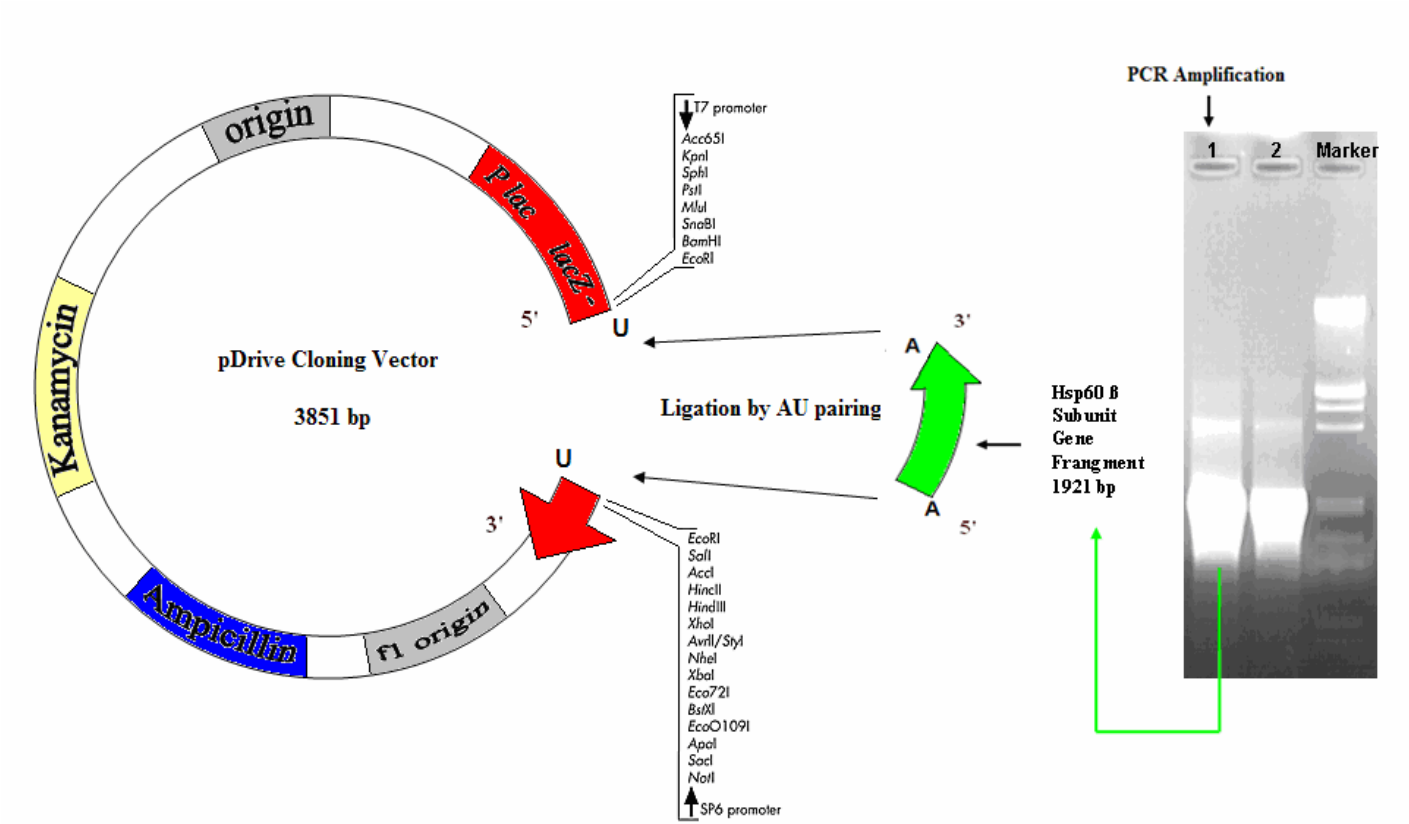

Figure 3.3: Schematic representation of cloning of PCR amplified 1921 bp Hsp60 β subunit gene fragment by using pDrive cloning vector (QIAGEN Inc. Valencia, USA). Marker: Lamda DNA *EcoRI/HindIII* Cut Molecular Weight Marker (MBI Fermentas, AB, Vilnuis)

A total of 134 and 15 putative recombinant (white-colored) colonies were obtained from Hsp60 α subunit and Hsp60 β subunit cloning experiments, respectively. Plasmid DNAs were isolated from 5 positive clones from each group (Figure 3.4).

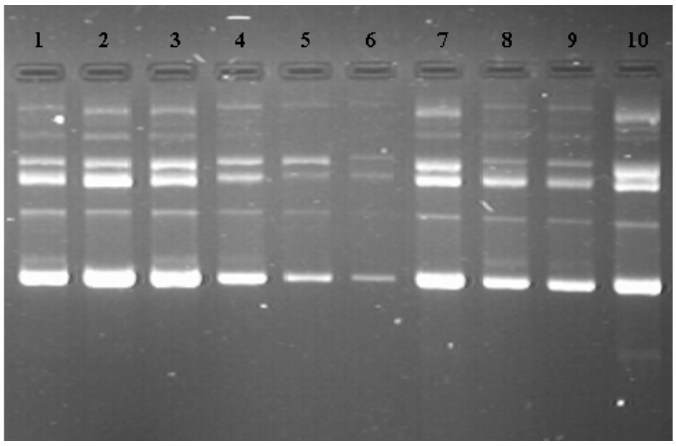

Figure 3.4: Plasmids isolated from putative recombinant colonies. Lane 1 to 5, pDrive plasmids (pDrive β_1 to β_5), expected to contain Hsp60 β subunit genes, Lane 6 to 10, pDrive plasmids (pDrive α_1 to α_5), expected to contain Hsp60 α subunit gene.

3.1.3. Characterization of Cloned DNA Fragments

3.1.3.1. Characterization of Putative Recombinant Plasmids with Hsp60 α and Hsp60 β Gene Fragments

Restriction maps of our genes of interest were constructed, based on their sequences which were available in the genomic databases, by using a software program (Restriction Mapper Version 3) as mentioned in the Materials and Methods, section 2.6 (Table 3.1). There are two *EcoRI* restriction sites in the MCS of the vector flanking the insertion site, and digestion with this enzyme could excise intact inserts. Digestions with *EcoRI* restriction endonuclease were performed to confirm the presence of Hsp60 α subunit gene fragment and

Table 3.1: Cut sites for a number of restriction enzymes that were determined by Restriction Mapper software program.

RESTRICTION MAPS				
Hsp60 α Subunit Gene (TVN1128) Fragment				
Non-Cutter Restriction Enzymes	*BamHI, EcoRI*, *HindIII, KpnI, SacI, SalI, SmaI, SphI*			
Cutter Restriction Enzymes	**Name**	**Sequence**	**Overhang**	**Cut Position**
	HaeII	RGCGCY	Three_prime	1828
	PstI	CTGCAG	Three_prime	40
	BsmI	GAATGC	Three_prime	1844
	AccI	GTMKAC	Five_prime	1326
	XbaI	TCTAGA	Five_prime	1647
	ApoI	RAATTY	Five_prime	47, 1423, 1853, 1901, 1926
Hsp60 β Subunit Gene (TVN0507) Fragment				
Non-Cutter Restriction Enzymes	*EcoRI, HindIII, KpnI, SalI, SmaI*			
Cutter Restriction Enzymes	**Name**	**Sequence**	**Overhang**	**Cut Position**
	PstI	CTGCAG	Three_prime	1431
	SphI	GCATGC	Three _prime	1892
	SacI	GAGCTC	Three _prime	644
	BsmI	GAATGC	Three _prime	878, 897
	AccI	GTMKAC	Five_prime	848
	BamHI	GGATCC	Five_prime	1219
	XbaI	TCTAGA	Five_prime	146

Hsp60 β gene fragment in putative recombinant plasmids which were isolated from white colonies. Since there is no restriction site for *EcoRI* in the Hsp60 α insert, the putative recombinant plasmids which were digested with *EcoRI* restriction enzyme yielded two fragments of 3851 bp and 1939 bp in length corresponding to linear pDrive cloning vector and insert, respectively. There is no restriction site for *EcoRI* in the Hsp60 β gene fragment, either. So, digestion with *EcoRI* restriction enzyme yielded two fragments of 3851 bp long and 1921 bp long, corresponding to linear pDrive cloning vector and Hsp60 β gene fragment, respectively.

All of the five pDrive α plasmids analysed by *EcoRI* digestion were recognized as true recombinants possibly including the Hsp60 α gene. Out of five pDrive β plasmids only pDrive β_4 appeared to contain Hsp60 β gene. Figures 3.5 and 3.6 show *EcoRI* digestion profiles of the putative recombinant plasmids.

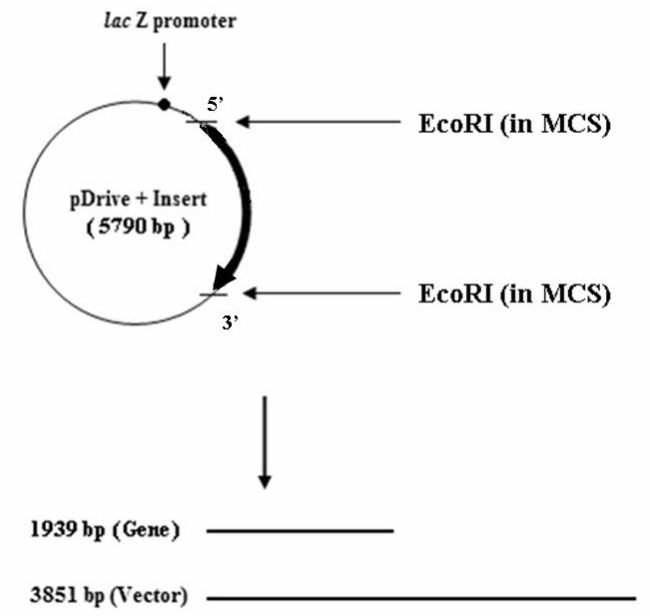

Figure 3.5: *EcoRI* digestion profile of a recombinant plasmid with Hsp 60 α subunit gene.

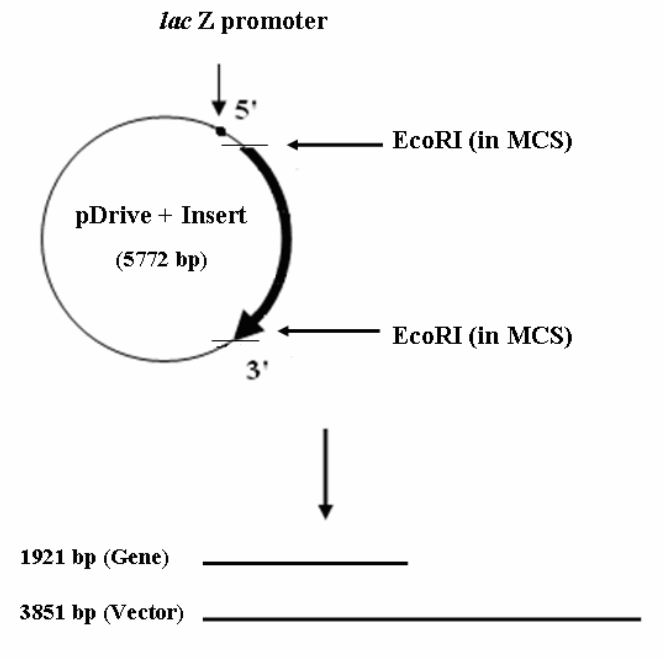

Figure 3.6: *EcoRI* digestion profile of a recombinant plasmid with Hsp60 β subunit gene.

3.1.3.2 Further Characterization of Recombinant Plasmids Containing Hsp60 α Subunit (TVN1128) Gene

Plasmids isolated from recombinant pDrive-α cells (Figure 3.4) were digested with *BamHI*, *HindIII*, *SacI* and *PstI* endonucleases for further structural characterization and restriction mapping.

There is single *BamHI* site in the MCS of the p-Drive-α recombinant vectors, and *BamHI* is a non-cutter for insert (Figure 3.8). *BamHI* digestion of pDrive α_1- α_5 plasmids yielded linearized recombinant plasmid DNA of 5790 bp (1939 bp insert + 3851 bp pDrive vector) as shown in the agarose gel picture (Figure 3.9).

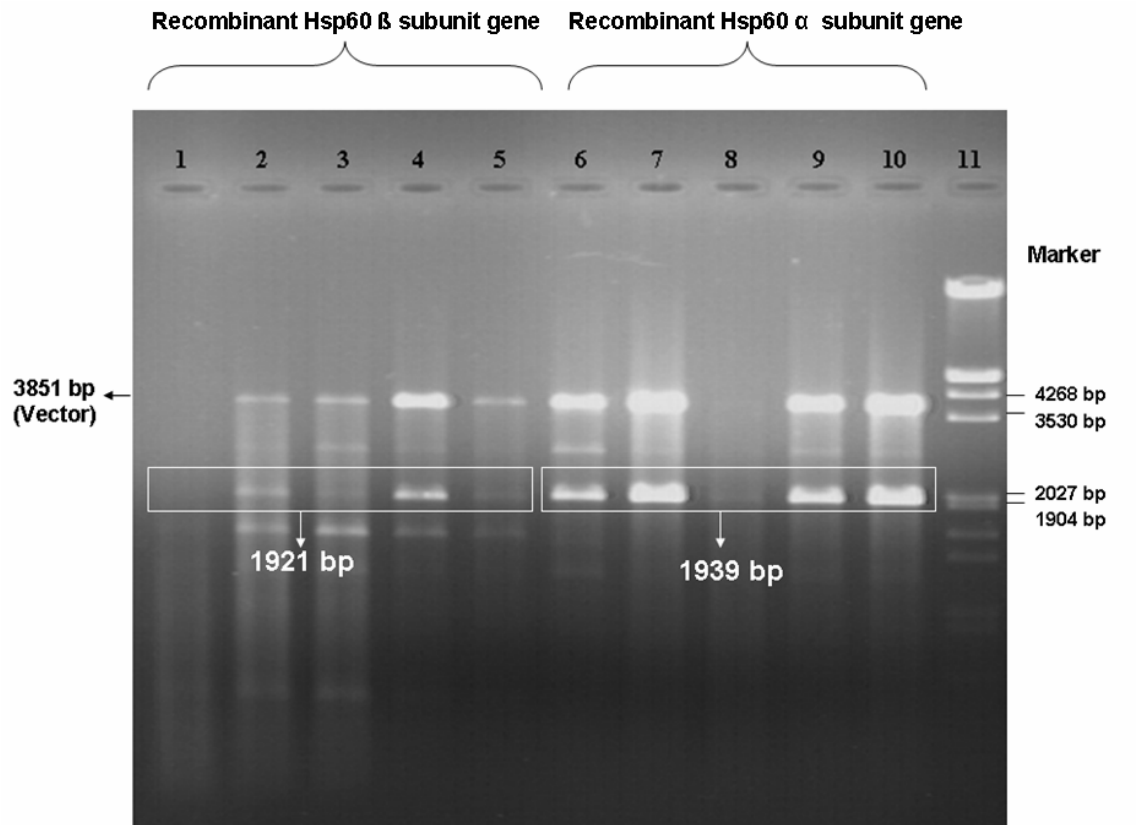

Figure 3.7: *EcoRI* digestion profiles of putative recombinant plasmids isolated from white colonies. Lane 1 to 5, pDrive plasmids, pDrive $ß_1$ to $ß_5$, presumed containing Hsp60 β subunit genes, Lane 6 to 10, pDrive plasmids, pDrive α_1 to α_5, expected to include Hsp60 α subunit genes. Lane 11 is the *EcoRI/HindIII* cut Lamda DNA molecular weight marker (MBI Fermentas, AB, Vilnius).

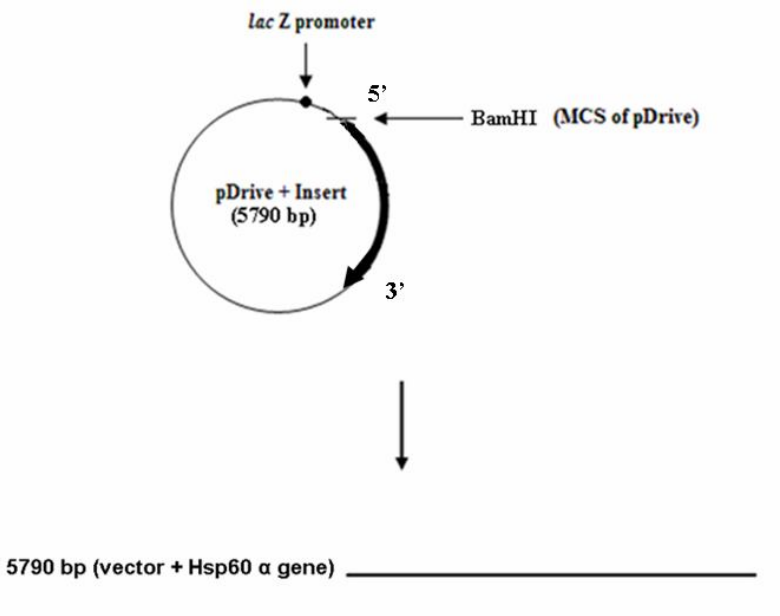

Figure 3.8: *BamHI* digestion profile of recombinant plasmid with Hsp60 α subunit gene (TVN1128).

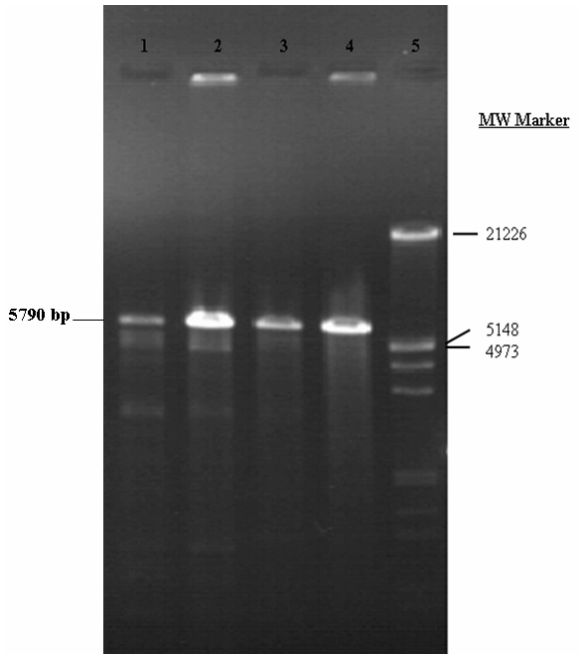

Figure 3.9: *BamHI* digestion profiles of pDrive-α1, pDrive-α2, pDrive-α4 and pDrive-α5 plasmids. *BamHI* digestion yielded 5790 bp linearized plasmid which includes TVN1128 gene (Lanes 1, 2, 3 and 4). Lane 5 *EcoRI*/*HindIII* cut Lambda DNA molecular weight marker (MBI Fermentas, AB, Vilnius).

BamHI has single cut site within MCS before 5' end of the gene, *HindIII* has single cut site within MCS after 3' end of the gene (Figure 3.10). Therefore, *BamHI* and *HindIII* digestion yielded 1939 bp long gene fragment and 3851 bp long linearized pDrive vector (Figure 3.11).

There is single *SacI* site in the MCS of the vector before 5' end of the gene. *SacI* is a non-cutter for the insert (Figure 3.12). *SacI* digestion of pDrive α_4 plasmid yielded linearized recombinant plasmid DNA of 5790 bp (1939 bp insert + 3851 bp pDrive vector) (Figure 3.13).

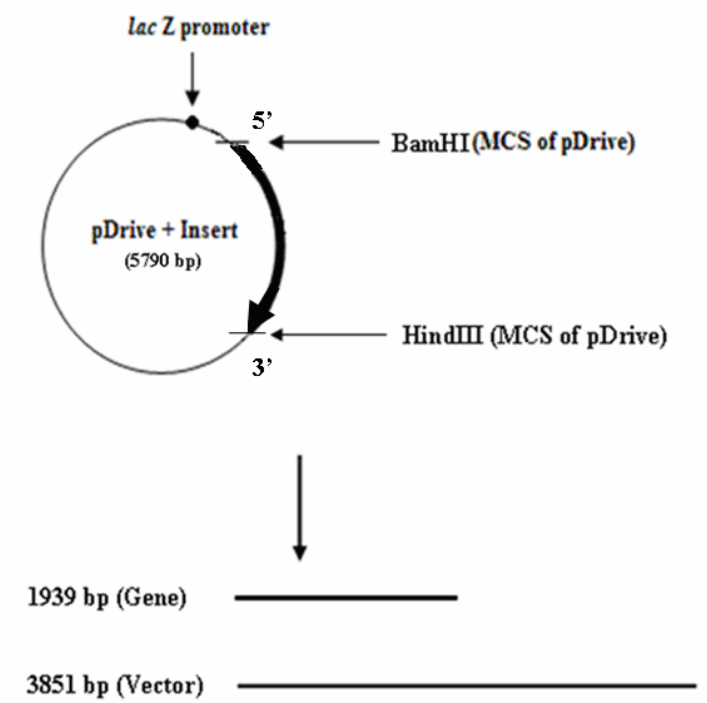

Figure 3.10: *BamHI* and *HindIII* double digestion profile of recombinant plasmid with Hsp60 α subunit gene (TVN1128).

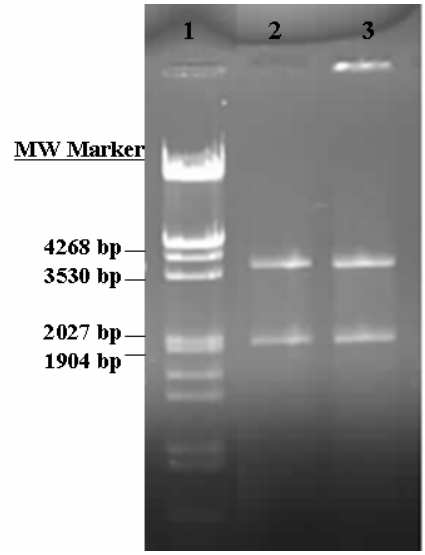

Figure 3.11: Restriction enzyme digestions of pDrive-α4 and pDrive-α5. Double digestion with *BamHI* and *HindIII* enzymes produced 1939 bp gene fragment and 3851 bp linearized pDrive vector (Lane 2 and 3). Lane 1 is the *EcoRI*/*HindIII* cut Lambda DNA molecular weight marker (MBI Fermentas, AB, Vilnius).

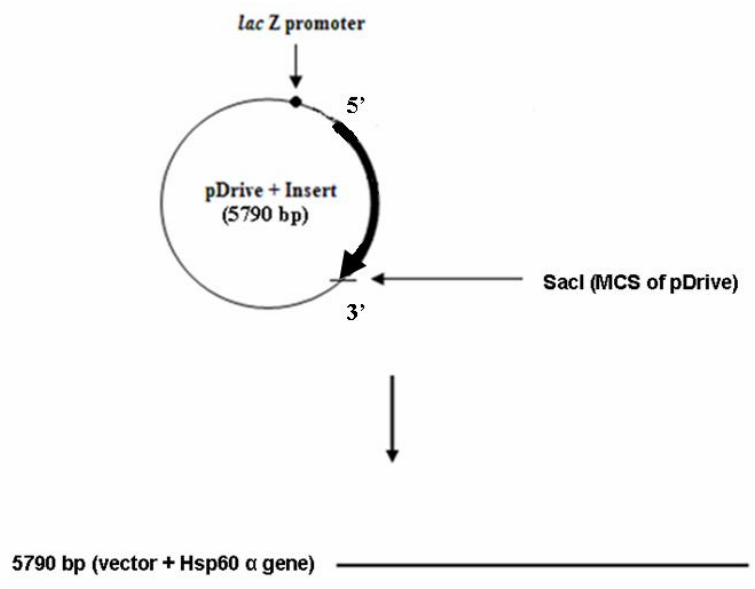

Figure 3.12: *SacI* digestion profile of recombinant plasmid construct with Hsp60 α subunit gene (TVN1128).

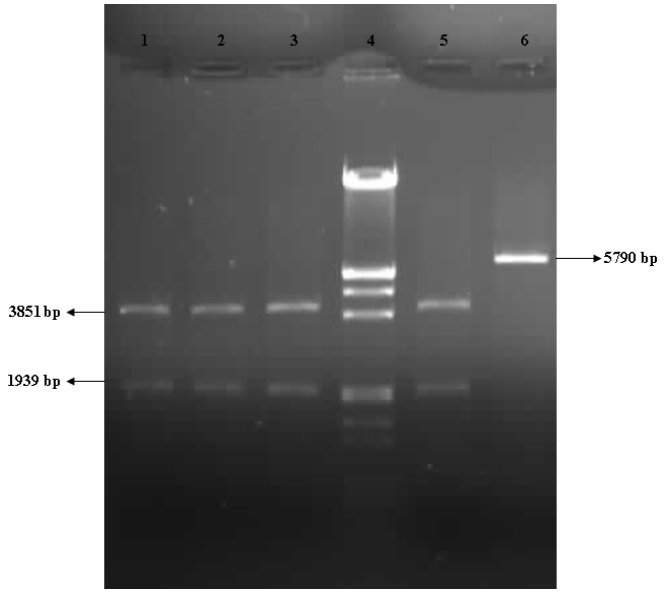

Figure 3.13: Restriction digestion profile of pDrive-α4. With *BamHI* and *SacI* enzymes the double digestion yielded 1939 bp long gene fragment and 3851 bp long linearized pDrive vector (Lanes 1, 2, 3 and 5). *SacI* digestion of pDrive-α4 yielded 5790 bp long linearized recombinant plasmid DNA (Lane 6). Lane 4 *EcoRI*/*HindIII* cut Lambda DNA molecular weight marker (MBI Fermentas, AB, Vilnius).

In pDrive-α_4 recombinant vector, *BamHI* has single cut site within MCS at 5' flanking sequence of the insert, *SacI* has single cut site within MCS at 3' flanking sequence of the insert. Both *BamHI* and *SacI* are non-cutter enzymes for insert (Figure 3.14). Therefore, *BamHI* and *SacI* digestion yielded a 1939 bp long gene fragment and a 3851 bp long linearized pDrive vector (Figure 3.13).

PstI has single cut site within MCS flanking the 5' end of the insert, and this enzyme cuts the gene at 40th bp from 5' end of the insert (Figure 3.15). *PstI* digestion yielded 40 bp and 5750 bp long fragments. (Figure 3.16)

Restriction digestion profiles obtained by gel electrophoresis was in good agreement with the restriction map derived by using Restriction Mapper

Version 3 program from the known sequence of Hsp60 α subunit gene (TVN1128) (Table 3.1). This result confirmed that we have successfully cloned Hsp60 α subunit gene of *T. volcanium* in pDrive cloning vector. Furthermore, based on the restriction enzyme analyses of the recombinant vectors (pDrive α_1, α_2, α_4 and α_5), it became clear that the gene fragment in pDrive-α4 was located in same direction as the *lac*Z promoter of the pDrive vector (Figure 3.17).

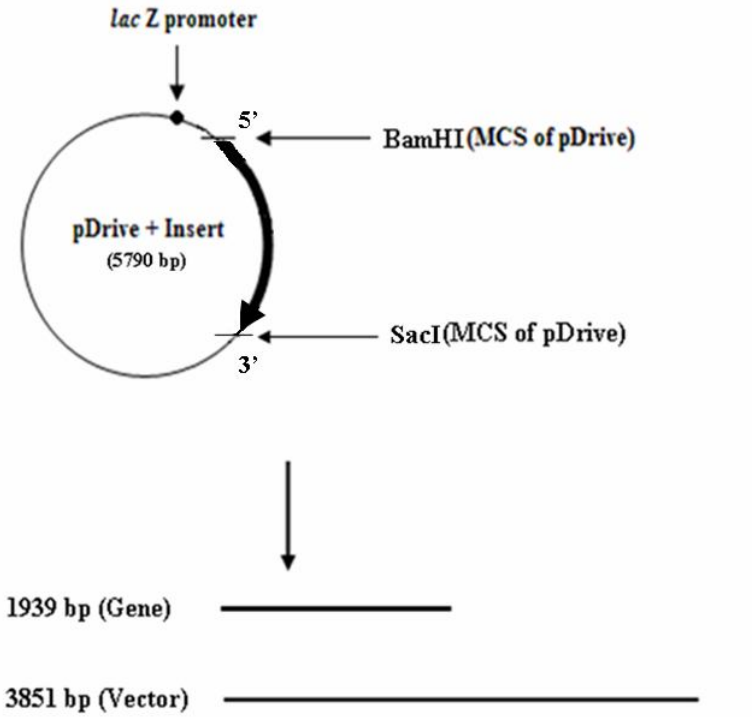

Figure 3.14: *BamHI* and *SacI* double digestion profile of recombinant plasmid with Hsp60 α subunit gene (TVN1128).

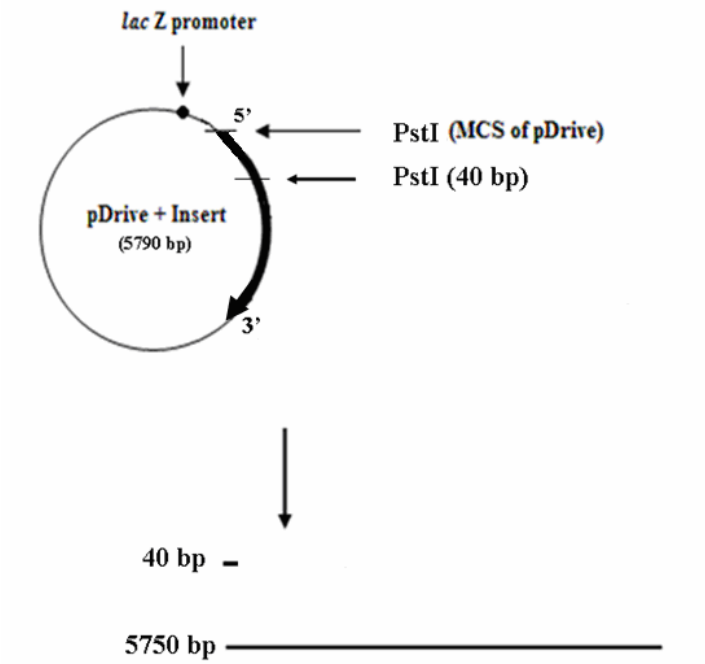

Figure 3.15: *PstI* digestion profile of the recombinant plasmid with Hsp60 α subunit gene (TVN1128).

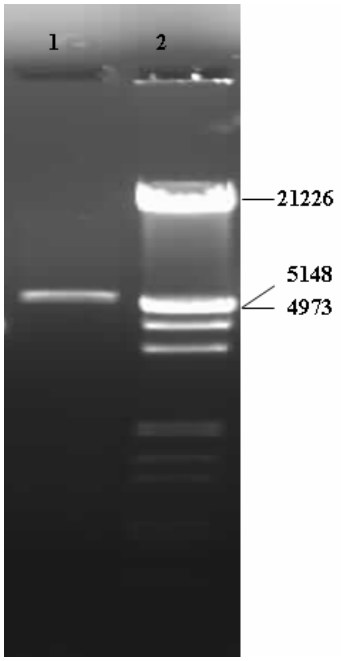

Figure 3.16: Restriction enzyme digestion of pDrive-α4. Digestion with *PstI* enzyme yielded 5750 bp and 40 bp fragments. 40 bp fragment is too small to be seen on gel (Lane 1). Lane 2 is the *EcoRI*/*HindIII* cut Lambda DNA molecular weight marker (MBI Fermentas, AB, Vilnius).

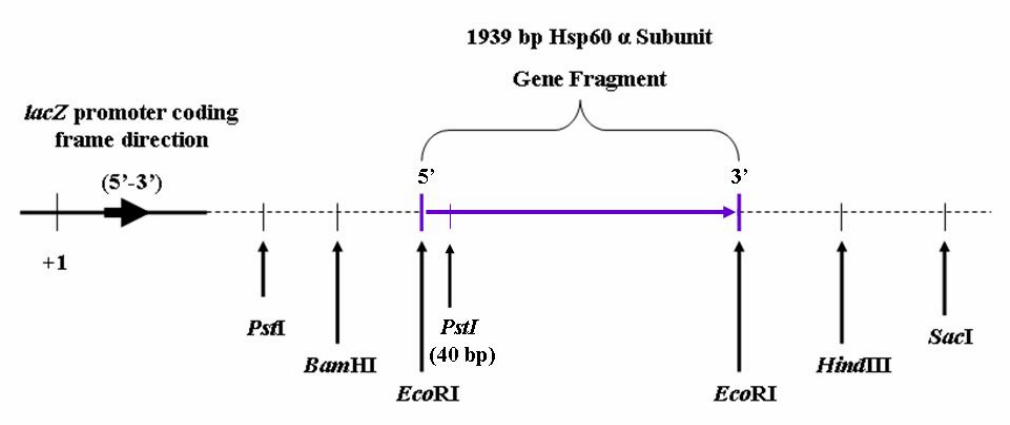

Figure 3.17: Schematic representation of the restriction map of recombinant plasmid (pDrive) which include Hsp60 α subunit gene.

3.1.3.3 Further Characterization of Recombinant Plasmids Containing Hsp60 β Subunit (TVN0507) Gene

Plasmids isolated from recombinant pDrive-β cells (Figure 3.4) were digested with *BamHI*, *HindIII* and *PstI* endonucleases for structural characterization and restriction mapping.

In the recombinant pDrive-β plasmids, *BamHI* has single cut site within MCS flanking the 5' end of the insert. The enzyme cuts the Hsp60 β subunit gene (TVN0507) at 1219th bp from 5' end. Therefore, if the gene is located in the same direction as the *lacZ* promoter, *BamHI* digestion yields 1219 bp long and 4553 bp long fragments (Figure 3.18). If the gene is located in the reverse direction with respect to *lacZ* promoter, *BamHI* digestion yields 702 bp long and 5070 bp long fragments (Figure 3.19).

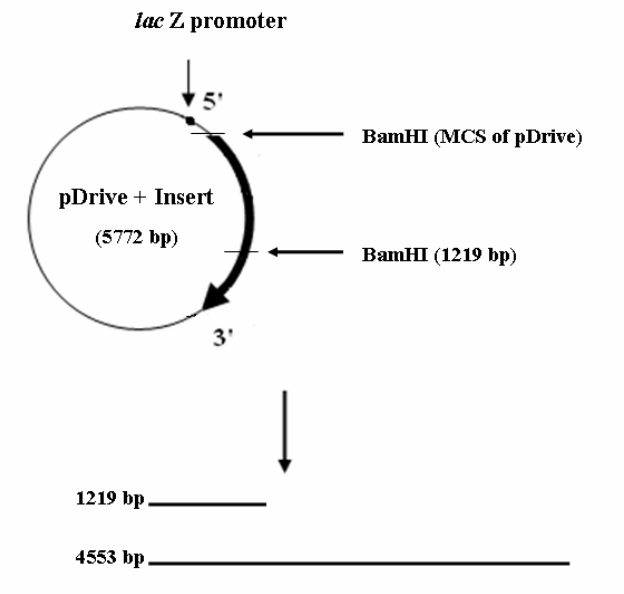

Figure 3.18: *BamHI* digestion profile of the recombinant plasmid with Hsp60 β subunit gene (TVN0507), if it is located in the same direction as the *lac*Z promoter.

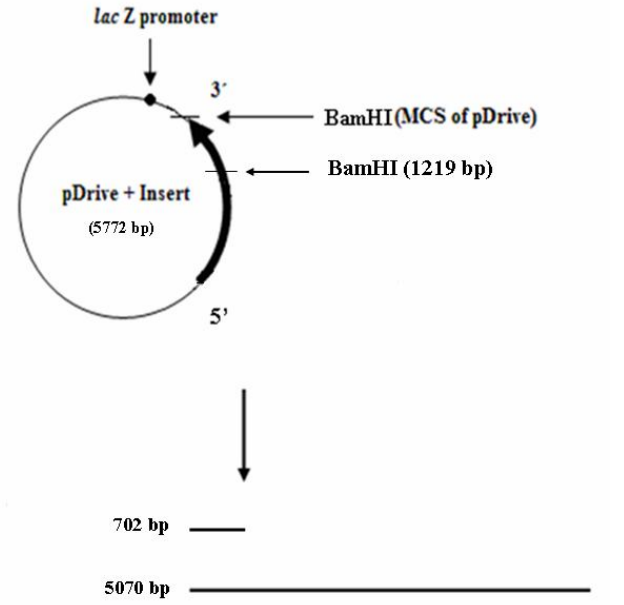

Figure 3.19: *Bam*HI digestion profile of recombinant plasmid construct with Hsp60 β subunit gene (TVN0507) if it is located in the reverse direction with respect to *lac*Z promoter.

Restriction digestion profiles on agarose gel revealed that pDrive-β3, pDrive-β4 and pDrive-β5 carry the gene in the same direction as *lac*Z promoter. But, pDrive-β2 carries the gene in the reverse direction relative to *lac*Z promoter (Figure 3.20).

There is a single *HindIII* site in the MCS of the recombinant vectors and *HindIII* is non-cutter for the gene (Figure 3.21). *HindIII* digestion of pDrive-β3, pDrive-β4 and pDrive-β5 yielded linearized recombinant plasmid DNA of 5772 bp long (1921 bp insert + 3851 bp pDrive vector) (Figure 3.22). *HindIII* digestion profiles of the pDrive-β plasmids, on agarose gel are shown in Figure 3.22.

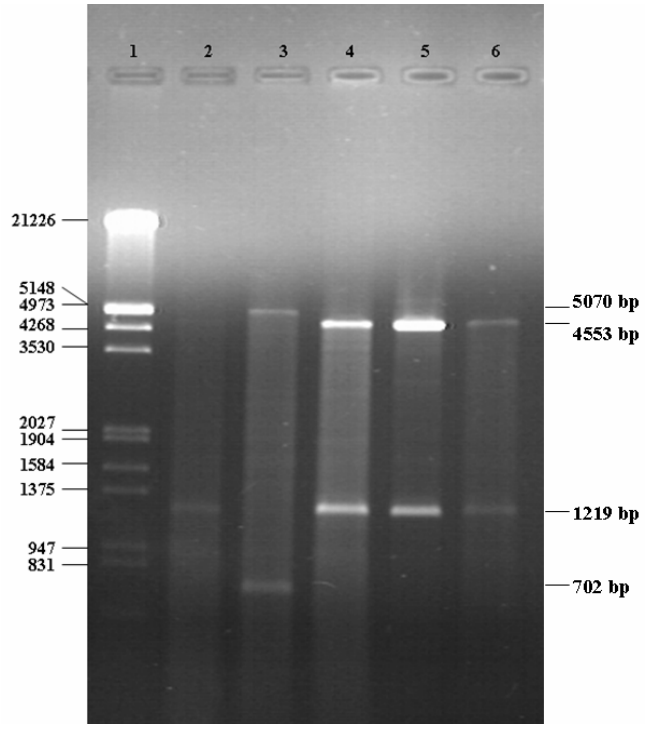

Figure 3.20: Restriction enzyme digestions of recombinant pDrive-β1, pDrive-β2, pDrive-β3, pDrive-β4 and pDrive-β5 plasmids. Digestion of pDrive-β2 with *Bam*HI enzyme yielded 5070 bp long and 702 bp long fragments (Lane 3). Digestions of pDrive-β3, β4 and β5 with *Bam*HI yielded 4553 bp long and 1219 bp long fragments (Lane 4,5, and 6). Lane 1 is the *EcoRI*/*HindIII* cut Lambda DNA molecular weight marker (MBI Fermentas, AB, Vilnius).

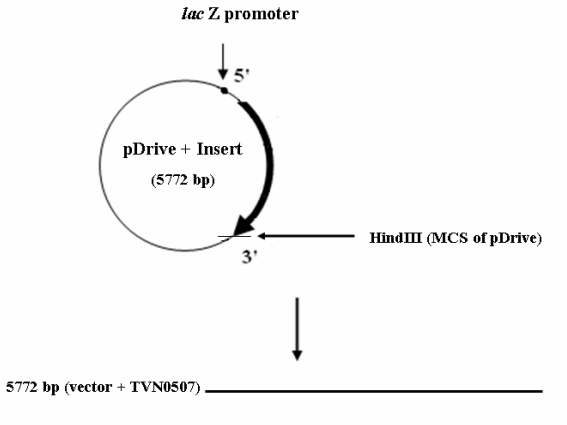

Figure 3.21: *HindIII* digestion profile of recombinant plasmid construct with Hsp60 β subunit gene (TVN0507).

EcoRI digestion profile of the recombinant pDrive-β plasmid with Hsp60 β subunit gene is given in Figure 3.22. Since *EcoRI* is a non-cutter enzyme for the Hsp60 β gene, digestion with this restriction enzyme released the insert (1921 bp) from vector DNA (3851 bp).

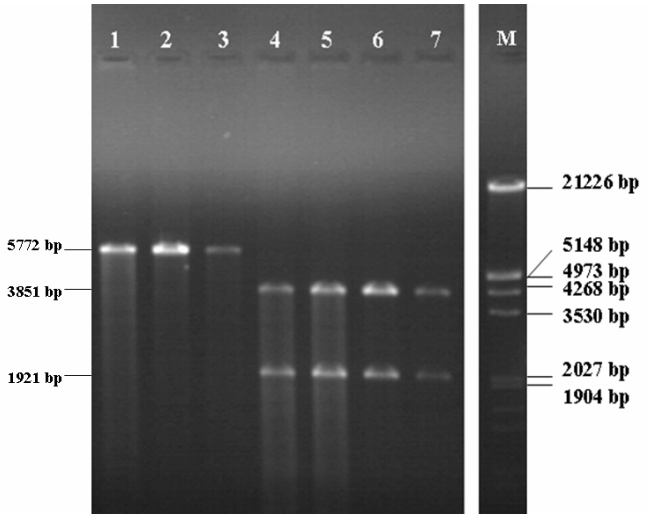

Figure 3.22: Restriction enzyme digestions of pDrive-β2, pDrive-β3, pDrive-β4, pDrive-β5. Digestion of pDrive-β3, β4 and β5 with *Hin*dIII enzyme yielded linearized recombinant plasmid DNA of 5772 bp (Lanes 1, 2 and 3). Digestions of pDrive-β2, β3, β4 and β5 with *Eco*RI yielded 3851 bp long and 1921 bp long fragments (Lanes 4,5, 6 and 7). **M** is the *EcoRI*/*HindIII* cut Lambda DNA molecular weight marker (MBI Fermentas, AB, Vilnius).

Additional plasmid DNAs were isolated from 7 more clones that are putative recombinant colonies (white-coloured) obtained from Hsp60 β cloning experiments (Figure 3.23). Among these, three plasmid DNAs were found to be in sufficient quantity as visualized on the gel. These three plasmids, pDrive β 6-8, were also characterized by restriction mapping.

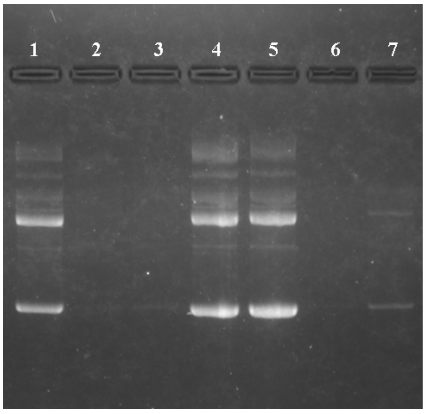

Figure 3.23: Plasmids isolated from putative recombinant colonies. Lane 1, colony β6; Lane 4, colony β7; Lane 5, colony β8 that were expected to be recombinants that include Hsp60 ß subunit gene (TVN0507). Enough amount of plasmid DNA can not be observed in lanes 2, 3, 6 and 7.

HindIII digestion of pDrive-β8 yielded linearized recombinant plasmid DNA of 5772 bp (1921 bp insert + 3851 bp pDrive vector) as depicted in Figure 3.21 and Figure 3.24.

In the pDrive β vectors, *BamHI* has single cut site within MCS flanking the 5' end of the insert, *HindIII* has single cut site within MCS flanking the 3' end of the insert. *BamHI* also cuts the gene at 1219th bp from 5' end (Figure 3.25). Therefore, *BamHI* and *HindIII* digestion yielded 702 bp long, 1219 bp long and 3851 bp long (pDrive vector) fragments (Figure 3.26).

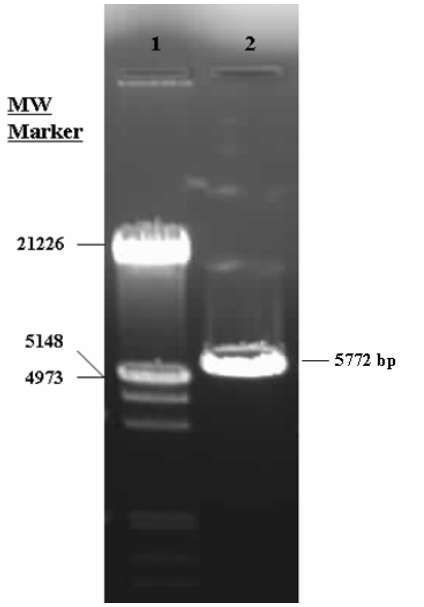

Figure 3.24: Restriction enzyme digestion of pDrive-β8. Digestion with *Hin*dIII enzyme yielded linearized recombinant plasmid DNA of 5772 bp (Lane 2). Lane 1 is the *EcoRI*/*HindIII* cut Lambda DNA molecular weight marker (MBI Fermentas, AB, Vilnius).

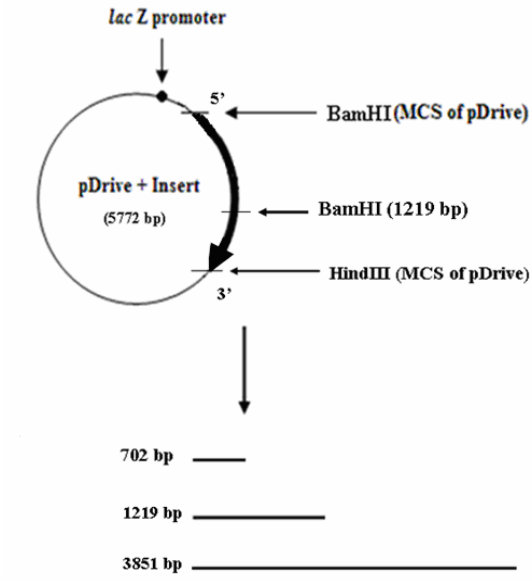

Figure 3.25: *Bam*HI and *Hin*dIII double digestion profile of recombinant plasmid construct with Hsp60 β subunit gene (TVN0507).

In the pDrive β vectors, *Pst*I has single cut site within MCS flanking the 5' end of the insert and it cuts the gene at 1431th bp from 5' end of the insert (Figure 3.27). Therefore, *Pst*I digestion yielded 1431 bp long and 4341 bp long fragments (Figure 3.28).

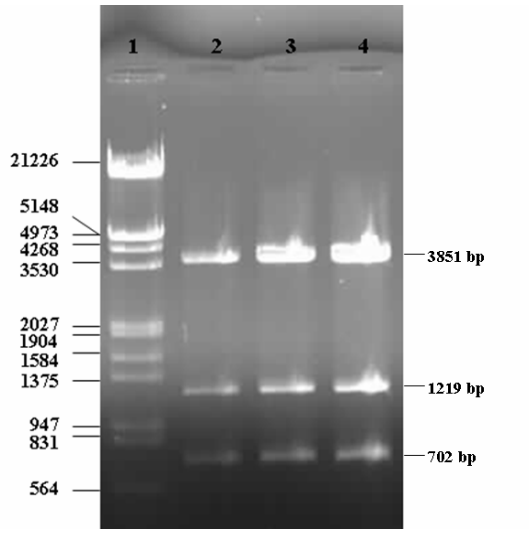

Figure 3.26: Restriction enzyme digestion of pDrive-β6, pDrive-β7 and pDrive-β8. Double digestion with *Hin*dIII and *Bam*HI enzymes yielded 702 bp long, 1219 bp long and 3851 bp long fragments (Lane 2, 3 and 4). Lane 1 is the *EcoRI*/*HindIII* cut Lambda DNA molecular weight marker (MBI Fermentas, AB, Vilnius).

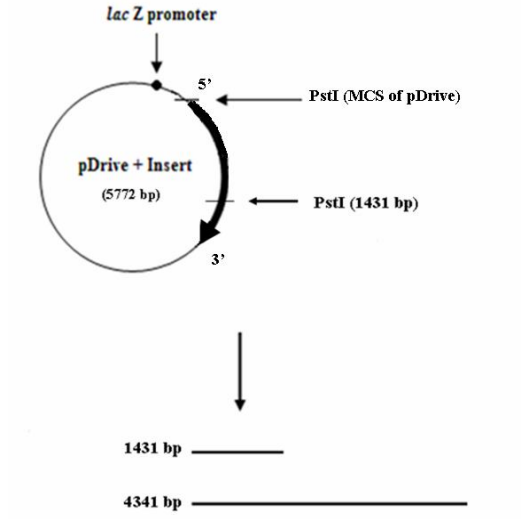

Figure 3.27: *PstI* digestion profile of recombinant plasmid with Hsp60 β subunit gene (TVN0507).

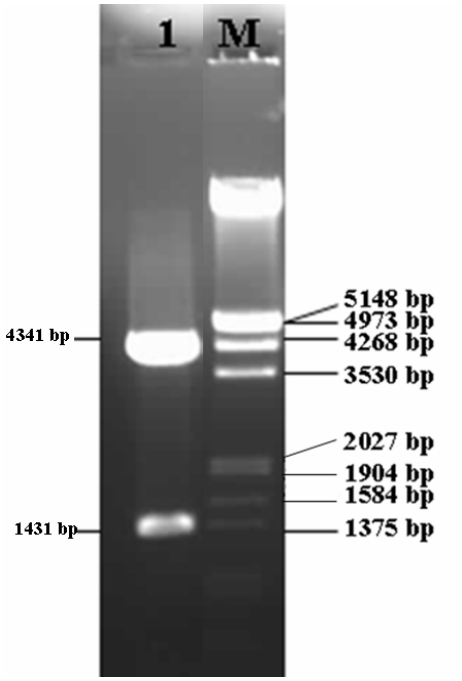

Figure 3.28: Restriction enzyme digestion of pDrive-β8. Digestion with *Pst*I enzyme produced 1431 bp long and 4341 bp long fragments (Lane 1). M: *EcoRI*/*HindIII* cut Lambda DNA molecular weight marker (MBI Fermentas, AB, Vilnius).

The restriction digestion profiles of the pDrive β plasmids were in good agreement with the restriction map derived by using Restriction Mapper Version 3 program from the known sequence of Hsp60 β subunit gene (TVN0507) (Table 3.1). This result confirmed that we have successfully cloned Hsp60 β subunit gene of *T. volcanium* in pDrive cloning vector. Furthermore, based on the restriction enzyme analyses of the recombinant vector, in the recombinant clone pDrive β2 the gene fragment was located in reverse and positioned in the recombinant clones pDrive β3, β4, β5 and β8 the gene cloned was in same direction as the *lac*Z promoter of the pDrive vector (Figures 3.18, 3.19 and 3.27). pDrive β6 and β7 plasmids were also determined as recombinant vectors (Figure 3.29).

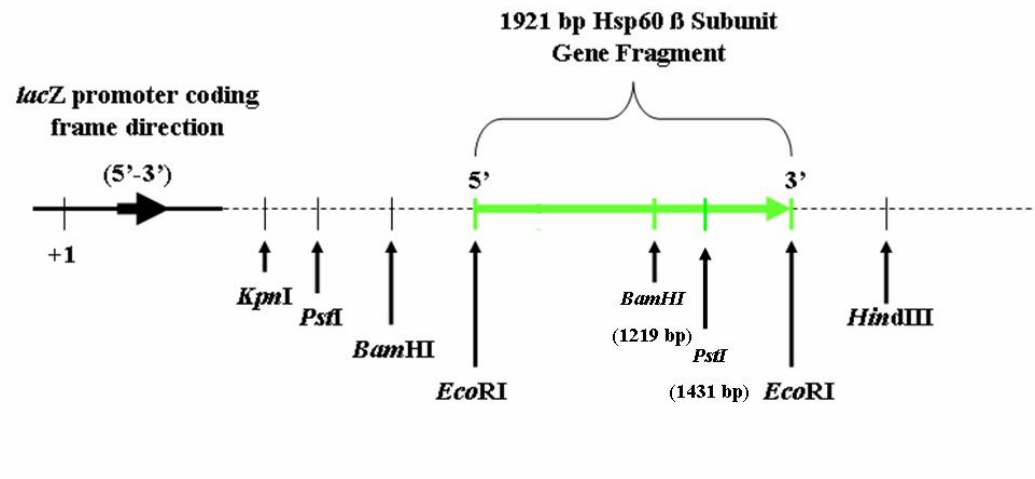

Figure 3.29: Schematic representation of the restriction map of recombinant pDrive ß plasmid which include Hsp60 β subunit gene.

3.1.4 Sequence Determination of Hsp60 α Subunit and Hsp60 β Subunit Genes

The sequence of inserted PCR products containing Hsp60 α subunit and Hsp60 β subunit genes were determined as described in 2.3.7 Section. Determined sequences are given in Figures 3.30 and 3.31.

3.1.5 Cloning of Hsp60 α and Hsp60 β Gene Fragments in pUC18 Vector For Co-expression

The Hsp60 α and Hsp60 β gene fragments obtained by digestion of the recombinant plasmids with restriction enzymes were ligated to pUC 18 cloning vector in succession. The pUC18 cloning vector provides blue/white colony screening. It also allows selection for ampicillin resistance. The vector also carries several unique restriction endonuclease recognition sites around the cloning site, providing easy cloning and restriction analysis of recombinant plasmids.

```
        taaaatttaactgtaaattacttactataacttacaggttttaggacgtga
aataagctaattttagtacagcccattttcgtaatatatactgtaatttttataaactcc
ttaattagtaaagtttatattgaagaacatatttatccggttagctaggtgatcagaaat
atgatgactggacaggttccaattctagttcttaaagaaggtacgcagagggaacagggc
 M  M  T  G  Q  V  P  I  L  V  L  K  E  G  T  Q  R  E  Q  G
aaaaacgcacagagaaacaatattgaggccgccaaggccattgcagatgctgtgaggact
 K  N  A  Q  R  N  N  I  E  A  A  K  A  I  A  D  A  V  R  T
acactgggcccgaagggcatggataagatgctggtagattcaataggggatataatcatc
 T  L  G  P  K  G  M  D  K  M  L  V  D  S  I  G  D  I  I  I
tcaaacgatggtgctacaattctaaaggagatggatgttgagcatcccacagcaaagatg
 S  N  D  G  A  T  I  L  K  E  M  D  V  E  H  P  T  A  K  M
atcgttgaagtttctaaggcacaggataccgccgtaggagatggaacaaccactgcggtc
 I  V  E  V  S  K  A  Q  D  T  A  V  G  D  G  T  T  T  A  V
gtgctctcaggagagcttctaaagcaagctgaaaccctcctggaccagggcgtgcatcca
 V  L  S  G  E  L  L  K  Q  A  E  T  L  L  D  Q  G  V  H  P
acagttatatccaacggatacagacttgcagtaaatgaggccaggaagattatagatgaa
 T  V  I  S  N  G  Y  R  L  A  V  N  E  A  R  K  I  I  D  E
atatctgtaaaatcgaccgatgatgaaacccttaggaaaatagctttgactgccctctca
 I  S  V  K  S  T  D  D  E  T  L  R  K  I  A  L  T  A  L  S
ggaaagaacaccgggctctccaatacattcctagcggatctggtagtaaaagcagttaac
 G  K  N  T  G  L  S  N  T  F  L  A  D  L  V  V  K  A  V  N
gctgtagccgaagagagggacggaaagataatagttgataccgccaatataaaggtagat
 A  V  A  E  E  R  D  G  K  I  I  V  D  T  A  N  I  K  V  D
aagaagagcggaggcagcatcaacgacactcagttcataagcggcatagtagttgacaag
 K  K  S  G  G  S  I  N  D  T  Q  F  I  S  G  I  V  V  D  K
gaaaaagtacattctaagatgccagatgtcgtcaaggatgcaaaaatagcgttgatagac
 E  K  V  H  S  K  M  P  D  V  V  K  D  A  K  I  A  L  I  D
tctgctctggaaataaagaagactgaaatagaagcaaaagtccagatatcagatccaagc
 S  A  L  E  I  K  K  T  E  I  E  A  K  V  Q  I  S  D  P  S
aaaatacaagacttcttgaaccaggaaactagcaccttcaaagagatggtagaaaagatc
 K  I  Q  D  F  L  N  Q  E  T  S  T  F  K  E  M  V  E  K  I
aagaagagcggagctaacgttgtcctatgccagaaaggtatcgatgatgtagcccagcac
 K  K  S  G  A  N  V  V  L  C  Q  K  G  I  D  D  V  A  Q  H
taccttgcaaaggaaggcatatacgcagtacgcagggtaaagaagagcgatatggagaaa
 Y  L  A  K  E  G  I  Y  A  V  R  R  V  K  K  S  D  M  E  K
ctggcaaaagctacaggtgcaaagatagtcacggatcttgatgaccttactccatcagta
 L  A  K  A  T  G  A  K  I  V  T  D  L  D  D  L  T  P  S  V
ctcggtgaagctgaaaaagtagaagagaggaagattggcgatgacaggatgacctttgta
 L  G  E  A  E  K  V  E  E  R  K  I  G  D  D  R  M  T  F  V
acaggttgcaaaaatccaaaagccgtgagtatacttatcaggggcggaacagaacacgtc
 T  G  C  K  N  P  K  A  V  S  I  L  I  R  G  G  T  E  H  V
gtttccgaagttgaaagagcactcaacgacgccataagggtcgtagccataacaaaggaa
 V  S  E  V  E  R  A  L  N  D  A  I  R  V  V  A  I  T  K  E
gatggcaaattcttatggggtggaggagccgtagaggctgagctagcaatgaggctagcc
 D  G  K  F  L  W  G  G  G  A  V  E  A  E  L  A  M  R  L  A
aagtatgccaacagtgtcggaggaagagagcaattagctatcgaagccttcgccaaggcc
 K  Y  A  N  S  V  G  G  R  E  Q  L  A  I  E  A  F  A  K  A
ttggagatcatacctaggacgttggctgaaaacgcaggcatagatccgataaacactctt
 L  E  I  I  P  R  T  L  A  E  N  A  G  I  D  P  I  N  T  L
atcaagctgaaatctgagcacgagaaaggcaagatatcaatgggcgtagatctagacagc
 I  K  L  K  S  E  H  E  K  G  K  I  S  M  G  V  D  L  D  S
aacggtgcaggcgacatgtcaaagaagggtgtaatagacccggtaagagtgaagactcac
 N  G  A  G  D  M  S  K  K  G  V  I  D  P  V  R  V  K  T  H
gcactcgaaagtgcagtagaagttgctacgatgatcctgcgtatagacgatgttatagcc
 A  L  E  S  A  V  E  V  A  T  M  I  L  R  I  D  D  V  I  A
agcaagaaatccacgccaccttctaaccagccaggccaaggagctggagcgccaggcggc
 S  K  K  S  T  P  P  S  N  Q  P  G  Q  G  A  G  A  P  G  G
ggaatgcctgagtattaaatttttatttttttaatatttt
 G  M  P  E  Y  -
```

Figure 3.30: Determined sequence and open reading frame for Hsp60 α subunit gene of *T. volcanium*.

aggaactaaaggagaaagttgaggatattatcaacggtcgatgttaaaacattattataa
attagagattatttctagaaatgcttatatagaagtttatttttactctgttagatagct
atgatagcgggacaaccaatattcattcttaaggaaggtacaaaaagagagagcggcaag
M I A G Q P I F I L K E G T K R E S G K
gatgcgatgaaagagaatatagaggcagcaattgcgatttcgaactctgtcagatccagc
D A M K E N I E A A I A I S N S V R S S
cttggcccaaggggaatggacaagatgctggtggattctcttggcgacatagtaattacc
L G P R G M D K M L V D S L G D I V I T
aacgacggtgttacaattctcaaagagatggatgtagaacaccctgctgccaaaatgatg
N D G V T I L K E M D V E H P A A K M M
gtagaggtatctaagacacaggattcctttgttggagatggaacaaccaccgcagtgatc
V E V S K T Q D S F V G D G T T T A V I
atcgctggcggcctactacagcaggctgaggcacttataaaccagaatgtacacccaacg
I A G G L L Q Q A E A L I N Q N V H P T
gtcatatctgaaggttacagaatggcttctgaagaggcaaagaggatcatagatgaaata
V I S E G Y R M A S E E A K R I I D E I
tcaacaaagatcggcaaagacgaaaaggagctccttataaagttggcacagacatcactt
S T K I G K D E K E L L I K L A Q T S L
aacagcaaaagtgcatctgtagcaaaggacaaactcgcagagatatcctatgaagctgtt
N S K S A S V A K D K L A E I S Y E A V
aaatctgtagcagagcttagggatgggaagtattacgtggattttgacaatatacaggtc
K S V A E L R D G K Y Y V D F D N I Q V
gtaaagaaacagggtggtgcaatagatgacactgcgttgataaacggaataatagtagac
V K K Q G G A I D D T A L I N G I I V D
aaggaaaaggtccaccctggaatgccggatgtagttaagaatgcaaagattgccctccta
K E K V H P G M P D V V K N A K I A L L
gatgccccactcgaaattaagaagcctgaatttgatacaaacctcaggatcgaagacccg
D A P L E I K K P E F D T N L R I E D P
agcatgatacagaagttcctagcgcaggaagaaaacatgctcagagagatggttgaaaaa
S M I Q K F L A Q E E N M L R E M V E K
attaaatccgtgggtgccaacgttgtaattacccagaagggaatagacgacatggcccag
I K S V G A N V V I T Q K G I D D M A Q
cactatctatcgaaagaagggatatacgcagtacgcagggtaaagaagagcgatatggac
H Y L S K E G I Y A V R R V K K S D M D
aaactcgcaaaagctacaggcgcgacagttgtctcaactatagatgagatttcggctagt
K L A K A T G A T V V S T I D E I S A S
gatcttggatccgctgacagagtagaacaagtcaaagttggagacgactacatgaccttt
D L G S A D R V E Q V K V G D D Y M T F
gttactggctgcaagaatccgaaagcggtaagtgttctagttagaggcgagactgaacac
V T G C K N P K A V S V L V R G E T E H
gttgttgatgaaatggagagatccataactgattcgctgcacgtagttgccagtgctctc
V V D E M E R S I T D S L H V V A S A L
gaggatggagcctataccgctggtggtggagcaactgcagcagagatagcagtaaggctc
E D G A Y T A G G G A T A A E I A V R L
agatcatatgcacagaaaataggtggcaggcagcagcttgcaattgaaaaattcgcagat
R S Y A Q K I G G R Q Q L A I E K F A D
gccatcgaagaagtgcccagagcccttgctgaaaacgccggattagatcctatagacata
A I E E V P R A L A E N A G L D P I D I
atactgaagctgagagctgaacacgcaaagggcaacaaatatgctggtgtaaatgtattc
I L K L R A E H A K G N K Y A G V N V F
agcggcgaaatagaggacatggttaacaacggagtcatagagccaataagggtgggcaag
S G E I E D M V N N G V I E P I R V G K
caggccattgaatctgcaaccgaagctgcaataatgatactccgcatagacgatgtgatt
Q A I E S A T E A A I M I L R I D D V I
gcgacaaagtcgagcggttcctcttcgaatccacctaagtcgccgtcttctgagtcctca
A T K S S G S S S N P P K S P S S E S S
tcaggtgaggactaaaatttaatgtaatacatttttaaaattatttttgttacgatt
S G E D -

Figure 3.31: Determined sequence and open reading frame for Hsp60 β subunit gene of *T. volcanium*

The subcloning scheme for the Hsp60 α subunit and Hsp60 β subunit gene fragments to pUC18 cloning vector to construct a co-expression vector is shown in Figure 3.32.

The cloned Hsp60 α subunit gene was removed from recombinant pDrive α4 plasmid through *Eco*RI digestion. pUC18 plasmid was also digested and linearized by *Eco*RI restriction endonuclease enzyme. The ligation of the Hsp60 α-subunit gene fragment to the pUC18 vector was carried out using T4 DNA ligase (MBI Fermentas, Lithuania) as described in 2.3.8.2 Section. Ligation samples were transferred into *E. coli* TG1 competent cells by transformation as also described in 2.3.8.2. Section. Then, plasmid isolation was performed in order to determine the recombinant pUC18 α plasmids. Isolated plasmids were characterized by *Eco*RI digestion.

EcoRI has a single cut site within MCS of pUC18 plasmid (Figure 3.33). Since Hsp60 α subunit gene (TVN1128) is flanked by *EcoRI* sites at both ends in the pDrive α vector and there is no cut site in the insert for *EcoRI*, *EcoRI* digestion yielded 1939 bp long insert and 2686 bp long pUC18 vector (Figure 3.34). Figure 3.34 illustrates the restriction profile of the recombinant pUC18 α plasmids.

After determination of recombinant pUC18 α plasmids, second step was to insert Hsp60 β subunit gene fragment to pUC18 α plasmids. The recombinant pDrive β3 plasmid which carries Hsp60 β subunit gene and the recombinant pUC18 α plasmid were both double digested with *Kpn*I and *Hind*III restriction endonuclease enzymes. Ligation of Hsp60 β subunit gene fragment to recombinant pUC18 α plasmid was performed as described in the 2.3.8.4 Section. *E.coli* TG1 cells were transformed with the putative recombinant plasmids as described before. Then, plasmid isolation was performed in order to determine the recombinant pUC18 α/β plasmids.

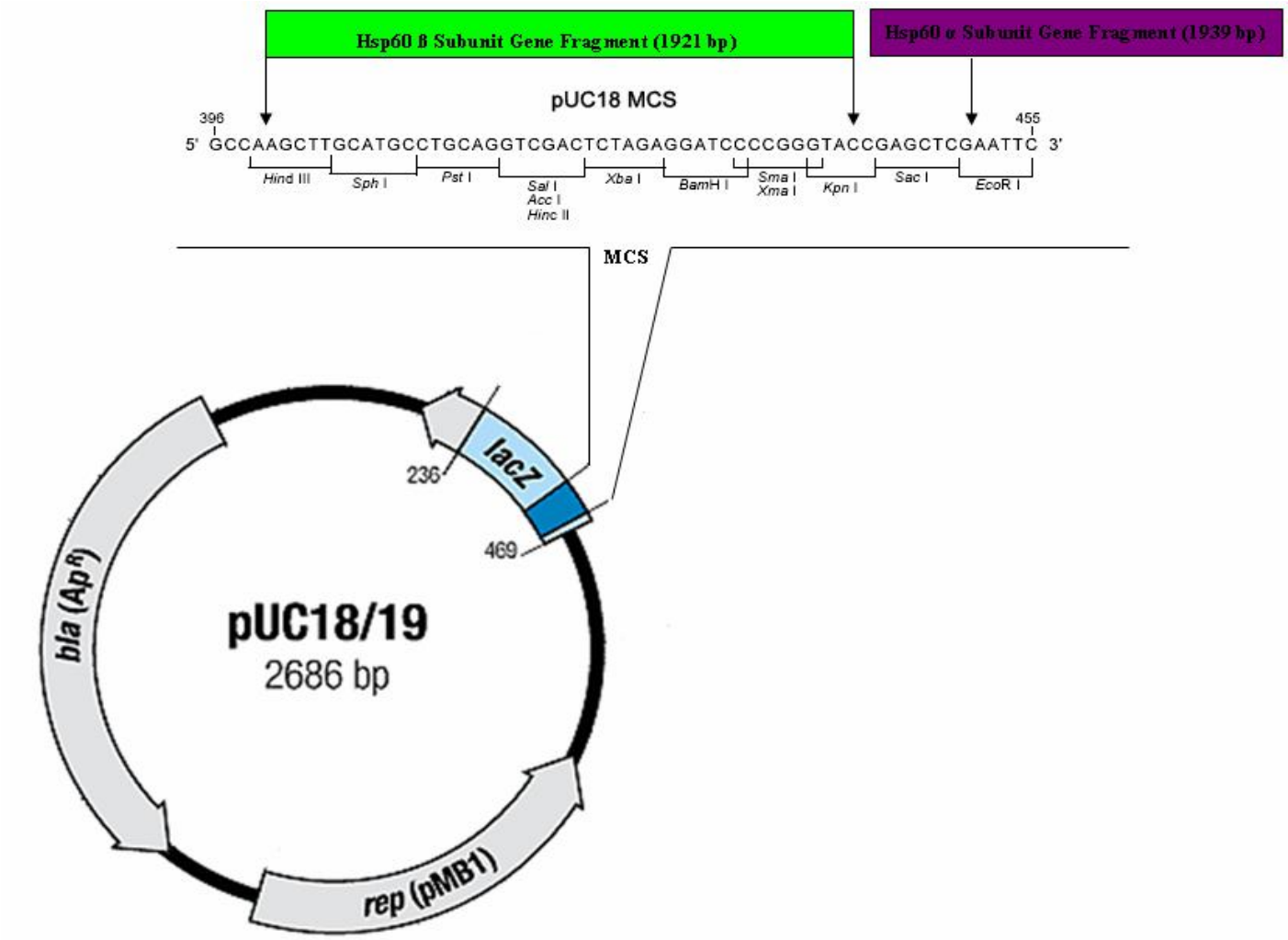

Figure 3.32: Schematic representation of subcloning of 1939 bp Hsp60 α subunit gene fragment and 1921 bp Hsp60 β subunit gene fragment to pUC18 vector (MBI Fermentas, AB, Vilnuis).

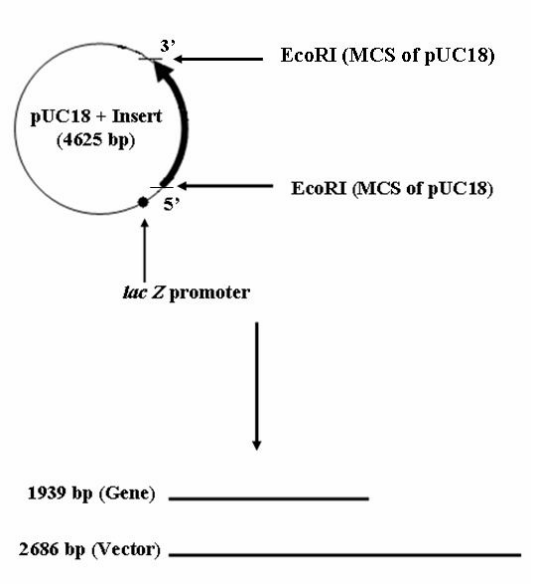

Figure 3.33: *EcoRI* digestion profile of recombinant pUC18 plasmid construct with Hsp60 α subunit gene (TVN1128).

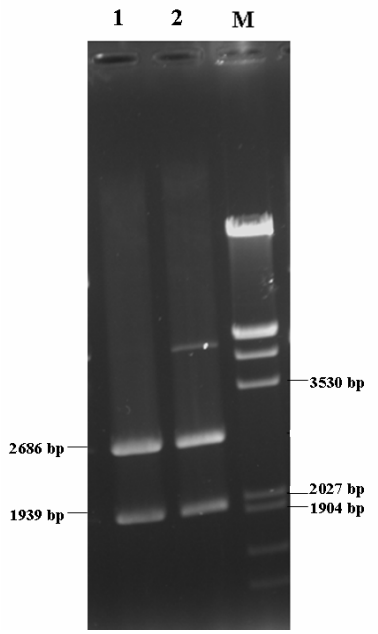

Figure 3.34: Restriction enzyme digestion of putative recombinant pUC18 α plasmids. Digestion with *EcoRI* enzyme yielded 1939 bp and 2686 bp fragments (Lanes 1 and 2) Lane 1 includes pUC-18 α/17 and lane 2 includes pUC-18 α/18. M is the *EcoRI* /*HindIII* cut Lambda DNA molecular weight marker (MBI Fermentas, AB, Vilnius).

*Kpn*I has single cut site within MCS of pUC18 plasmid and it is non-cutter for both Hsp60 α subunit gene (TVN1128) and Hsp60 β subunit gene (TVN0507) (Figure 3.35). *Kpn*I digestion yielded linearized recombinant plasmid DNA of 6546 bp (1939 bp Hsp60 α subunit gene + 1921 bp Hsp 60 β subunit gene + 2686 bp pUC18 vector) (Figure 3.36).

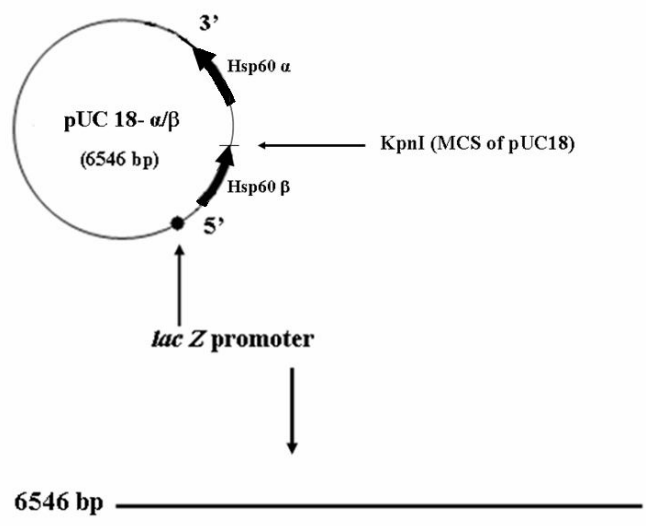

Figure 3.35: *KpnI* digestion profile of recombinant pUC18 plasmid construct with Hsp60 α subunit gene and Hsp 60 β subunit gene.

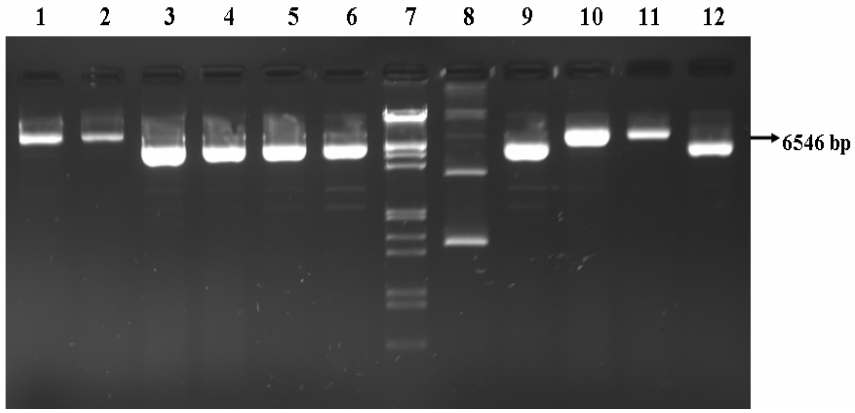

Figure 3.36: *KpnI* restriction enzyme digestion of putative recombinant pUC18-α/β plasmids: lane 1: p-3; lane 2: p-4; lane 3: p-11; lane 4: p-12; lane 5: p-13; lane 6: p-14; lane 7: the *EcoRI* /*HindIII* cut Lambda DNA molecular weight marker (MBI Fermentas, AB, Vilnius); lane 8: p-15; lane 9: p-16; lane 10: p-19; lane 11: p-9; lane 12: p-20.

Recombinant pUC18-α/β plasmids p-3, p-4, p-9 and p-19 yielded 6546 bp fragment when linearized by *KpnI*.

EcoRI is a non-cutter for both Hsp60 α subunit gene (TVN1128) and Hsp60 β subunit gene (TVN0507). *Eco*RI has single cut site within MCS of pUC18 plasmid. Hsp60 α subunit gene was ligated to pUC18 plasmid at this *EcoRI* site. Hsp60 β subunit gene was removed from *KpnI-HindIII* cut sites of recombinant pDrive β plasmid and ligated to pUC18 α plasmid at these sites. Since Hsp60 β subunit gene is flanked by *EcoRI* sites at both ends in the pDrive β vector and *EcoRI* sites are between *KpnI* and *HindIII* cut sites in the recombinant pUC18 vector, Hsp60 β gene was flanked by *EcoRI* sites at both end. *EcoRI* digestion of pUC18-α/β plasmid yielded 1939 bp Hsp60 α subunit gene, 1921 bp Hsp60 β subunit gene and 2686 bp pUC18 vector (Figure 3.37). Figure 3.37 illustrates the restriction profile of the recombinant pUC18 α/β plasmids.

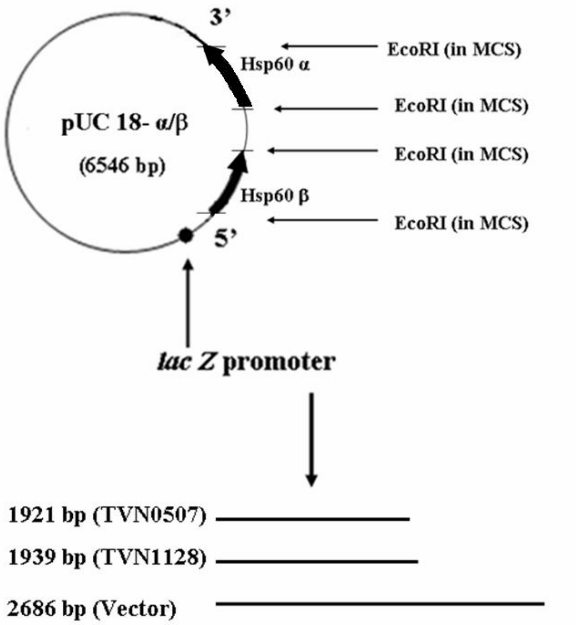

Figure 3.37: *Eco*RI digestion profile of recombinant plasmid construct with Hsp60 α subunit gene and Hsp60 β subunit gene.

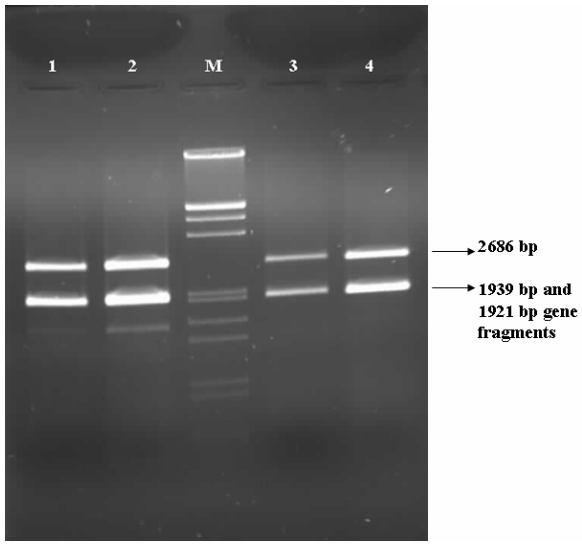

Figure 3.38: Restriction enzyme digestion of putative recombinant pUC18-α/β plasmids. Digestion with EcoRI enzyme yielded 1921 bp, 1939 bp and 2686 bp fragments. (Lane 1, 2, 3, and 4) Lane 1 contains pUC 18- α/β 9, lane 2 contains pUC 18-α/β19, lane 4 contains pUC 18- α/β4 and lane 5 contains pUC 18-α/β3. M: *EcoR* /*HindIII* cut Lambda DNA molecular weight marker (MBI Fermentas, AB, Vilnius).

3.2 Chaperonin Activity of Hsp60 Protein From *Thermoplasma volcanium*

Citrate synthase from porcine heart was denatured with GdmCl as described in the Material and Methods. Renaturation was performed after 1:100 dilution of the denatured citrate synthase in renaturation buffer at 3 different temperatures (30°C, 50°C and 57°C) for 2,5 h, in the presence (test) and absence (control) of recombinant thermosome.

Thermosome induced refolding was observed when renaturation was carried out 50°C for 2,5 h (Figure 3.39). Under this condition, citrate synthase activities associated with control and test were ΔmA_{412}/min:19.0 and ΔmA_{412}/min:24.0 respectively.

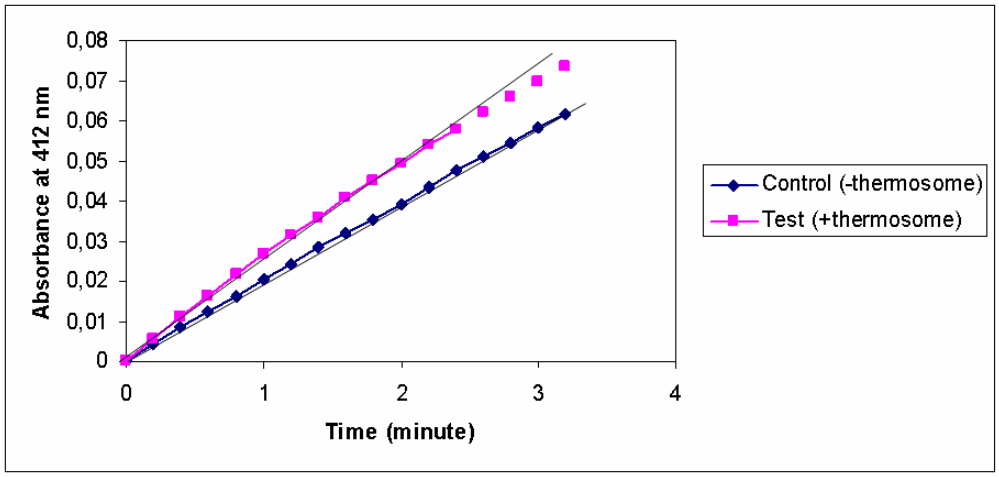

Figure 3.39: Time courses of reactivation of chemically (by 6 M GdmCl) denatured porcine heart citrate synthase assisted by recombinant *T. volcanium* chaperonin.

The effect of thermosome on refolding was not apparent when refolding was carried out at 30°C and 57°C for 2,5 h (Table 3.2).

Table 3.2: Renaturation after 1:100 dilution of the denatured citrate synthase in renaturation buffer at 3 different temperatures (30°C, 50°C and 57°C) for 2,5 h, in the presence (test) and absence (control) of recombinant thermosome.

	30°C		50°C		57°C	
	1,5 h	2,5 h	1,5 h	2,5 h	1,5 h	2,5 h
ΔmA_{412}/min (Control)	43,46	34,8	19,4	19,4	19,8	22
ΔmA_{412}/min (Test)	20,7	19,7	16,5	24	18,7	19,12

3.3. Stress Response of *Thermoplasma volcanium* Culture

3.3.1 Heat-Shock Response of *Thermoplasma volcanium* Culture

T. volcanium cells were grown until mid-exponential phase at 60°C and then, the temperature was shifted to 65°C, 70°C, 75°C and 78°C for 2 h in different experiments and then, incubation was carried out at 60°C. Control cultures were allowed to grow at 60°C. The cell growth was monitored through spectrophotometric measurements of the cell density at 540 nm., in a time dependent manner as mentioned in Section 2.5.1.

Exposure of the culture to heat shock at 65°C for 2 hours induced cell growth slightly as compared to the control which was not exposed to the heat shock (Figure 3.40). There was no significant effect of heat shock on culture growth as compared to control.

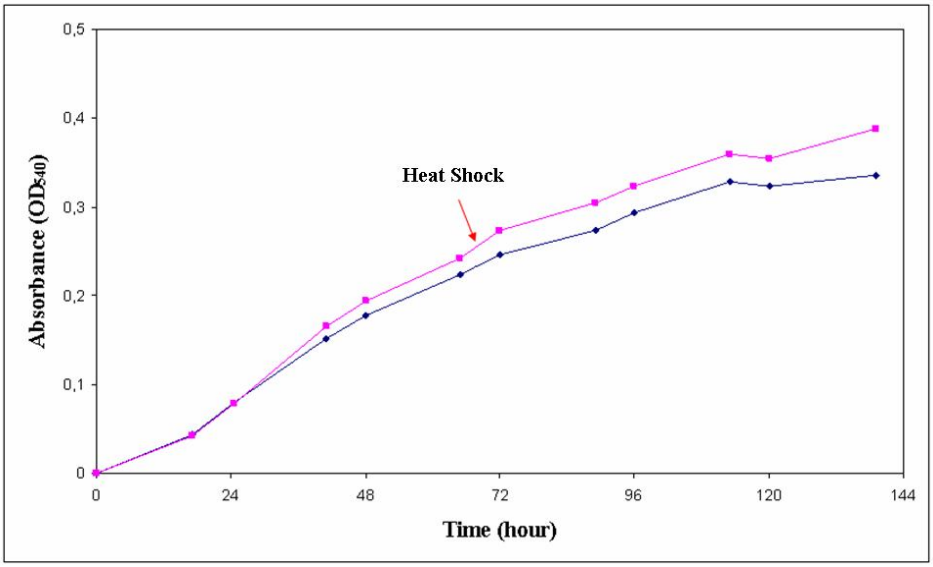

Figure 3.40: Effect of heat shock at 65°C for 2 h on the growth of *Thermoplasma volcanium*. Heat-shocked *T. volcanium* culture, Control *T. volcanium* culture. Heat shock was applied at 67th hour of the incubation.

Just after application of heat shock at 70°C, pausing in cell growth was observed but cells recovered in the following hours and heat shocked cells grew faster ($\Delta Abs_{540}xh^{-1} = 2,4x10^{-3}$) as compared to the control cells which were not exposed to the heat shock ($\Delta Abs_{540}xh^{-1} = 1,3x10^{-3}$) (Figure 3.41).

Before heat shock the growth rates of the test and control cultures were the same. Just after heat shock application at 75°C, pausing of the cell growth was observed but the cells recovered in the following hours and heat shocked cells grew faster ($\Delta Abs_{540}xh^{-1} = 7,9x10^{-4}$) as compared to the control cells which were not exposed to the heat shock ($\Delta Abs_{540}xh^{-1} = 5,5x10^{-4}$) (Figure 3.42).

The growth rates of new cultures initiated by the inocula from control culture and heat shock exposed (at 75°C) culture were almost the same. The growth rate of the culture that inoculated from heat shock exposed culture was $\Delta Abs_{540}xh^{-1} = 2,4x10^{-3}$ and the growth rate of the culture inoculated from control culture was $\Delta Abs_{540}xh^{-1} = 2,3x10^{-3}$. A short lag was observed in the new culture started with inoculum from heat shocked culture (Figure 3.43).

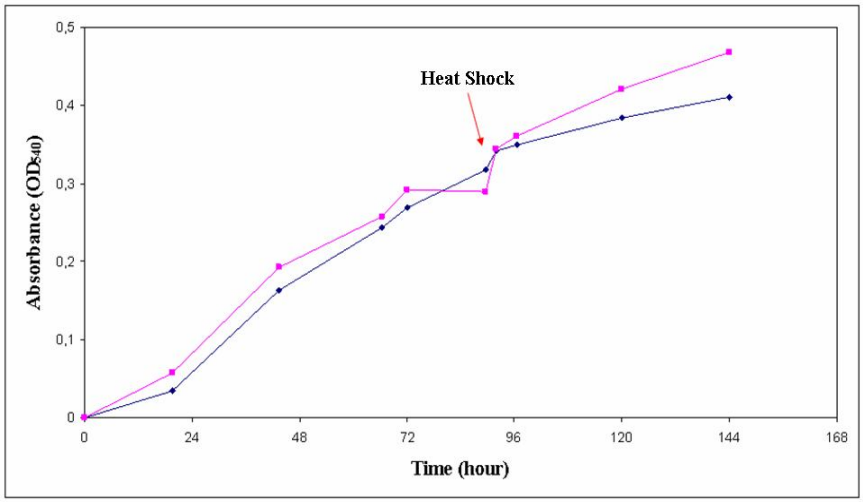

Figure 3.41: Effect of heat shock at 70°C for 2 h on the growth of *Thermoplasma volcanium*. Heat-shocked *T. volcanium* culture, Control *T. volcanium* culture. Heat shock was applied at 90th hour of the incubation.

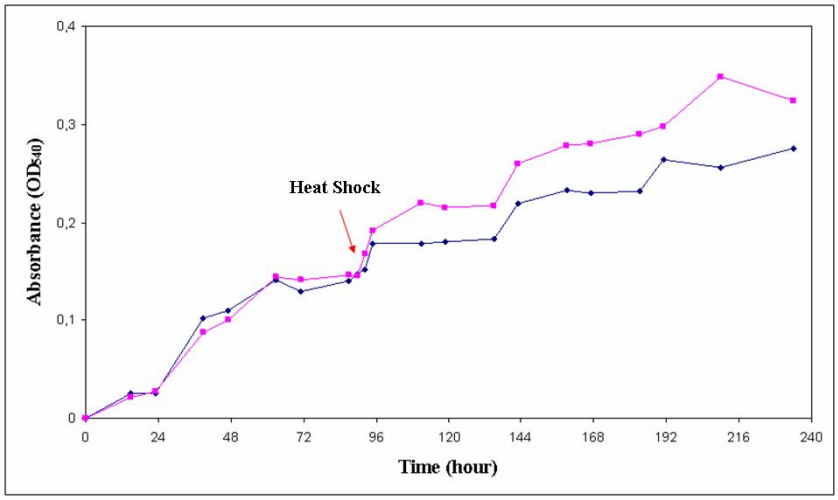

Figure 3.42: Effect of heat shock at 75°C for 2 h on the growth of *Thermoplasma volcanium*. Heat-shocked *T. volcanium* culture Control *T. volcanium* culture. Heat shock was applied at 90th hour of the incubation.

Retardation of cell growth was observed by heat-shock application at 78°C. Cell death and lysis should account for the decrease in absorbance after heat-shock (Figure 3.44).

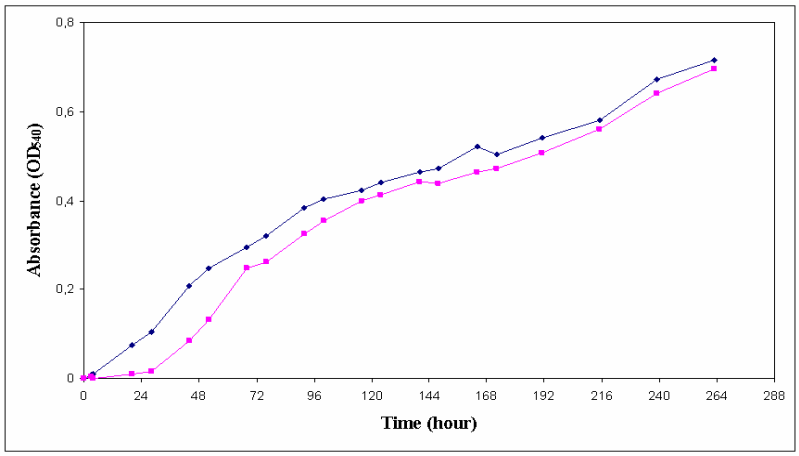

Figure 3.43: Effect of heat shock at 75°C for 2 h on the growth of new cultures of *Thermoplasma volcanium*. *T. volcanium* culture was started by the inoculum from heat shocked (75°C, 2 h) culture Control *T. volcanium* culture was started by the inoculum from control culture.

The new culture initiated by inoculation of fresh medium with 2h heat-shocked (at 78°C) culture of *T. volcanium* did not grow, as revealed by the OD measurements at 540 nm (Figure 3.45).

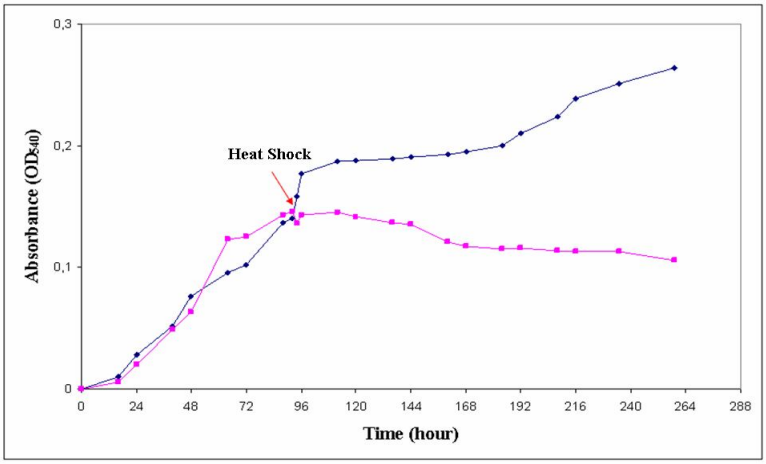

Figure 3.44: Effect of heat shock at 78°C for 2 h on the growth of *Thermoplasma volcanium*. Heat-shocked *T. volcanium* culture that exposed to heat shock Control *T. volcanium* culture. Heat shock was applied at 92th hour of the incubation.

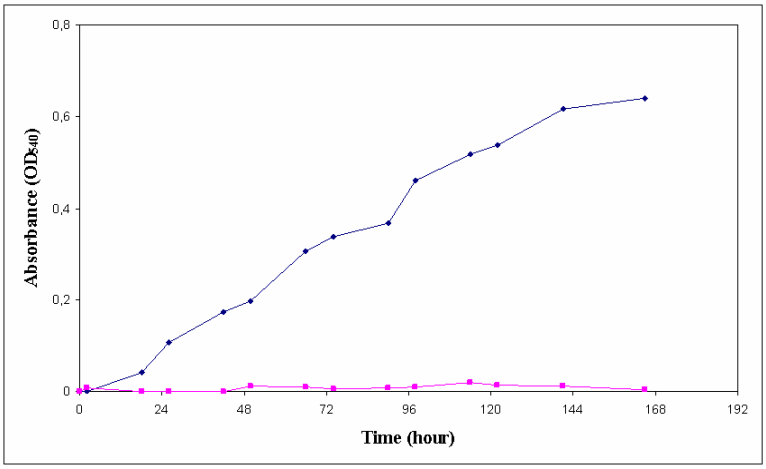

Figure 3.45: Effect of heat shock at 78°C for 2 h on the growth of new cultures of *Thermoplasma volcanium*. *T. volcanium* culture was started by the inoculum from heat shocked (78°C, 2 h) culture Control *T. volcanium* culture was started by the inoculum from control culture.

3.3.2 Oxidative Stress Response of *Thermoplasma volcanium* Culture

Different concentrations of H_2O_2 were added to *T. volcanium* cell cultures at the time of inoculation to observe their effects on growth of cells and to decide on the concentration to be used in RNA isolation experiments. The cultures supplemented with 0,025 mM H_2O_2, 0,05 mM H_2O_2, 0,075 mM H_2O_2 and 0,1 mM H_2O_2 could not grow, indicating toxic effect of H_2O_2 at concentrations ≥ 0,025 mM. Although growth was retarded about 72 h in the culture supplemented with 0,01 mM H_2O_2, there was a sharp increase in the growth thereafter, so that same absorbance value was reached as the control culture. At 0,005 mM H_2O_2 concentration the growth rate was slightly lower than the control culture (Figure 3.46).

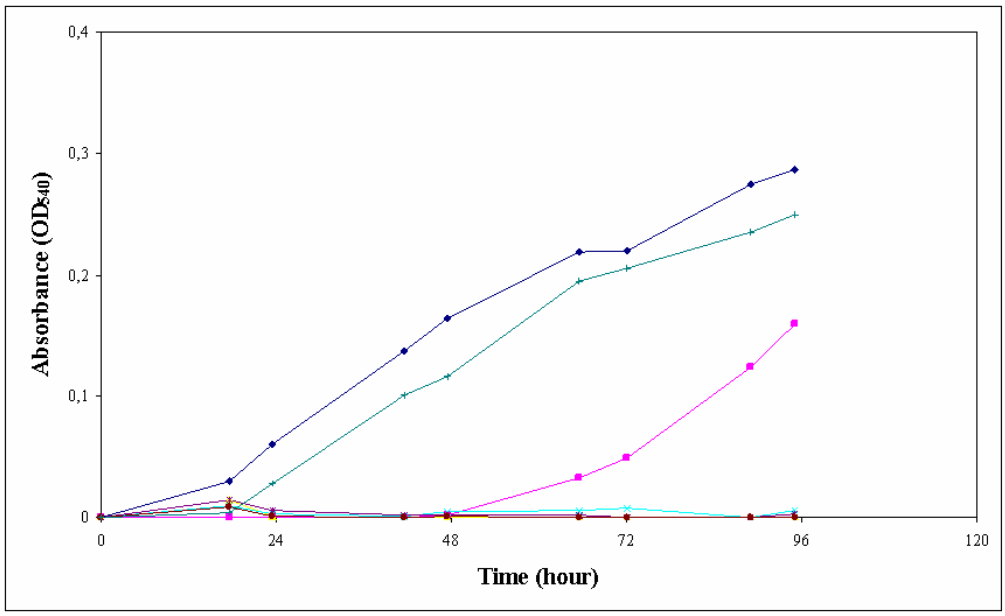

Figure 3.46: Effect of different concentrations of H_2O_2 on the growth of *Thermoplasma volcanium*. Control culture; Culture grown in 0,01 mM H_2O_2; Culture grown in 0,025 mM H_2O_2; Culture grown in 0,05 mM H_2O_2; Culture grown in 0,075 mM H_2O_2 ; Culture grown in 0,1 mM. H_2O_2; Culture grown in 0,005 mM H_2O_2.

Figure 3.47 shows time course effect of H_2O_2 (0,005-0,025 mM) on the growth of *T. volcanium*. The growth was inhibited by addition of 0,025-0,01 mM concentration of H_2O_2. The cultures supplemented with 0,01 mM H_2O_2 was arrested for 48 h following H_2O_2 addition, but cells then recovered as revealed by increase in the growth rate ($\Delta Abs_{540}xh^{-1} = 4,78x10^{-3}$).

Although 0,005 mM H_2O_2 addition resulted in a lag of about 20h, then growth rate ($\Delta Abs_{540}xh^{-1} = 3,98x10^{-3}$) increased to the level of the control culture ($\Delta Abs_{540}xh^{-1} = 3,79x10^{-3}$) for 72 h.

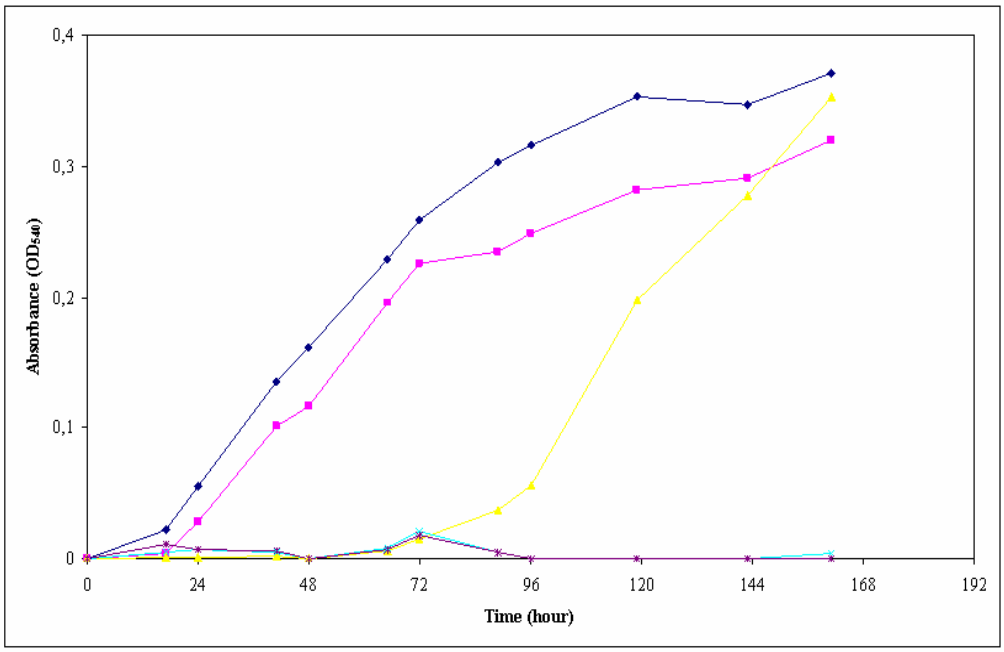

Figure 3.47: Effect of oxidative stress at different concentrations of H_2O_2 on the growth of *Thermoplasma volcanium*. Control culture; Culture grown in 0,005 mM H_2O_2; Culture grown in 0,01 mM H_2O_2; Culture grown in 0,015 mM H_2O_2; Culture grown in 0,025 mM H_2O_2.

To see the effect of H_2O_2 to log phase cells, the cultures were grown under standart conditions at 60°C until mid-log phase is reached (OD_{540}=0,220). Then, between 0,008 mM and 0,05 mM H_2O_2 was added into flasks and growth

was continued for ~78 h more. Time courses of the growth was followed by spectrophotometric measurements of absorbances at 540 nm.

When cultures supplemented with 0,008 mM H_2O_2, growth of *T. volcanium* culture appeared to be induced ($\Delta Abs_{540}xh^{-1}$ = 2,96x10^{-3}) as compared to control culture which is not supplemented ($\Delta Abs_{540}xh^{-1}$ = 2,65x10^{-3}) (Figure 3.48).

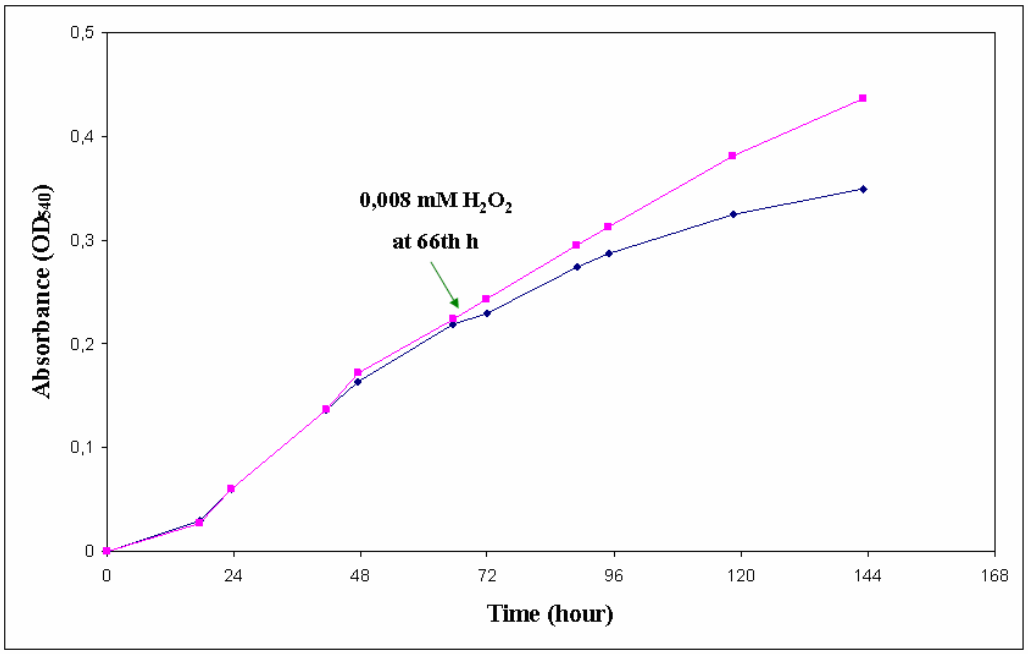

Figure 3.48: Effect of oxidative stress on the growth of *Thermoplasma volcanium*. Control H_2O_2 was added at 66th hour of culture. Concentration of H_2O_2 was 0,008 mM.

At > 0,01 mM H_2O_2 concentrations, the growth of the cultures were retarded in a concentration dependent manner when compared to control culture (Figures 3.49-3.51). The growth rates at 0,01 mM, 0,02 mM and 0,03 mM H_2O_2 concentrations were $\Delta Abs_{540}xh^{-1}$ = 2,13x10^{-3}, $\Delta Abs_{540}xh^{-1}$ = 1,83x10^{-3}, and $\Delta Abs_{540}xh^{-1}$ = 1,27x10^{-3}, respectively. The control growth rate was $\Delta Abs_{540}xh^{-1}$ = 2x10^{-3}.

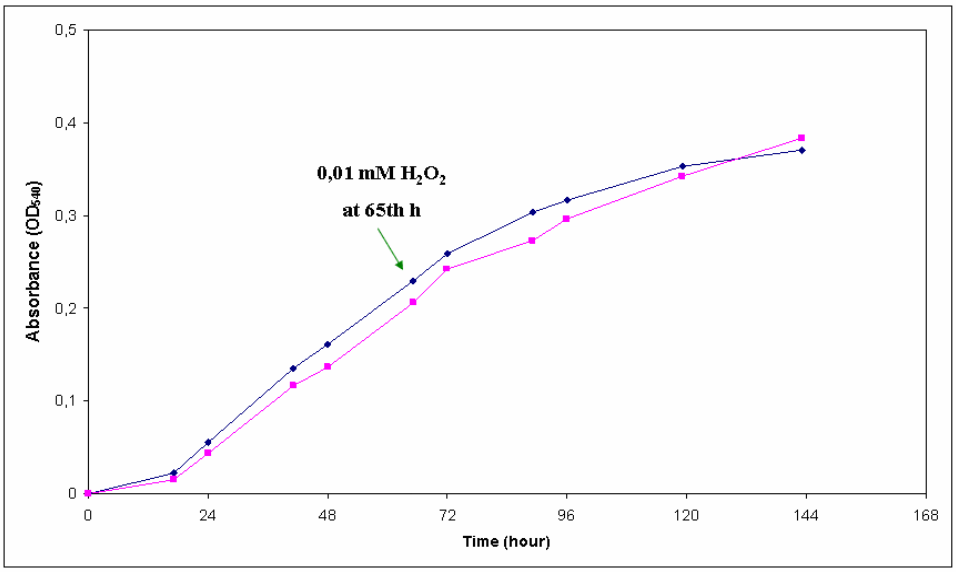

Figure 3.49: Effect of oxidative stress on the growth of *Thermoplasma volcanium*. Control H_2O_2 was added at 65th hour of culture. Concentration of H_2O_2 was 0,01 mM.

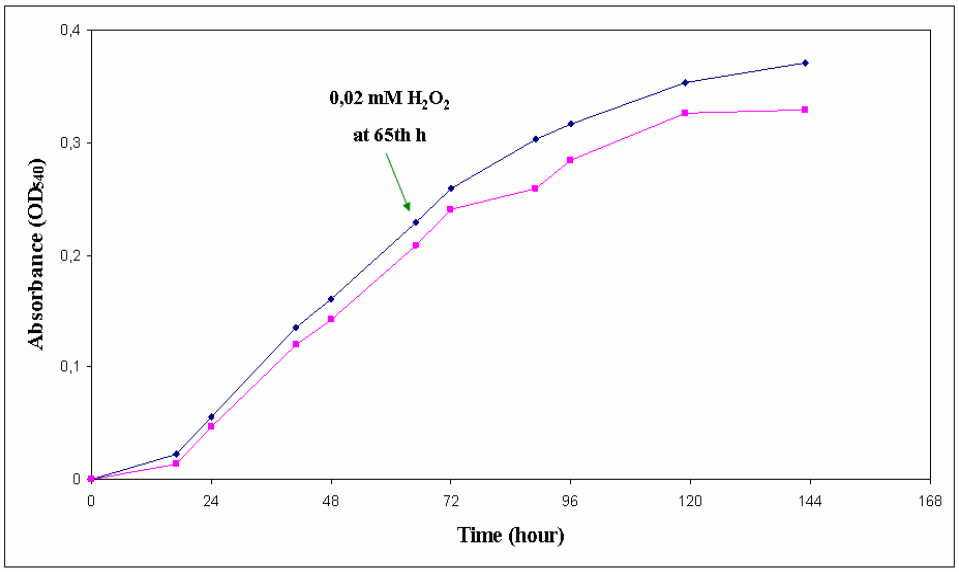

Figure 3.50: Effect of oxidative stress on the growth of *Thermoplasma volcanium*. Control H_2O_2 was added at 65th hour of culture. Concentration of H_2O_2 was 0,02 mM.

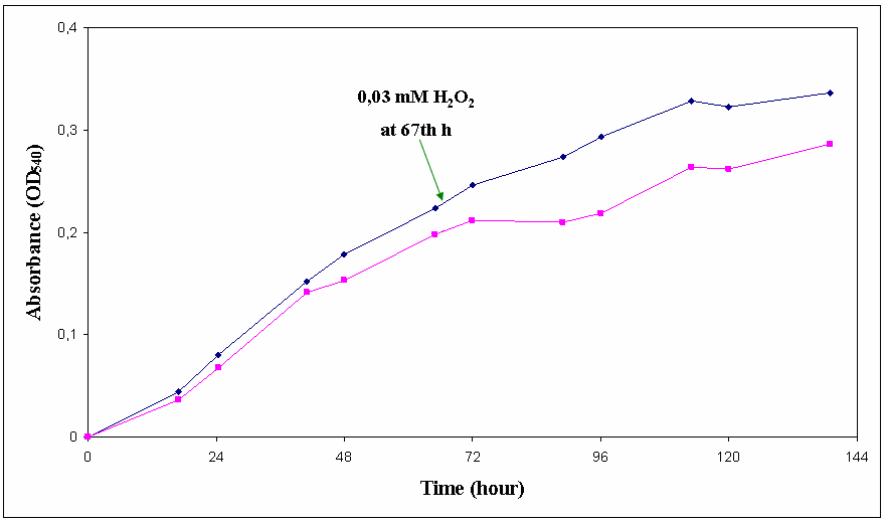

Figure 3.51: Effect of oxidative stress on the growth of *Thermoplasma volcanium*. Control H_2O_2 was added at 67th hour of culture. Concentration of H_2O_2 was 0,03 mM.

Supplementation of mid-log phase culture with 0,05 mM H_2O_2 seems to inhibit the growth of *T. volcanium* culture as could be seen in the growth curve (Figure 3.52). The growth rate at 0,05 mM H_2O_2 was $\Delta Abs_{540} x h^{-1} = 1,59 \times 10^{-3}$ and the control growth rate was $\Delta Abs_{540} x h^{-1} = 2,48 \times 10^{-3}$.

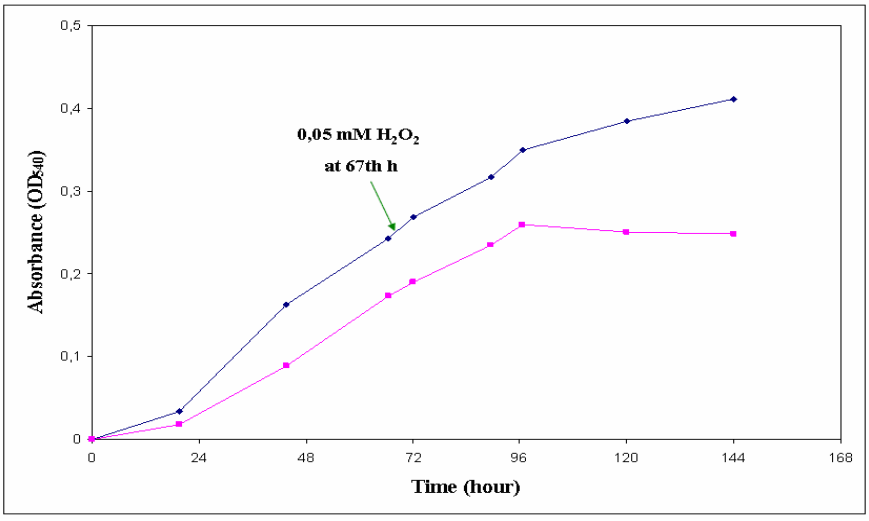

Figure 3.52: Effect of oxidative stress on the growth of *Thermoplasma volcanium*. Control H_2O_2 was added at 67th hour of culture. Concentration of H_2O_2 was 0,05 mM.

3.3.3 RNA Isolations

Isolation of RNA were performed as mentioned in 2.5.3 Section. Experimental conditions were optimized to isolate control and test RNA samples from *T. volcanium* cultures heat-shocked at 3 different temperatures (65°C, 70°C and 75°C) and also from cultures exposed to oxidative stress at 4 different concentrations of H_2O_2 (0,008 mM, 0,01 mM, 0,02 mM, 0,03 mM and 0,05 mM). Culture samples were taken in a time dependent manner to isolate RNA. Purity of RNA samples were checked by formamide agarose gel electrophoresis and measurement of absorbances at 260 nm and 280 nm as mentioned in 2.5.4 Section.

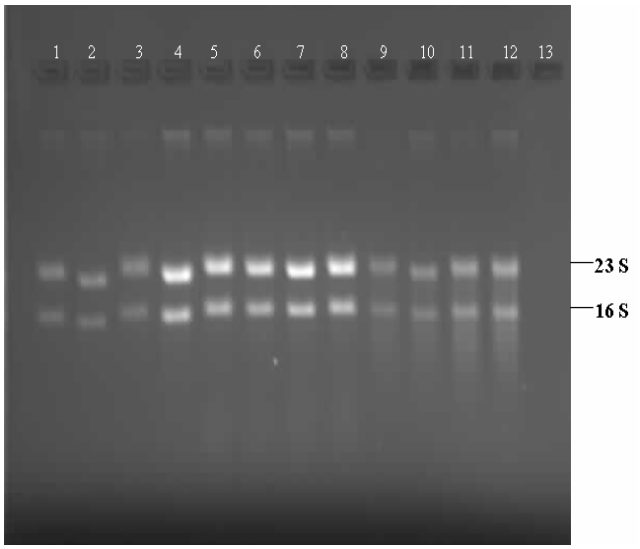

Figure 3.53: Agarose gel electrophoresis of the RNA samples isolated from *T. volcanium* cells under heat shock or oxidative stress conditions. Lane 1 to 4: control RNA samples isolated at 30th, 60th, 90th and 120th minutes after 72 h growth of the *T. volcanium* culture, respectively. Lane 5 to 8: RNA samples from heat-shocked (after 72 h growth) culture at 65°C, which were isolated at 30th, 60th, 90th and 120th minutes of the heat-shock. Lane 9 to 12: RNA samples from H_2O_2 exposed (0,03 mM) culture (after 72 h growth) which were isolated at 30th, 60th, 90th and 120th minutes of the oxidative stress, respectively.

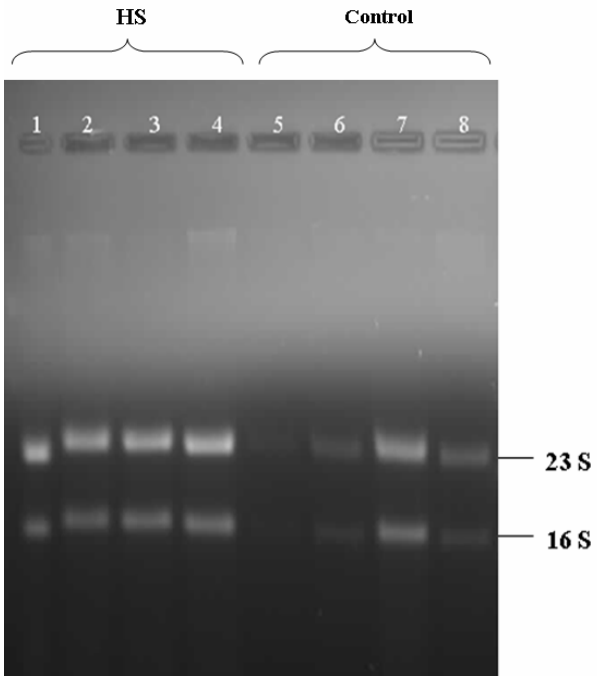

Figure 3.54: Agarose gel electrophoresis of the RNA samples isolated from *T. volcanium* cells under heat shock conditions. Lane 1 to 4: RNA samples from heat-shocked (after 72 h growth) culture at 70°C, which were isolated at 30th, 60th, 90th and 120th minutes of the heat-shock. Lane 5 to 8: control RNA samples isolated at 30th, 60th, 90th and 120th minutes, after 72h growth of the *T. volcanium* cells, respectively. HS: heat-shock.

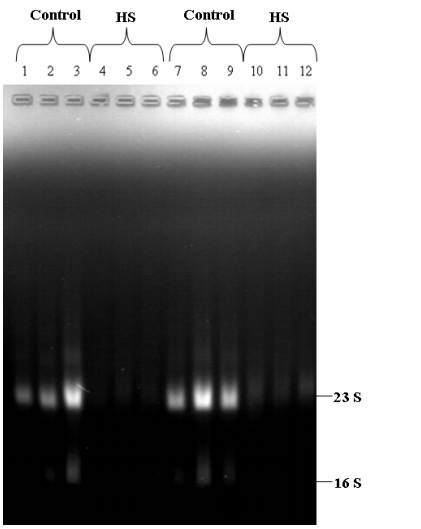

Figure 3.55: Agarose gel electrophoresis of the RNA samples isolated under heat shock conditions. Lane 1 to 3 and 7 to 9: control RNA samples isolated at 120th minute after 72 h growth of the *T. volcanium* culture. Different volumes of the culture (2, 3, 4 ml for lanes 1-6 and 3, 4, 5 ml for lanes 7-12) were used for the isolation. Lane 4 to 6 and 10 to 12: RNA samples from heat-shocked (after 72 h growth) culture at 75°C, which were isolated at 120th minutes of the heat-shock. HS: heat-shock.

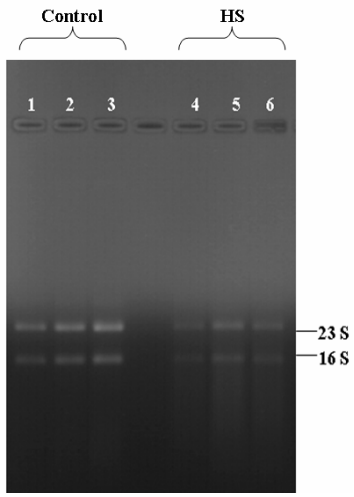

Figure 3.56: Gel electrophoresis of the RNA samples isolated under heat shock conditions. Lanes 1 to 3: 3, 4, 5 ml control RNA samples which were isolated at 120th minute after 72 h growth of the *T. volcanium* culture. Lanes 4 to 6: 3, 4, 5 ml RNA samples from heat-shocked (after 72 h growth) culture at 70°C, which were isolated at 120th minutes of the heat shock. HS: heat-shock.

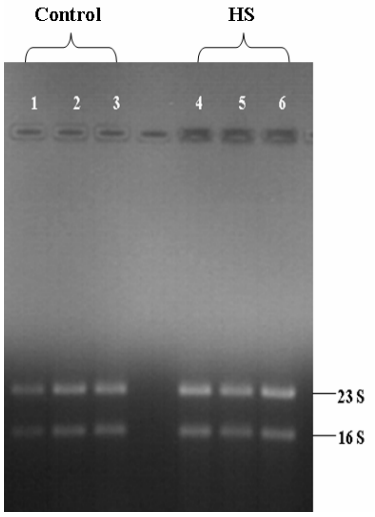

Figure 3.57: Gel electrophoresis of the RNA samples isolated under heat shock conditions. Lanes 1 to 3: control RNA samples (3, 4, 5 ml) which were isolated at 120th minute following 72 h growth of *T. volcanium* cells. Lanes 4 to 6: RNA samples (3, 4, 5 ml) from heat-shocked (after 72 h growth) culture at 65°C, which were isolated at 120th minutes of the heat-shock. HS: heat-shock.

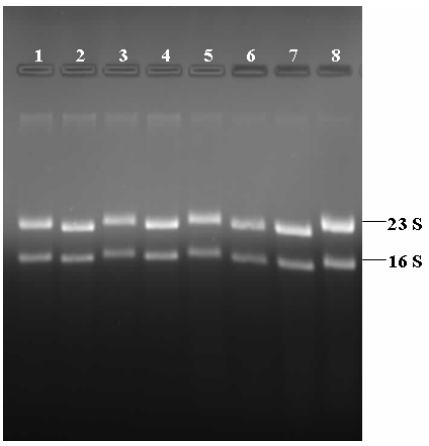

Figure 3.58: Gel electrophoresis of the RNA samples isolated under oxidative stress condition. Lane 1 to 4: control RNA samples which were isolated at 15th, 30th, 45th and 60th minutes after 72 h growth of the *T. volcanium* culture, respectively. Lane 5 to 8: RNA samples from H_2O_2 (0,008 mM) exposed culture which were isolated at 15th, 30th, 45th and 60th minutes of the oxidative stress (exposed to 72nd hour of the growth), respectively.

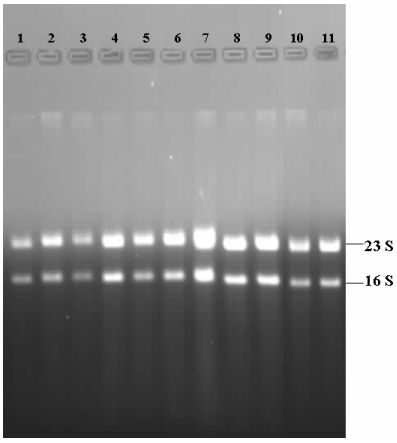

Figure 3.59: Agarose gel electrophoresis of the RNA samples isolated under oxidative stress conditions. Lanes 1 to 4: control RNA samples which were isolated at 30th, 60th, 90th and 120th minutes after 72 h growth of the *T. volcanium* cells, respectively. Lanes 5 to 8: RNA samples from H_2O_2 exposed (0,01 mM) culture which were isolated at 30th, 60th, 90th and 120th minutes of the oxidative stress (exposed to 72nd hour of the growth), respectively. Lanes 9, 10 and 11: RNA samples from H_2O_2 exposed (0,02 mM) culture, which were isolated at 30th, 90th and 120th minutes of the oxidative stress (exposed to 72nd hour of the growth), respectively.

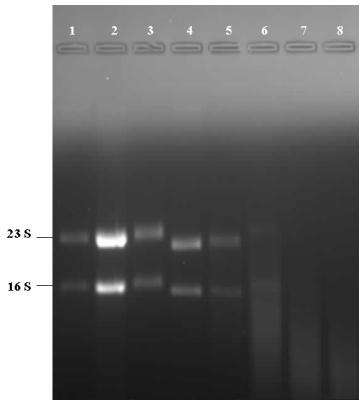

Figure 3.60: Agarose gel electrophoresis of the RNA samples isolated under oxidative stress condition. Lanes 1 to 4: control RNA samples which were isolated at 15th, 30th, 45th and 60th minutes after 72 h growth of the *T. volcanium* cells, respectively. Lanes 5 to 8: RNA samples from H_2O_2 (0,05 mM) exposed culture which were isolated at 15th, 30th, 45th and 60th minutes of the oxidative stress (exposed to 72nd hour of the growth), respectively.

In order to calculate the concentration and estimate the purity of RNA samples, absorbance at 260 nm. (A_{260}) and absorbance at 280 nm. (A_{280}) were measured, and A_{260}/A_{280} ratios were determined (Table 3.3).

Table 3.3: Concentrations and the A_{260}/A_{280} ratios of RNA samples

Figure No.	RNA Sample No.	A_{260}/A_{280}	Concentration (µg/µl)	Figure No.	RNA Sample No.	A_{260}/A_{280}	Concentration (µg/µl)
3.51	1	1,2	0,7	**3.55**	1	1,2	0,6
	2	1,2	0,7		3	1,23	0,63
	3	1,15	0,64		4	1,2	0,7
	4	1,24	0,87		5	1,2	0,62
	5	1,26	0,81		6	1,38	0,81
	6	1,2	0,74	**3.56**	1	1,121	0,7
	7	1,2	0,88		2	1,250	0,79
	8	1,2	0,76		3	1,150	0,64
	9	1	0,91		4	1,196	0,74
	10	1,3	0,97		5	1,127	0,66
	11	0,9	0,9		6	1,186	0,77
	12	1,1	0,88		7	1,250	0,79
3.52	1	1	0,61		8	1,265	0,8
	2	1	0,64	**3.57**	1	1,1	0,9
	3	1	0,64		2	1,1	0,94
	4	1,2	0,87		3	1,1	0,78
	5	1,6	0,87		4	1,14	0,74
	6	1	0,57		5	1,13	0,74
	7	1,1	0,63		6	1,16	0,87
	8	1,2	0,82		7	1,18	0,8
3.53	3	1,4	0,74		8	0,8	0,97
	6	1,3	0,81		9	1	0,97
	9	1,3	0,74		10	1,1	0,84
	12	1,4	0,89		11	1,2	0,9
3.54	1	1,2	0,62		12	1	0,72
	2	1,2	0,68	**3.58**	1	1	0,52
	3	1,26	0,67		2	1,2	0,74
	4	1,2	0,58		5	1	0,61
	5	1,24	0,67		6	1,2	0,9
	6	1,2	0,6				

3.3.4 Reverse PCR Experiments

3.3.4.1 cDNA Synthesis by Reverse PCR

Reverse PCR experiments to synthesize cDNAs of Hsp60 α and Hsp60 ß subunit genes from total RNA were described in 2.5.5.2 Section. cDNA for Hsp60 β gene which was synthesized by using reverse Real Time PCR primer is shown in Figure 3.61.

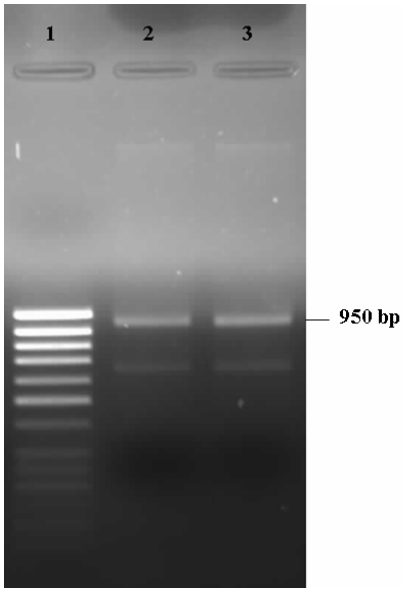

Figure 3.61: cDNAs for Hsp60 β gene synthesized from control RNA isolated from 120th min after 72 h growth. Lane 1: the O'GeneRuler 50 bp DNA Ladder (MBI Fermentas, AB, Vilnius). Lanes 2 and 3: cDNAs for Hsp60 β gene synthesized from control RNA isolated from 120th min after 72 h growth.

3.3.4.2 cDNA Amplification by Real-Time PCR

Reverse transcription PCR experiments were performed as described in 2.5.5 Section. cDNAs for Hsp60 α and Hsp60 β genes which were amplified by PCR are 399 bp and 581 bp amplicons as shown in Figure 3.62.

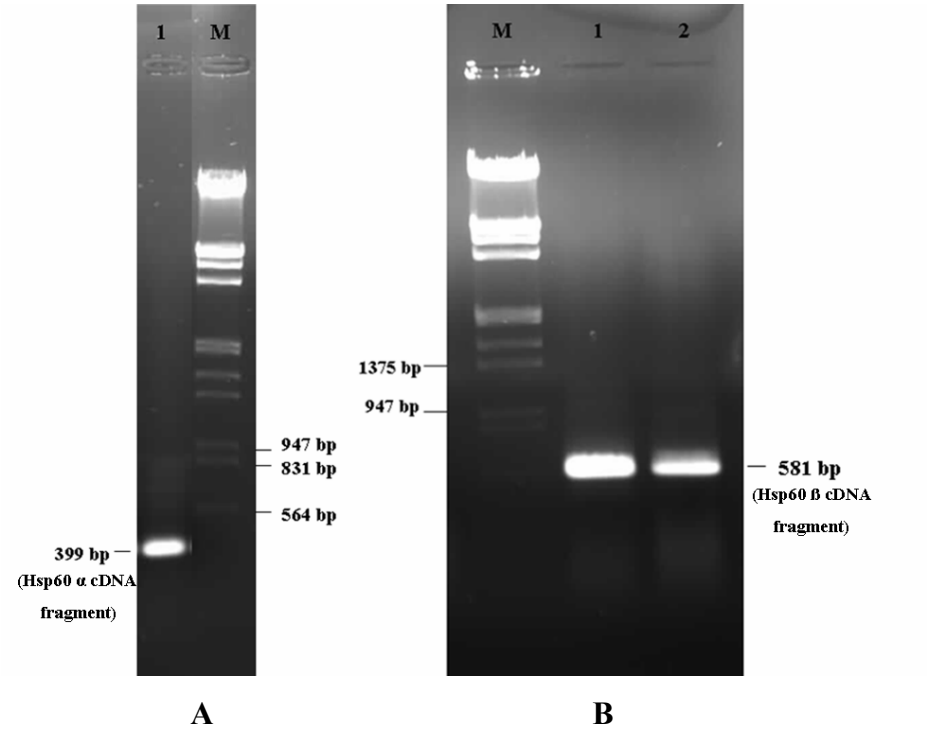

Figure 3.62: cDNAs for Hsp60 α and Hsp60 β genes synthesized from heat shock exposed RNA samples. **M** is the *EcoRI*/*HindIII* cut Lambda DNA molecular weight marker (MBI Fermentas, AB, Vilnius). Panel A, lane 1: cDNA for Hsp60 α gene synthesized from RNA isolated from 120 min heat-shocked sample at 65°C. Panel B, lanes 1 and 2: cDNAs for Hsp60 β gene synthesized from RNA isolated from 120 min heat-shocked samples at 65°C.

3.3.5 Effect of Heat-Shock on Differential Expression of Hsp60 α Subunit Gene

Heat shock at 65°C for 2 hours induced expression of Hsp60 α subunit gene, which is evident from lower crossing point (CP) values for the tests as compared to controls (Figures 3.63-3.66). The real-time PCR experiments showed that, induction of Hsp60 α gene expression continued throughout the 2h heat-shock, as revealed by the CP values for the amplification of 30 min, 60 min, 90 min and 120 min samples (Figures 3.63-3.66). The lower the crossing point (CP) the earlier the amplification of sample (cDNA) is expected. Melting point analyses showed that amplifications in Real-Time PCR was specific for *T. volcanium* Hsp60 α gene, and the average Tm was 86,75°C (± 0,40).

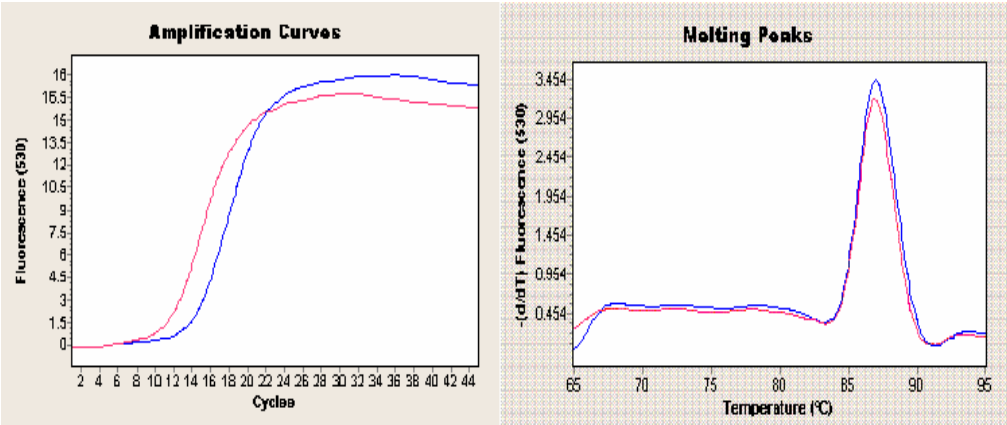

Figure 3.63: Real-time PCR graphics of control and heat-shocked samples at 65°C for 30 min. _____ Control (30th min following 72 h growth) CP: 13,31 _____ Test (30 min heat-shock at 65°C) CP: 10,67

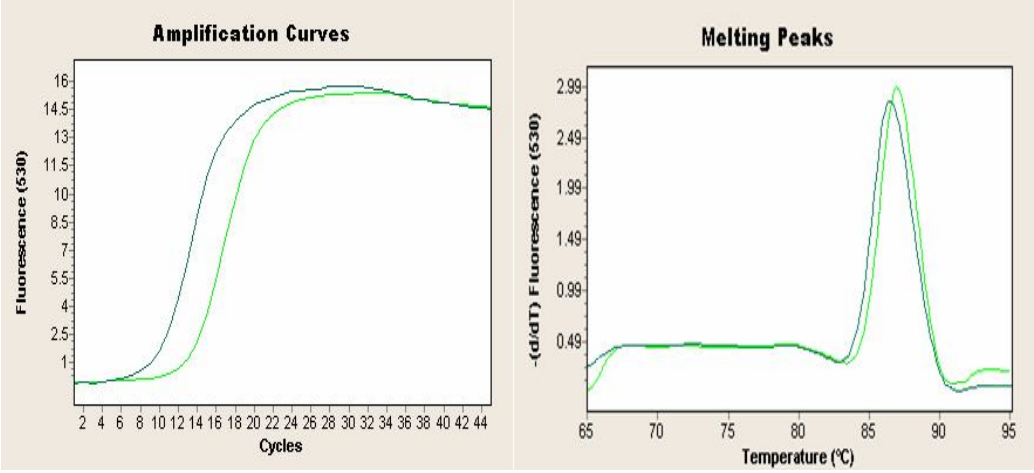

Figure 3.64: Real-time PCR graphics of control and heat-shocked samples at 65°C for 60 min. Control (60th min following 72 h growth) CP: 12,54 Test (60 min heat-shock at 65°C) CP: 8,94

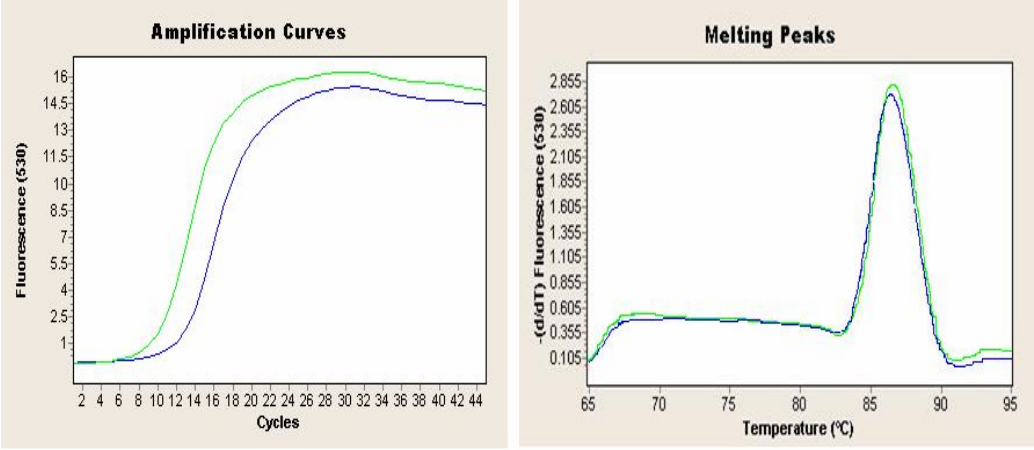

Figure 3.65: Real-time PCR graphics of control and heat-shocked samples at 65°C for 90 min. Control (90th min following 72 h growth) CP: 11,72 Test (90 min heat-shock at 65°C) CP: 9,01

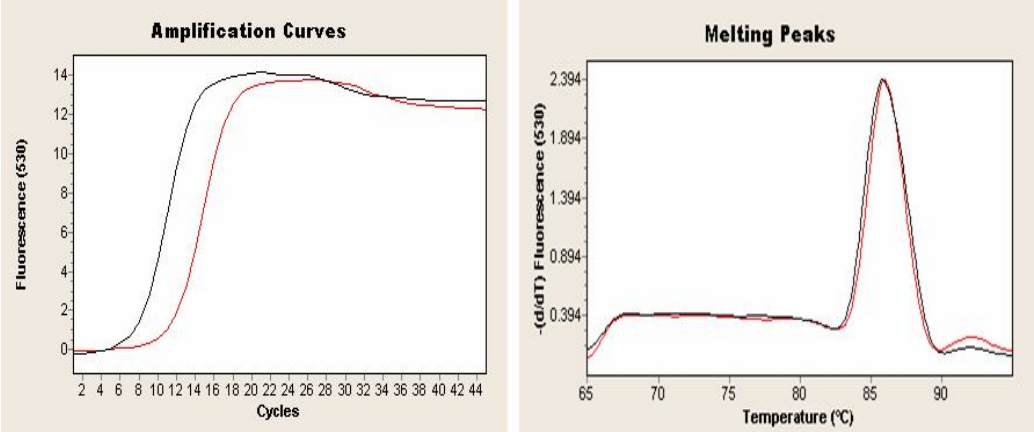

Figure 3.66: Real-time PCR graphics of control and heat-shocked samples at 65°C for 120 min. ——— Control (120th min following 72 h growth) CP: 10,63 ——— Test (120 min heat-shock at 65°C) CP: 6,78

Heat shock at 70°C also induced expression of Hsp60 α subunit gene which is evident from lower CP values of the tests as compared to controls (Figures 3.67-3.70). Continuous induction of Hsp60 α gene was observed throughout 2h heat-shock as shown in the Figures 3.67-3.70. The CP values for the amplification of 30 min, 60 min, 90 min and 120 min samples were smaller than that of the controls. The PCR amplifications all were specific for Hsp60 α gene and average Tm for Hsp60 α was 86,68°C (± 0,1).

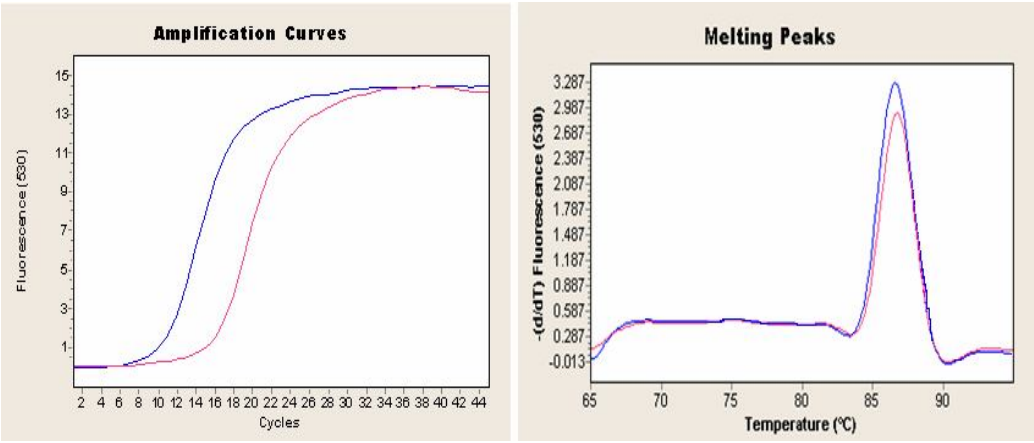

Figure 3.67: Real-time PCR graphics of control and heat-shocked samples at 70°C for 30 min. ——— Control at 30th min. CP:15,07 ——— Test (30 min heat shock application) CP: 9,77

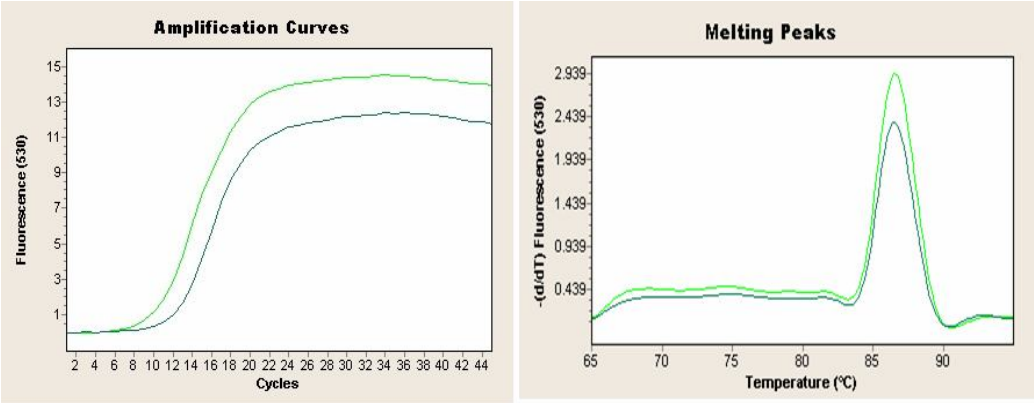

Figure 3.68: Real-time PCR graphics of control and heat-shocked samples at 70°C for 60 min. Control at 60th min. CP: 11,50 Test (60 min heat-shock application) CP: 9,51

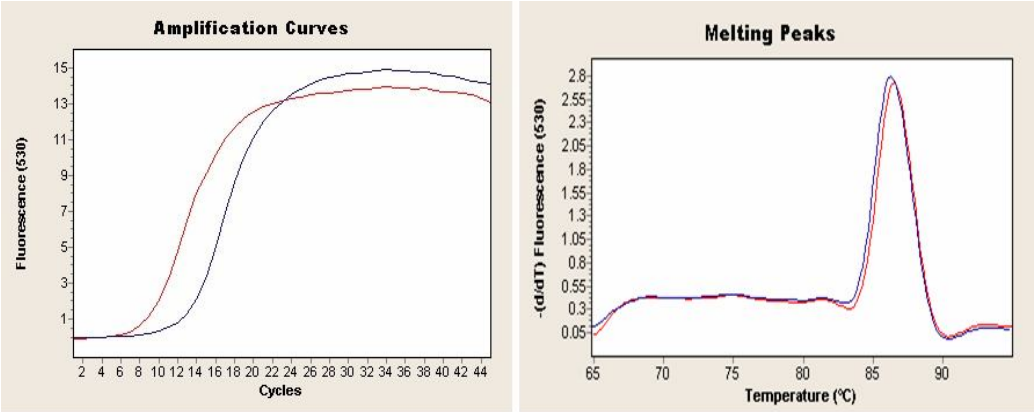

Figure 3.69: Real-time PCR graphics of control and heat-shocked samples at 70°C for 90 min. Control at 90th min. CP: 12,29 Test (90 min heat-shock application) CP: 8,04

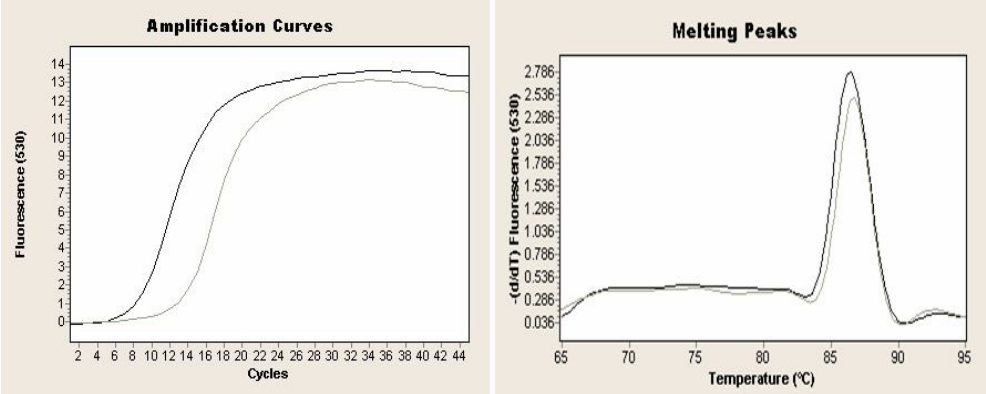

Figure 3.70: Real-time PCR graphics of control and heat-shocked samples at 70°C for 120 min. _____ Control at 120th min. CP:12,55 _____ Test (120 min heat-shock application) CP: 7,51

The real-time PCR experiments for which cDNA templates prepared from RNA samples of the 75°C 2 hours heat-shocked culture, yielded amplifications with the same CP values for both test and control. This result showed that heat shock at 75°C for 2 hours did not induce expression of Hsp60 α subunit gene (Figure 3.71). Amplifications were specific for Hsp60 α gene, Tm being 86,2°C (± 0,13).

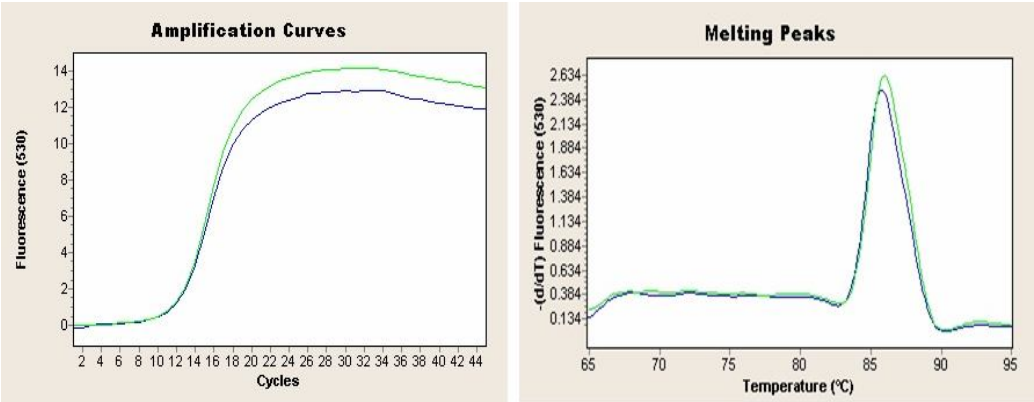

Figure 3.71: Real-time PCR graphics of control and heat-shocked samples at 75°C for 120 min. _____ Control at 120th min CP: 11,14 _____ Test (120 min heat-shock application) CP: 11,17

CPs and Tms for amplification of Hsp60 α cDNA at 65˚C, 70˚C and 75˚C heat-shock are listed in the Table 3.4.

Table 3.4: CP and Tm values for the study of Hsp60 α gene's differential expression as a response to heat-shock.

Heat Shock Temperature	Time (minute)	CP	Tm	Figure
65˚C	30 (Control)	13,31	87,16	Figure 3.60
	30 (Test)	10,67	87,08	Figure 3.60
	60 (Control)	12,54	87,15	Figure 3.61
	60 (Test)	8,94	86,79	Figure 3.61
	90 (Control)	11,72	86,71	Figure 3.62
	90 (Test)	9,01	86,82	Figure 3.62
	120 (Control)	10,63	86,13	Figure 3.63
	120 (Test)	6,78	86,18	Figure 3.63
70˚C	30 (Control)	15,07	86,85	Figure 3.64
	30 (Test)	9,77	86,68	Figure 3.64
	60 (Control)	11,50	86,67	Figure 3.65
	60 (Test)	9,51	86,69	Figure 3.65
	90 (Control)	12,29	86,49	Figure 3.66
	90 (Test)	8,04	86,66	Figure 3.66
	120 (Control)	12,55	86,78	Figure 3.67
	120 (Test)	7,51	86,59	Figure 3.67
75˚C	120 (Control)	11,14	86,11	Figure 3.68
	120 (Test)	11,17	86,29	Figure 3.68

3.3.6 Effect of Heat-Shock on Differential Expression of Hsp60 β Subunit Gene

Heat shock at 65°C for 2 hours induced expression of Tpv Hsp60 β subunit gene. Induction was observed for 30 min, 60 min, 90 min and 120 min samples as revealed by real-time PCR graphics and lower CP values of the tests as compared to controls (Figures 3.72-3.75). Amplifications all were specific for the Tpv Hsp60 β subunit gene and average Tm for Hsp60 β was 86,45°C (±1,7).

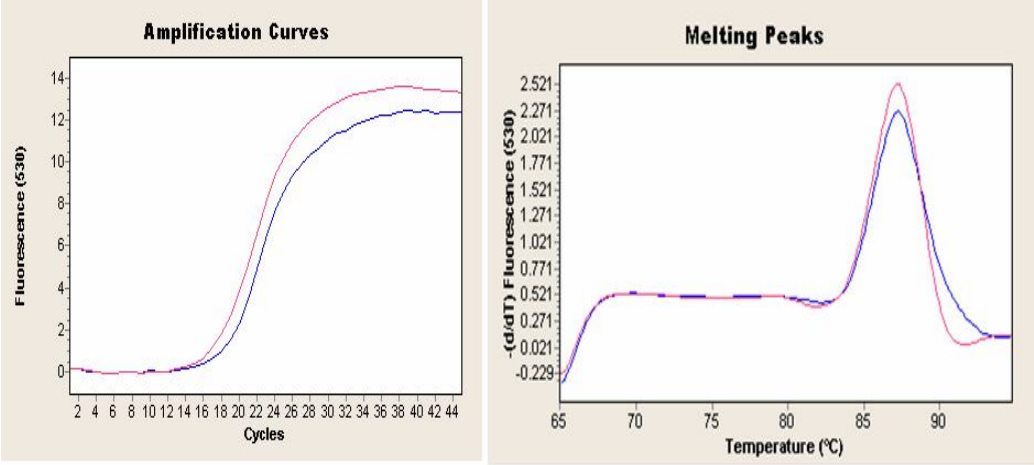

Figure 3.72: Real-time PCR graphics of control and heat-shocked samples at 65°C for 30 minutes. ——— Control (30th min following 72 h growth) CP:17,77 ——— Test (30 min heat-shock application) CP: 16,77

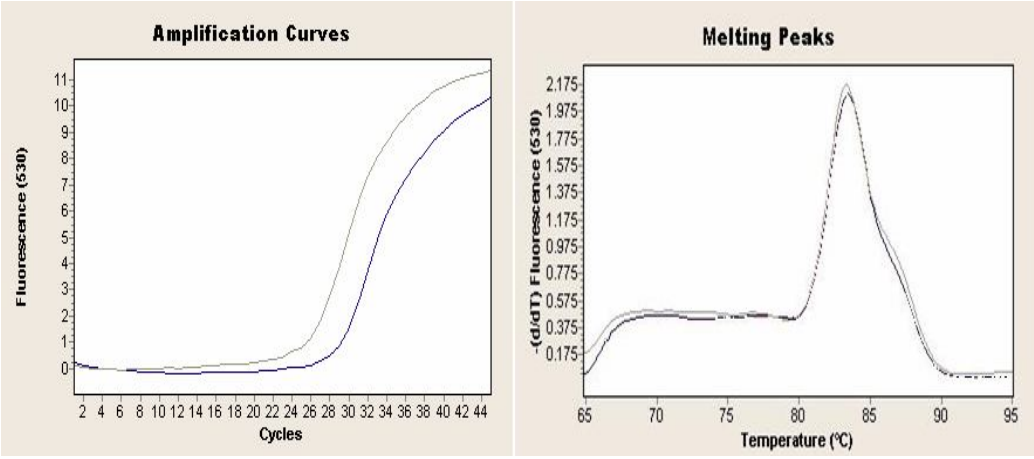

Figure 3.73: Real-time PCR graphics of control and heat-shocked samples at 65°C for 60 min. ——— Control (60th min following 72 h growth) CP: 27,71 ——— Test (60 min heat-shock application) CP: 25,13

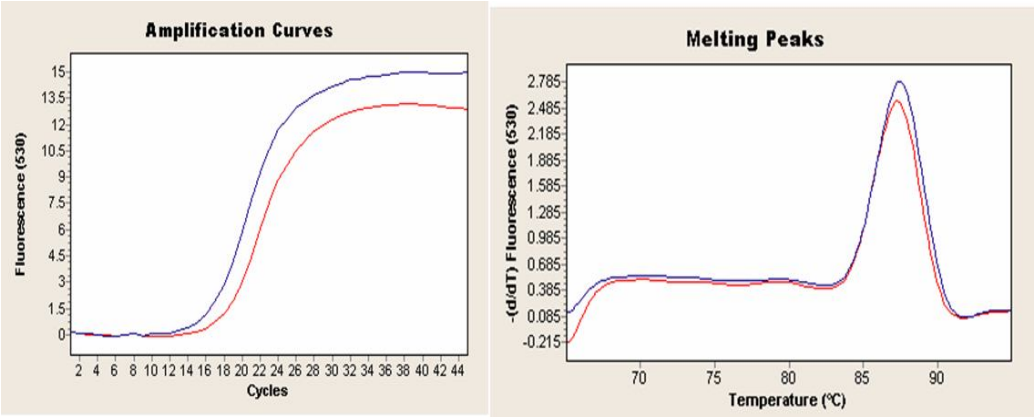

Figure 3.74: Real-time PCR graphics of control and heat-shocked samples at 65°C for 90 min. ——— Control (90th min following 72 h growth) CP: 17,18 ——— Test (90 min heat-shock application) CP: 15,80

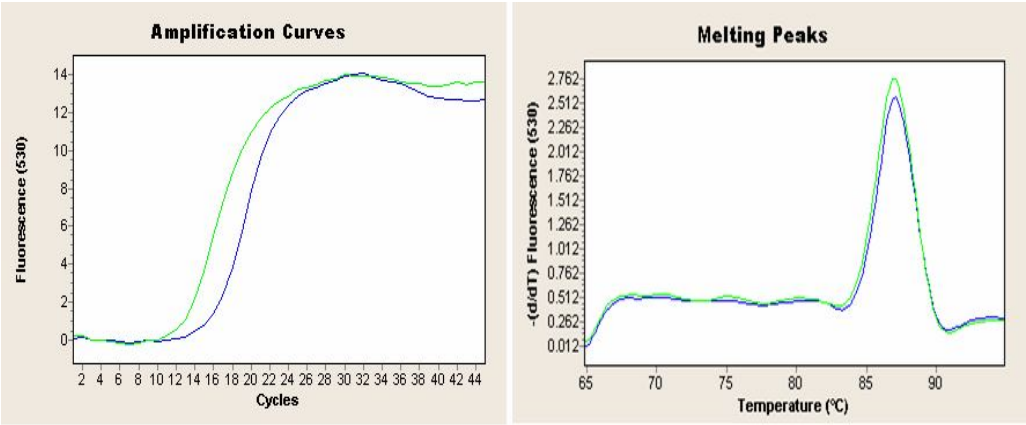

Figure 3.75: Real-time PCR graphics of control and heat-shocked samples at 65°C for 120 min. ——— Control (120th min following 72 h growth) CP: 14,94 ——— Test (120 min heat-shock application) CP: 11,82

Hsp60 β subunit gene expression is also induced by heat shock at 70°C for 2 hours. Induction was observed in the all test samples (30 min, 60 min, 90 min and 120 min), as could be seen in the real-time PCR graphics and lower CP values of the tests as compared to controls. The amplifications were all Hsp60 β gene specific and average Tm was 86,98°C (±0,19) (Figures 3.76-3.79).

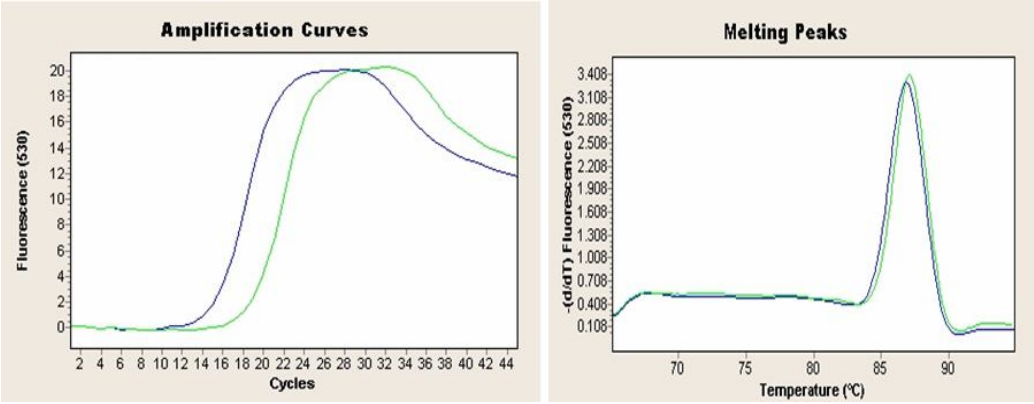

Figure 3.76: Real-time PCR graphics of control and heat-shocked samples at 70°C for 30 min. ——— Control (30th min following 72 h growth) CP: 17,66 ——— Test (30 min heat-shock) CP: 14

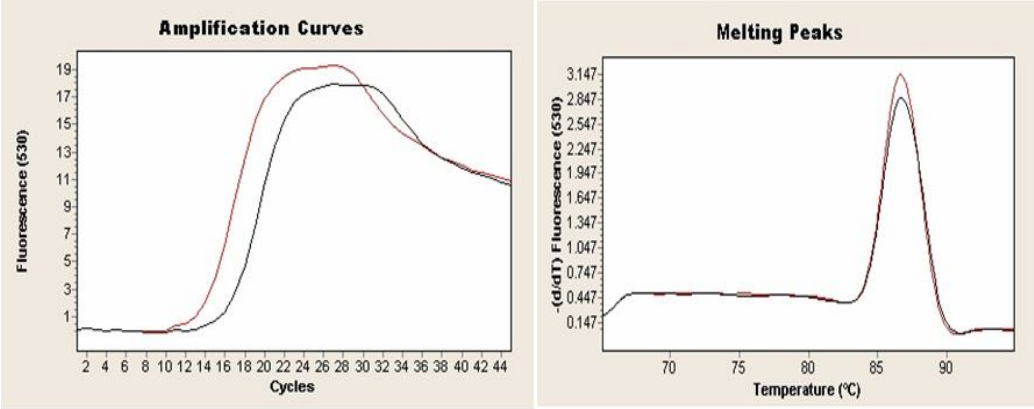

Figure 3.77: Real-time PCR graphics of control and heat-shocked samples at 70°C for 60 min. ——— Control (60th min following 72 h growth) CP: 15,15 ——— Test (60 min heat-shock) CP: 12,76

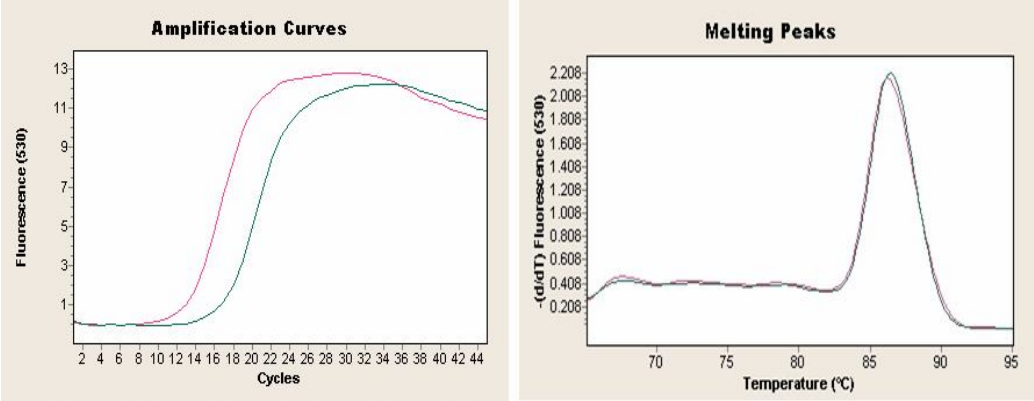

Figure 3.78: Real-time PCR graphics of control and heat-shocked samples at 70°C for 90 min. ——— Control (90th min following 72 h growth) CP: 16,02 ——— Test (90 min heat-shock) CP: 12,44

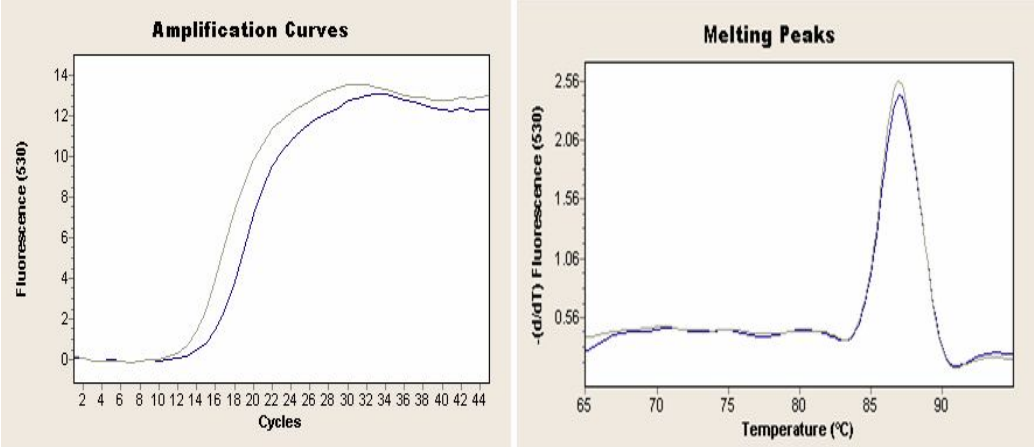

Figure 3.79: Real-time PCR graphics of control and heat-shocked samples at 70°C for 120 min. ——— Control (120th min following 72 h growth) CP: 14,59 ——— Test (120 min heat-shock) CP: 12,62

Induction in the expression of Hsp60 β gene was not observed, in response to heat shock at 75°C for 2 hours. Amplification in the control started earlier (CP:15,69) than test (CP:16,69) (Figure 3.80). Amplifications were specific for Hsp60 β gene, Tm being 87,4°C (±0,18).

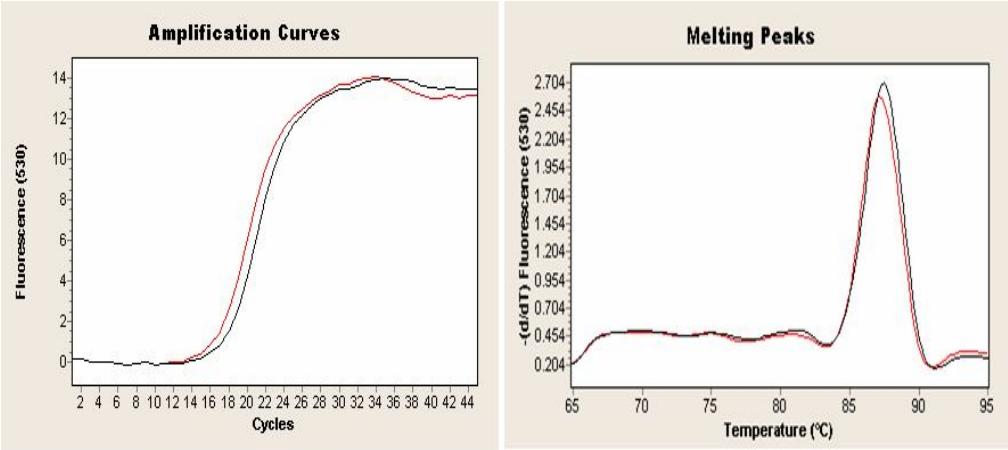

Figure 3.80: Real-time PCR graphics of control and heat-shocked samples at 75°C for 120 min. ——— Control (120th min following 72 h growth) CP: 15,69 ——— Test (120 min heat-shock application) CP: 16,69

CPs and Tms for amplification of Hsp60 β cDNA at 65˚C, 70˚C and 75˚C heat-shock are listed in the table 3.5.

Table 3.5: CP and Tm values for the study of Hsp60 β gene's differential expression as a response to heat-shock.

Heat Shock Temperature	Time (minute)	CP	Tm	Figure
65˚C	30 (Control)	17,77	87,49	Figure 3.69
	30 (Test)	16,77	87,40	Figure 3.69
	60 (Control)	27,71	84,02	Figure 3.70
	60 (Test)	25,13	86,55	Figure 3.70
	90 (Control)	17,18	87,43	Figure 3.71
	90 (Test)	15,80	87,59	Figure 3.71
	120 (Control)	14,94	87,17	Figure 3.72
	120 (Test)	11,82	87,12	Figure 3.72
70˚C	30 (Control)	17,66	87,23	Figure 3.73
	30 (Test)	14	87,02	Figure 3.73
	60 (Control)	15,15	86,95	Figure 3.74
	60 (Test)	12,76	86,85	Figure 3.74
	90 (Control)	16,02	86,77	Figure 3.75
	90 (Test)	12,44	86,71	Figure 3.75
	120 (Control)	14,59	87,16	Figure 3.76
	120 (Test)	12,62	87,12	Figure 3.76
75˚C	120 (Control)	15,69	87,3	Figure 3.77
	120 (Test)	16,69	87,55	Figure 3.77

3.3.7 Effect of Oxidative Stress on Differential Expression of Hsp60 α Subunit Gene

Oxidative stress, by exposure of mid-log phase culture to 0,008 mM H_2O_2 did not induce expression of Hsp60 α subunit gene during 45 minutes (Figures 3.81-3.83). After 60 min exposure to H_2O_2, amplification of test cDNA was slightly earlier than control cDNA as revealed by Real-time PCR graphics and CP values (Figure 3.84). This might indicate that H_2O_2 stress at 0,008 mM concentration begins to induce expression of Hsp60 α subunit gene starting from the 60th minute of exposure (Figure 3.84).

Oxidative stress imposed by 0,01 mM H_2O_2 addition to mid-log culture induced expression of Hsp60 α subunit gene increasingly for 90 minutes (Figures 3.85-3.87). But induction was not observed at the 120th min of H_2O_2 application (Figure 3.88).

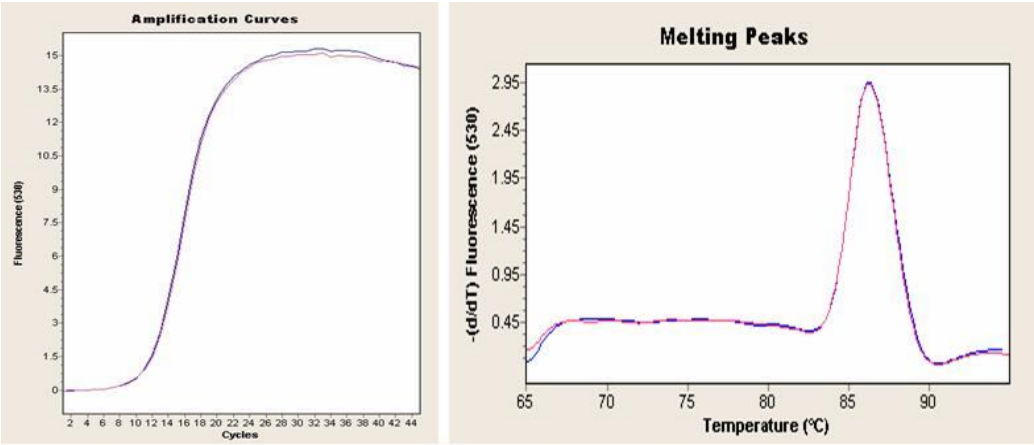

Figure 3.81: Real-time PCR graphics of control and 0,008 mM H_2O_2 exposed samples (for 15 min). ——— Control (15th min. following 72 h growth) CP:11 ——— Test (15 min after addition of 0,008 mM H_2O_2) CP:11,16

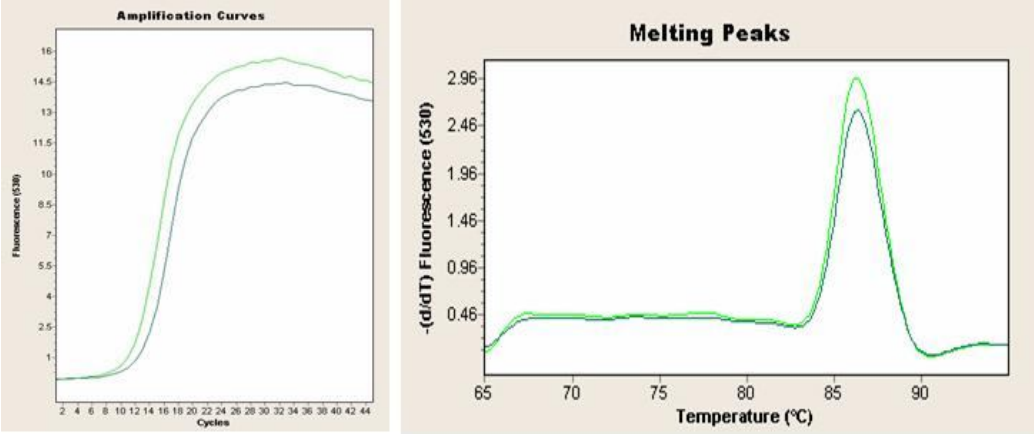

Figure 3.82: Real-time PCR graphics of control and 0,008 mM H_2O_2 exposed samples (for 30 min). _____ Control (30th min. following 72 h growth) CP: 10,83 _____ Test (30 min after addition of 0,008 mM H_2O_2) CP: 12,33

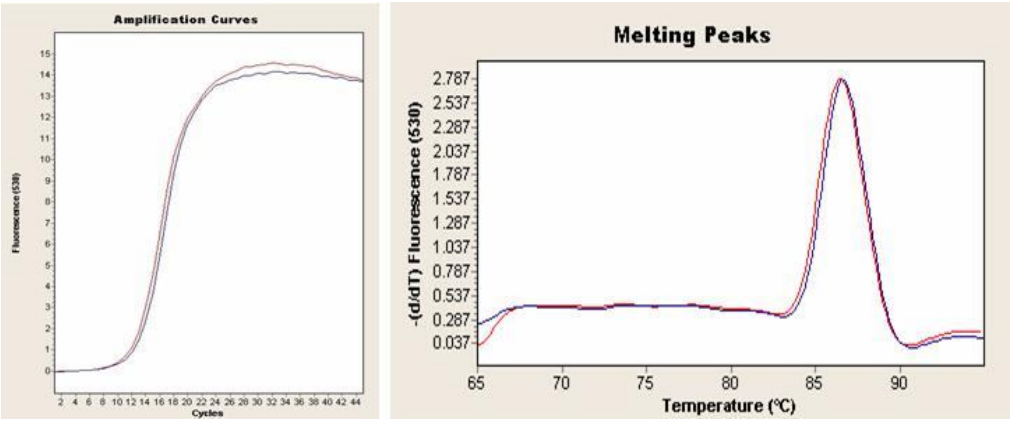

Figure 3.83: Real-time PCR graphics of control and 0,008 mM H_2O_2 exposed samples (for 45 min). _____ Control (45th min. following 72 h growth) CP: 11,61 _____ Test (45 min after addition of 0,008 mM H_2O_2) CP: 12,13

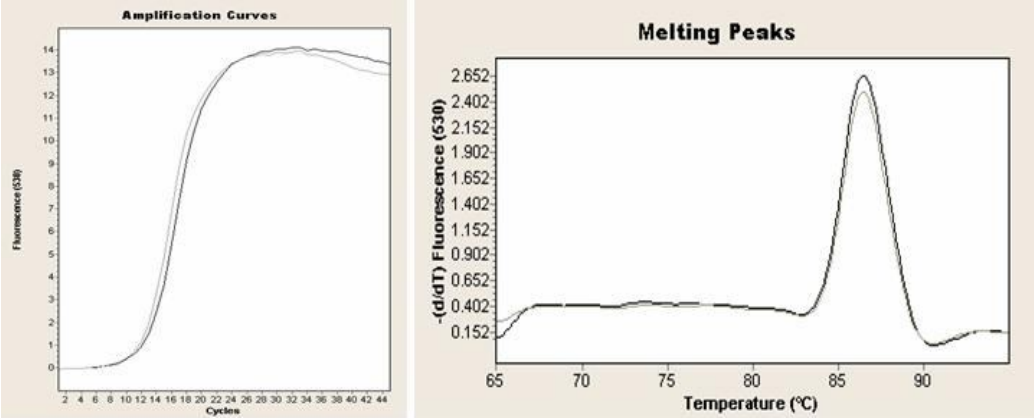

Figure 3.84: Real-time PCR graphics of control and 0,008 mM H_2O_2 exposed samples (for 60 min). ——— Control (60th min. following 72 h growth) CP: 12,09 ——— Test (60 min after addition of 0,008 mM H_2O_2) CP: 11,35

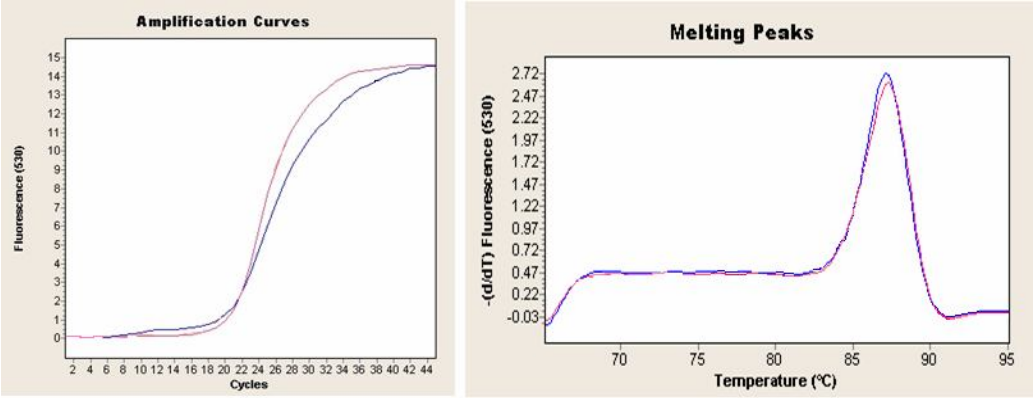

Figure 3.85: Real-time PCR graphics of control and 0,01 mM H_2O_2 exposed samples (for 30 min). ——— Control (30th min. following 72 h growth) CP: 19,95 ——— Test (30 min after addition of 0,01 mM H_2O_2) CP: 19,78

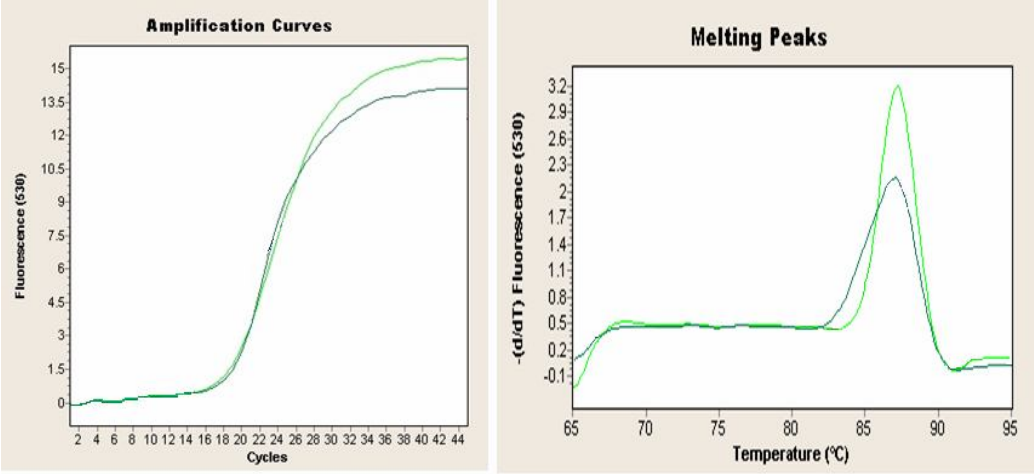

Figure 3.86: Real-time PCR graphics of control and 0,01 mM H_2O_2 exposed samples (for 60 min). Control (60th min. following 72 h growth) CP: 18,16 Test (60 min after addition of 0,01 mM H_2O_2) CP:17,97

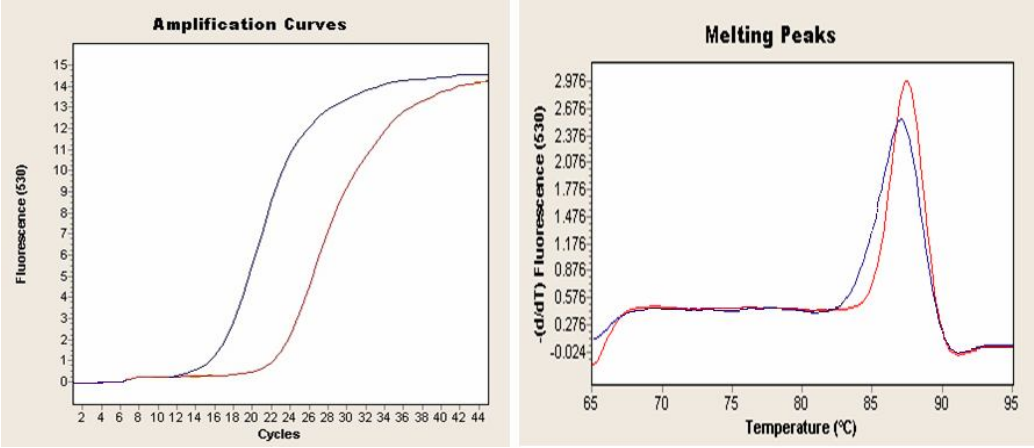

Figure 3.87: Real-time PCR graphics of control and 0,01 mM H_2O_2 exposed samples (for 90 min). Control (90th min. following 72 h growth) CP: 21,93 Test (90 min after addition of 0,01 mM H_2O_2) CP: 15,82

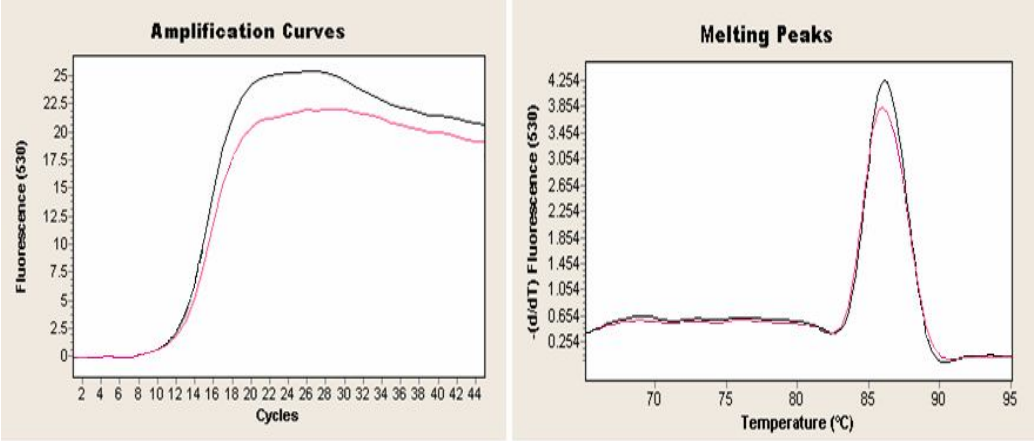

Figure 3.88: Real-time PCR graphics of control and 0,01 mM H_2O_2 exposed samples (for 120 min). ——— Control (120th min. following 72 h growth) CP: 11,29 ——— Test (120 min. after addition of 0,01 mM H_2O_2) CP: 11,51

Exposure of the mid-log phase cultures to 0,02 mM H_2O_2 induced expression of Hsp60 α subunit gene increasingly for the 120 minutes (Figures 3.89-3.92).

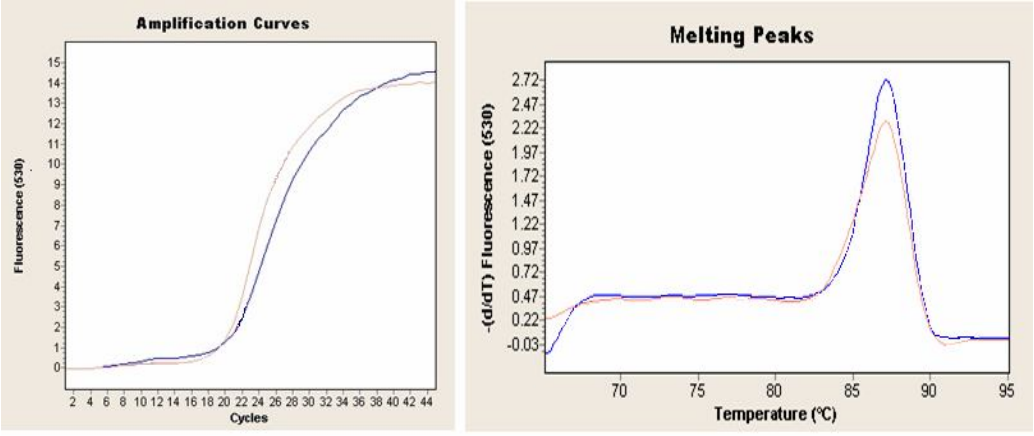

Figure 3.89: Real-time PCR graphics of control and 0,02 mM H_2O_2 exposed samples (for 30 min). ——— Control (30th min. following 72 h growth) CP: 19,95 ——— Test (30 min after addition of 0,02 mM H_2O_2) CP: 18,89

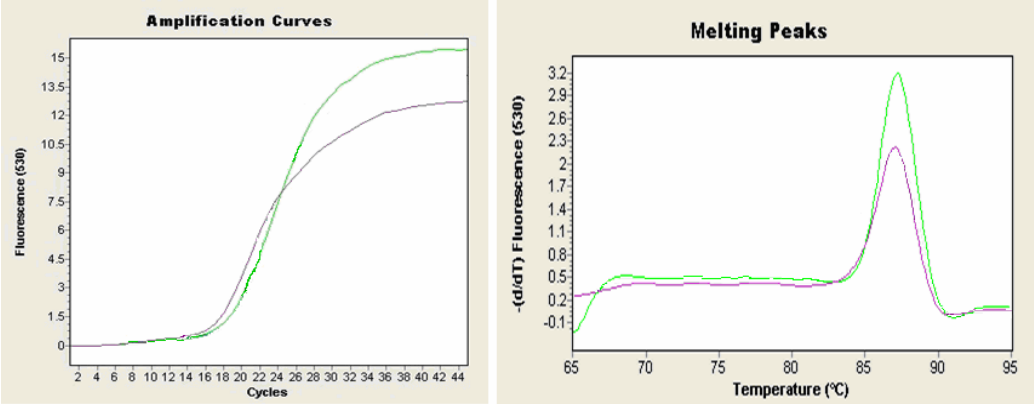

Figure 3.90: Real-time PCR graphics of control and 0,02 mM H_2O_2 exposed samples (for 60 min). Control (60th min. following 72 h growth) CP: 18,16 Test (60 min after addition of 0,02 mM H_2O_2) CP: 16,32

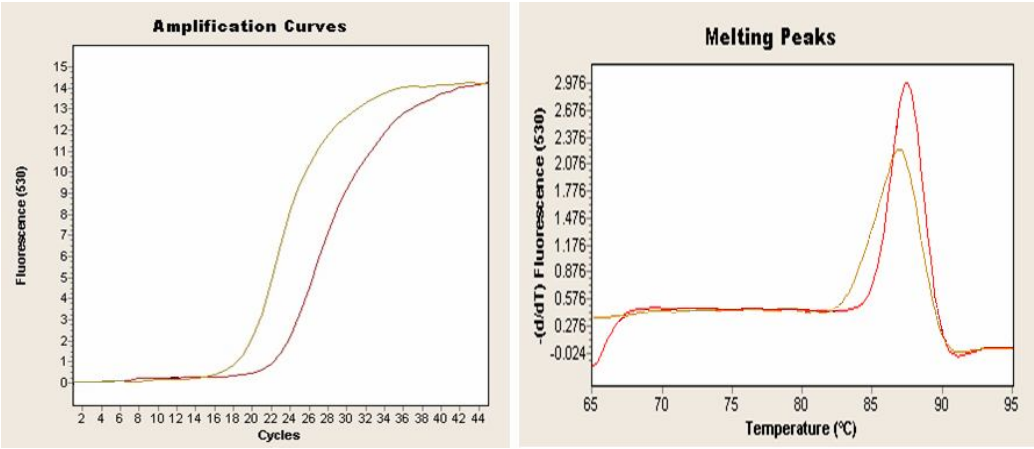

Figure 3.91: Real-time PCR graphics of control and 0,02 mM H_2O_2 exposed samples (for 90 min). Control (90th min. following 72 h growth) CP: 21,93 Test (90 min after addition of 0,02 mM H_2O_2) CP: 18,19

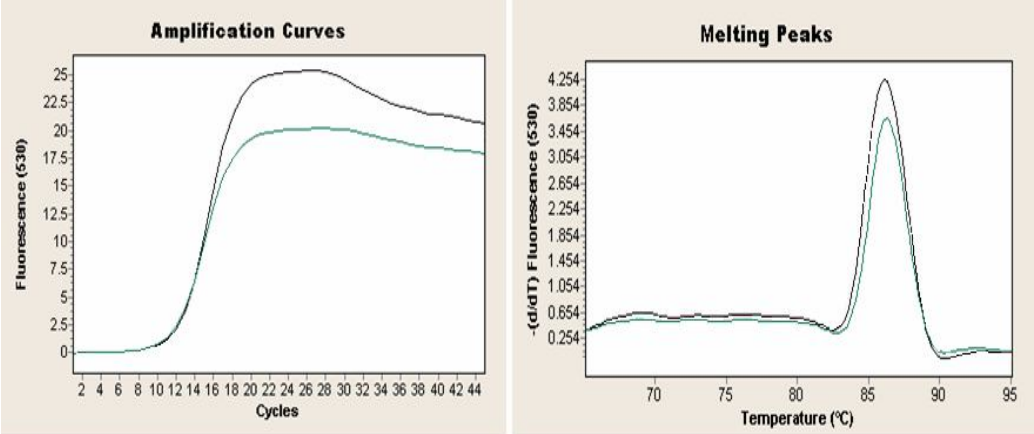

Figure 3.92: Real-time PCR graphics of control and 0,02 mM H_2O_2 exposed samples (for 120 min). ——— Control (120th min. following 72 h growth) CP: 11,29 ——— Test (120 min after addition of 0,02 mM H_2O_2) CP: 10,79

Induction of expression of Hsp60 α subunit gene started 60 min later following the addition of 0,03 mM H_2O_2 to mid-log culture and induction lasted 90 min (Figures 3.93-3.96). There was no induction of Hsp60 α subunit gene expression within first 30 minutes of H_2O_2 addition (Figure 3.93). Induction was not obsered at 120th min of the H_2O_2 addition (Figure 3.96).

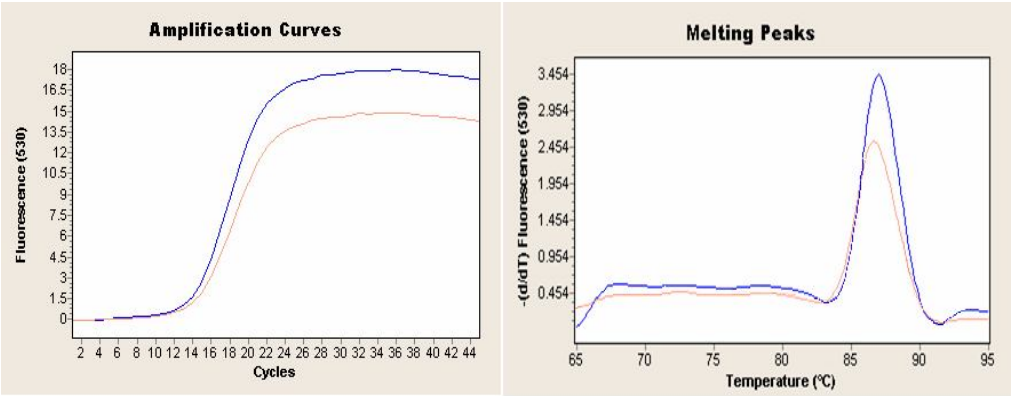

Figure 3.93: Real-time PCR graphics of control and 0,03 mM H_2O_2 exposed samples (for 30 min). ——— Control (30th min. following 72 h growth) CP: 13,31 ——— Test (30 min after addition of 0,03 mM H_2O_2) CP: 13,73

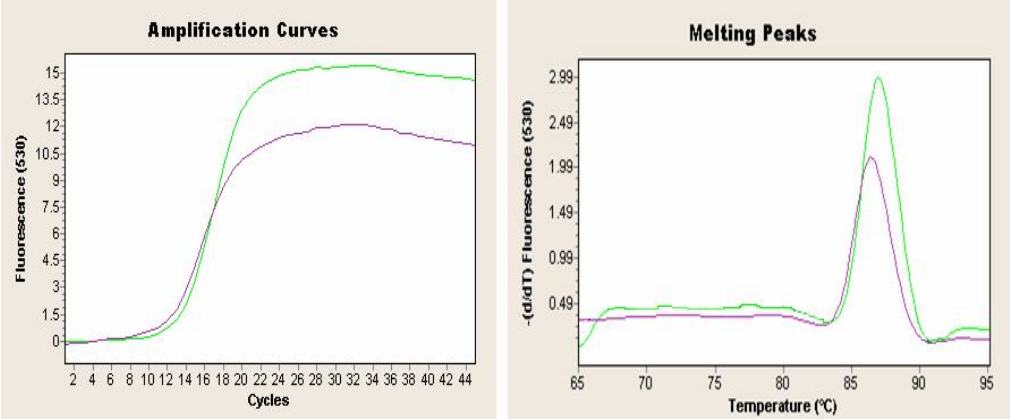

Figure 3.94: Real-time PCR graphics of control and 0,03 mM H_2O_2 exposed samples (for 60 min). ——— Control (60th min. following 72 h growth) CP: 12,54 ——— Test (60 min after addition of 0,03 mM H_2O_2) CP: 11,48

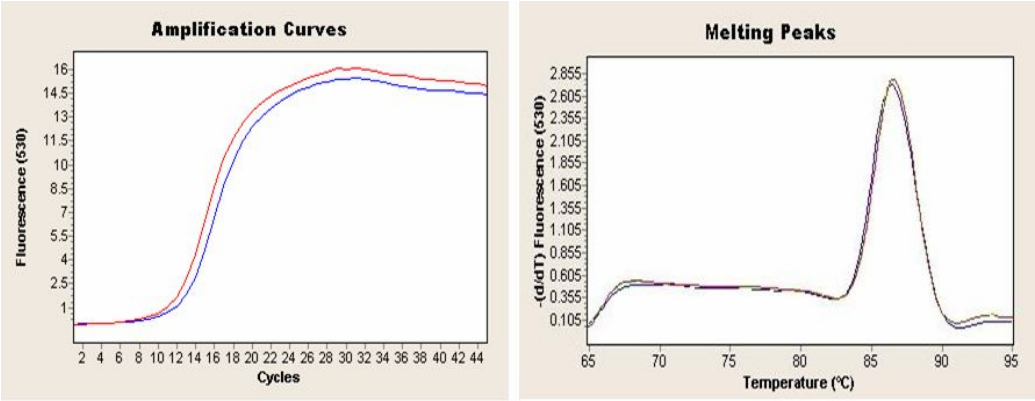

Figure 3.95: Real-time PCR graphics of control and 0,03 mM H_2O_2 exposed samples (for 90 min). ——— Control (90th min. following 72 h growth) CP: 11,72 ——— Test (90 min after addition of 0,03 mM H_2O_2) CP: 10,91

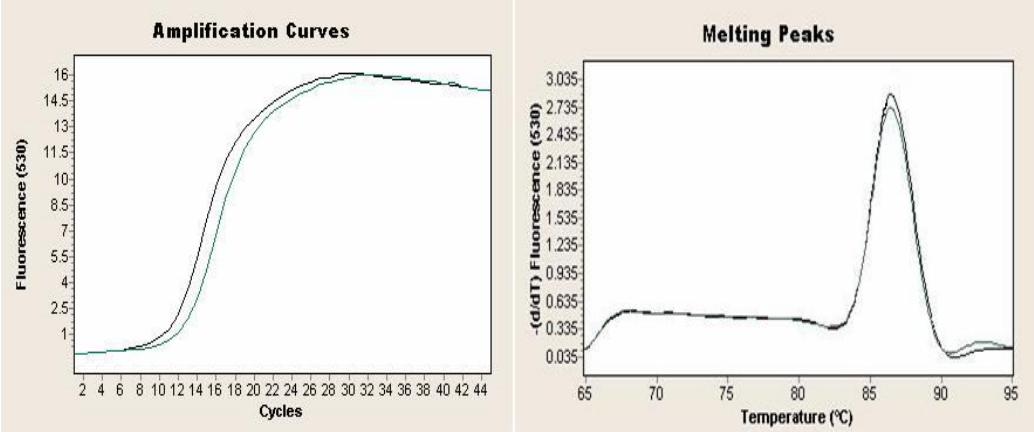

Figure 3.96: Real-time PCR graphics of control and 0,03 mM H_2O_2 exposed samples (for 120 min). ——— Control (120th min. following 72 h growth) CP: 10,32 ——— Test (120 min after addition of 0,03 mM H_2O_2) CP: 11,69

H_2O_2 stress at 0,05 mM concentration induced expression of Hsp60 α subunit gene during first 30 minutes (Figures 3.97 and 3.98). Since cell growth was significantly retarded after H_2O_2 addition at this concentration, the amount of RNA isolated from the samples was very low, especially after 30th min of the addition. For this reason, Real-Time PCR for 45 and 60 min samples could not be performed.

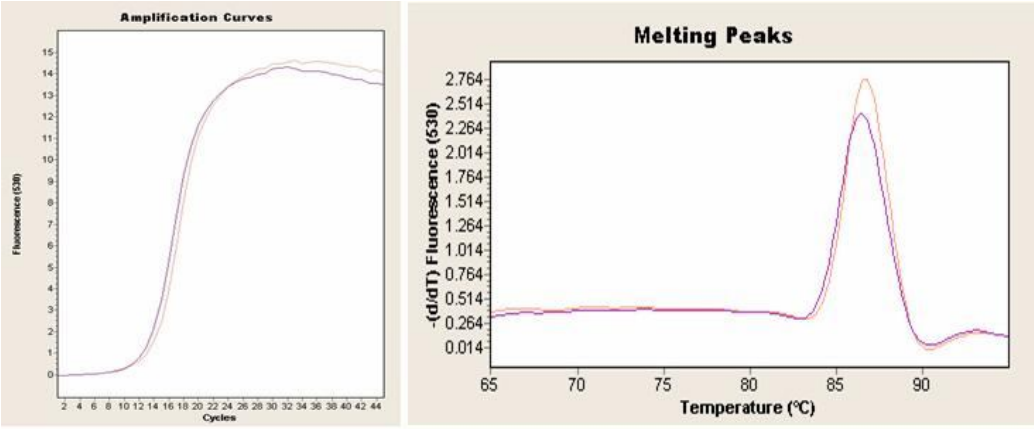

Figure 3.97: Real-time PCR graphics of control and 0,05 mM H_2O_2 exposed samples (for 15 min). ——— Control (15th min. following 72 h growth) CP: 13,01 ——— Test (15 min. after addition of 0,05 mM H_2O_2) CP: 12,21

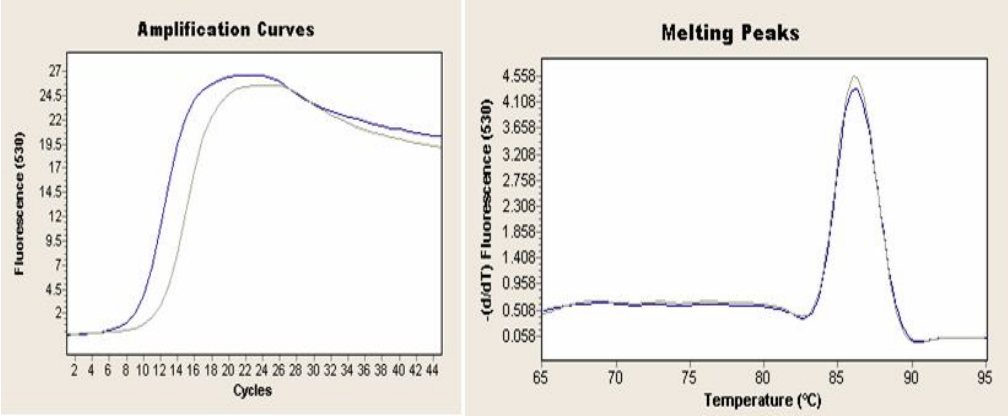

Figure 3.98: Real-time PCR graphics of control and 0,05 mM H_2O_2 exposed samples (for 30 min). ——— Control (30th min. following 72 h growth) CP: 10,83 ——— Test (30 min. after additon of 0,05 mM H_2O_2) CP: 8,20

CPs and Tms for differential expression of Hsp60 α gene as a response to oxidative stress by 0,008, 0,01, 0,02, 0,03 and 0,05 mM H_2O_2 are listed in the table 3.6.

3.3.8 Effect of Oxidative Stress on Differential Expression of Hsp60 β Subunit Gene

Oxidative stress, imposed by additon of 0,008 mM H_2O_2 to mid-log phase culture did not induce expression of Hsp60 β subunit gene during 60 minutes (Figures 3.99-3.102).

Table 3.6: CP and Tm values for Real Time PCR performed to analyze differential expression of Hsp60 α gene as a response to oxidative stress.

H_2O_2 [mM]	Time	CP	Tm	Figure
0,008	15 (Control)	11	86,47	Figure 3.78
	15 (Test)	11,16	86,48	Figure 3.78
	30 (Control)	10,83	86,50	Figure 3.79
	30 (Test)	12,33	86,53	Figure 3.79
	45 (Control)	11,61	86,63	Figure 3.80
	45 (Test)	12,13	86,79	Figure 3.80
	60 (Control)	12,09	86,65	Figure 3.81
	60 (Test)	11,35	86,62	Figure 3.81
0,01	30 (Control)	19,95	87,28	Figure 3.82
	30 (Test)	19,78	87,38	Figure 3.82
	60 (Control)	18,16	87,34	Figure 3.83
	60 (Test)	17,97	87,13	Figure 3.83
	90 (Control)	21,93	87,60	Figure 3.84
	90 (Test)	15,82	87,18	Figure 3.84
	120 (Control)	11,29	86,31	Figure 3.85
	120 (Test)	11,51	86,30	Figure 3.85
0,02	30 (Control)	19,95	87,28	Figure 3.86
	30 (Test)	18,89	87,19	Figure 3.86
	60 (Control)	18,16	87,34	Figure 3.87
	60 (Test)	16,32	87,19	Figure 3.87
	90 (Control)	21,93	87,60	Figure 3.88
	90 (Test)	18,19	87,07	Figure 3.88
	120 (Control)	11,29	86,31	Figure 3.89
	120 (Test)	10,79	86,42	Figure 3.89
0,03	30 (Control)	13,31	87,16	Figure 3.90
	30 (Test)	13,73	86,91	Figure 3.90
	60 (Control)	12,54	87,15	Figure 3.91
	60 (Test)	11,48	86,60	Figure 3.91
	90 (Control)	11,72	86,71	Figure 3.92
	90 (Test)	10,91	86,79	Figure 3.92
	120 (Control)	10,32	86,69	Figure 3.93
	120 (Test)	11,69	86,64	Figure 3.93
0,05	15 (Control)	13,01	86,79	Figure 3.94
	15 (Test)	12,21	86,60	Figure 3.94
	30 (Control)	10,83	86,33	Figure 3.95
	30 (Test)	8,20	86,34	Figure 3.95

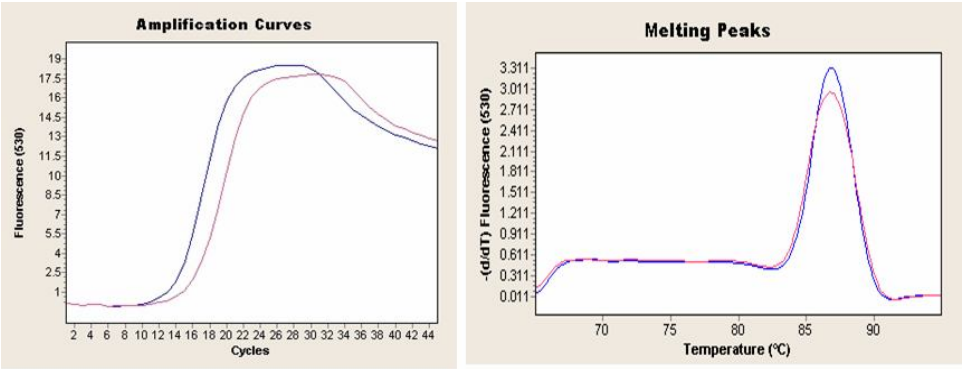

Figure 3.99: Real-time PCR graphics of control and oxidatively stressed (by 0,008 mM H_2O_2) samples at 15th min. ——— Control (at 15th min. of 72 h growth) CP: 13,03 ——— Test (at 15th min. following addition of 0,008 mM H_2O_2) CP: 15,10

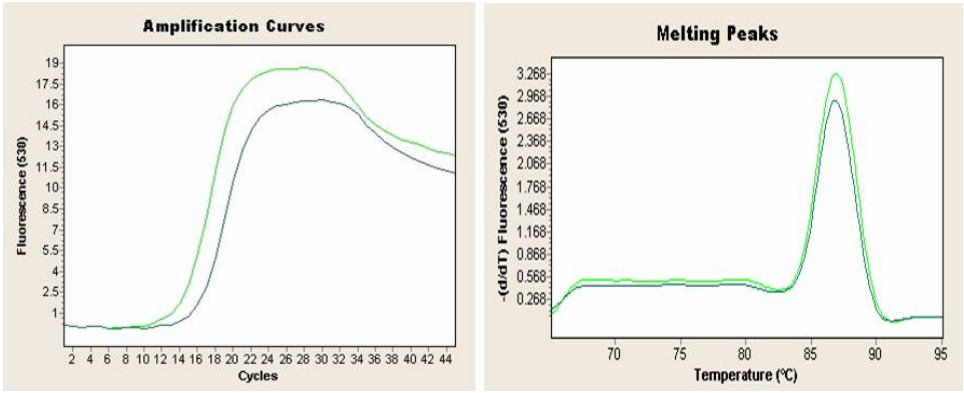

Figure 3.100: Real-time PCR graphics of control and oxidatively stressed (by 0,008 mM H_2O_2) samples at 30th min. ——— Control (at 30th min. of 72 h growth) CP: 13,15 ——— Test (at 30th min. following addition of 0,008 mM H_2O_2) CP: 14,90

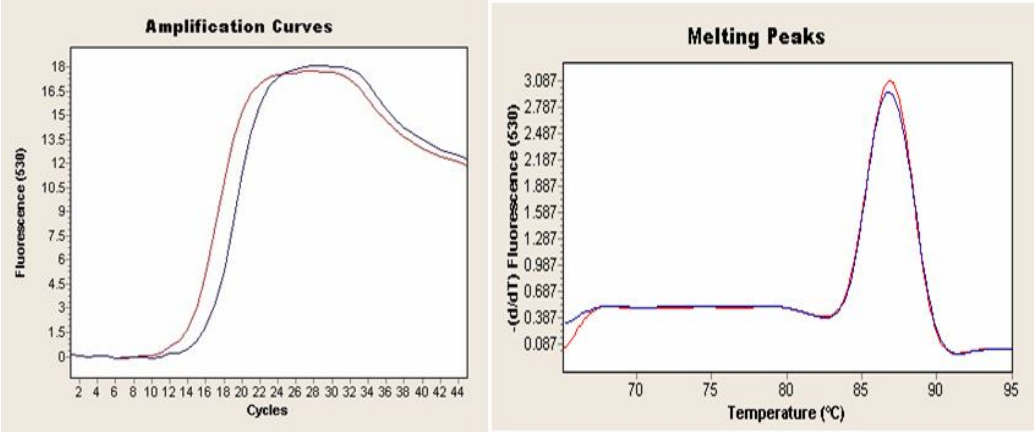

Figure 3.101: Real-time PCR graphics of control and oxidatively stressed (by 0,008 mM H_2O_2) samples at 45th min. _____ Control (at 45th min. of 72 h growth) CP: 13,08 _____ Test (at 45th min. following addition of 0,008 mM H_2O_2) CP: 14,97

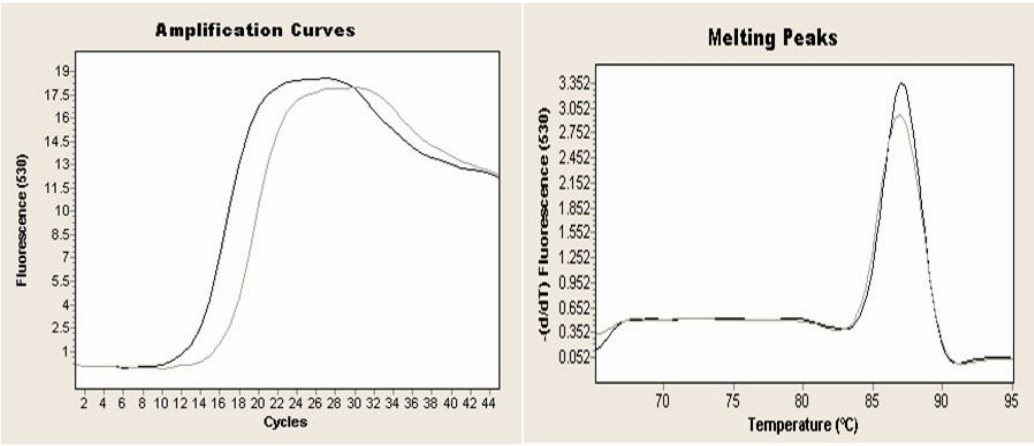

Figure 3.102: Real-time PCR graphics of control and oxidatively stressed (by 0,008 mM H_2O_2) samples at 60th min. _____ Control (at 60th min. of 72 h growth) CP: 12,51 _____ Test (at 60th min. following addition of 0,008 mM H_2O_2) CP: 15,25

H_2O_2 stress at 0,01 mM concentration induced expression of Hsp60 β subunit gene for 90 minutes (Figures 3.103, 3.104 and 3.105). However, no induction was observed, at this concentration, at 120th min of the H_2O_2 addition (Figure 3.106).

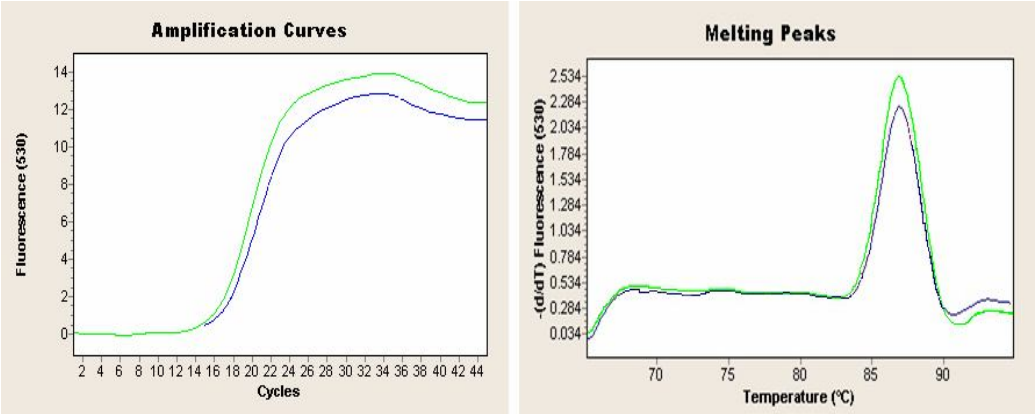

Figure 3.103: Real-time PCR graphics of control and oxidatively stressed (by 0,01 mM H_2O_2) samples at 30th min. Control (at 30th min. of 72 h growth) CP: 15,92 Test (at 30th min. following addition of 0,01 mM H_2O_2) CP: 15,45

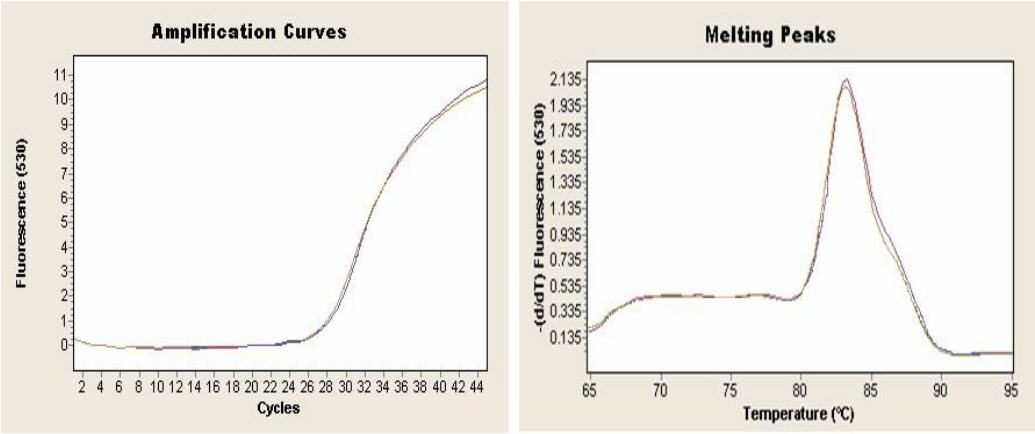

Figure 3.104: Real-time PCR graphics of control and oxidatively stressed (by 0,01 mM H_2O_2) samples at 60th min. Control (at 60th min. of 72 h growth) CP: 26,97 Test (at 60th min. following addition of 0,01 mM H_2O_2) CP: 26,61

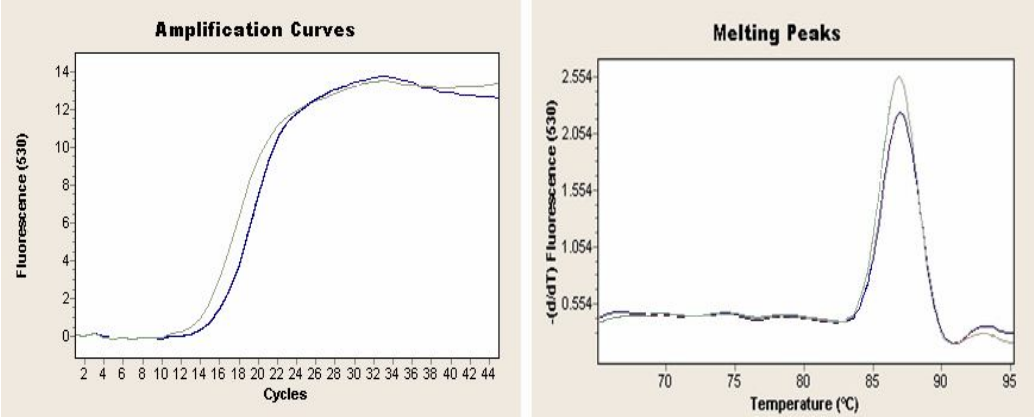

Figure 3.105: Real-time PCR graphics of control and oxidatively stressed (by 0,01 mM H_2O_2) samples at 90th min. Control (at 90th min. of 72 h growth) CP: 14,77 Test (at 90th min. following addition of 0,01 mM H_2O_2) CP: 13,29

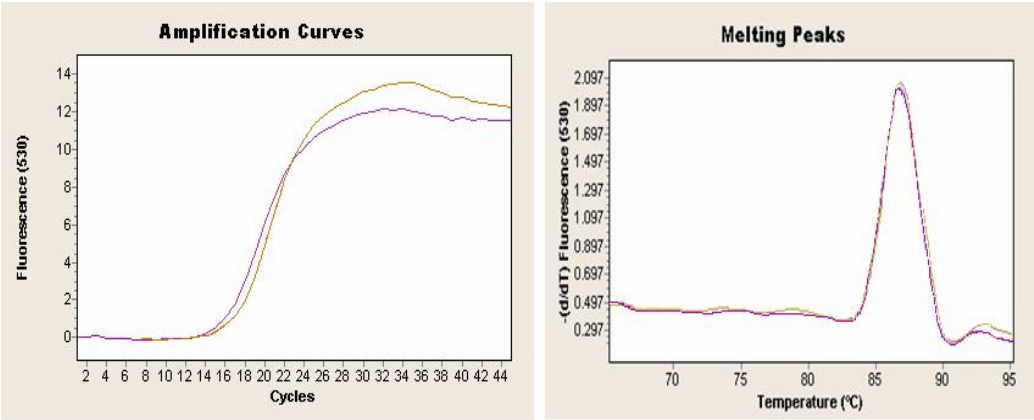

Figure 3.106: Real-time PCR graphics of control and oxidatively stressed (by 0,01 mM H_2O_2) samples at 120th min. Control (at 120th min. of 72 h growth) CP: 14,90 Test (at 120th min. following addition of H_2O_2) CP: 16,10

H_2O_2 stress at 0,02 mM H_2O_2 concentration induced expression of Hsp60 β subunit gene at 60th minute (Figures 3.107 and 3.108). Induction was not observed after 90th min following H_2O_2 addition (Figures 3.109 and 3.110).

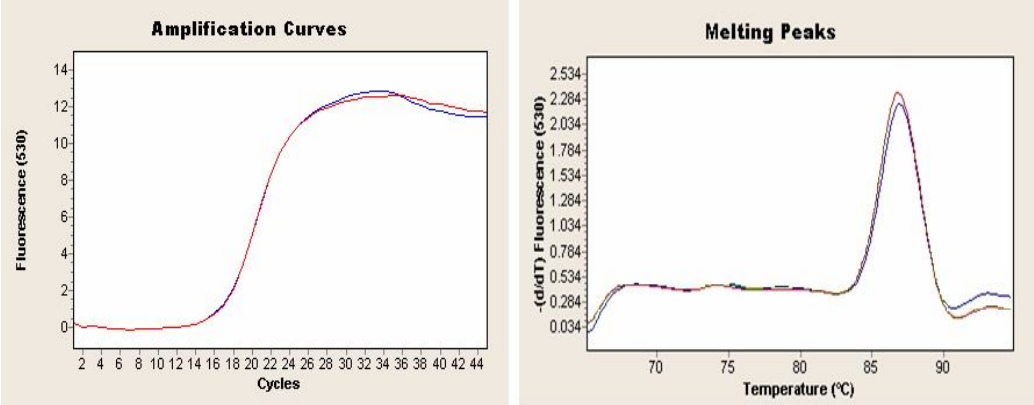

Figure 3.107: Real-time PCR graphics of control and oxidatively stressed (by 0,02 mM H_2O_2) samples at 30th min. ——— Control (at 30th min. of 72 h growth) CP: 15,92 ——— Test (at 30th min. following addition of 0,02 mM H_2O_2) CP: 15,93

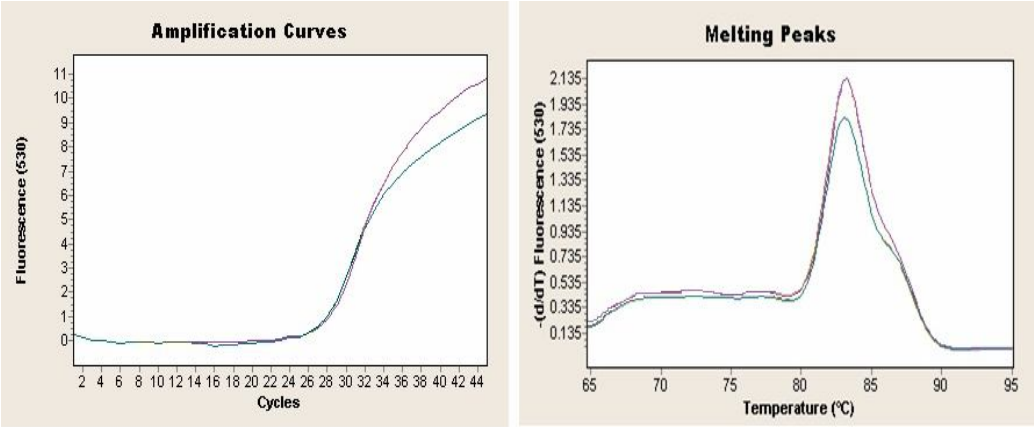

Figure 3.108: Real-time PCR graphics of control and oxidatively stressed (by 0,02 mM H_2O_2) samples at 60th min. ——— Control (at 60th min. of 72 h growth) CP: 26,97 ——— Test (at 60th min. following addition of 0,02 mM H_2O_2) CP: 26,34

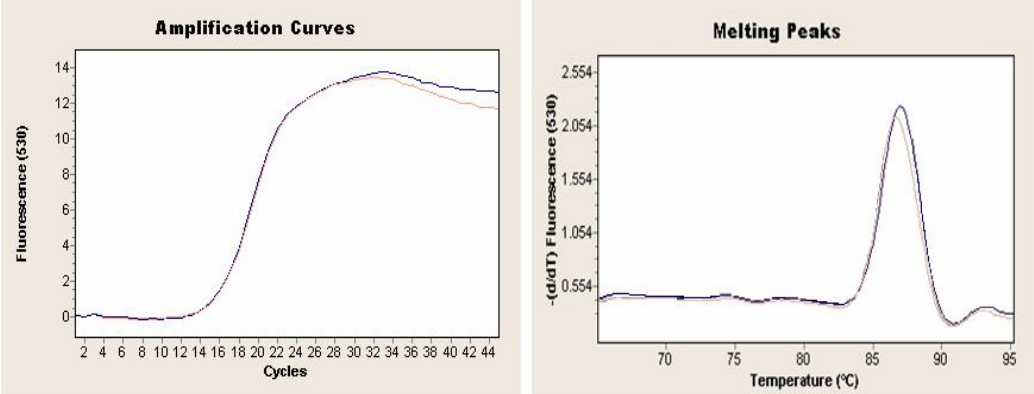

Figure 3.109: Real-time PCR graphics of control and oxidatively stressed (by 0,02 mM H_2O_2) samples at 90th min. Control (at 90th min. of 72 h growth) CP: 14,77 Test (at 90th min. following addition of 0,02 mM H_2O_2) CP: 14,86

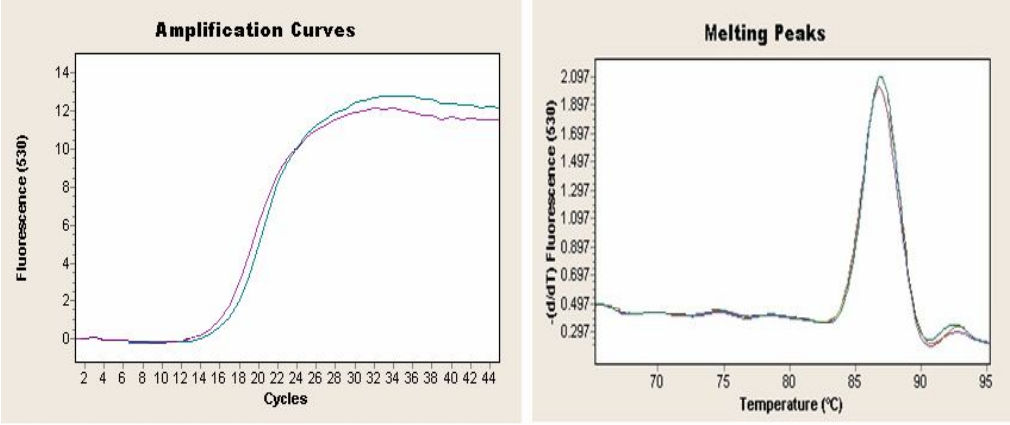

Figure 3.110: Real-time PCR graphics of control and oxidatively stressed (by 0,02 mM H_2O_2) samples at 120th min. Control (at 120th min. of 72 h growth) CP: 14,90 Test (at 120th min. following addition of 0,02 mM H_2O_2) CP: 15,84

Induction of Hsp60 β subunit gene expression was not observed at 0,03 mM H_2O_2 addition up to 60 minutes (Figures 3.111 and 3.112). H_2O_2 stress at 0,03 mM concentration increasingly induced expression of the β-subunit gene at 90th min and 120th min (Figures 3.113 and 3.114).

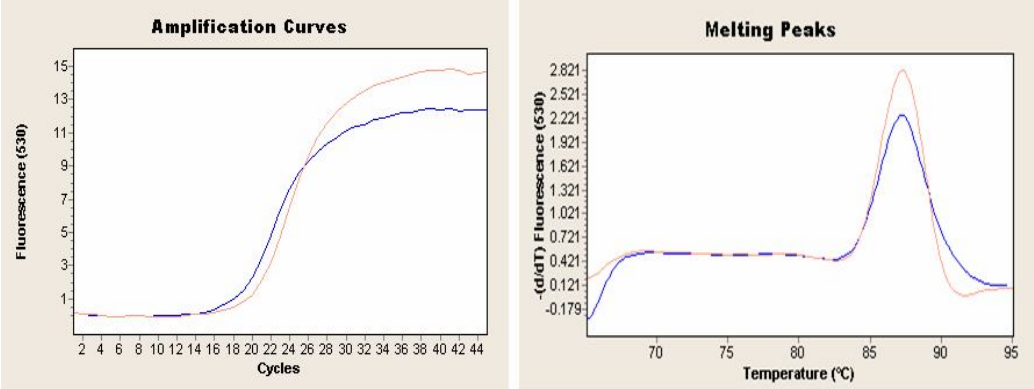

Figure 3.111: Real-time PCR graphics of control and H_2O_2 exposed samples at 30th min. Control (at 30th min. following 72 h growth) CP: 17,77 Test (30 min after 0,03 mM H_2O_2 addition) CP: 19,37

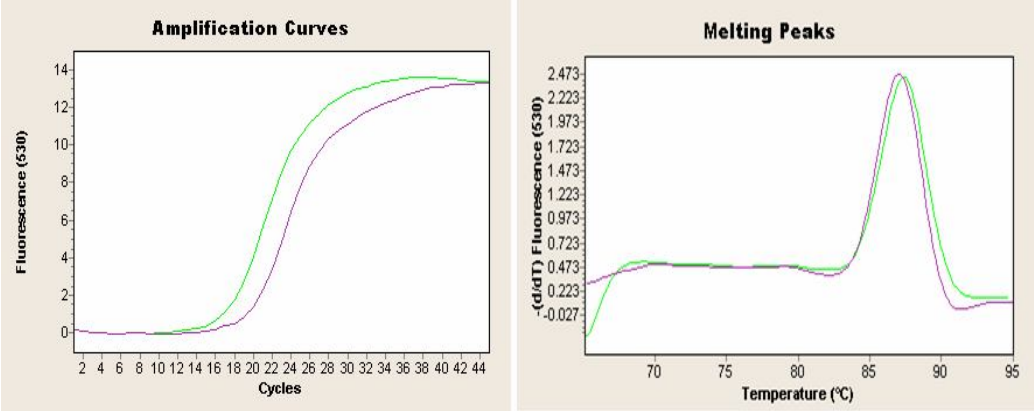

Figure 3.112: Real-time PCR graphics of control and H_2O_2 exposed samples at 60th min. Control (at 60th min. following 72 h growth) CP: 16,54 Test (60 min after 0,03 mM H_2O_2 addition) CP: 18,88

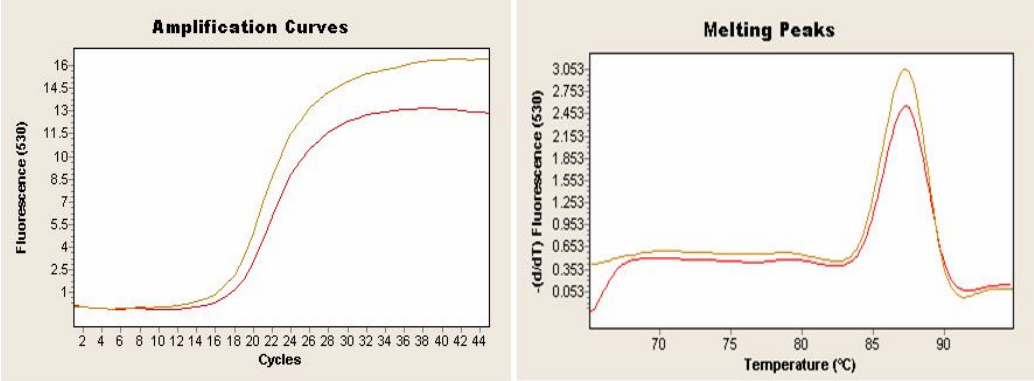

Figure 3.113: Real-time PCR graphics of control and H_2O_2 exposed samples at 90th min. Control (at 90th min. following 72 h growth) CP: 17,18 Test (90 min after 0,03 mM H_2O_2 addition) CP: 16,54

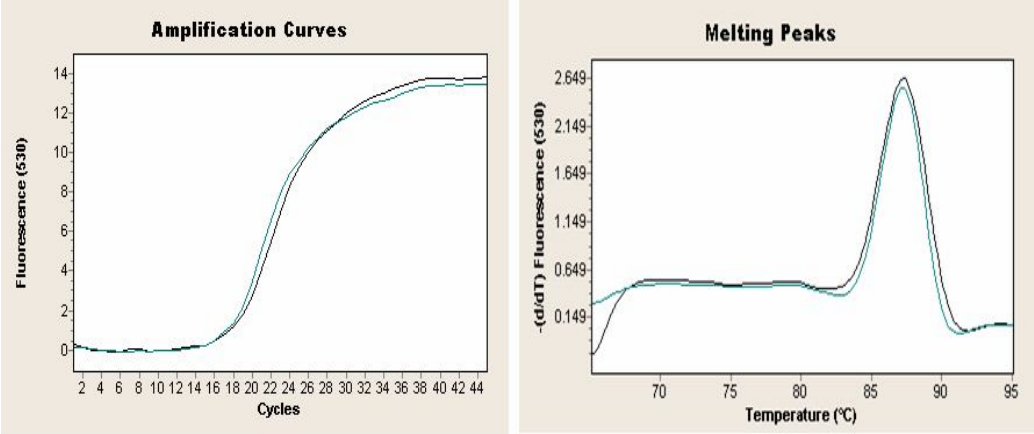

Figure 3.114: Real-time PCR graphics of control and H_2O_2 exposed samples at 120th min. Control (at 120th min. following 72 h growth) CP: 17,51 Test (120 min after 0,03 mM H_2O_2 addition) CP: 16,74

At 0,05 mM H_2O_2 concentration Hsp60 β subunit gene expression gradually increased for 1 h following H_2O_2 addition (Figures 3.115 and 3.116).

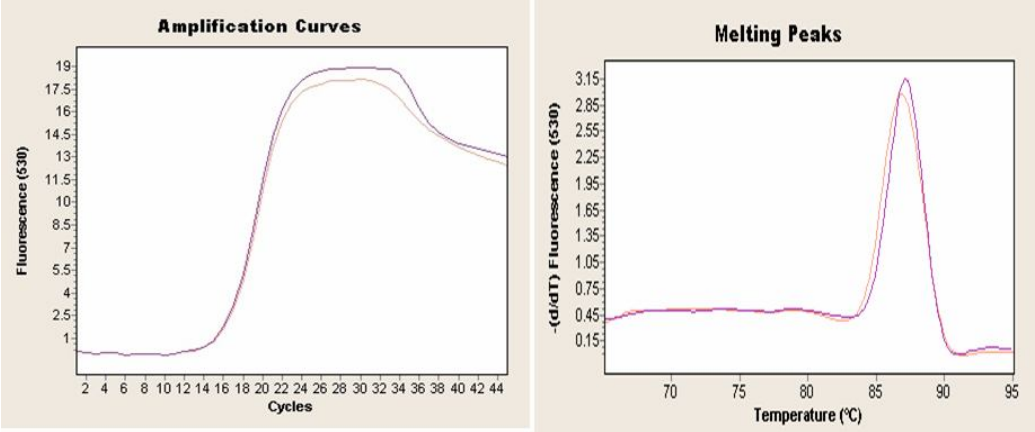

Figure 3.115: Real-time PCR graphics of control and H_2O_2 exposed samples at 15th min. Control (at 15th min. after 72 h growth) CP: 15,16 Test (at 15th min. of 0,05 mM H_2O_2 addition) CP: 15,08

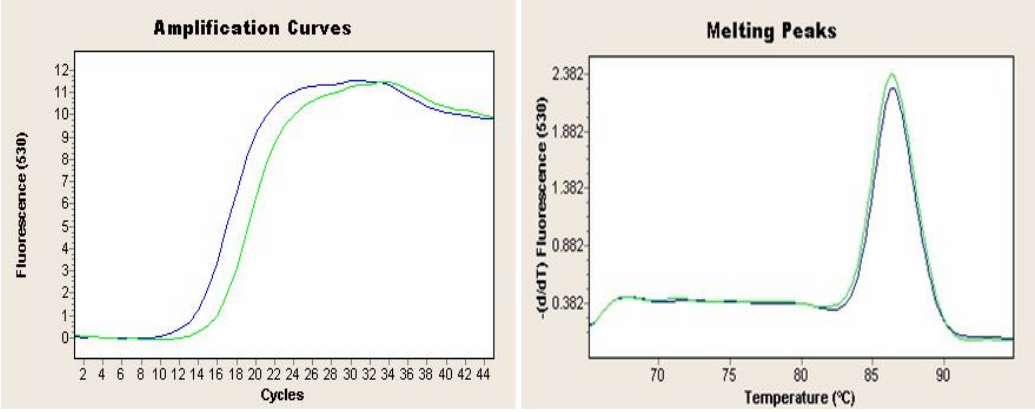

Figure 3.116: Real-time PCR graphics of control and H_2O_2 exposed samples at 30th min. Control (at 30th minute after 72 h growth) CP: 14,80 Test (at 30th min. of 0,05 mM H_2O_2 addition) CP: 12,85

CPs and Tms for differential expression of Hsp60 β gene as a response to oxidative stress induced by 0,008, 0,01, 0,02, 0,03 and 0,05 mM H_2O_2 are listed in the table 3.7

Table 3.7: CP and Tm values for Real Time PCR performed to study differential expression of Hsp60 β gene as a response to oxidative stress.

H_2O_2 [mM]	Time	CP	Tm	Figure
0,008	15 (Control)	13,03	87,02	Figure 3.96
	15 (Test)	15,10	87,08	Figure 3.96
	30 (Control)	13,15	87,13	Figure 3.97
	30 (Test)	14,90	87,03	Figure 3.97
	45 (Control)	13,08	87,08	Figure 3.98
	45 (Test)	14,97	87,08	Figure 3.98
	60 (Control)	12,51	87,23	Figure 3.99
	60 (Test)	15,25	87,16	Figure 3.99
0,01	30 (Control)	15,92	87,04	Figure 3.100
	30 (Test)	15,45	87,08	Figure 3.100
	60 (Control)	26,97	86,46	Figure 3.101
	60 (Test)	26,61	86,61	Figure 3.101
	90 (Control)	14,77	87,08	Figure 3.102
	90 (Test)	13,29	86,99	Figure 3.102
	120 (Control)	14,90	86,91	Figure 3.103
	120 (Test)	16,10	87,01	Figure 3.103
0,02	30 (Control)	15,92	87,04	Figure 3.104
	30 (Test)	15,93	87,01	Figure 3.104
	60 (Control)	26,97	86,46	Figure 3.105
	60 (Test)	26,34	86,61	Figure 3.105
	90 (Control)	14,77	87,08	Figure 3.106
	90 (Test)	14,86	86,94	Figure 3.106
	120 (Control)	14,90	86,91	Figure 3.107
	120 (Test)	15,84	87,01	Figure 3.107
0,03	30 (Control)	17,77	87,49	Figure 3.108
	30 (Test)	19,37	87,49	Figure 3.108
	60 (Control)	16,54	87,54	Figure 3.109
	60 (Test)	18,88	87,24	Figure 3.109
	90 (Control)	17,18	87,43	Figure 3.110
	90 (Test)	16,54	87,41	Figure 3.110
	120 (Control)	17,51	87,50	Figure 3.111
	120 (Test)	16,74	87,40	Figure 3.111
0,05	15 (Control)	15,16	87,06	Figure 3.112
	15 (Test)	15,08	87,29	Figure 3.112
	30 (Control)	14,80	86,62	Figure 3.113
	30 (Test)	12,85	86,64	Figure 3.113

3.3.9 Band Density Analysis of Hsp60 α Subunit (TVN1128) cDNA Samples Amplified From RNA Samples Isolated From Heat-Shocked and Control Cultures

Densitometric analysis of the cDNA bands was performed by using Scion Image Version Beta 4.0.2 software as an alternative method for quantifying expression of Hsp60 α and β genes as response to heat shock and oxidative stress by real-time PCR. For 65°C heat-shock experiment, the relative cDNA band quantities were as follows: 2691,66 ± 122,09 RPA (30 min control); 2856,33 ± 115,76 RPA (30 min test); 2686,33 ± 155,00 RPA (60 min control); and 2952 ± 53,33 RPA (60 min test) (Figure 3.117 Panel A). Relative band quantities of cDNA samples synthesized from RNA isolated from 120 min heat shocked culture at 65°C and control culture sample were 6110,66 ± 303,45 RPA and 5590 ± 182,26 RPA, respectively (Figure 3.117 Panel B).

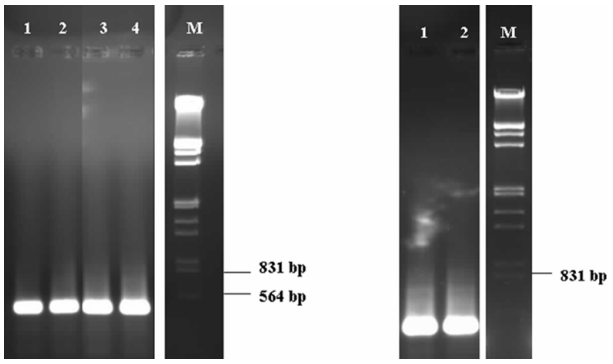

Figure 3.117: Agarose gel electrophoresis of cDNA samples synthesized and amplified by TVN1128 Real Time PCR primers. Panel A lanes 1 and 2: cDNAs synthesized from control RNA isolated from 30th min and 60th min after 72 h growth, respectively. Lanes 3 and 4: cDNAs synthesized from RNA isolated from 30 min and 60 min heat shocked samples at 65°C, respectively. Panel B lane 1: cDNA synthesized from control RNA isolated from 120th min after 72 h growth. Lane 2: cDNA synthesized from RNA isolated from 120 min heat shocked sample at 65°C. **M** is *EcoRI*/*HindIII* cut Lambda DNA molecular weight marker (MBI Fermentas, AB, Vilnius).

In conclusion, there is a good agreement between the results of RT-PCR and cDNA band density analysis for expression of Hsp60 α gene when *T. volcanium* was exposed to heat shock at 65°C, for 30, 60 and 120 minutes.

Also, there is a good agreement between the results of RT-PCR and cDNA band density analysis for heat shock exposure of *T. volcanium* at 70°C, for 30-120 min, and representative result for 90 min and 120 min heat-shock are illustrated in Figure 3.118.

For example, relative band quantities for cDNAs synthesized from RNA isolated from 90 min heat shock culture at 70°C and control culture were 1383,66 ± 17,04 RPA and 1226,33 ± 33,08 RPA respectively (Figure 3.118 Panel A). Relative band quantities of cDNA samples synthesized from RNA isolated from 120 min heat shocked culture at 70°C and control culture sample were 6818±92,37 RPA and 6030,33±44,30 RPA, respectively (Figure 3.118 Panel B).

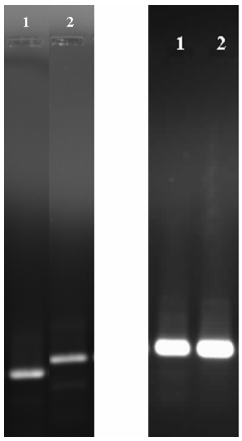

Figure 3.118: Agarose gel electrophoresis of cDNA samples synthesized and amplified by TVN1128 Real Time PCR primers. Panel A lane 1: cDNA synthesized from RNA isolated from 90 min heat shocked samples at 70°C. Lane 2: cDNA synthesized from control RNA isolated from 90th min after 72 h growth. Panel B lane 1: cDNA synthesized from control RNA isolated from 120th min after 72 h growth. Lane 2: cDNA isolated from 120 min heat shocked sample at 70°C.

For 75°C heat shock experiment, the relative cDNA band quantities were 5499,33 ± 57,07 RPA (120 min control) and 5175 ± 41,90 RPA (120 min test) (Figure 3.119). This result also is in agreement with the results of RT-PCR result.

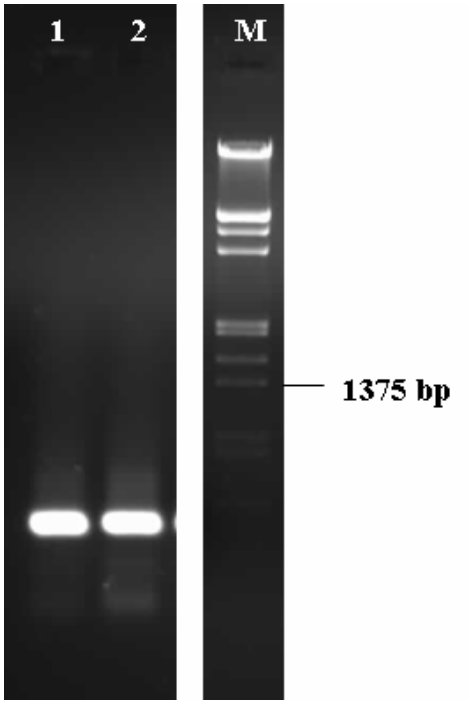

Figure 3.119: Agarose gel electrophoresis of cDNA samples synthesized and amplified by TVN1128 Real Time PCR primers. Lane 1: cDNA synthesized from control RNA isolated from 120th min after 72 h growth. Lane 2: cDNA sythesized from RNA isolated from 120 min heat shocked sample at 75°C. **M** stands for the *EcoRI* /*HindIII* cut Lambda DNA molecular weight marker (MBI Fermentas, AB, Vilnius).

3.3.10 Band Density Analysis of Hsp60 β Subunit (TVN0507) cDNA Samples Amplified From RNA Samples Isolated From Heat-Shocked And Control Cultures

For 65°C heat shock experiment, the relative cDNA band quantities were: 838,66 ± 18,15 RPA (30 min control); 1350,66 ± 63,36 RPA (30 min test); 1460,33 ± 99,68 RPA (90 min control) and 1509,66 ± 78,50 RPA (90 min test) (Figure 3.120 Panel A). Relative band quantities of cDNA samples synthesized from RNA isolated from 60 min heat shocked culture at 65°C and control culture sample were 6872±884,41 RPA and 5238±109,24 RPA, respectively (Figure 3.120 Panel B).

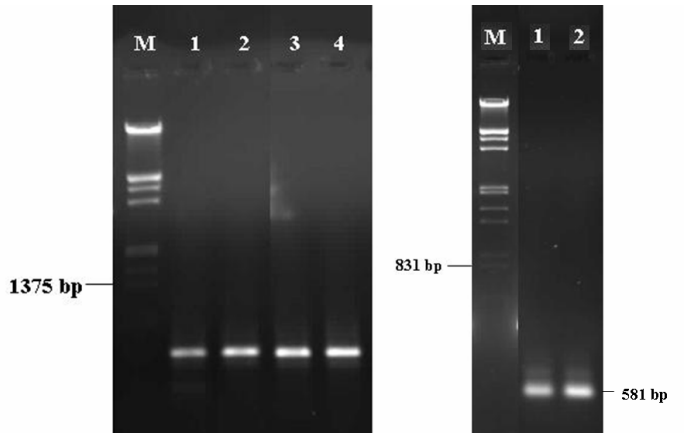

Figure 3.120: Agarose gel electrophoresis of cDNA samples synthesized and amplified by TVN0507 Real Time PCR primers. M stands for the *EcoRI* /*HindIII* cut Lambda DNA molecular weight marker (MBI Fermentas, AB, Vilnius). Panel A lanes 1 and 3: cDNAs synthesized from control RNA isolated from 30th and 90th minutes after 72 h growth, respectively. Lanes 2 and 4: cDNAs synthesized from RNA isolated from 30 min and 90 min heat shock exposed samples at 65°C, respectively. Panel B lane 1: cDNA synthesized from control RNA isolated from 60th minute after 72 h growth. Lane 2: cDNA synthesized from RNA isolated from 60 min heat shocked sample at 65°C.

Relative band quantities of cDNA samples synthesized from RNA isolated from 120 min heat shocked culture at 65°C and control culture sample were: 7329,66 ± 287,97 RPA and 6609,33 ± 137,31 RPA respectively. These results of band quantity measurements were in agreement with those of Real-Time PCR experiments for 65°C heat-shock (Figure 3.121 Panel A).

For 70°C and 75°C heat-shock, also the results of band quantity measurements were consistent with those Real-Time PCR experiments. Some representative cDNA amplification results related to these experiments are illustrated in Figure 3.121 Panel B-C.

Relative band quantities of cDNA samples synthesized from RNA isolated from 30 min heat-shocked culture at 70°C were: 6124,33 ± 187,91 RPA (30 min test); 6256,33 ± 142,72 RPA (30 min control). Relative band quantities of cDNA samples synthesized from RNA isolated from 120 min heat-shocked culture at 75°C were: 5137,66 ± 421,09 RPA (120 min control); 4208,33 ± 115,82 RPA (120 min test) (Figure 3.121 Panel B-C).

3.3.11 Band Density Analysis of Hsp60 α Subunit (TVN1128) cDNA Samples Amplified From RNA Samples Isolated H_2O_2 Stress Exposed and Control Cultures

Band quantity measurements also supported the RT-PCR results, so that cDNA band densities were lower than that of controls up to 45th min of 0,008 mM H_2O_2 exposure, but the opposite (i.e. higher relative band quantity of test) was found at 60th min. of exposure. Representative results of these experiments is shown in the Figure 3.119. The relative cDNA band quantities were: 3633,33 ± 67,5 RPA (15 min control); 3495,66 ± 2 RPA (15 min test); 3567 ± 110 RPA (60 min control); 3709,33 ± 63,6 RPA (60 min test) (Figure 3.122).

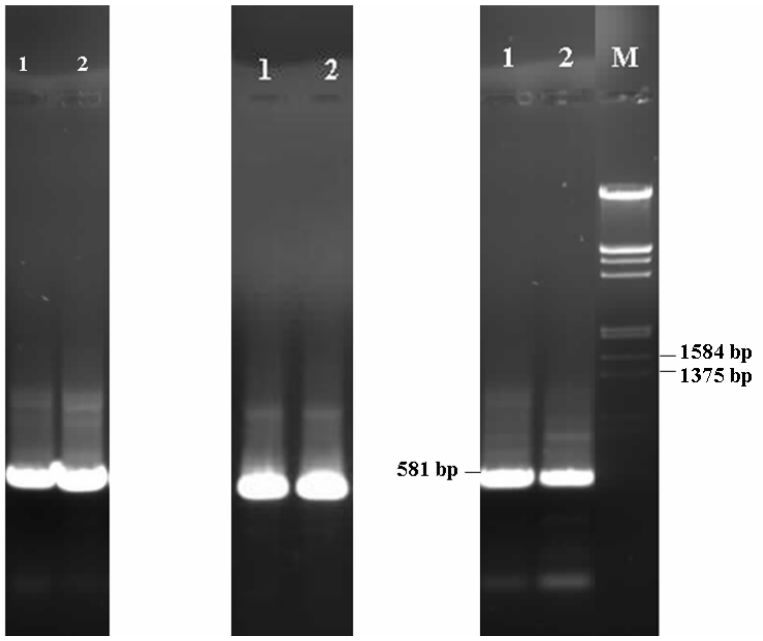

Figure 3.121: Agarose gel electrophoresis of cDNA samples synthesized and amplified by TVN0507 Real Time PCR primers. Panel A lane 1: cDNA synthesized from control RNA isolated from 120 min after 72 h growth. Lane 2: cDNA synthesized from RNA isolated from 120 min heat shocked sample at 65°C. Panel B lane 1: cDNA synthesized from RNA isolated from 30 min heat shocked sample at 70°C. Lane 2: cDNA synthesized from control RNA isolated from culture at 30th minute after 72 h growth. Panel C lane 1: cDNA synthesized from control RNA isolated from 120 min after 72 h growth. Lane 2: cDNA synthesized from RNA isolated from 120 min heat shocked sample at 75°C. M stands for the *EcoRI*/*HindIII* cut Lambda DNA molecular weight marker (MBI Fermentas, AB, Vilnius).

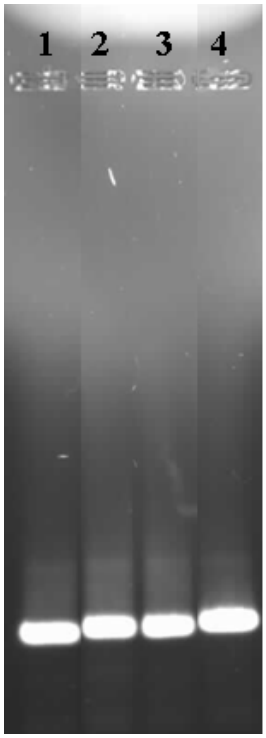

Figure 3.122: Agarose gel electrophoresis of cDNA samples synthesized and amplified by TVN1128 Real Time PCR primers. Lanes 1 and 2: cDNAs synthesized from control RNA isolated from 15th min and 60th min after 72 h growth, respectively. Lanes 3 and 4: cDNAs synthesized from RNA isolated from 15 min. and 60 min. oxidatively stressed samples at 0,008 mM H_2O_2 concentration, respectively.

Relative band quantity analysis, also revealed Hsp60 α gene expression was induced for 90 min at 0,01 mM H_2O_2 promoted oxidative stress, but induction was observed throughout 120 min exposure to 0,02 mM H_2O_2. These results were in agreement with RT-PCR results. Some representative cDNA amplification results related to these experiments are illustrated in Figure 3.123. Relative band quantities of cDNA samples synthesized from RNA isolated from 120 min oxidatively stressed cultures at 0,01 mM and 0,02 mM H_2O_2 concentration and control culture sample were: 2857±78,62 RPA (120 min control) and 2682±39,04 RPA (120 min test oxidatively stressed at 0,01 mM H_2O_2 concentration), 4919,66±39,8 RPA (120 min test oxidatively stressed at 0,02 mM H_2O_2 concentration) (Figure 3.123).

Figure 3.123: Agarose gel electrophoresis of cDNA samples synthesized and amplified by TVN1128 Real Time PCR primers. Lane 1: cDNA synthesized from control RNA isolated from 120 min after 72 hour growth. Lane 2: cDNA synthesized from RNA isolated from 120 min oxidatively stressed sample at 0,01 mM H_2O_2 concentration. Lane 3: negative control. Lane 4: cDNA synthesized from RNA isolated from 120 min oxidatively stressed sample at 0,02 mM H_2O_2 concentration.

There was also a good agreement between the results of RT-PCR and cDNA band density analysis for 0,03 mM H_2O_2 exposure of *T. volcanium* cultures at 30th min, 60th min and 90th min of the oxidative stress. Representative results of these experiments are shown in Figure 3.124. The relative cDNA band quantities were: 2691,66 ± 122,09 RPA (30 min control); 1895,66 ± 33,53 RPA (30 min test); 2686,33 ± 155,00 RPA (60 min control); 2691 ± 29,71 RPA (60 min test) and 2162,66 ± 181,56 RPA (90 min control); 2268,66 ± 172,17 RPA (90 min test) (Figure 3.124 Panel A and Panel B).

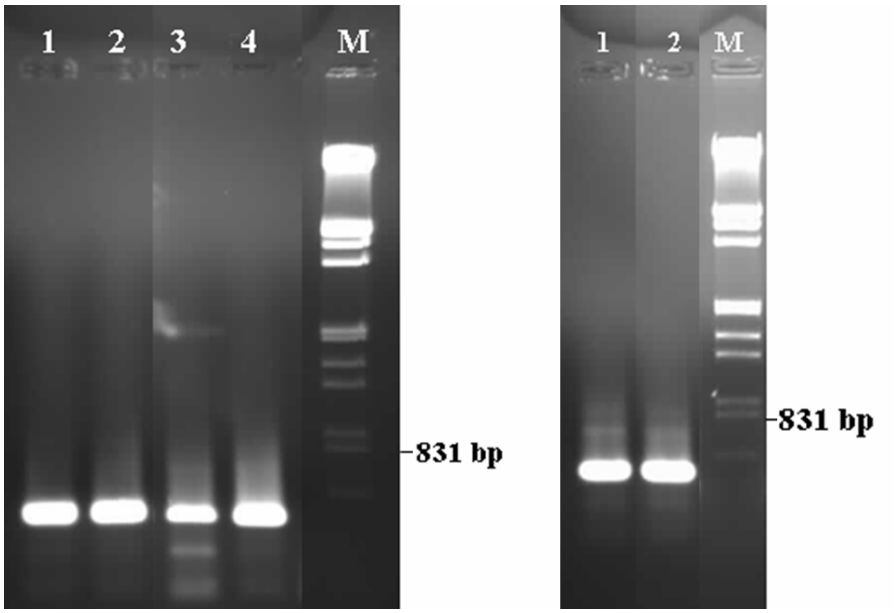

Figure 3.124: Agarose gel electrophoresis of cDNA samples synthesized and amplified by TVN1128 Real Time PCR primers. Panel A lanes 1 and 2: cDNAs synthesized from control RNA isolated from 30 min and 60 min after 72 h growth, respectively. Lane 3 and 4: cDNA synthesized from RNA isolated from 30 min and 60 min oxidatively stressed samples at 0,03 mM H_2O_2 concentration, respectively. Panel B lane 1: cDNA synthesized from control RNA isolated from 90 min after 72 h growth. Lane 2: cDNA synthesized from RNA isolated from 90 min oxidatively stressed sample at 0,03 mM H_2O_2 concentration. M stands for the *EcoRI*/*HindIII* cut Lambda DNA molecular weight marker (MBI Fermentas, AB, Vilnius).

The band quantity measurement results also supported the results obtained by Real-Time PCR, for oxidative stress experiment at 0,05 mM H_2O_2 concentration for 15 min and 30 min. The result for cDNA samples from RNA isolated from 30 min oxidatively stressed culture is shown in Figure 3. 125. The relative cDNA band quantities of cDNA samples for the test and control were: 4378 ± 277,0253 RPA (30 min test) and 4348,33 ± 107,2256 RPA (30 min control) (Figure 3.125).

Figure 3.125: Agarose gel electrophoresis of cDNA samples synthesized and amplified by TVN1128 Real Time PCR primers. Lane 1: cDNA synthesized from RNA isolated from 30 min oxidatively stressed sample at 0,05 mM H_2O_2 concentration. Lane 2: cDNA synthesized from control RNA isolated from 30 min after 72 h growth.

3.3.12 Band Density Analysis of Hsp60 β Subunit (TVN0507) cDNA Samples Amplified From RNA Samples Isolated From H_2O_2 Stress Exposed and Control Cultures

In agreement with Real-Time PCR results, relative band density measurements also showed that oxidative stress at 0,008 mM H_2O_2 concentration for 15-60 min did not induce Hsp60 β gene expression. Results for this experiment are given in the Figure 3.126. Relative band quantities of cDNA samples synthesized from RNA isolated from 15 min, 30 min, 45 min and 60 min oxidatively stressed cultures and control cultures sample were: 2995,3±46 RPA (15 min control); 2523±15,3 RPA (15 min test); 2853±58,6 RPA (30 min control); 2366,6±56 RPA (30 min test); 2645±73,65 RPA (45 min control); 2440,3±8,96 RPA (45 min test); 2418,6±54,12 RPA (60 min control); 2381±48,5 RPA (60 min test) (Figure 3.126).

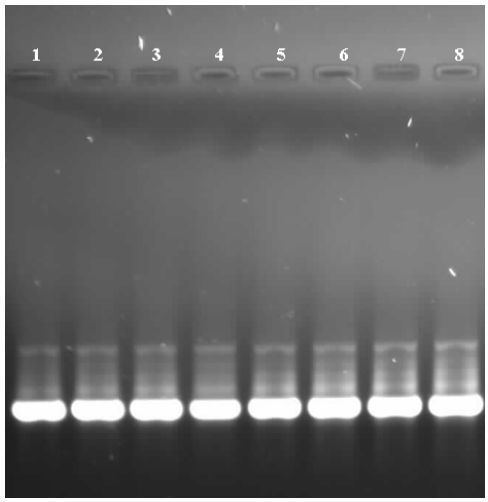

Figure 3.126: Agarose gel electrophoresis of cDNA samples synthesized and amplified by TVN0507 real time pcr primers. Lanes 1 to 4: cDNAs synthesized from control RNA isolated from 15 min, 30 min, 45 min and 60 min after 72 h growth. Lanes 5 to 8: cDNA synthesized from RNA isolated from 15 min, 30 min, 45 min and 60 min oxidatively stressed samples at 0,008 mM H_2O_2 concentration.

For oxidative stress experiment at 0,01 mM H_2O_2 concentration, relative band quantity analysis of cDNA samples synthesized from RNA isolated from 30-90 min oxidatively stressed culture indicated that Hsp60 β gene expression was induced and no induction was observed at 120th min of H_2O_2 exposure. This result was in agreement with the Real-Time PCR result. Representative gel photographs of cDNA samples are given in the Figure 3.127. Relative band quantities of the test and control culture samples were: 1104±104,75 RPA (60 min control); 1328,66±11,72 RPA (60 min test); 3829,66±110,54 RPA (90 min control); 3858,66±261,51 RPA (90 min test); 3801,66±223,94 RPA (120 min control); 3319,66±195,43 RPA (120 min test) (Figure 3.127 Panel A and Panel B).

For oxidative stress experiment at 0,02 mM H_2O_2 concentration, relative band quantities of cDNA samples synthesized from RNA isolated from 30 min and

60 min showed that Hsp60 β gene expression was not induced. After 90th minute of the H_2O_2 exposure there was an increase in the gene expression. Representative results of these experiments are shown in the Figure 3.127 Panel B. Relative band quantities of the test and control cDNA samples of 90 min and 120 min oxidatively stressed cultures were: 3829,66±110,54 RPA (90 min control); 3629,33±207,76 RPA (90 min test); 3801,66±223,94 RPA (120 min control); 3099,33±225,78 RPA (120 min test). Relative band quantities of cDNA samples synthesized from RNA isolated from control culture samples are the same as that of the oxidative stress experiment at 0,01 mM H_2O_2 concentration. Because same control samples were used as in the oxidative stress experiments at 0,01 mM and 0,02 mM H_2O_2 concentrations (Figure 3.127).

There is also agreement between the results of RT-PCR and cDNA band density analysis for oxidative stress exposure of *T. volcanium* at 0,03 mM between 30th-120th min. As an example, for oxidative stress experiment at 0,03 mM H_2O_2 concentration, relative band quantities of cDNA samples synthesized from RNA isolated from 120 min oxidatively stressed culture and control culture samples were: 838,66±18,15 RPA (120 min control) and 1852,66 ± 147,63 RPA (120 min test) (Figure 3.128).

The cDNA band density analysis for oxidative stress imposed by the exposure of *T. volcanium* at 0,05 mM yielded results that are in agreement with the Real-Time PCR results. Under this condition induction of Hsp60 β gene expression continued for 60 min. Representative result for 15 min H_2O_2 exposure is shown in Figure 3.129. Relative band quantities of cDNA samples for the test and control were: 2289,6±42,7 RPA (15 min control) and 2533,3±22 RPA (15 min test) (Figure 3.129).

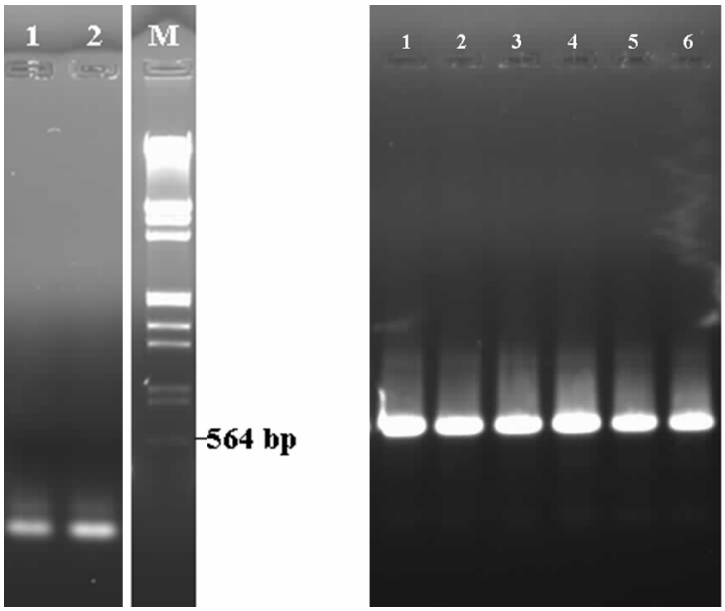

Figure 3.127: Agarose gel electrophoresis of cDNA samples synthesized and amplified by TVN0507 Real Time PCR primers. Panel A lane 1: cDNA synthesized from control RNA isolated from 60 min. after 72 h growth. Lane 2: cDNA synthesized from RNA isolated from 60 min oxidatively stressed sample at 0,01 mM H_2O_2 concentration. **M** stands for the *EcoRI* /*HindIII* cut Lambda DNA molecular weight marker (MBI Fermentas, AB, Vilnius). Panel B lanes 1 and 4: cDNAs sythesized from control RNA isolated from 90 min and 120 min. after 72 h growth, respectively. Lanes 2 and 5: cDNAs synthesized from RNA isolated from 90 min and 120 min oxidatively stressed samples at 0,01 mM H_2O_2 concentration, respectively. Lanes 3 and 6: cDNAs synthesized from RNA isolated from 90 min and 120 min oxidatively stressed samples at 0,02 mM H_2O_2 concentration, respectively.

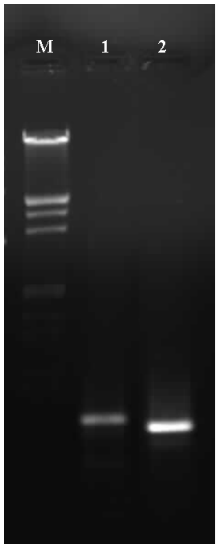

Figure 3.128: Agarose gel electrophoresis of cDNA samples synthesized and amplified by TVN0507 Real Time PCR primers. **M** is the *EcoRI*/*HindIII* cut Lambda DNA molecular weight marker (MBI Fermentas, AB, Vilnius). Lane 1 cDNA synthesized from control RNA isolated from 120 min. after 72 h growth. Lane 2: cDNA synthesized from RNA isolated from 120 min oxidatively stressed samples at 0,03 mM H_2O_2 concentration.

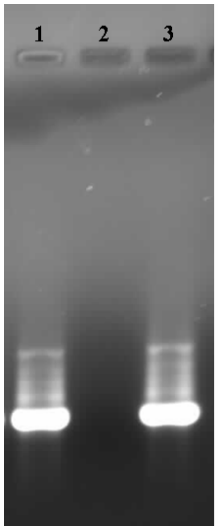

Figure 3.129: Agarose gel electrophoresis of cDNA samples synthesized and amplified by TVN0507 Real Time PCR primers. Lane 1: cDNA synthesized from control RNA isolated from 15 min after 72 h growth. Lane 2: negative control. Lane 3: cDNA synthesized from RNA isolated from 15 min oxidatively stressed samples at 0,05 mM H_2O_2 concentration.

3.4 Multiple Sequence Alignments of *T. volcanium* Hsp60 α and β Subunit Proteins

3.4.1 Sequence Alignments of *T. volcanium* Hsp60 α Subunit With Several Eukaryal, Archaeal and Bacterial Hsp60 Proteins

TVN1128 gene encodes Hsp60 α subunit protein of 549 aa length. This protein has a predicted molecular mass of 58272.76 Da and a theoretical pI of 5.8261. The *T. volcanium* Hsp60 α has the greatest similarity to *T. acidophilum* thermosome alpha chain. Multiple sequence alignments of amino acid sequence of *T. volcanium* Hsp60 α subunit protein with several eukaryal, archaeal and bacterial Hsp60 proteins were achieved by using Clustal W 1.83 program as described in Section 2.6. Protein sequences of Hsp60 subunits of organisms were derived from the online-database of NCBI (Figure 3.130). Scores of this alignment are given in Table 3.8. The sequence alignment of *T. volcanium* Hsp60 α protein with homologs from other organisms shows that this protein is more closely related to *T. acidophilum* thermosome alpha chain (CAC12109) (94%) and *Picrophilus torridus* thermosome subunit (AAT43320) (80%). All members of the Euryarchaeota and Crenarchaeota are clustered together. The identity between the *T. volcanium* Hsp60 α and Hsp60 proteins from other archaeabacteria (except Halobacteria) is 50-60%. There is a 60% sequence similarity between *T. volcanium* Hsp60 α and Hsp60 β (BAB59649). The lowest similarity (19-24%) was found between the sequence of *T. volcanium* Hsp60 α subunit and GroEL sequences of some bacteria, i.e. *Clostridium tetani* (AAO36881), *Bacillus subtilis* (NP_388484), *Rhodococcus* sp. (YP_702111), *Mycoplasma genitalum* (NP_073065), *Bacillus cereus* (NP_830146), *B. thuringiensis* (YP_893164) and *Entorococcus faecalis* (NP_ 816272). On the other hand, various eukaryotic organisms including human appear to have Hsp60 proteins with amino acid sequence identity of 37-39% to *T. volcanium* Hsp60 α protein (Table 3.8).

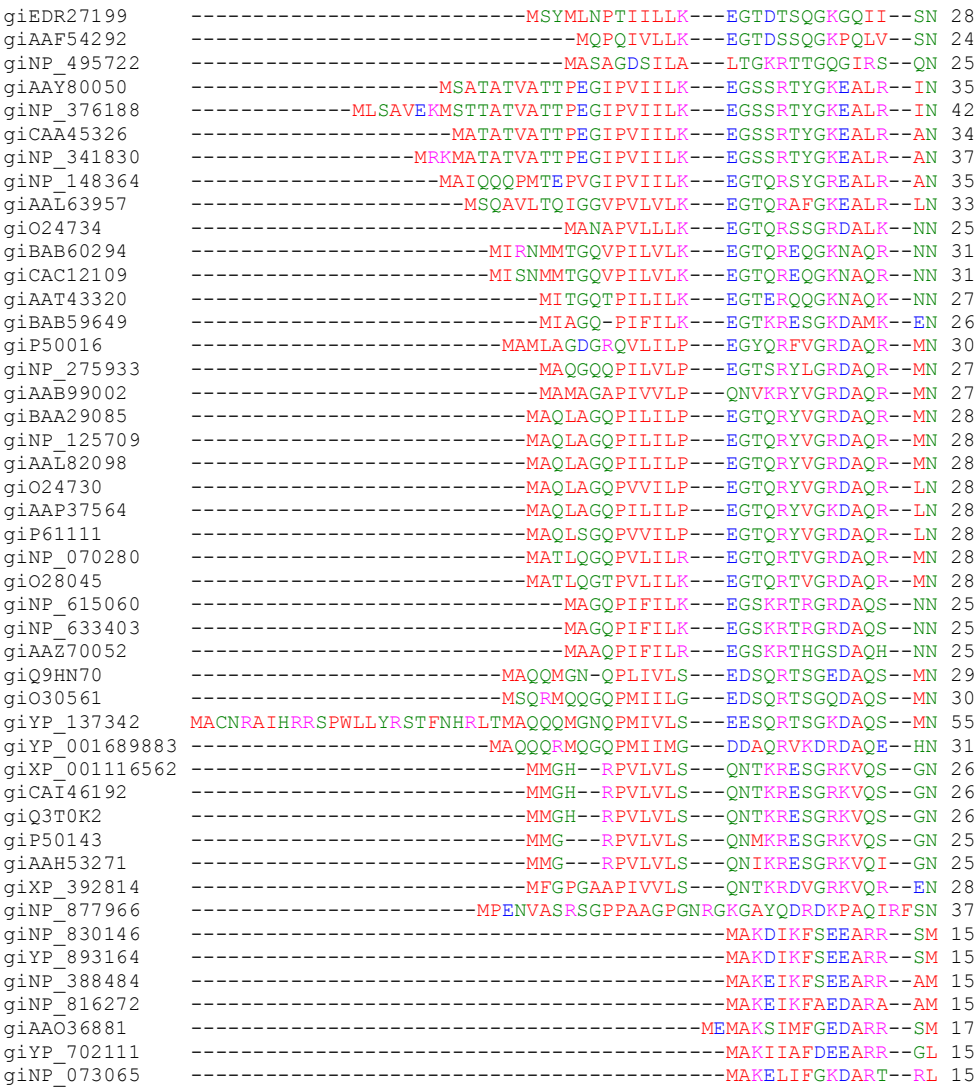

Figure 3.130: Clustal type multiple sequence alignments of amino acid sequence of *T. volcanium* Hsp60 α subunit protein with several eukaryal, archaeal and bacterial Hsp60 proteins. (*) conserved residues along all Hsp60 proteins, (.) and (:) conserved substitutions of amino acids residues.

Conserved sequences related to feature 1 and feature 2 were indicated by # and # symbols on the multiple sequence alignment, respectively.

```
                              #### #####             #
giEDR27199      INACQAIANIVKTTLGPRGMDKLFIE-NGKILVTNDGATVMKNLDIVHP----AAKALVD 83
giAAF54292      INACQSIVDAVRTTLGPRGMDKLIVDAHGKATISNDGATIMKLLEIIHP----AAKTLVD 80
giNP_495722     VTAAVAIANIVKSSLGPVGLDKMLVDDVGDVIVTNDGATILKQLEVEHP----AGKVLVE 81
giAAY80050      IAAVKAVEEALKTTYGPRGMDKMLVDSLGDITITNDGATILDKMDLQHP----AAKLLVQ 91
giNP_376188     IAAVKAVEEALKSTYGPRGMDKMLVDSLGDITITNDGATILDKMDLQHP----AAKLLVQ 98
giCAA45326      IAAVKAIEEALKSTYGPRGMDKMFVDSLGDITITNDGATILDKMDLQHP----TGKLLVQ 90
giNP_341830     IAAVKAIEEALKSTYGPRGMDKMLVDSLGDITITNDGATILDKMDLQHP----TGKLLVQ 93
giNP_148364     IMAVRAIAQILKTTYGPKGMDKMLVDSLGDITITNNGATILDKMDVAHP----AAKMLVQ 91
giAAL63957      IMIARAIAEVMRTTLGPKGMDKMLIDSLGDITITNDGATILDEMDVQHP----IAKLLVE 89
giO24734        ILAAVTLAEMLKSSLGPRGLDKMLIDSFGDVTITNDGATIVKEMEIQHP----AAKLLVE 81
giBAB60294      IEAAKAIADAVRTTLGPKGMDKMLVDSIGDIIISNDGATILKEMDVEHP----TAKMIVE 87
giCAC12109      IEAAKAIADAVRTTLGPKGMDKMLVDSIGDIIISNDGATILKEMDVEHP----TAKMIVE 87
giAAT43320      IEAAKAIADAVRTTLGPKGMDKMLVDSIGDIVITNDGATILKEMDIDHP----TAKMLVE 83
giBAB59649      IEAAIAISNSVRSSLGPRGMDKMLVDSLGDIVITNDGVTILKEMDVEHP----AAKMMVE 82
giP50016        IMAARVVAETVRTTLGPMGMDKMLVDEMGDVVVTNDGVTILEEMDIEHP----AAKMVVE 86
giNP_275933     ILAGKILAETVRTTLGPKGMDKMLVDSLGDIVVTNDGVTILKEMDIEHP----AAKMLVE 83
giAAB99002      ILAGRIIAETVRTTLGPKGMDKMLVDELGDIVVTNDGVTILKEMSVEHP----AAKMLIE 83
giBAA29085      ILAARIIAETVRTTLGPKGMDKMLVDSLGDIVITNDGATILDEMDIQHP----AAKMMVE 84
giNP_125709     ILAARIIAETVRTTLGPKGMDKMLVDSLGDIVITNDGATILDEMDIQHP----AAKMMVE 84
giAAL82098      ILAARIVAETIRTTLGPKGMDKMLVDSLGDIVITNDGATILDEMDIQHP----AAKMMVE 84
giO24730        ILAARIIAETVRTTLGPKGMDKMLVDSLGDIVITNDGATILDEMDIQHP----AAKMMVE 84
giAAP37564      ILAARIVAETVRTTLGPKGMDKMLVDSLGDIVITNDGATILDEMDIQHP----AAKMMVE 84
giP61111        ILAARIIAETVRTTLGPKGMDKMLVDSLGDIVVTNDGATILDKIDLQHP----AAKMMVE 84
giNP_070280     IMAARVIAEAVRSTLGPKGMDKMLVDSLGDVVITNDGVTILKEIDVEHP----AAKMIIE 84
giO28045        IMAARVIAEAVKSTLGPKGMDKMLVDSLGDVVITNDGVTILKEMDVEHP----AAKMIIE 84
giNP_615060     IMAAKAVAEAVRTTLGPKGMDKMLVDSMGDVVITNDGATILKEMDIEHP----AAKMVVE 81
giNP_633403     IMAAKAVAEAVRTTLGPKGMDKMLVDSMGDVVITNDGATILKEMDIEHP----AAKMVVE 81
giAAZ70052      IMAAKAVAEAVRTTLGPKGMDKMLVDSMGDVVITNDGATILKEMDIEHP----GAKMIVE 81
giQ9HN70        ITAGKAVAESVRTTLGPKGMDKMLVDSSGEVVVTNDGVTILKEMDIEHP----AANMIVE 85
giO30561        ITAGKAVAEAVRTTLGPKGMDKMLVDSGGQVVVTNDGVTILKEMDIDHP----AANMIVE 86
giYP_137342     ITAGTAVAEAVRTTLGPKGMDKMLVDNSGSVVVTNDGVTILDEMDIEHP----AANMIVE 111
giYP_001689883  ISAARAVADAVRSTLGPKGMDKMLVSSMGDVTVTNDGVTILQEMDIDNP----TAEMIVE 87
giXP_001116562  INAAKTIADIIRTCLGPKSMMKMLLDPMGGIVMTNDGNAILREIQVQHP----AAKSMIE 82
giCAI46192      INAAKTIADIIRTCLGPKSMMKMLLDPMGGIVMTNDGNAILREIQVQHP----AAKSMIE 82
giQ3T0K2        INAAKTIADIIRTCLGPKSMMKMLLDPMGGIVMTNDGNAILREIQVQHP----AAKSMIE 82
giP50143        INAAKTIADIIRTCLGPRAMMKMLLDPMGGIVMTNDGNAILREIQVQHP----AAKSMIE 81
giAAH53271      ISAAKTIADIIRTCLGPRAMMKMLLDPMGGIVMTNDGNAILREIQVQHP----AAKSMIE 81
giXP_392814     IQAGKAIADVIRTCLGPQAMLKMLMDPMGGIVMTNDGNAILREITVQHP----AGKSMIE 84
giNP_877966     ISAAKAVADAIRTSLGPKGMDKMIQDGKGDVTITNDGATILKQMQVLHP----AARMLVE 93
giNP_830146     LRGVDTLANAVKVTLGPKGRNVVLEKKFGSPLITNDGVTIAKEIELEDAFENMGAKLVAE 75
giYP_893164     LRGVDTLANAVKVTLGPKGRNVVLEKKFGSPLITNDGVTIAKEIELEDAFENMGAKLVAE 75
giNP_388484     LRGVDALADAVKVTLGPKGRNVVLEKKFGSPLITNDGVTIAKEIELEDAFENMGAKLVAE 75
giNP_816272     LRGVDVLADTVKVTLGPKGRNVVLEKSFGSPLITNDGVTIAKEIELEDHFENMGAKLVSE 75
giAAO36881      QKGVDILADTVKVTMGPKGRNVVLDKKFGAPLITNDGVTIAREIELEDAYENMGAQLVKE 77
giYP_702111     ERGLNALADAVKVTLGPKGRNVVLEKKWGAPTITNDGVSIAKEIELEDPYEKIGAELVKE 75
giNP_073065     LQGINKIANAVKVTVGPKGQNVILERKFANPLITNDGVTIAKEIELSDPVENIGAKVISV 75
                      : : ::   ** .   ::    .   ::*:* ::   : : .      .. :
```

Figure 3.130: continued

```
                        #####
giEDR27199      IAMAQDSEVGDGTTTVVVLAGELLAQAKKLIEDGIHPQVIIKGYRMASNKAREVVNTMKI 143
giAAF54292      IAKSQDAEVGDGTTSVVLLAGEFLKQVKPFVEEGVHPRVIIKAIRKALQLCMEKINEMAV 140
giNP_495722     LAQLQDEEVGDGTTSVVIVAAELLKRADELVKQKVHPTTIINGYRLACKEAVKYISENIS 141
giAAY80050      IAKGQDEETADGTKTAVIFSGELVKKAEELLYKEIHPTIIVSGYKKAEEMAIKTI-EEIS 150
giNP_376188     IAKGQDEETADGTKTAVILAGELVKKAEELLYKEIHPTIIVSGFKKAEEQALKTI-EEIA 157
giCAA45326      IAKGQDEETADGTKTAVILAGELAKKAEDLLYKEIHPTIIVSGYKKAEEIALKTI-QDIA 149
giNP_341830     IAKGQDEETADGTKTAVILAGELAKKAEDLLYKEIHPTIIVSGYKKAEEIALKTI-QEIA 152
giNP_148364     ISKGQEDEAGDGTKTTVIFAGELLKEAEKLLDINIHPTIIVEGYKEALRKASEVI-ESIA 150
giAAL63957      ISKSQEEEAGDGTTTAVVLAGALLEEAEKLLEKNIHPTVIVSGFKKALDVAAEHL-RKVA 148
giO24734        AAKAQDAEVGDGTTSAVVLAGLLLDKADDLLDQNIHPTIIIEGYKKALNKSLEII-DQLA 140
giBAB60294      VSKAQDTAVGDGTTTAVVLSGELLKQAETLLDQGVHPTVISNGYRLAVNEARKII-DEIS 146
giCAC12109      VSKAQDTAVGDGTTTAVVLSGELLKQAETLLDQGVHPTVISNGYRLAVNEARKII-DEIA 146
giAAT43320      ASKSQDTAVGDGTTTVVVLAGELLKQAESLLEQGVHSTVIASGYHLAVTEAKKQL-DSLA 142
giBAB59649      VSKTQDSFVGDGTTTAVIIAGGLLQQAEALINQNVHPTVISEGYRMASEEAKRII-DEIS 141
giP50016        VAKTQEDEVGDGTTTAVVLAGELLHKAEDLLQQDIHPTVIARGYRMAVEKAEEIL-EEIA 145
giNP_275933     VAKTQEDEVGDGTTTAVIIAGELLKKAENLLEMEIHPTIIAMGYRQAAEKAQEIL-DDIA 142
giAAB99002      VAKTQEKEVGDGTTTAVVIAGELLRKAEELLDQNIHPSVIINGYEMARNKAVEEL-KSIA 142
giBAA29085      VAKTQDKEAGDGTTTAVVIAGELLKKAEELLDQNIHPSIIIKGYTLASQKAQEIL-DSIA 143
giNP_125709     VAKTQDKEAGDGTTTAVVIAGELLKKAEELLDQNIHPSIVIKGYMLAAEKAQEIL-DSIA 143
giAAL82098      VAKTQDKEAGDGTTTAVVIAGELLRKAEELLDQNIHPSIIIKGYTLAAQKAQEIL-ENIA 143
giO24730        VAKTQDKEAGDGTTTAVVIAGELLRKAEELLDQNIHPSIIIKGYALAAEKAQEIL-DEIA 143
giAAP37564      VAKTQDKEAGDGTTTAVVIAGELLRKAEELLNQNIHPTIIVKGYTLAAEKAQEIL-ESIA 143
giP61111        VAKTQDKEAGDGTTTAVVIAGELLRKAEELLDQNIHPSIIIKGYALAAEKAQEIL-DEIA 143
giNP_070280     VAKTQDNEVGDGTTTAVVLAGELLKRAEELLDQEIHPAIIANGYRYAAEKALEIL-NEIA 143
giO28045        VAKTQDNEVGDGTTTAVVLAGELLKKAEELLDQDIHPTVIARGYRMAANKAVEIL-ESIA 143
giNP_615060     VSKTQDEQVGDGTTSAAVVAGELLKKAEDLIEQEIHPTIIASGYRLAAEKAVEVL-NSLA 140
giNP_633403     VSKTQDDEVGDGTTSAAVVAGELLNKAEDLIEQEIHPTIIASGYRLAAEKAIEVL-NSLA 140
giAAZ70052      VAKTQDAEVGDGTTTAAVLAGEFLTKAEDLLESGVHPTVIASGYRLAADQATKTI-DTIT 140
giQ9HN70        VAETQETEVGDGTTTSVVVSGELLSEAETLLEQDIHATTLAQGYRQAAEKAKELL-DDAA 144
giO30561        VSETQEDEVGDGTTTAVINAGELLDQAEDLLDSDVHATTIAQGYRQAAEKAKEVL-EDNA 145
giYP_137342     VAQTQEDEVGDGTTTAVVMAGELLSKAEELLDQDIHASILAQGYRQAAEKAKEIL-EDNA 170
giYP_001689883 VAETQEDEAGDGTTTAVAIAGELLKNAEDLLERDIHPTAIIKGYNLAAEQAREEV-DNVA 146
giXP_001116562 ISRTQDEEVGDGTTSVIILAGEMLSVAEHFLEQQMHPTVVISAYRKALDDMISTL-KKIS 141
giCAI46192      ISRTQDEEVGDGTTSVIILAGEMLSVAEHFLEQQMHPTVVISAYRKALDDMISTL-KKIS 141
giQ3T0K2        ISRTQDEEVGDGTTSVIILAGEMLSVAEHFLEQQMHPTVVISAYRKALDDMISTL-KKIS 141
giP50143        ISRTQDEEVGDGTTSVIILAGEMLSVAEQFLEQQMHPTVIISAYRKALDDMVNTL-KEIS 140
giAAH53271      ISRTQDEEVGDGTTSVIILAGEMLSVAEQFLEQQMHPTVVIGAYRQALDDMLNIL-KDIS 140
giXP_392814     IARTQDEEVGDGTTSVIVLAGEILATAEPFLEQNMHPTVIIRAYRQALEDIVTILNEQVS 144
giNP_877966     LSKAQDIEAGDGTTSVVIIAGSLLDSCTKLLQKGIHPTIISESFQKALEKGLEIL-TDMS 152
giNP_830146     VASKTNDVAGDGTTTATVLAQAMIREGLKNVTAGANPMGLRKGIEKAVTAAIEEL-KTIS 134
giYP_893164     VASKTNDVAGDGTTTATVLAQAMIREGLKNVTAGANPMGLRKGIEKAVVAAVEEL-KTIS 134
giNP_388484     VASKTNDVAGDGTTTATVLAQAMIREGLKNVTAGANPVGVRKGMEQAVAVAIENL-KEIS 134
giNP_816272     VASKTNDIAGDGTTTATVLTQAIVREGLKNVTAGANPLGIRRGIELATKTAVEEL-HNIS 134
giAAO36881      VATKTNDVAGDGTTTATLLAQAIIREGLKNVTGGANPMLVRRGIQMAVEEAVKGI-KEIS 136
giYP_702111     VAKKTDDVAGDGTTTATVLAQALVREGLRNVAAGANPLGLKRGIEKAVEAVTVRL-LETA 134
giNP_073065     AAVSTNDIAGDGTTTATILAQEMTNRGIEIINKGANPVNIRRGIEDASLLIIKEL-EKYS 134
                 :   :  ..***.:    :  :       :    :.  :  .   *       :
```

Figure 3.130: continued

```
giEDR27199      DFD---KKDLM---EYLKNCAKTSMQSKLIAMQR--EHFTNIVVQSVMHLDDK------- 188
giAAF54292      QIVEQSKDQQR---ALLEKCAATAMSSKLIHQQK--DFFSRIVVDAVLSLDEL------- 188
giNP_495722     FTS---DSIGR---QSVVNAAKTSMSSKIIGPDA--DFFGELVVDAAEAVRVENN-GKVT 192
giAAY80050      TKVSVNDT------EILRKVALTSLSSKAVAGAR--EHLADIVVKAITQVAE-LRGDKWY 201
giNP_376188     QKVSVNDM------DILKKVAMTSLNSKAVAGAR--EYLADIVAKAVTQVAE-LRGDRWY 208
giCAA45326      QPVSINDT------DVLRKVALTSLGSKAVAGAR--EYLADLVVKAVAQVAE-LRGDKWY 200
giNP_341830     QPVTINDT------DVLRKVALTSLGSKAVAGAR--EYLADLVVKAVAQVAE-LRGDKWY 203
giNP_148364     EPVSYDDV------EKLKLIAKTSLNSKAVAEAR--DYFAELAVEAVRTVAE-RRGDRWY 201
giAAL63957      IPVNRTDV------DTLRKIAMTSMGGKISETVK--EYFADLAVKAVLQVAE-ERNGKWY 199
giO24734        TKIDVSNLNSLATRDQLKKIVYTTMSSKFIAGGEEMDKIMNMVIDAVSIVAEPLPEGGYN 200
giBAB60294      VKS--TDD------ETLRKIALTALSGKNTGLSN--TFLADLVVKAVNAVAEERD-GKII 195
giCAC12109      EKS--TDD------ATLRKIALTALSGKNTGLSN--DFLADLVVKAVNAVAEVRD-GKTI 195
giAAT43320      IKA--DDE------ETLKRIAITALSGKNTSVAP--EFLADLVIKAVNAVAEERD-GKVI 191
giBAB59649      TKIGKDEK------ELLIKLAQTSLNSKSASVAK--DKLAEISYEAVKSVAELRD-GKYY 192
giP50016        EEIDPDDE------ETLKKIAKTAMTGKGVEKAR--DYLAELVVKAVKQVAEEED-GEIV 196
giNP_275933     --IDASDR------DTLMKVAMTAMTGKGTEKAR--EPLAELIVDAVKQVE--ED-GE-- 187
giAAB99002      KEVKPEDT------EMLKKIAMTSITGKGAEKAR--EQLAEIVVEAVRAVVDEET-GK-- 191
giBAA29085      KEVKPDDE------EVLLKAAMTAITGKAAEEER--EYLAKLAVEAVKLVAEEKD-GKLK 194
giNP_125709     KEVKPDDE------EVLLKAAMTAITGKAAEEER--EYLAKLAVEAVKLVAEEKD-GKFK 194
giAAL82098      KEVKPDDE------EILLKAAMTSITGKAAEEER--EYLAKLAVEAVKLVAEKED-GKYK 194
giO24730        KDVDVEDR------EILKKAAVTSITGKAAEEER--EYLAEIAVEAVKQVAEKVG-ETYK 194
giAAP37564      KDVSPMDE------EILMKAATTAITGKAAEEER--EYLAKLAVDAVKLVAEEVD-GKYI 194
giP61111        IRVDPDDE------ETLLKIAATSITGKNAESHK--ELLAKLAVEAVKQVAEKKD-GKYV 194
giNP_070280     IPISKDDD------EILKKIATTAMTGKGAEVAI--DKLAEIAVNAVKMIAEESN-GQVE 194
giO28045        MDIDVEDE------ETLKKIAATAITGKHSEYAL--DHLSSLVVEAVKRVAEKVD-DRYK 194
giNP_615060     MNVEMSNR------ELLVSIAETAMTGKGAEASK--KLLSGIAVDAVTSVVDTN--GKKT 190
giNP_633403     MSVDMGNR------DLLLSIAETAMTGKGAESSK--KLLAEIAVDAVTSVVDTN--GKMS 190
giAAZ70052      ISASPEDT------ETLEKIAATAITGKGAEAQK--EHLSRLAVKAVKSVAEISEDGKIT 192
giQ9HN70        IDVSADDT------ETLEKIAATAMTGKGAENAK--GVLSDLVVRAVQSVADDND----- 191
giO30561        IEVTEDDR------ETLTKIAATAMTGKGAESAK--DLLSELVVDAVLAVKDDDG----- 192
giYP_137342     IDVDADDT------ETLEKVAATAMTGKGAESSK--DVLAELVVRAAQSVVDDDGS---- 218
giYP_001689883 VDVDPDDK------DLIRSVAETSMTGKGAELDK--ELLSSIIYDAVNQVAVETNDGGIV 198
giXP_001116562 IPVDINDS------DMMLNIINSSITTKAISRWS--SLACNIALDAVKTVQFEEN-GRKE 192
giCAI46192      IPVDISDS------DMMLNIINSSITTKAISRWS--SLACNIALDAVKMVQFEEN-GRKE 192
giQ3T0K2        IPVDTSNR------DTMLNIINSSITTKVISRWS--SLACNIALDAVKTVQFEEN-GRKE 192
giP50143        TPVDTNDR------ELMLKIINSAINTKAIKLWA--DMACGIALDAVKTVELEEN-GRKE 191
giAAH53271      TPVDVSNR------DMMLKIINSAINTKALSRWS--TLACNIALDAVRTVELEEN-GRKE 191
giXP_392814     IDLDCNDK------NKMIQVINSCVRTKFIGRWC--ELACQIALDAVYTVLLEEN-GRRE 195
giNP_877966     RPVQLSDR------ETLLNSATTSLNSKVVSQYS--SLLSPMSVNAVMKVIDPAT--ATS 202
giNP_830146     KPIEGKSS--------IAQVAAISAADEEVGQLIA-EAMERVGNDGVITLEESKG----- 180
giYP_893164     KPIEGKSS--------IAQVAAISAADEEVGQLIA-EAMERVGNDGVITLEESKG----- 180
giNP_388484     KPIEGKES--------IAQVAAISAADEEVGSLIA-EAMERVGNDGVITIEESKG----- 180
giNP_816272     SVVDSKEA--------IAQVAAVSSGSEKVGQLIA-DAMEKVGNDGVITIEESKG----- 180
giAAO36881      KPVEGKED--------IARVAAISADDKEIGKLIA-DAMEKVGNEGVITVEESNT----- 182
giYP_702111     KEIDTKEQ--------IAATAGISAGDPSIGELIA-EAMDKVGKEGVITVEESNT----- 180
giNP_073065     KKINTNEE--------IEQVAAISSGSKEIGKLIA-QAMALVGKNGVITTDDAKT----- 180
                      .         :                     :    .
```

Figure 3.130: continued

```
giEDR27199      LDIDM-IGIKKEQGGSLEDSFTLEGVAFKKCFSYAGFEQQPKLFYKPKILCLNIELELKK 247
giAAF54292      LPLNM-IGIKKVTGGSLEESQLVSGVAFKKTFSYAGFEMAPKSYDNCKIALLNIELELKA 247
giNP_495722     YPINA-VNVLKAHGKSARESVLVKGYALNCTVASQAMPLR---VQNAKIACLDFSLMKAK 248
giAAY80050      VDLDN-VQIVKKHGGSINDTQIVYGIIVDKEVVHPGMPKR---VENAKIALLDASLEVEK 257
giNP_376188     VDLDN-IQIVKKHGGSINDTQIIYGIVVDKEVVHPGMPKR---VENAKIALLDASLEVEK 264
giCAA45326      VDLDN-VQIVKKHGGSINDTQLVYGIVVDKEVVHPGMPKR---IENAKIALLDASLEVEK 256
giNP_341830     VDLDN-VQIVKKHGGSVNDTQLVYGIVVDKEVVHPGMPKR---IENAKIALLDASLEVEK 259
giNP_148364     VDLNN-IQIVKKHGGSLRDTRLVRGIVLDKEVVHPDMPRR---VENARIALLDTPLEIEK 257
giAAL63957      VDLDN-IQIVKKHGGSLLDTQLVYGIVVDKEVVHAAMPKR---VVNAKIALLDAPLEVEK 255
giO24734        VPLDL-IKIDKKKGGSIEDSMLVHGLVLDKEVVHPGMPRR---VEKAKIAVLDAALEVEK 256
giBAB60294      VDTAN-IKVDKKSGGSINDTQFISGIVVDKEKVHSKMPDV---VKDAKIALIDSALEIKK 251
giCAC12109      VDTAN-IKVDKKNGGSVNDTQFISGIVIDKEKVHSKMPDV---VKNAKIALIDSALEIKK 251
giAAT43320      VDTAN-IKVDKKNGGSATDTQFISGLIIDKEKVHSKMPSV---VKNAKIALINSALEIKK 247
giBAB59649      VDFDN-IQVVKKQGGAIDDTALINGIIVDKEKVHPGMPDV---VKNAKIALLDAPLEIKK 248
giP50016        IDTDH-IKLEKKEGGGLEDTELVKGMVIDKERVHPGMPRR---VENAKIALLNCPIEVKE 252
giNP_275933     VEKDH-IKIEKKEGAAVDDSTLVQGVIIDKERVHPGMPKK---VENAKIALLNCPIEVKE 243
giAAB99002      VDKDL-IKVEKKEGAPIEETKLIRGVVIDKERVNPQMPKK---VENAKIALLNCPIEVKE 247
giBAA29085      VDIDN-IKLEKKEGGAVRDTRLIRGVVIDKEVVHPGMPKR---IENAKIALINDALEVKE 250
giNP_125709     VDIDN-IKFEKKEGGAVSDTKLIRGVVIDKEVVHPGMPKR---VEKAKIALINDALEVKE 250
giAAL82098      VDIDN-IKLEKKEGGSVRDTQLIRGVVIDKEVVHPGMPKR---VEKAKIALINDALEVKE 250
giO24730        VDLDN-IKFEKKEGGSVKDTQLIKGVVIDKEVVHPGMPKR---VEGAKIALINEALEVKE 250
giAAP37564      VDIDN-IKLEKKEGGSVRDTQLIKGVVIDKERVHPGMPKK---VENAKIALINEALEVKE 250
giP61111        VDLDN-IKFEKKAGEGVEESELVRGVVIDKEVVHPRMPKR---VENAKIALINEALEVKK 250
giNP_070280     VNTDY-IKIEKRQGGSIEETELVDGIVLDKEVVHPGMPKR---VENAKILLLDSALEVKE 250
giO28045        VDEDN-IKLEKRQGGSVADTKLVNGIVIDKEVVHPGMPKR---VKNAKIAVLKAALEVKE 250
giNP_615060     IDKDN-ISVVKKVGGRIEDSELIPGMIIDKERVHTNMPEK---VKDAKIALLNSAIELKD 246
giNP_633403     VDKEN-ISVVKKVGGKTEDSELIPGMIIDKERVHTNMPEK---VKDAKIALLNTAIELKD 246
giAAZ70052      VDIED-IKVEKRPGGSIKDSEIVDGVIVDKERVHPAMPEV---VENAKILLLSVPIELKK 248
giQ9HN70        VDTDN-VKVEKVTGGAIENSELIEGVIVDKERVSENMPYA---VEDANIALVDDGLEVQE 247
giO30561        IDTNN-VSIEKVVGGTIDNSELVEGVIVDKERVDENMPYA---VEDANIAILDDALEVRE 248
giYP_137342     VDTDN-IQIETVVGGATDESELVEGVIVDKERVHDNMPFA---VEDADVALLDTAIEVPE 274
giYP_001689883 VDAAN-INIETQTGHGVNESQLLRGAAISKDPVHDQMPAA---VEDADVLLLNEAIEVEE 254
giXP_001116562 IDIKKYAKVEKIPGGIIEDSCVLRGVMINKDVTHPRMRRY---IKNPRIVHVDSSLEYKK 249
giCAI46192      IDIKKYARVEKIPGGIIEDSCVLRGVMINKDVTHPRMRRY---IKNPRIVLLDSSLEYKK 249
giQ3T0K2        IDIKKYARVEKIPGGIIEDSCVLRGVMINKDVTHPRMRRY---IKNPRIVLLDSSLEYKK 249
giP50143        IDIKKYAKVEKIPGGIIEDSCVLRGVMVNKDVTHPKMRRL---IKNPRIILLDCSLEYKK 248
giAAH53271      IDIKKYAKVEKVPGGIIEDSCVLRGVMVNKDVTHPRMRRL---IKNPRIVLLDCSLEYKK 248
giXP_392814     IDIKRYAKVEKIPGGTIEDSTVLKGVMFNKDVTHPKMRRH---IKNPRIVLLDCSLEYKK 252
giNP_877966     VDLRD-IKIVKKLGGTIDDCELVEGLVLTQKVANSGITR----VEKAKIGLIQFCLSAPK 257
giNP_830146     ----FTTELDVVEGMQFDRGYASPYMITDSDKMEAVLDNPYILITDKKISNIQEILPVLE 236
giYP_893164     ----FTTELDVVEGMQFDRGYASPYMITDSDKMEAVLDNPYILITDKKISNIQEILPVLE 236
giNP_388484     ----FTTELEVVEGMQFDRGYASPYMVTDSDKMEAVLDNPYILITDKKITNIQEILPVLE 236
giNP_816272     ----IETELDVVEGMQFDRGYLSQYMVTDNDKMEAVLENPYILITDKKISNIQDILPLLE 236
giAAO36881      ----MGTELDVVEGMQFDRGYVSPYMVTDTEKMEASLDDAYILITDKKITNIQEILPVLE 238
giYP_702111     ----FGLQLELTEGMRFDKGYISAYFATDPERQEAVLEDAYILLVSSKISTVKDLLPLLE 236
giNP_073065     ----INTTLETTEGIEFKGTYASPYMVSDQEKMEVVLEQPKILVSSLKINTIKEILPLLE 236
                        .    *                      :          :  :.  :
```

Figure 3.130: continued

Figure 3.130: continued

```
giEDR27199      QY----FADRKIFCAGRVEEDDMKRVCLATGAQVQTTVSELN------DSVLG-TCGKFE 348
giAAF54292      QY----FADRDIFCAGRVPEEDLKRTMKACGGAVMTTANDIK------PNVLG-LCEHFE 348
giNP_495722     KQ----FVESGAMAVRRCKKSDLKRIAKATGATLTVSLATLEGDEAFDASLLG-HADEIV 355
giAAY80050      HY----LAKKGILAVRRAKKSDLEKLARATGGRVVSNIDELT------SQDLG-YATLVE 358
giNP_376188     HY----LAKKGILAVRRAKKSDLEKLARATGGRVVSNIDELT------PQDLG-YAALVE 365
giCAA45326      HY----LAKKGILAVRRAKKSDLEKLARATGGRVISNIDELT------SQDLG-YAALVE 357
giNP_341830     HY----LAKKGILAVRRAKKSDLEKLARATGGRVISNIDELT------SQDLG-YAALVE 360
giNP_148364     HF----LAKKGILAVRRVKRSDIEKIARATGARIVTDIEDLR------PEDLG-YAELVE 358
giAAL63957      YY----LAKAGILAVRRVKRSDIEKLVRATGARLVTSIEDLT------EADLG-FAGLVE 356
giO24734        HF----LAKKGILAVRRVKRSDIEKLEKALGARIISSIKDAT------PEDLG-YAELVE 357
giBAB60294      HY----LAKEGIYAVRRVKKSDMEKLAKATGAKIVTDLDDLT------PSVLG-EAEKVE 352
giCAC12109      HY----LAKEGIYAVRRVKKSDMEKLAKATGAKIVTDLDDLT------PSVLG-EAETVE 352
giAAT43320      YY----LAKEGIYAVRRVKQSDMEKLAKATGAKIVTDLDDLT------PDSLG-TAEKVE 348
giBAB59649      HY----LSKEGIYAVRRVKKSDMDKLAKATGATVVSTIDEIS------ASDLG-SADRVE 349
giP50016        HY----LAKKGILAVRRVKKSDMQKLARATGARIVTNIDDLS------EEDLG-EAEVVE 353
giNP_275933     HY----LAKAGVLAVRRVKKSDMEKLSKATGANIVTNIEDLS------PEDLG-EAGVVS 344
giAAB99002      HY----LAKKGILAVRRVKKSDMEKLAKATGARIVTKIDDLT------PEDLG-EAGLVE 348
giBAA29085      HY----LAKYGILAVRRVKKSDMEKLAKATGAKIVTNIRDLT------PEDLG-EAELVE 351
giNP_125709     HY----LAKYGILAVRRVKKSDMEKLAKATGAKIVTNIRDLT------PEDLG-EAELVE 351
giAAL82098      HY----LAKYGIMAVRRVKKSDMEKLAKATGAKIVTNIRDLT------PEDLG-YAELVE 351
giO24730        HY----LAKYGIMAVRRVKKSDMEKLAKATGAKIVTNVRDLT------PEDLG-EAELVE 351
giAAP37564      HY----LAKAGILAVRRVKKSDMEKLAKATGAKIVTNVRDLT------PDDLG-YAELVE 351
giP61111        HY----LAKYGIMAVRRVKKSDMEKLAKATGAKIVTNVKDLT------PEDLG-YAEVVE 351
giNP_070280     YY----LAKAGVLAVRRVKKSDMEKLAKATGAKVLTDLRDIS------SEDLG-EAALVE 351
giO28045        YY----LAKAGILAVRRVKQSDIEKIAKACGAKIITDLREIT------SADLG-EAELVE 351
giNP_615060     HY----LAKAGIFAIRRVKKSDMEKLARATGGKLITNLDEIT------PEDLG-FAKLVE 347
giNP_633403     HY----LAKAGIFAVRRVKKSDMEKLARATGGKLITNLDEIV------PEDLG-FAKLVE 347
giAAZ70052      YY----MTKAGIFGMRRVKKSDMDKLSRATGAKIITSLDEIE------ESDLG-HAGLVE 349
giQ9HN70        HY----LAKEGILAVRRAKSDDFTRLSRATGATPVSNVNDIE------AADLG-AAGSVA 348
giO30561        HY----LAKEGILAVRRAKSSDLKRLARATGGRVVSSLDDIE------ADDLG-FAGSVG 349
giYP_137342     HY----LAQEGILAVRRAKKSDIEALSRSTGARIISNIDDIE------ADDLG-FAGSVA 375
giYP_001689883 HY----LAKEGILAVRRTKKSDIEFLTNVLDASVVTDLDAAS------EADV--VAGSVT 354
giXP_001116562 HY----LMRANITAIRRVRKTDNNRIARACGARIVSRPEELR------EDDVGTGAGLLE 351
giCAI46192      HY----LMRANITAIRRVRKTDNNRIARACGARIVSRPEELR------EDDVGTGAGLLE 351
giQ3T0K2        HY----LMRANITAIRRVRKTDNNRIARACGARIVSRPEELR------EEDVGTGAGLLE 351
giP50143        HY----LVKANITAVRRVRKTDNNRIARACGARIASRTDELR------EEDVGTGAGLFE 350
giAAH53271      HY----LMKANITAIRRIRKTDNNRIARACGARIASRTDELT------EDDVGTGAGLFE 350
giXP_392814     HY----LVKAGISAIRRLRKSDINRIARACGATVVNRTEELR------DEDVGTRAGLFE 354
giNP_877966     HF----LNKMKIMVVKDIEREDIEFICKTIGTKPVAHIDQFT------PDMLG-SAELAE 363
giNP_830146     LTGGEVITEELGRDLKSATVESLGRAGKVVVTKENTTVVEGVGSTEQIEARIGQIRAQLE 352
giYP_893164     LTGGEVITEELGRDLKSATVESLGRAGKVVVTKENTTVVEGVGSTEQIEARIGQIRAQLE 352
giNP_388484     LTGGEVITEDLGLDLKSTQIAQLGRASKVVVTKENTTIVEGAGETDKISARVTQIRAQVE 352
giNP_816272     LTGGTVITDDLGLELKDTTIENLGNASKVVVDKDNTTIVEGAGSKEAIDARVHLIKNQIG 352
giAAO36881      LTGGQVISEEIGRDLKDVTVDMLGRAESVKITKETTTIVNGKGNKKEIEDRVNQIKAQIE 354
giYP_702111     LTGGEVISEEVGLSLETAGLELLGQARKVVITKDETTIVEGAGDPEAIAGRVAQIRAEIE 352
giNP_073065     SSGTLAYNNEINSGFKDVTVDNLGDARKVQIAKEKTTVIGGKGNKDKIKKHVELLNGRLK 352
                                                                          :
```

Figure 3.130: continued

```
giEDR27199      EQQIGKERYNLFSG-CTAA-KSSTIILRGGGEHFIDEAERSLHDAIMIVRRALKHKQMVT 406
giAAF54292      ERQVGGERFNLFQG-CPNA-KTSTLILRGGAEQFLEETERSLHDAIMIVRRTIKHDSVVA 406
giNP_495722     QERISDDELILIKG-PKSR-TASSIILRGANDVMLDEMERSVHDSLCVVRRVLESKKLVA 413
giAAY80050      ERKIGEDKMVFIEG-AKNP-KAVSILIRGGLERVVDETERALRDALGTVADVVRDGRAIA 416
giNP_376188     ERKVGEDKMVFVEG-AKNP-KAVSILIRGGLERVVDETERALRDALGTVADVIRDGRAVA 423
giCAA45326      ERKVGEDKMVFVEG-AKNP-KSVSILIRGGLERVVDETERALRDALGTVADVIRDGRAVA 415
giNP_341830     ERKVGEDKMVFVEG-AKNP-KSVSILIRGGLERVVDETERALRDALGTVADVIRDGRAVA 418
giNP_148364     ERKVGEDKMVFIEG-AKNP-KSVTILLRGGFERLVDEAERSLHDALSVVADAIMDGKIVA 416
giAAL63957      ERRVGDEKMVFVEQ-CKNP-KAVSILVRGGFERLVDEAERNLDDALSVVSDVVEDPYILP 414
giO24734        ERRVGNDKMVFIEG-AKNP-KAVNILLRGSNDMALDEAERSINDALHSLRNVLMKPMIVA 415
giBAB60294      ERKIGDDRMTFVTG-CKNP-KAVSILIRGGTEHVVSEVERALNDAIRVVAITKEDGKFLW 410
giCAC12109      ERKIGDDRMTFVMG-CKNP-KAVSILIRGGTDHVVSEVERALNDAIRVVAITKEDGKFLW 410
giAAT43320      ERKIGDDRMTFITG-AKNP-KAVSILIRGGTEHVVDEIERALHDAIRVVAITKEDGKYLP 406
giBAB59649      QVKVGDDYMTFVTG-CKNP-KAVSVLVRGETEHVVDEMERSITDSLHVVASALEDGAYTA 407
giP50016        EKKVAGDKMIFVEG-CKDP-KAVTILIRGGTEHVVDEAERAIEDAIGVVAAALEDGKVVA 411
giNP_275933     EKKISGEEMIFVEE-CKEP-KAVTILVRGSTEHVVSEVERAIEDAIGVVAATVEDGKVVA 402
giAAB99002      ERKVAGDAMIFVEQ-CKHP-KAVTILARGSTEHVVEEVARAIDDAIGVVKCALEEGKIVA 406
giBAA29085      ERKVAGENMIFVEG-CKNP-KAVTILIRGGTEHVVDEVERALEDAIKVVKDILEDGKIIA 409
giNP_125709     ERKVAGENMIFVEG-CKNP-KAVTILIRGGTEHVVDEVERALEDAVKVVKDILEDGKIIA 409
giAAL82098      ERKVAGESMIFVEG-CQNP-KAVTILIRGGTEHVVDEVERALEDAIKVVKDILEDGKILA 409
giO24730        QRKVAGENMIFVEG-CKNP-KAVTILIRGGTEHVVDEVERALEDAVKVVKDIVEDGKIVA 409
giAAP37564      ERKVAGENMVFVEG-CKNP-KAVTILIRGGTEHVVDEVERALEDAIKVVKDIVEDGKIVA 409
giP61111        ERKLAGENMIFVEG-CKNP-KAVTILIRGGTEHVIDEVERALEDAVKVVKDVMEDGAVLP 409
giNP_070280     ERKVGDEKMVFVTG-CKNP-KAVTILVRGGTEHVVEEIARGIEDAVRAVACAVEDGKVVV 409
giO28045        ERKVGDEKMVFIEG-CKNP-KAVTILIRGGSEHVVDEVERSLQDAIKVVKTALESGKVVA 409
giNP_615060     EKKVGGDSMTFVTG-CDNP-KAVTILLRGGTEHVVDSVDSALEDALRVVGVAIEDEKLVS 405
giNP_633403     EKKVGGDSMTFVTG-CDNP-KAVTILLRGGTEHVVDSIDSALEDALRVVGVAIEDEKLVA 405
giAAZ70052      EKDVTGSRMTFVTG-CKDS-KATSILLRGGTEHVVEGIERALEDALRVVGVALEDQKIVV 407
giQ9HN70        QKDIGGDERIFVED-VEEA-KSVTLILRGGTEHVVDEVERAIEDSLGVVRVTLEDGQVMP 406
giO30561        QKDVGGDERIFVED-VEDA-KSVTLILRGGTEHVVDELERAIEDSLGVVRTTLEDGKVLP 407
giYP_137342     QKDIAGDERIFVED-VEDA-RAVTMILRGGTEHVVDEVERAIEDSLGVVAATLEDGKVLP 433
giYP_001689883 RD--SDDELFYVEGESEQA-HGVTLLLRGSTDHVVDELERGVSDALDVSAQTLSDGRVLP 411
giXP_001116562 IKKIGDEYFTFITE-CKDP-KACTILLRGASKEILSEVERNLQDAMQVCRNVLLDPQLVP 409
giCAI46192      IKKIGDEYFTFITD-CKDP-KACTILLRGASKEILSEVERNLQDAMQVCRNVLLDPQLVP 409
giQ3T0K2        IKKIGDEYFTFITE-CKDP-KACTILLRGASKEILSEVERNLQDAMQVCRNVLLDPQLVP 409
giP50143        IKKIGDEYFTFITD-CKDP-KACTIVLRGASKEILAEVERNLQDAMQVCRNVVIDPYLVP 408
giAAH53271      VKKIGDEYFTFVTE-CKDP-KACTILLRGASKEILAEVERNLQDAMQVCRNVLLDPYLLP 408
giXP_392814     IKKVGDEYFCFITE-CKDP-KACTIILRGASKDVLNETERNLQDALHVARNLLIEPKLVP 412
giNP_877966     EVSLNGSGKLFKITGCTSPGKTVTIVVRGSNKLVIEEAERSIHDALCVIRCLVKKRALIA 423
giNP_830146     ETTSEFDREKLQERLAKLAGGVPVIKVGAATETELKERKLRIEDALNSTRAAVEEG-IVA 411
giYP_893164     ETTSEFDREKLQERLAKLAGGVAVIKVGAATETELKERKLRIEDALNSTRAAVEEG-IVA 411
giNP_388484     ETTSEFDREKLQERLAKLAGGVAVIKVGAATETELKERKLRIEDALNSTRAAVEEG-IVS 411
giNP_816272     ETTSDFDREKLQERLAKLAGGVAVVKVGAATETELKELKLRIEDALNATRAAVEEG-MVS 411
giAAO36881      ETTSEFDREKLQERLAKLAGGVAVIKVGAATETELKERKLRIEDALAATKAAVEEG-IIP 413
giYP_702111     NSDSDYDREKLQERLAKLAGGVAVIKAGAATEVELKERKHRIEDAVRNAKAAVEEG-IVA 411
giNP_073065     QTTDKYDSDLIKERIAYLSQGVAVIRVGGATELAQKELKLRIEDALNSTKAAVEEG-IIA 411
                       .                 :   .   .         : *::
```

Figure 3.130: continued

```
giEDR27199      GGGAVEMEISRQLKEYAMTIE----------GKIQYVILGYAKAFEGIPRQLADNAGFDP 456
giAAF54292      GGGAIEMELSKLLRDYSRTIA----------GKEQLLIAAIAKGLEIIPRQLCDNAGFDA 456
giNP_495722     GGGAVETSLSLFLETYAQTLS----------SREQLAVAEFASALLIIPKVLASNAARDS 463
giAAY80050      GGGAVETEIAKRLRKYAPQVG----------GKEQLAIEAYANALESLVMILIENGGFDP 466
giNP_376188     GGGAVELEIAKRLRKYAPQIG----------GKEQLAIEAYASALENLVMILIENGGYDP 473
giCAA45326      GGGAVEIEIAKRLRKYAPQVG----------GKEQLAIEAYANAIEGLIMILAENAGLDP 465
giNP_341830     GGGAVEIEIAKRLRKYAPQVG----------GKEQLAIEAYANAIEGLIMILAENAGLDP 468
giNP_148364     GGGAVEAEVAKVLYEYASKLP----------GKTQLAVEAFARAVEALPQALAHNAGHDP 466
giAAL63957      AGGAAEIEAAKAVRAFAPKVG----------GREQYAVEAFARALEVIPKALAENAGLDP 464
giO24734        GGGAVETELALRLREYARSVG----------GKEQLAIEKFAEALEEIPMILAETAGMEP 465
giBAB60294      GGGAVEAELAMRLAKYANSVG----------GREQLAIEAFAKALEIIPRTLAENAGIDP 460
giCAC12109      GGGAVEAELAMRLAKYANSVG----------GREQLAIEAFAKALEIIPRTLAENAGIDP 460
giAAT43320      GGGAIEAELSMKIRDYANSVG----------GREQLAIEAFAKALEIIPRTLAENAGMDP 456
giBAB59649      GGGATAAEIAVRLRSYAQKIG----------GRQQLAIEKFADAIEEVPRALAENAGLDP 457
giP50016        GGGAPEVEVARQLRDFADGVE----------GREQLAVEAFADALEIIPRTLAENSGLDP 461
giNP_275933     GGGAPEIEIAKRLKDYADSIS----------GREQLAVSAFAEALEIVPKTLAENAGLDS 452
giAAB99002      GGGATEIELAKRLRKFAESVA----------GREQLAVKAFADALEVIPRTLAENSGLDP 456
giBAA29085      GGGASEIELSIKLDEYAKEVG----------GKEQLAIEAFAEALKVIPRTLAENAGLDP 459
giNP_125709     GGGAAEIELSIKLDEYAKEVG----------GKEQLAIEAFAEALKVIPRTLAENAGLDP 459
giAAL82098      GGGAPEIELAIRLDEYAKEVG----------GKEQLAIEAFAEALKVIPRTLAENAGLDP 459
giO24730        AGGAPEIELSIRLDEYAKEVG----------GKEQLAIEAFAEALKVIPRTLAENAGLDP 459
giAAP37564      GGGASEIELAIRLDEYAKEVG----------GKEQLAIEAFADALKVIPRTLAENAGLDP 459
giP61111        AGGAPEIELAIRLDEYAKQVG----------GKEALAIENFADALKIIPKTLAENAGLDT 459
giNP_070280     GAGAPEIEVSLKLREWAPSLG----------GREQLAVEAFATALEIIPRTLAENAGLDP 459
giO28045        GGGAPEIEVALKIRDWAPTLG----------GREQLAAEAFASALEVIPRALAENSGLDP 459
giNP_615060     GGGSPEVEVALRLQEYAATLE----------GREQLAVKAYSEALEVIPRTLAENAGLDP 455
giNP_633403     GGGSPEVEVALRLQEYAATLE----------GREQLAVKAYSEALEVIPRTLAENAGLDP 455
giAAZ70052      GGGSPEIELSLRLKEYAATLK----------GREQLAVMKFAESLEIIPSTLAENAGLDP 457
giQ9HN70        GGGAPETELAMQLRDFADSVG----------GREQLAVEAFADALEVIPRTLAENAGHDP 456
giO30561        GGGAPETELSLQLREFADSVG----------GREQLAVEAFAEALDIIPRTLAENAGLDP 457
giYP_137342     GGGAPETQLALGLRDHADSVG----------GREQLAVEAFADAIDVIPRTLAENAGLDP 483
giYP_001689883 GGGATEVEVASRLRDFADSVS----------GREQLAVEAFADSLELVPRVLAENAGLDS 461
giXP_001116562 GGGASEMAVAHALTEKSKAMT----------GVEQWPYRAVAQALEVIPRTLIQNCGAST 459
giCAI46192      GGGASEMAVAHALTEKSKAMT----------GVEQWPYRAVAQALEVIPRTLIQNCGAST 459
giQ3T0K2        GGGASEMAVAHALTEKSKAMT----------GVEQWPYRAVAQALEVIPRTLIQNCGAST 459
giP50143        GGGASEMSVAHILTEKSKTMT----------GVEQWPYRAVAQALEVIPRTLIQNCGAST 458
giAAH53271      GGGAVEMEVSHRLTERSRAMT----------GVEQWPYRAVAQALEVVPRTLIQNCGASA 458
giXP_392814     GGGAVEMAVSRLLTEKAARLA----------GVEQWPYKAVAQALEIIPRTLAQNCGANT 462
giNP_877966     GGGAPEIELALRLTEYSRTLS----------GMESYCVRAFADAMEVIPSTLAENAGLNP 473
giNP_830146     GGGTSLMNVYTKVASIVAE------------GDEATGINIVLRALEEPVRQIAINAGLEG 459
giYP_893164     GGGTSLMNVYTKVASIVAE------------GDEATGINIVLRALEEPVRQIAINAGLEG 459
giNP_388484     GGGTALVNVYNKVAAVEAE------------GDAQTGINIVLRALEEPIRQIAHNAGLEG 459
giNP_816272     GGGTALVNVIGKVAALEAE------------GDVATGIKIVVRALEEPIRQIAENAGYEG 459
giAAO36881      GGGTAYAMVIKEVEKLNSET-----------HDIKLGIDIVKKSLEEPVRQIACNAGVEG 462
giYP_702111     GGGVALLQSAPALDDLKLE------------GDEATGANIVRVALEAPLKQIAFNAGLEP 459
giNP_073065     GGGVGLLNASCVLTNSKLKERYENETSVENIKEILLGFEIVQKSLEAPARQIIQNSGVDP 471
                ..*         :                                  ..      :  . . .
```

Figure 3.130: continued

```
giEDR27199      TNILNLLRKKHAEGGL--------WYGVNVNEEGILD-MMEAQVWEPALIKLNAIAAATE 507
giAAF54292      TNILNKLRQKHAQGGQ--------WYGVDINKEDISD-NYEQCVWEPSIIKINALTAAAE 507
giNP_495722     TDLVTKLRAYHSKAQLIPQLQHLKWAGLDLEEGTIRD-NKEAGILEPALSKVKSLKFATE 522
giAAY80050      IELLVKLRSAHENETN-------KWHGINVYTGQIQD-MWSLGVIEPAVVKMNAIKAATE 518
giNP_376188     IDLLVKLRSAHENEAN-------KWYGINVFTGQVED-MWKLGVIEPAVVKMNAIKAATE 525
giCAA45326      IDKLMQLRSLHENETN-------KWYGLNLFTGNPED-MWKLGVIEPALVKMNAIKAATE 517
giNP_341830     IDKLMQLRSLHENETN-------KWYGLNLFTGNPED-MWKLGVIEPALVKMNAVKAATE 520
giNP_148364     IEVLVKLRSAHEKPEN-------KWYGVDLDTGEIVD-MWSRGVLEPMRVKLNALKAATE 518
giAAL63957      IDILTELTHKHEQTDG-------WKYGLDVYQGKVVD-MVSLGLVEPLTVKINALKVAVE 516
giO24734        IQTLMDLRAKHAKG-L-------INAGVDVMNGKIADDMLALNVLEPVRVKAQVLKSAVE 517
giBAB60294      INTLIKLKSEHE-KGK-------ISMGVDLDSNGAGD-MSKKGVIDPVRVKTHALESAVE 511
giCAC12109      INTLIKLKAEHE-KGR-------ISVGVDLDNNGVGD-MKAKGVVDPLRVKTHALESAVE 511
giAAT43320      INTLIKLKAEHE-KSN-------KNYGINLNENKIDD-MVKLGVFDTYRVKQHALESAVE 507
giBAB59649      IDIILKLRAEHA-KGN-------KYAGVNVFSGEIED-MVNNGVIEPIRVGKQAIESATE 508
giP50016        IDVLVQLRAKHE-DGQ-------VTAGIDVYDGDVKD-MLEEGVVEPLRVKTQALASATE 512
giNP_275933     IDVLVDLRAAHE-ES--------TYMGIDVFDGKIVD-MKEAGVIEPHRVKKQAIQSAAE 502
giAAB99002      IDMLVKLRAAHEKEGG-------EVYGLDVFEGEVVD-MLEKGVVEPLKVKTQAIDSATE 508
giBAA29085      IETLVKVIAAHK-EKG-------QTIGIDVYEGEPAD-MMERGVIEPVRVKKQAIKSASE 510
giNP_125709     IETLVKVIAAHK-EKG-------PTIGIDVYEGEPAD-MMERGVIEPVRVKKQAIKSASE 510
giAAL82098      IETLVKVIAAHK-EKG-------PTIGVDVYEGEPAD-MLERGVIEPLRVKKQAIKSASE 510
giO24730        IETLVKVIAAHK-EKG-------PTIGVDVFEGEPAD-MLERGVIAPVRVPKQAIKSASE 510
giAAP37564      VDVLVKVTAAHK-DKG-------ATIGVDVFAGEPAD-MLERGVIEPLRVKKQAIKSASE 510
giP61111        VEMLVKVISEHK-NRG-------LGIGIDVFEGKPAD-MLEKGIIEPLRVKKQAIKSASE 510
giNP_070280     IDVLVELKAAHE-KGQ-------KYAGVDVDTGKVVD-MKERGVFEPLRVKTQAIGSATE 510
giO28045        IDILVELRKAHE-EGK-------TTYGVDVFSGEVAC-MKERGVLEPLKVKTQAITSATE 510
giNP_615060     IDMLMELRSQHEKGM--------KTAGLDVYEGKVVD-MWNNFVVEPLRVKTQVINAATE 506
giNP_633403     IDMLMELRSQHEKGM--------KTAGLNVYEGKVVD-MWENFVVEPLRVKTQVINAATE 506
giAAZ70052      IDMLVEMRSQHEKGN--------KRAGLNVYTGKIED-MFENNVVEPLRIKTQAINAATE 508
giQ9HN70        IDSLVDLRSQHDGGD--------TEAGLDAYNGDVID-MESEGIVEPLRVKTQAIESATE 507
giO30561        IDSLVDLRSRHDGGE--------FAAGLDAYTGEVID-MEEEGVVEPLRVKTQAIESATE 508
giYP_137342     IDSLVDLRSKHDGGA--------VTSGLDAYTGEVVD-MEEDGVVEPLRVKTQAVESATE 534
giYP_001689883 IDTLVDLRSAHENDDD-------EHIGLNVLSGDLED-TFEAGVVEPAHAKEQAVTSASE 513
giXP_001116562 IRLLTSLRAKHTQENC-------ETWGVNGETGTLVD-MKELGIWEPLAVKLQTYKTAVE 511
giCAI46192      IRLLTSLRAKHTQENC-------ETWGVNGETGTLVD-MKELGIWEPLAVKLQTYKTAVE 511
giQ3T0K2        IRLLTSLRAKHTQENC-------ETWGVNGETGTLVD-MKELGIWEPLAVKLQTYKTAVE 511
giP50143        IRILTSLRAKHTQEGC-------QTWGVDGEAGVLAD-MKELGIWEPLAVKLQTYKTAVE 510
giAAH53271      IRVLTSLRAKHTQEGN-------SSWGVNGETGTLAD-MEQLGIWEPLAVKAQTYKTAVE 510
giXP_392814     IRTLTALRAKHATEG--------MTWGIDGETGQLVD-MKEHGIWEPLSVKLQTYKTAIE 513
giNP_877966     ISTVTELRNRHAQGE--------KTTGINVRKGGISN-ILEEMVVQPLLVSVSALTLATE 524
giNP_830146     SVVVERLKGEKV------------GVGFNAATGEWVN-MLESGIVDPAKVTRSALQNAAS 506
giYP_893164     SVVVERLKGEKV------------GVGFNAATGEWVN-MLETGIVDPAKVTRSALQNAAS 506
giNP_388484     SVIVERLKNEEI------------GVGFNAATGEWVN-MIEKGIVDPTKVTRSALQNAAS 506
giNP_816272     SVIVDKLKNVDL------------GIGFNAANGEWVN-MVEAGIVDPTKVTRSALQNAAS 506
giAAO36881      SIVIEKVKHSEA------------GIGYDALNNEYVN-MIKAGIVDPTKVSRSALQNAAS 509
giYP_702111     GVVAEKVRNLPA------------GHGLNASTNEYGD-LLEAGINDPVKVTRSALQNAAS 506
giNP_073065     VKILSELKNEKT------------GVGFDAETKKKVD-MIANGIIDPTKVTKTALEKAAS 518
                      :                  * :             :  .          * .
```

Figure 3.130: continued

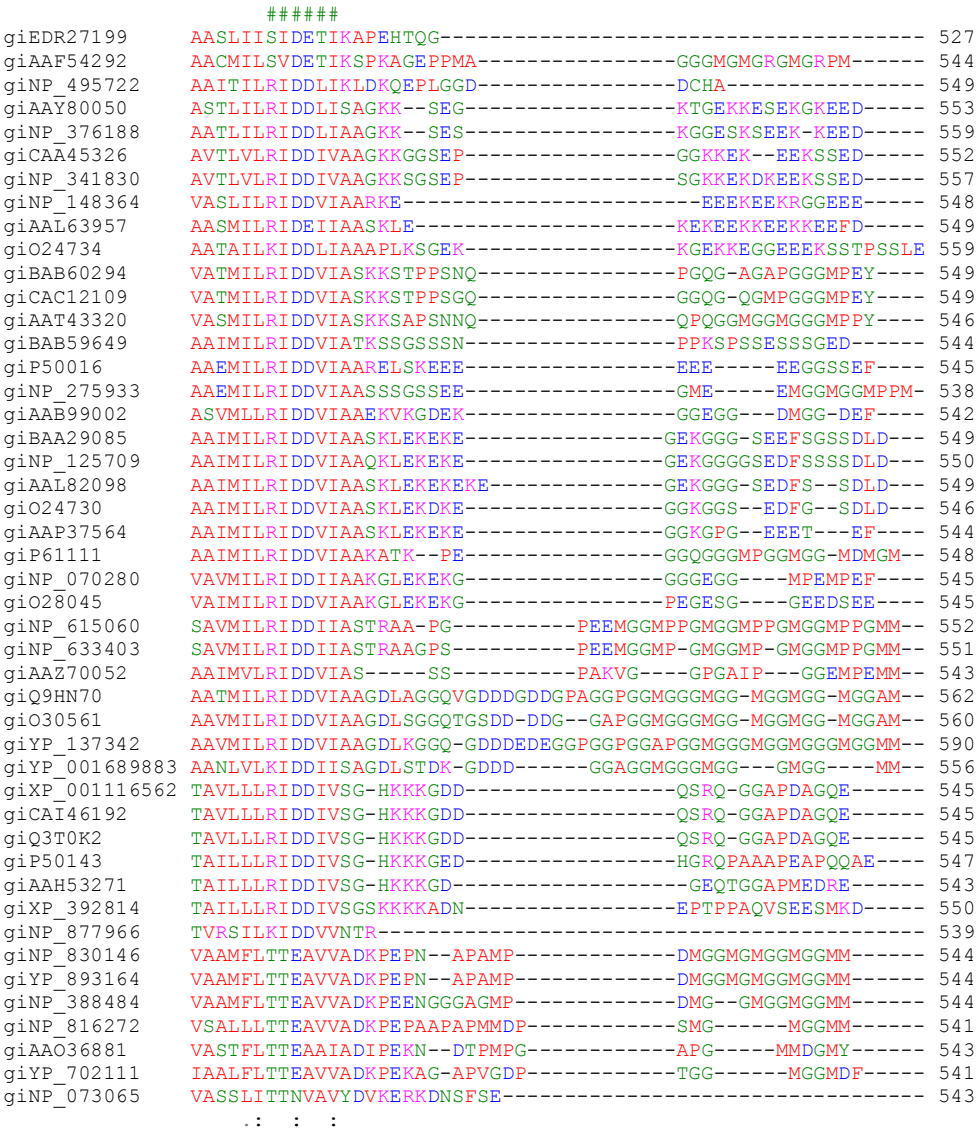

Figure 3.130

[giEDR27199: source organism= *Entamoeba dispar* SAW760, product= T-complex protein 1 subunit eta, putative, length= 527 aa;
giAAF54292: source organism= *Drosophila melanogaster*, product= CG8351-PA (GO_component: chaperonin-containing T-complex), length= 544 aa;
giNP_495722: source organism= *Caenorhabditis elegans*, product= chaperonin containing TCP-1 family member (cct-1), lenght= 549 aa;
giAAY80050: source organism= *Sulfolobus acidocaldarius* DSM 639, product= thermosome beta subunit, length= 553 aa;
giNP_376188: source organism= *Sulfolobus tokodaii* str. 7, product= thermosome, beta subunit, lenght= 559 aa;

giCAA45326: source organism= *Sulfolobus shibatae*, product= thermophilic factor 55, length= 552 aa;
giNP_341830: source organism= *Sulfolobus solfataricus* P2, product= thermosome subunit beta, length= 557 aa;
giNP_148364: source organism= *Aeropyrum pernix* K1, product= thermosome beta subunit, length= 548 aa;
giAAL63957: source organism= *Pyrobaculum aerophilum* str. IM2, product= thermosome (chaperonin) alpha subunit, length= 549 aa;
giO24734: source organism= *Sulfolobus tokodaii*, product= thermosome subunit alpha, length= 559 aa;
giBAB60294: source organism= *Thermoplasma volcanium* GSS1, product= archaeal chaperonin [group II], length= 549 aa;
giCAC12109: source organism= *Thermoplasma acidophilum*, product= thermosome, alpha chain, length= 549 aa;
giAAT43320: source organism= *Picrophilus torridus* DSM 9790, product= thermosome subunit, length= 546 aa;
giBAB59649: source organism= *Thermoplasma volcanium* GSS1, product= archaeal chaperonin [group II], length= 544 aa;
giP50016: source organism= *Methanopyrus kandleri*, product= thermosome subunit, length= 545 aa;
giNP_275933: source organism= *Methanothermobacter thermautotrophicus* str. Delta H, product= chaperonin, length= 538 aa;
giAAB99002: source organism= *Methanocaldococcus jannaschii* DSM 2661, product= thermosome (ths), lenght= 542 aa;
giBAA29085: source organism= *Pyrococcus horikoshii* OT3, product= hypothetical thermophilic factor, length= 549 aa;
giNP_125709: source organism= *Pyrococcus abyssi* GE5, product= thermosome, subunit alpha, length= 550 aa;
giAAL82098: source organism= *Pyrococcus furiosus* DSM 3638, product= thermosome, single subunit, length= 549 aa;
giO24730: source organism= Thermococcus sp. KS-1, product= thermosome subunit beta, lengh= 546 aa;
giAAP37564: source organism= *Thermococcus litoralis*, product= thermosome alpha subunit, length= 544 aa;
giP61111: source organism= *Thermococcus kodakarensis* KOD1, product= thermosome subunit alpha, length= 548 aa;
giNP_070280: source organism= *Archaeoglobus fulgidus* DSM 4304, product= thermosome, subunit beta (thsB), length= 545 aa;
giO28045: source organism= *Archaeoglobus fulgidus*, product= thermosome subunit alpha, length= 545 aa;
giNP_615060: source organism= *Methanosarcina acetivorans* C2A, product= Hsp60, length= 552 aa;
giNP_633403: source organism= *Methanosarcina mazei* Go1, product= thermosome, alpha subunit, length= 551 aa;
giAAZ70052: source organism= *Methanosarcina barkeri* str. Fusaro product= Hsp60, length= 543 aa;
giQ9HN70: source organism= *Halobacterium salinarum*, product= thermosome subunit alpha, length= 562 aa;

giO30561: source organism= *Haloferax volcanii*, product= thermosome subunit 1, length= 560 aa;
giYP_137342: source organism= *Haloarcula marismortui* ATCC 43049, product= thermosome alpha subunit, length= 590 aa;
giYP_001689883: source organism= *Halobacterium salinarum* R1, product= thermosome subunit 2, length= 556 aa;
giQ3T0K2: source organism= *Bos taurus*, product= T-complex protein 1 subunit gamma, length= 545 aa;
giXP_001116562: source organism= *Macaca mulatta*, product= similar to chaperonin containing TCP1, subunit 3 isoform a isoform 4, length= 545 aa;
giCAI46192: source organism= *Homo sapiens*, product= hypothetical protein; T-complex protein 1, gamma subunit= 545 aa;
giP50143: source organism= *Xenopus laevis*, product= T-complex protein 1 subunit gamma, length= 547 aa;
giAAH53271: source organism= *Danio rerio*, product= chaperonin containing TCP1, subunit 3 (gamma), length= 543 aa;
giXP_392814: source organism= *Apis mellifera*, product= similar to T-complex protein 1 subunit gamma(TCP-1-gamma) (CCT-gamma), length= 550 aa; giNP_877966: source organism= *Rattus norvegicus*, product= chaperonin subunit 4 (delta), length= 539 aa;
giNP_830146: source organism= *Bacillus cereus* ATCC 14579, product= chaperonin GroEL, length= 544 aa;
giYP_893164: source organism= *Bacillus thuringiensis* str. Al Hakam, product= chaperonin GroEL, length= 544 aa;
giNP_388484: source organism= *Bacillus subtilis* subsp. subtilis str. 168, product= chaperonin GroEL, length= 544 aa;
giNP_816272: source organism= *Enterococcus faecalis* V583, product= chaperonin, 60 kDa, length= 541 aa;
giAAO36881: source organism= *Clostridium tetani* E88, product= 60 kDa chaperonin groEL, length= 543 aa;
giYP_702111: source organism= Rhodococcus sp. RHA1, product=chaperonin GroEL, length= 541 aa;
giNP_073065: source organism= *Mycoplasma genitalium* G37, product= chaperonin GroEL, length= 543 aa]

Phylogenetic tree constructed by this alignment shows that bacterial and eukaryotic Hsp60 α or GroEL proteins are more closely related to one another than they are to archaeal proteins (Figure 3.131). Hsp60 subunit proteins used in multiple sequence alignment are abbreviated in phylogenetic tree in order to make evaluation easier (Figure 3.131). The classification scheme in this tree, almost follow the systematic hierarchy among the organisms.

Table 3.8: Scores of multiple sequence alignment of *T. volcanium* Hsp60α subunit protein with several archaeal Hsp60 proteins.

Chaperonin source	Percent identity with chaperonin subunits from																												
	1	2	3	4	5	6	7	8	9	10	11	12	13	14	15	16	17	18	19	20	21	22	23	24	25	26	27	28	29
(1) TvolcaniumAlpha	100	60	94	80	59	59	59	60	57	57	59	57	55	57	54	58	56	57	52	50	52	51	52	52	52	52	52	50	45
(2) TvolcaniumBeta		100	59	57	57	57	56	57	57	55	56	53	53	54	53	57	56	54	50	50	53	50	54	54	53	52	50	49	44
(3) TacidophilumAlpha			100	79	60	60	59	60	58	57	59	58	55	56	54	58	56	57	52	50	51	50	52	51	52	51	52	51	45
(4) PtorridusThsSubunit				100	57	59	58	58	56	55	57	56	55	56	56	56	56	54	51	49	51	51	51	50	50	51	53	50	45
(5) AfulgidusBeta					100	67	68	68	75	69	66	64	61	61	62	67	66	65	55	58	53	59	55	53	53	56	57	53	50
(6) PhorikoshiiTF						100	97	89	70	69	93	80	58	58	59	88	67	70	55	57	55	55	56	55	55	59	58	54	49
(7) PabyssiAlpha							100	88	70	69	92	79	69	58	59	89	67	70	55	56	55	55	56	54	55	58	57	54	50
(8) TlitoralisAlpha								100	70	70	88	79	60	60	60	87	69	70	55	57	57	55	59	57	57	59	59	54	51
(9) AfulgidusAlpha									100	69	69	64	58	59	58	69	62	66	56	58	54	56	56	54	54	57	57	55	49
(10) MkandleriThsSubunit										100	70	65	61	61	61	67	71	70	60	63	54	62	55	54	54	58	57	53	53
(11) PfuriosusThsSSubunit											100	80	59	58	59	90	67	70	54	57	55	55	56	54	55	58	58	54	50
(12) TkodakarensisAlpha												100	58	57	59	81	65	67	56	58	53	55	54	54	53	54	55	51	53
(13) MacetivoransHsp60													100	69	93	58	60	60	57	58	48	59	49	48	48	49	50	47	49
(14) MbarkeriHsp60														100	68	57	59	57	56	56	49	57	50	50	49	46	50	46	48
(15) MmazeiAlpha															100	59	61	59	57	60	49	59	50	49	49	50	50	47	50
(16) TspKS-1Beta																100	66	69	54	56	56	54	57	55	55	58	57	55	49
(17) MthermautotrophicusChp																	100	69	60	61	52	59	53	52	52	52	54	50	52
(18) MjannaschiiThs																		100	56	59	52	56	54	52	52	54	54	50	50
(19) HsalinarumAlpha																			100	78	46	79	44	45	44	44	48	43	53
(20) HmarismortuiAlpha																				100	47	79	46	46	46	46	48	44	57
(21) SacidocaldariusBeta																					100	47	90	86	85	64	58	52	43
(22) HvolcaniiThsSubunit1																						100	46	47	46	46	48	44	55
(23) StokodaiiBeta																							100	87	86	65	59	52	44
(24) SshibataeTF55																								100	97	64	60	52	43
(25) SsolfataricusBeta																									100	64	60	52	43
(26) ApernixBeta																										100	61	54	42
(27) PaerophilumAlpha																											100	51	43
(28) StokodaiiAlpha																												100	40
(29) HsalinarumThsSubunit2																													100

Table 3.9: Scores of multiple sequence alignment of *T. volcanium* Hsp60 α subunit protein with several eukaryal Hsp60 proteins and bacterial GroEL proteins.

Chaperonin source	Percent identity with chaperonin subunits from																	
	1	30	31	32	33	34	35	36	37	38	39	40	41	42	43	44	45	46
(1) TvolcaniumAlpha	100	38	38	38	37	37	37	37	39	37	38	24	20	22	23	19	19	19
(30) EdisparTCP1eta		100	30	31	33	30	31	30	59	30	35	17	17	18	15	18	18	18
(31) DrerioTCP1gamma			100	86	69	84	32	84	29	84	30	14	14	18	14	14	14	16
(32) XlaevisTCP1gamma				100	72	86	32	86	31	86	32	16	16	19	15	16	16	17
(33) AmelliferaTCP1gamma					100	71	30	71	30	71	33	18	14	20	16	19	19	19
(34) BtaurusTCP1gamma						100	32	98	29	98	31	16	16	19	18	19	19	17
(35) RnorvegicusDelta							100	32	30	32	32	17	15	18	20	18	18	15
(36) MmulattaSimilartoTCP1gamma								100	28	98	31	15	16	19	16	17	17	17
(37) DmelanogasterCCT									100	29	34	16	15	19	19	19	19	18
(38) HsapiensTCP1gamma										100	31	15	14	19	17	17	16	17
(39) CelegansCCT1											100	17	15	17	13	12	16	18
(40) CtetaniGroEL												100	48	70	60	71	71	66
(41) MgenitalumGroEL													100	49	44	49	49	48
(42) BsubtilisGroEL														100	64	87	87	78
(43) RspRHA1GroEL															100	64	64	61
(44) BcereusGroEL																100	99	76
(45) BthuringiensisGroEL																	100	77
(46) Efaecalis60kdChaperonin																		100

Thermosome proteins of methanogenic species are clustered as two different groups. *Methanosarcina acetivorans* Hsp60 protein, *Methanosarcina mazei* thermosome alpha subunit and *Methanosarcina barkeri* Hsp60 protein are clustered as a sub-branch. These organisms belong to the class Methanomicrobia and genus Methanosarcina. They are mesophilic methanogens with optimal growth temperatures of 37°C. *M. kandleri* thermosome subunit, *M. thermautotrophicus* chaperonin protein and *M. jannaschii* thermosome form a distinct branch. *M. kandleri* and *M. thermautotrophicus* belong to the class Methanopyri. *M. jannaschii* belongs to the class *Methanococci*. These methanogens are either thermophilic or hyperthermophilic. Optimum growh temperature of the organisms in this distinct branch is higher than that of methanogens which belong to the class Methanomicrobia (Figure 3.131).

In Euryarchaeota, Hsp60 α proteins of mesophilic methanogens (*Methanosarcina*, optimum growth temperature 37°C) appeared to be more close to Halobacteria (optimum growth temperature 37-45°C) then thermophilic methanogens, and clustered together. Hsp60 α subunits of hyperthermophilic members of Euryarchaeota, other than hyperthermophilic methanogens (i.e. *Archaeoglobus*, *Pyrococcus*, *Thermococcus*) are classified in the same group. These proteins seem to be more close to eukaryotic and bacterial orthologs and share the most recent ancestor. Hsp60 α proteins of hyperthermophilic archaea in Crenarchaeota (i.e. *Sulfolobus*, *Aeropyrum* and *Pyrobaculum* sp.) are clustered together. Eukaryotic and bacterial Hsp60 proteins form a sub-branch. GroEL proteins are clustered together. All eukaryotic Hsp60 proteins are not clustered together, TCP-1 subunits of *E. dispar*, *D. melanogaster* and *C. elegans* seem to be more close to bacterial proteins. Hsp60 α proteins of the archaea in phylum Euryarchaeota (i.e. *Thermoplasma* and *Picrophilus*) fall into same cluster. Proteins of hyperthermophilic members of the Crenarchaeota phylum, formed a distinct branch being more related to the eucarya/bacteria group than other archaea.

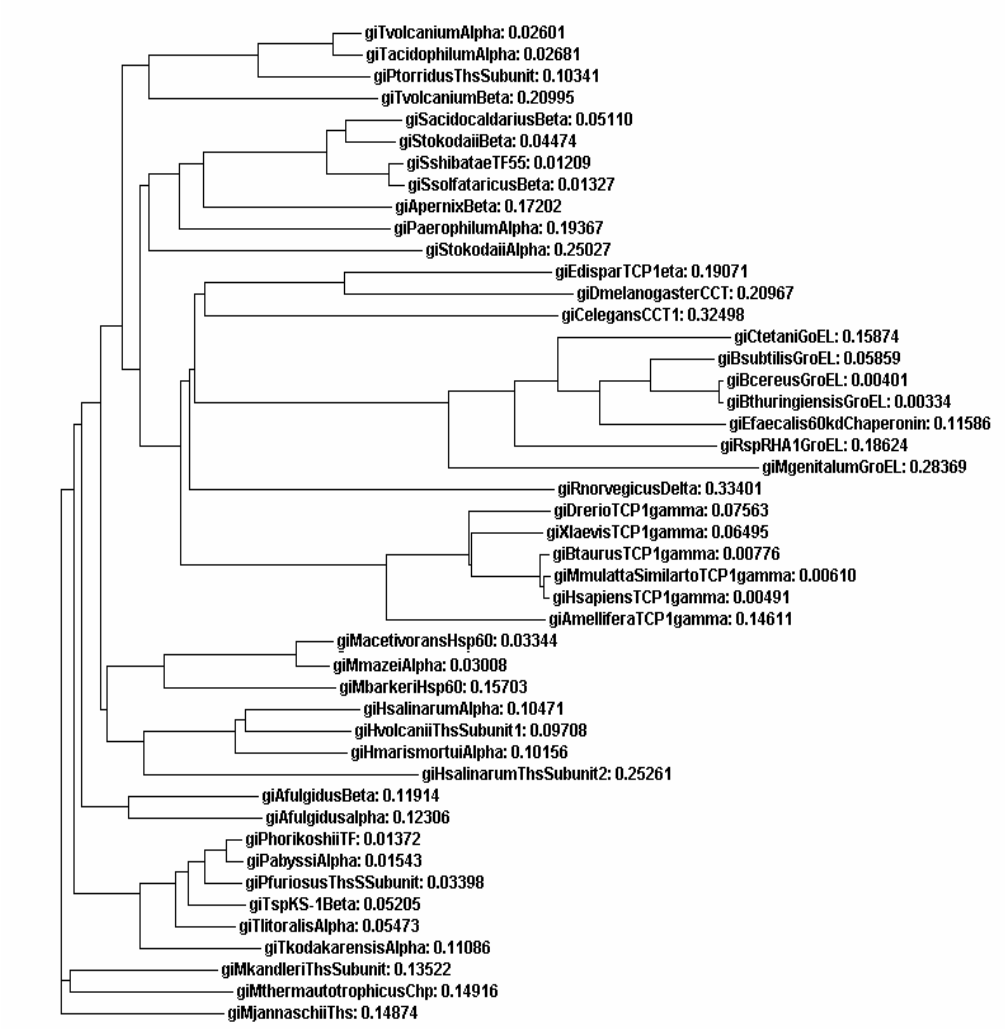

Figure 3.131: Phylogenetic tree constructed by clustal type multiple sequence alignments of amino acid sequence of *T. volcanium* Hsp60 α subunit protein with several eukaryal, archaeal and bacterial Hsp60 proteins (Clustal W -1.83). The numbers indicate the calculated distances of organisms to the closest branching point.

3.4.2 Sequence Alignments of *T. volcanium* Hsp60 α Subunit With Several Archaeal Hsp60 Proteins

Multiple sequence alignments of amino acid sequence of *T. volcanium* Hsp60α subunit protein with several archaeal Hsp60 proteins were performed by using Clustal W 1.83 as described in 2.6 Section. Protein sequences of Hsp60 subunits of organisms were derived from the online-database of NCBI (Figure 3.132). The archaeal Hsp60 subunit proteins are the same proteins used in Section 3.4.1. Scores of this alignment is given in Table 3.8. Hsp60 subunit proteins used in multiple sequence alignment are abbreviated in score table and phylogenetic tree (Table 3.8 and Figure 3.133).

```
giBAB60294      ------------------------MIRNMMTGQVPILVLKEGTQREQGKNAQRNNIEAAK 36
giCAC12109      ------------------------MISNMMTGQVPILVLKEGTQREQGKNAQRNNIEAAK 36
giAAT43320      ----------------------------MITGQTPILILKEGTERQQGKNAQKNNIEAAK 32
giBAB59649      ----------------------------MIAGQ-PIFILKEGTKRESGKDAMKENIEAAI 31
giAAY80050      ---------------------MSATATVATTPEGIPVIILKEGSSRTYGKEALRINIAAVK 40
giNP_376188     -------------MLSAVEKMSTTATVATTPEGIPVIILKEGSSRTYGKEALRINIAAVK 47
giCAA45326      ---------------------MATATVATTPEGIPVIILKEGSSRTYGKEALRANIAAVK 39
giNP_341830     ------------------MRKMATATVATTPEGIPVIILKEGSSRTYGKEALRANIAAVK 42
giNP_148364     ---------------------MAIQQQPMTEPVGIPVIILKEGTQRSYGREALRANIMAVR 40
giAAL63957      ----------------------MSQAVLTQIGGVPVLVLKEGTQRAFGKEALRLNIMIAR 38
giO24734        ----------------------------MANAPVLLLKEGTQRSSGRDALKNNILAAV 30
giP50016        ------------------------MAMLAGDGRQVLILPEGYQRFVGRDAQRMNIMAAR 35
giNP_275933     ----------------------------MAQGQQPILVLPEGTSRYLGRDAQRMNILAGK 32
giAAB99002      ----------------------------MAMAGAPIVVLPQNVKRYVGRDAQRMNILAGR 32
giBAA29085      ----------------------------MAQLAGQPILILPEGTQRYVGRDAQRMNILAAR 33
giNP_125709     ----------------------------MAQLAGQPILILPEGTQRYVGRDAQRMNILAAR 33
giAAL82098      ----------------------------MAQLAGQPILILPEGTQRYVGRDAQRMNILAAR 33
giO24730        ----------------------------MAQLAGQPVVILPEGTQRYVGRDAQRLNILAAR 33
giAAP37564      ----------------------------MAQLAGQPILILPEGTQRYVGKDAQRLNILAAR 33
giP61111        ----------------------------MAQLSGQPVVILPEGTQRYVGRDAQRLNILAAR 33
giNP_070280     ----------------------------MATLQGQPVLILREGTQRTVGRDAQRMNIMAAR 33
giO28045        ----------------------------MATLQGTPVLILKEGTQRTVGRDAQRMNIMAAR 33
giNP_615060     ------------------------------MAGQPIFILKEGSKRTRGRDAQSNNIMAAK 30
giNP_633403     ------------------------------MAGQPIFILKEGSKRTRGRDAQSNNIMAAK 30
giAAZ70052      ------------------------------MAAQPIFILREGSKRTHGSDAQHNNIMAAK 30
giQ9HN70        --------------------------MAQQMGN-QPLIVLSEDSQRTSGEDAQSMNITAGK 34
giO30561        --------------------------MSQRMQQGQPMIILGEDSQRTSGQDAQSMNITAGK 35
giYP_137342     MACNRAIHRRSPWLLYRSTFNHRLTMAQQQMGNQPMIVLSEESQRTSGKDAQSMNITAGT 60
giYP_001689883----------------------MAQQQRMQGQPMIIMGDDAQRVKDRDAQEHNISAAR 36
                                                 :.:: :  .*  . :*   **
```

Figure 3.132: Clustal type multiple sequence alignments of amino acid sequence of *T. volcanium* Hsp60α subunit protein with several archaeal Hsp60 proteins.

Conserved sequences related to feature 1, feature 2 and feature 3 were indicated by #, #, and # symbols on the multiple sequence alignments, respectively.

```
giBAB60294      AIADAVRTTLGPKGMDKMLVDSIGDIIISNDGATILKEMDVEHPTAKMIVEVSKAQDTAV 96
giCAC12109      AIADAVRTTLGPKGMDKMLVDSIGDIIISNDGATILKEMDVEHPTAKMIVEVSKAQDTAV 96
giAAT43320      AIADAVRTTLGPKGMDKMLVDSIGDIVITNDGATILKEMDIDHPTAKMLVEASKSQDTAV 92
giBAB59649      AISNSVRSSLGPRGMDKMLVDSLGDIVITNDGVTILKEMDVEHPAAKMMVEVSKTQDSFV 91
giAAY80050      AVEEALKTTYGPRGMDKMLVDSLGDITITNDGATILDKMDLQHPAAKLLVQIAKGQDEET 100
giNP_376188     AVEEALKSTYGPRGMDKMLVDSLGDITITNDGATILDKMDLQHPAAKLLVQIAKGQDEET 107
giCAA45326      AIEEALKSTYGPRGMDKMFVDSLGDITITNDGATILDKMDLQHPTGKLLVQIAKGQDEET 99
giNP_341830     AIEEALKSTYGPRGMDKMLVDSLGDITITNDGATILDKMDLQHPTGKLLVQIAKGQDEET 102
giNP_148364     AIAQILKTTYGPKGMDKMLVDSLGDITITNNGATILDKMDVAHPAAKMLVQISKGQEDEA 100
giAAL63957      AIAEVMRTTLGPKGMDKMLIDSLGDITITNDGATILDEMDVQHPIAKLLVEISKSQEEEA 98
giO24734        TLAEMLKSSLGPRGLDKMLIDSFGDVTITNDGATIVKEMEIQHPAAKLLVEAAKAQDAEV 90
giP50016        VVAETVRTTLGPMGMDKMLVDEMGDVVVTNDGVTILEEMDIEHPAAKMVVEVAKTQEDEV 95
giNP_275933     ILAETVRTTLGPKGMDKMLVDSLGDIVVTNDGVTILKEMDIEHPAAKMLVEVAKTQEDEV 92
giAAB99002      IIAETVRTTLGPKGMDKMLVDELGDIVVTNDGVTILKEMSVEHPAAKMLIEVAKTQEKEV 92
giBAA29085      IIAETVRTTLGPKGMDKMLVDSLGDIVITNDGATILDEMDIQHPAAKMMVEVAKTQDKEA 93
giNP_125709     IIAETVRTTLGPKGMDKMLVDSLGDIVITNDGATILDEMDIQHPAAKMMVEVAKTQDKEA 93
giAAL82098      IVAETIRTTLGPKGMDKMLVDSLGDIVITNDGATILDEMDIQHPAAKMMVEVAKTQDKEA 93
giO24730        IIAETVRTTLGPKGMDKMLVDSLGDIVITNDGATILDEMDIQHPAAKMMVEVAKTQDKEA 93
giAAP37564      IVAETVRTTLGPKGMDKMLVDSLGDIVITNDGATILDEMDIQHPAAKMMVEVAKTQDKEA 93
giP61111        IIAETVRTTLGPKGMDKMLVDSLGDIVVTNDGATILDKIDLQHPAAKMMVEVAKTQDKEA 93
giNP_070280     VIAEAVRSTLGPKGMDKMLVDSLGDVVITNDGVTILKEIDVEHPAAKMIIEVAKTQDNEV 93
giO28045        VIAEAVKSTLGPKGMDKMLVDSLGDVVITNDGVTILKEMDVEHPAAKMIIEVAKTQDNEV 93
giNP_615060     AVAEAVRTTLGPKGMDKMLVDSMGDVVITNDGATILKEMDIEHPAAKMVVEVSKTQDEQV 90
giNP_633403     AVAEAVRTTLGPKGMDKMLVDSMGDVVITNDGATILKEMDIEHPAAKMVVEVSKTQDDEV 90
giAAZ70052      AVAEAVRTTLGPKGMDKMLVDSMGDVVITNDGATILKEMDIEHPGAKMIVEVAKTQDAEV 90
giQ9HN70        AVAESVRTTLGPKGMDKMLVDSSGEVVVTNDGVTILKEMDIEHPAANMIVEVAETQETEV 94
giO30561        AVAEAVRTTLGPKGMDKMLVDSGGQVVVTNDGVTILKEMDIDHPAANMIVEVSETQEDEV 95
giYP_137342     AVAEAVRTTLGPKGMDKMLVDNSGSVVVTNDGVTILDEMDIEHPAANMIVEVAQTQEDEV 120
giYP_001689883AVADAVRSTLGPKGMDKMLVSSMGDVTVTNDGVTILQEMDIDNPTAEMIVEVAETQEDEA 96
                : : :::: ** *:***::.. *.: ::*:*.**:.::.: :* .::::: :: *:  .
                #####
giBAB60294      GDGTTTAVVLSGELLKQAETLLDQGVHPTVISNGYRLAVNEARKIIDEISVKS--TDD-- 152
giCAC12109      GDGTTTAVVLSGELLKQAETLLDQGVHPTVISNGYRLAVNEARKIIDEIAEKS--TDD-- 152
giAAT43320      GDGTTTVVVLAGELLKQAESLLEQGVHSTVIASGYHLAVTEAKKQLDSLAIKA--DDE-- 148
giBAB59649      GDGTTTAVIIAGGLLQQAEALINQNVHPTVISEGYRMASEEAKRIIDEISTKIGKDEK-- 149
giAAY80050      ADGTKTAVIFSGELVKKAEELLYKEIHPTIIVSGYKKAEEMAIKTIEEISTKVSVNDT-- 158
giNP_376188     ADGTKTAVILAGELVKKAEELLYKEIHPTIIVSGFKKAEEQALKTIEEIAQKVSVNDM-- 165
giCAA45326      ADGTKTAVILAGELAKKAEDLLYKEIHPTIIVSGYKKAEEIALKTIQDIAQPVSINDT-- 157
giNP_341830     ADGTKTAVILAGELAKKAEDLLYKEIHPTIIVSGYKKAEEIALKTIQEIAQPVTINDT-- 160
giNP_148364     GDGTKTTVIFAGELLKEAEKLLDINIHPTIIVEGYKEALRKASEVIESIAEPVSYDDV-- 158
giAAL63957      GDGTTTAVVLAGALLEEAEKLLEKNIHPTVIVSGFKKALDVAAEHLRKVAIPVNRTDV-- 156
giO24734        GDGTTSAVVLAGLLLDKADDLLDQNIHPTIIIEGYKKALNKSLEIIDQLATKIDVSNLNS 150
giP50016        GDGTTTAVVLAGELLHKAEDLLQQDIHPTVIARGYRMAVEKAEEILEEIAEEIDPDDE-- 153
giNP_275933     GDGTTTAVIIAGELLKKAENLLEMEIHPTIIAMGYRQAAEKAQEILDDIA--IDASDR-- 148
giAAB99002      GDGTTTAVVIAGELLRKAEELLDQNIHPSVIINGYEMARNKAVEELKSIAKEVKPEDT-- 150
giBAA29085      GDGTTTAVVIAGELLKKAEELLDQNIHPSIIIKGYTLASQKAQEILDSIAKEVKPDDE-- 151
giNP_125709     GDGTTTAVVIAGELLKKAEELLDQNIHPSIVIKGYMLAAEKAQEILDSIAKEVKPDDE-- 151
giAAL82098      GDGTTTAVVIAGELLRKAEELLDQNIHPSIIIKGYTLAAQKAQEILENIAKEVKPDDE-- 151
giO24730        GDGTTTAVVIAGELLRKAEELLDQNIHPSIIIKGYALAAEKAQEILDEIAKDVDVEDR-- 151
giAAP37564      GDGTTTAVVIAGELLRKAEELLNQNIHPTIIVKGYTLAAEKAQEILESIAKDVSPMDE-- 151
giP61111        GDGTTTAVVIAGELLRKAEELLDQNIHPSIIIKGYALAAEKAQEILDEIAIRVDPDDE-- 151
giNP_070280     GDGTTTAVVLAGELLKRAEELLDQEIHPAIIANGYRYAAEKALEILNEIAIPISKDDD-- 151
giO28045        GDGTTTAVVLAGELLKKAEELLDQDIHPTVIARGYRMAANKAVEILESIAMDIDVEDE-- 151
giNP_615060     GDGTTSAAVVAGELLKKAEDLIEQEIHPTIIASGYRLAAEKAVEVLNSLAMNVEMSNR-- 148
giNP_633403     GDGTTSAAVVAGELLNKAEDLIEQEIHPTIIASGYRLAAEKAIEVLNSLAMSVDMGNR-- 148
giAAZ70052      GDGTTTAAVLAGEFLTKAEDLLESGVHPTVIASGYRLAADQATKTIDTITISASPEDT-- 148
giQ9HN70        GDGTTTSVVVSGELLSEAETLLEQDIHATTLAQGYRQAAEKAKELLDDAAIDVSADDT-- 152
giO30561        GDGTTTAVINAGELLDQAEDLLDSDVHATTIAQGYRQAAEKAKEVLEDNAIEVTEDDR-- 153
giYP_137342     GDGTTTAVVMAGELLSKAEELLDQDIHASILAQGYRQAAEKAKEILEDNAIDVDADDT-- 178
giYP_001689883GDGTTTAVAIAGELLKNAEDLLERDIHPTAIIKGYNLAAEQAREEVDNVAVDVDPDDK-- 154
                .***.: .  :* :  .*: *:   :*.: :  *:  *   : . :   :      :
```

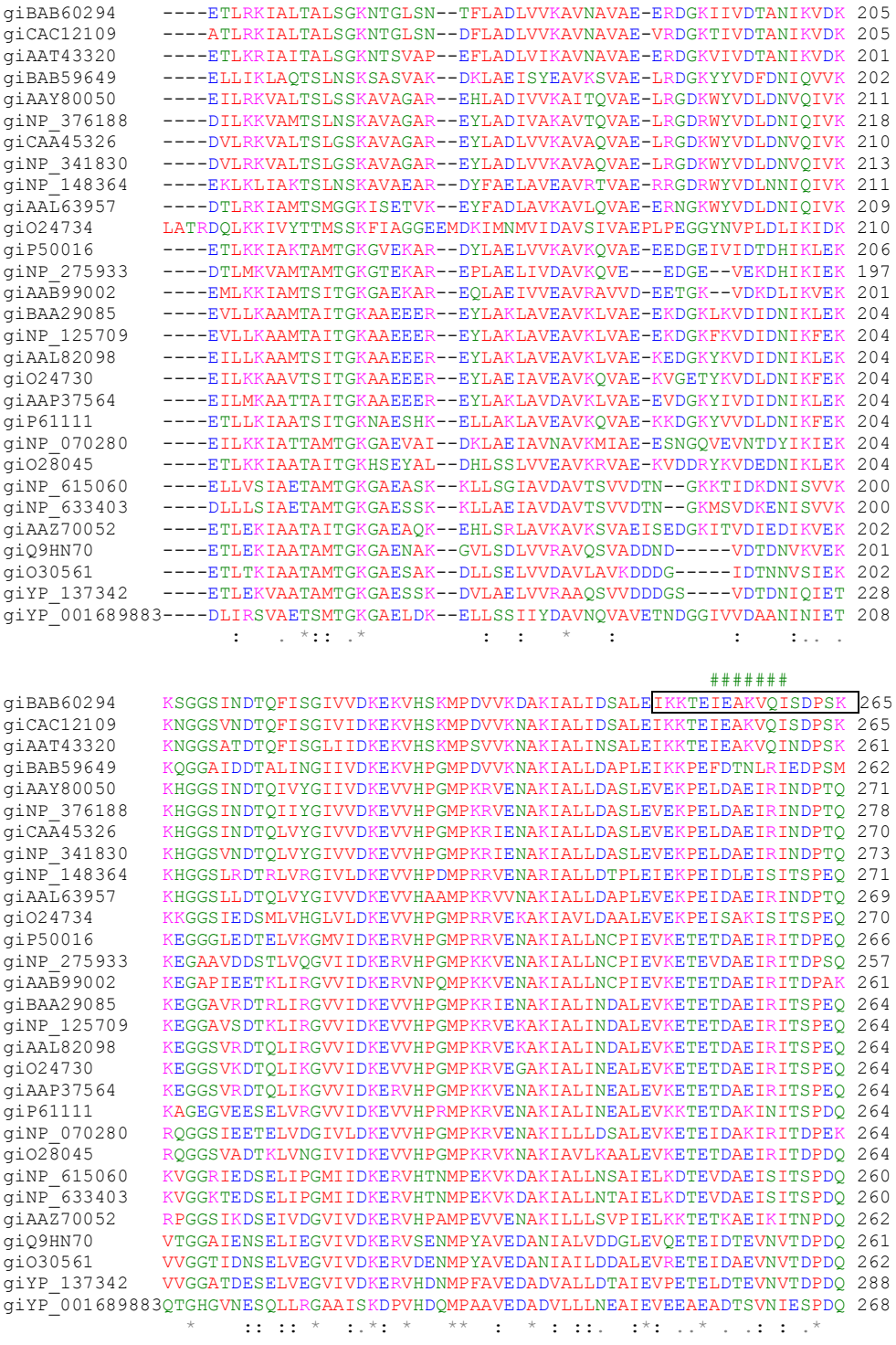

Figure 3.132: continued

```
giBAB60294      IQDFLNQETSTFKEMVEKIKKSGANVVLCQKGIDDVAQHYLAKEGIYAVRRVKKSDMEKL 325
giCAC12109      IQDFLNQETNTFKQMVEKIKKSGANVVLCQKGIDDVAQHYLAKEGIYAVRRVKKSDMEKL 325
giAAT43320      IQEFLDQETDTFKEMVEKVKKSGANVLLCQKGIDDTAQYYLAKEGIYAVRRVKQSDMEKL 321
giBAB59649      IQKFLAQEENMLREMVEKIKSVGANVVITQKGIDDMAQHYLSKEGIYAVRRVKKSDMDKL 322
giAAY80050      MKKFLDEEENILKEKVDKIAQTGANVVICQKGIDEVAQHYLAKKGILAVRRAKKSDLEKL 331
giNP_376188     MKKFLEEEENLLKEKVDKIAATGANVVICQKGIDEVAQHYLAKKGILAVRRAKKSDLEKL 338
giCAA45326      MHKFLEEEENILKEKVDKIAATGANVVICQKGIDEVAQHYLAKKGILAVRRAKKSDLEKL 330
giNP_341830     MHKFLEEEENILKEKVDKIAATGANVVICQKGIDEVAQHYLAKKGILAVRRAKKSDLEKL 333
giNP_148364     IKALYEKQERILQEKIEKIAATGANVVITQKGIDDVAQHFLAKKGILAVRRVKRSDIEKI 331
giAAL63957      MRAFLEEEERILRGYVDKLKSLGVTVLFTTKGIDDIAQYYLAKAGILAVRRVKRSDIEKL 329
giO24734        IKAFLDEEAKYLKDMVDKLASIGANVVICQKGIDDVAQHFLAKKGILAVRRVKRSDIEKL 330
giP50016        LQAFIEEEERMLSEMVDKIAETGANVVFCQKGIDDLAQHYLAKKGILAVRRVKKSDMQKL 326
giNP_275933     MQAFIEQEEQMIRDMVNSIVDTGANVLFCQKGIDDLAQHYLAKAGVLAVRRVKKSDMEKL 317
giAAB99002      LMEFIEQEEKMIKDMVEKIAATGANVVFCQKGIDDLAQHYLAKKGILAVRRVKKSDMEKL 321
giBAA29085      LQAFLEQEEKMLKEMVDKIKEVGANVVFVQKGIDDLAQHYLAKYGILAVRRVKKSDMEKL 324
giNP_125709     LQAFLEQEEKMLKEMVDKIKEVGANVVFVQKGIDDLAQHYLAKYGILAVRRVKKSDMEKL 324
giAAL82098      LQAFLEQEERMLREMVEKIKEVGANVVFVQKGIDDLAQHYLAKYGIMAVRRVKKSDMEKL 324
giO24730        LQAFLEQEEKMLREMVDKIKEVGANVVFVQKGIDDLAQHYLAKYGIMAVRRVKKSDMEKL 324
giAAP37564      LQAFLEQEEKMIKEMVDKIVATGANVVFCQKGIDDLAQHYLAKAGILAVRRVKKSDMEKL 324
giP61111        LMSFLEQEEKMLKDMVDHIAQTGANVVFVQKGIDDLAQHYLAKYGIMAVRRVKKSDMEKL 324
giNP_070280     LQKFIEQEEAMLKEMVDKIVNAGANVVFCQKGIDDLAQYYLAKAGVLAVRRVKKSDMEKL 324
giO28045        LMKFIEQEEKMLKEMVDRLAEAGANVVFCQKGIDDLAQYYLAKAGILAVRRVKQSDIEKI 324
giNP_615060     LQSFLDQEEAMLKKIVQKVISSGANVVFCQKGVEDLAQHYLAKAGIFAIRRVKKSDMEKL 320
giNP_633403     LQSFLDQEEQMLKKIVQKVINSGANVVFCQKGVEDLAQHYLAKAGIFAVRRVKKSDMEKL 320
giAAZ70052      MQLFLDQEEAMLKEIVDKVIKTGANVVFCQKGIDDLAQYYMTKAGIFGMRRVKKSDMDKL 322
giQ9HN70        LQNFLDQEEEQLKEMVDALKDAGANVVFADSGIDDMAQHYLAKEGILAVRRAKSDDFTRL 321
giO30561        LQQFLDQEEKQLKEMVDQLVEVGADAVFVGDGIDDMAQHYLAKEGILAVRRAKSSDLKRL 322
giYP_137342     LQQFLDQEEEQLKEMVDQLAEAGADVVFCQKGIDDMAQHYLAQEGILAVRRAKKSDIEAL 348
giYP_001689883LQSFLDQEEKQLKEKVQQIADTGANVVFCQKGIDDMAQHYLAKEGILAVRRTKKSDIEFL 328
                :  :  ::   :   :: :   *. .::  .*::: **::::: *: .:**.* .*:  :

giBAB60294      AKATGAKIVTDLDDLTPSVLGEAEKVEERKIGDDRMTFVTG-CKNPKAVSILIRGGTEHV 384
giCAC12109      AKATGAKIVTDLDDLTPSVLGEAETVEERKIGDDRMTFVMG-CKNPKAVSILIRGGTDHV 384
giAAT43320      AKATGAKIVTDLDDLTPDSLGTAEKVEERKIGDDRMTFITG-AKNPKAVSILIRGGTEHV 380
giBAB59649      AKATGATVVSTIDEISASDLGSADRVEQVKVGDDYMTFVTG-CKNPKAVSVLVRGETEHV 381
giAAY80050      ARATGGRVVSNIDELTSQDLGYATLVEERKIGEDKMVFIEG-AKNPKAVSILIRGGLERV 390
giNP_376188     ARATGGRVVSNIDELTPQDLGYAALVEERKVGEDKMVFVEG-AKNPKAVSILIRGGLERV 397
giCAA45326      ARATGGRVISNIDELTSQDLGYAALVEERKVGEDKMVFVEG-AKNPKSVSILIRGGLERV 389
giNP_341830     ARATGGRVISNIDELTSQDLGYAALVEERKVGEDKMVFVEG-AKNPKSVSILIRGGLERV 392
giNP_148364     ARATGARIVTDIEDLRPEDLGYAELVEERKVGEDKMVFIEG-AKNPKSVTILLRGGFERL 390
giAAL63957      VRATGARLVTSIEDLTEADLGFAGLVEERRVGDEKMVFVEQ-CKNPKAVSILVRGGFERL 388
giO24734        EKALGARIISSIKDATPEDLGYAELVEERRVGNDKMVFIEG-AKNPKAVNILLRGSNDMA 389
giP50016        ARATGARIVTNIDDLSEEDLGEAEVVEEKKVAGDKMIFVEG-CKDPKAVTILIRGGTEHV 385
giNP_275933     SKATGANIVTNIEDLSPEDLGEAGVVSEKKISGEEMIFVEE-CKEPKAVTILVRGSTEHV 376
giAAB99002      AKATGARIVTKIDDLTPEDLGEAGLVEERKVAGDAMIFVEQ-CKHPKAVTILARGSTEHV 380
giBAA29085      AKATGAKIVTNIRDLTPEDLGEAELVEERKVAGENMIFVEG-CKNPKAVTILIRGGTEHV 383
giNP_125709     AKATGAKIVTNIRDLTPEDLGEAELVEERKVAGENMIFVEG-CKNPKAVTILIRGGTEHV 383
giAAL82098      AKATGAKIVTNIRDLTPEDLGYAELVEERKVAGESMIFVEG-CQNPKAVTILIRGGTEHV 383
giO24730        AKATGAKIVTNVRDLTPEDLGEAELVEQRKVAGENMIFVEG-CKNPKAVTILIRGGTEHV 383
giAAP37564      AKATGAKIVTNVRDLTPDDLGYAELVEERKVAGENMVFVEG-CKNPKAVTILIRGGTEHV 383
giP61111        AKATGAKIVTNVKDLTPEDLGYAEVVEERKLAGENMIFVEG-CKNPKAVTILIRGGTEHV 383
giNP_070280     AKATGAKVLTDLRDISSEDLGEAALVEERKVGDEKMVFVTG-CKNPKAVTILVRGGTEHV 383
giO28045        AKACGAKIITDLREITSADLGEAELVEERKVGDEKMVFIEG-CKNPKAVTILIRGGSEHV 383
giNP_615060     ARATGGKLITNLDEITPEDLGFAKLVEEKKVGGDSMTFVTG-CDNPKAVTILLRGGTEHV 379
giNP_633403     ARATGGKLITNLDEIVPEDLGFAKLVEEKKVGGDSMTFVTG-CDNPKAVTILLRGGTEHV 379
giAAZ70052      SRATGAKIITSLDEIEESDLGHAGLVEEKDVTGSRMTFVTG-CKDSKATSILLRGGTEHV 381
giQ9HN70        SRATGATPVSNVNDIEAADLGAAGSVAQKDIGGDERIFVED-VEEAKSVTLILRGGTEHV 380
giO30561        ARATGGRVVSSLDDIEADDLGFAGSVGQKDVGGDERIFVED-VEDAKSVTLILRGGTEHV 381
giYP_137342     SRSTGARIISNIDDIEADDLGFAGSVAQKDIAGDERIFVED-VEDARAVTMILRGGTEHV 407
giYP_001689883TNVLDASVVTDLDAASEADV-VAGSVTRD--SDDELFYVEGESEQAHGVTLLLRGSTDHV 385
                .  ..  :: :       :  *  * .     .   ::    ...:...:: **  :
```

Figure 3.132: continued

```
giBAB60294      VSEVERALNDAIRVVAITKEDGKFLWGGGAVEAELAMRLAKYANSVGGREQLAIEAFAKA 444
giCAC12109      VSEVERALNDAIRVVAITKEDGKFLWGGGAVEAELAMRLAKYANSVGGREQLAIEAFAKA 444
giAAT43320      VDEIERALHDAIRVVAITKEDGKYLPGGGAIEAELSMKIRDYANSVGGREQLAIEAFAKA 440
giBAB59649      VDEMERSITDSLHVVASALEDGAYTAGGGATAAEIAVRLRSYAQKIGGRQQLAIEKFADA 441
giAAY80050      VDETERALRDALGTVADVVRDGRAIAGGGAVETEIAKRLRKYAPQVGGKEQLAIEAYANA 450
giNP_376188     VDETERALRDALGTVADVIRDGRAVAGGGAVELEIAKRLRKYAPQIGGKEQLAIEAYASA 457
giCAA45326      VDETERALRDALGTVADVIRDGRAVAGGGAVEIEIAKRLRKYAPQVGGKEQLAIEAYANA 449
giNP_341830     VDETERALRDALGTVADVIRDGRAVAGGGAVEIEIAKRLRKYAPQVGGKEQLAIEAYANA 452
giNP_148364     VDEAERSLHDALSVVADAIMDGKIVAGGGAVEAEVAKVLYEYASKLPGKTQLAVEAFARA 450
giAAL63957      VDEAERNLDDALSVVSDVVEDPYILPAGGAAEIEAAKAVRAFAPKVGGREQYAVEAFARA 448
giO24734        LDEAERSINDALHSLRNVLMKPMIVAGGGAVETELALRLREYARSVGGKEQLAIEKFAEA 449
giP50016        VDEAERAIEDAIGVVAAALEDGKVVAGGGAPEVEVARQLRDFADGVEGREQLAVEAFADA 445
giNP_275933     VSEVERAIEDAIGVVAATVEDGKVVAGGGAPEIEIAKRLKDYADSISGREQLAVSAFAEA 436
giAAB99002      VEEVARAIDDAIGVVKCALEEGKIVAGGGATEIELAKRLRKFAESVAGREQLAVKAFADA 440
giBAA29085      VDEVERALEDAIKVVKDILEDGKIIAGGGASEIELSIKLDEYAKEVGGKEQLAIEAFAEA 443
giNP_125709     VDEVERALEDAVKVVKDILEDGKIIAGGGAAEIELSIKLDEYAKEVGGKEQLAIEAFAEA 443
giAAL82098      VDEVERALEDAIKVVKDILEDGKILAGGGAPEIELAIRLDEYAKEVGGKEQLAIEAFAEA 443
giO24730        VDEVERALEDAVKVVKDIVEDGKIVAAGGAPEIELSIRLDEYAKEVGGKEQLAIEAFAEA 443
giAAP37564      VDEVERALEDAIKVVKDIVEDGKIVAGGGASEIELAIRLDEYAKEVGGKEQLAIEAFADA 443
giP61111        IDEVERALEDAVKVVKDVMEDGAVLPAGGAPEIELAIRLDEYAKQVGGKEALAIENFADA 443
giNP_070280     VEEIARGIEDAVRAVACAVEDGKVVVGAGAPEIEVSLKLREWAPSLGGREQLAVEAFATA 443
giO28045        VDEVERSLQDAIKVVKTALESGKVVAGGGAPEIEVALKIRDWAPTLGGREQLAAEAFASA 443
giNP_615060     VDSVDSALEDALRVVGVAIEDEKLVSGGGSPEVEVALRLQEYAATLEGREQLAVKAYSEA 439
giNP_633403     VDSIDSALEDALRVVGVAIEDEKLVAGGGSPEVEVALRLQEYAATLEGREQLAVKAYSEA 439
giAAZ70052      VEGIERALEDALRVVGVALEDQKIVVGGGSPEIELSLRLKEYAATLKGREQLAVMKFAES 441
giQ9HN70        VDEVERAIEDSLGVVRVTLEDGQVMPGGGAPETELAMQLRDFADSVGGREQLAVEAFADA 440
giO30561        VDELERAIEDSLGVVRTTLEDGKVLPGGGAPETELSLQLREFADSVGGREQLAVEAFAEA 441
giYP_137342     VDEVERAIEDSLGVVAATLEDGKVLPGGGAPETQLALGLRDHADSVGGREQLAVEAFADA 467
giYP_001689883VDELERGVSDALDVSAQTLSDGRVLPGGGATEVEVASRLRDFADSVSGREQLAVEAFADS 445
               :.     : *::        .     ..*:   : :  :   *  : *:   *   :: :

                          # ##  #
giBAB60294      LEIIPRTLAENAGIDPINTLIKLKSEHEKG-KISMGVDLDSNGAGD-MSKKGVIDPVRVK 502
giCAC12109      LEIIPRTLAENAGIDPINTLIKLKAEHEKG-RISVGVDLDNNGVGD-MKAKGVVDPLRVK 502
giAAT43320      LEIIPRTLAENAGMDPINTLIKLKAEHEKS-NKNYGINLNENKIDD-MVKLGVFDTYRVK 498
giBAB59649      IEEVPRALAENAGLDPIDIILKLRAEHAKG-NKYAGVNVFSGEIED-MVNNGVIEPIRVG 499
giAAY80050      LESLVMILIENGGFDPIELLVKLRSAHENETNKWHGINVYTGQIQD-MWSLGVIEPAVVK 509
giNP_376188     LENLVMILIENGGYDPIDLLVKLRSAHENEANKWYGINVFTGQVED-MWKLGVIEPAVVK 516
giCAA45326      IEGLIMILAENAGLDPIDKLMQLRSLHENETNKWYGLNLFTGNPED-MWKLGVIEPALVK 508
giNP_341830     IEGLIMILAENAGLDPIDKLMQLRSLHENETNKWYGLNLFTGNPED-MWKLGVIEPALVK 511
giNP_148364     VEALPQALAHNAGHDPIEVLVKLRSAHEKPENKWYGVDLDTGEIVD-MWSRGVLEPMRVK 509
giAAL63957      LEVIPKALAENAGLDPIDILTELTHKHEQTDGWKYGLDVYQGKVVD-MVSLGLVEPLTVK 507
giO24734        LEEIPMILAETAGMEPIQTLMDLRAKHAKG-LINAGVDVMNGKIADDMLALNVLEPVRVK 508
giP50016        LEIIPRTLAENSGLDPIDVLVQLRAKHE-DGQVTAGIDVYDGDVKD-MLEEGVVEPLRVK 503
giNP_275933     LEIVPKTLAENAGLDSIDVLVDLRAAHE-ES-TYMGIDVFDGKIVD-MKEAGVIEPHRVK 493
giAAB99002      LEVIPRTLAENSGLDPIDMLVKLRAAHEKEGGEVYGLDVFEGEVVD-MLEKGVVEPLKVK 499
giBAA29085      LKVIPRTLAENAGLDPIETLVKVIAAHK-EKGQTIGIDVYEGEPAD-MMERGVIEPVRVK 501
giNP_125709     LKVIPRTLAENAGLDPIETLVKVIAAHK-EKGPTIGIDVYEGEPAD-MMERGVIEPVRVK 501
giAAL82098      LKVIPRTLAENAGLDPIETLVKVIAAHK-EKGPTIGVDVYEGEPAD-MLERGVIEPLRVK 501
giO24730        LKVIPRTLAENAGLDPIETLVKVIAAHK-EKGPTIGVDVFEGEPAD-MLERGVIAPVRVP 501
giAAP37564      LKVIPRTLAENAGLDPVDVLVKVTAAHK-DKGATIGVDVFAGEPAD-MLERGVIEPLRVK 501
giP61111        LKIIPKTLAENAGLDTVEMLVKVISEHK-NRGLGIGIDVFEGKPAD-MLEKGIIEPLRVK 501
giNP_070280     LEIIPRTLAENAGLDPIDVLVELKAAHE-KGQKYAGVDVDTGKVVD-MKERGVFEPLRVK 501
giO28045        LEVIPRALAENSGLDPIDILVELRKAHE-EGKTTYGVDVFSGEVAC-MKERGVLEPLKVK 501
giNP_615060     LEVIPRTLAENAGLDPIDMLMELRSQHEKGM-KTAGLDVYEGKVVD-MWNNFVVEPLRVK 497
giNP_633403     LEVIPRTLAENAGLDPIDMLMELRSQHEKGM-KTAGLNVYEGKVVD-MWENFVVEPLRVK 497
giAAZ70052      LEIIPSTLAENAGLDPIDMLVEMRSQHEKGN-KRAGLNVYTGKIED-MFENNVVEPLRIK 499
giQ9HN70        LEVIPRTLAENAGHDPIDSLVDLRSQHDGGD-TEAGLDAYNGDVID-MESEGIVEPLRVK 498
giO30561        LDIIPRTLAENAGLDPIDSLVDLRSRHDGGE-FAAGLDAYTGEVID-MEEEGVVEPLRVK 499
giYP_137342     IDVIPRTLAENAGLDPIDSLVDLRSKHDGGA-VTSGLDAYTGEVVD-MEEDGVVEPLRVK 525
giYP_001689883LELVPRVLAENAGLDSIDTLVDLRSAHENDDDEHIGLNVLSGDLED-TFEAGVVEPAHAK 504
               :. :   * ...* :.:: : .:   *        *::   .          :. .
```

Figure 3.132: continued

```
                              ######
giBAB60294      THALESAVEVATMILRIDDVIASKKSTPPSN---------QPGQG-AGAPGGGMPEY--- 549
giCAC12109      THALESAVEVATMILRIDDVIASKKSTPPSG---------QGGQG-QGMPGGGMPEY--- 549
giAAT43320      QHALESAVEVASMILRIDDVIASKKSAPSNN---------QQPQGGMGGMGGGMPPY--- 546
giBAB59649      KQAIESATEAAIMILRIDDVIATKSSGSSSN----------PPKSPSSESSSGED----- 544
giAAY80050      MNAIKAATEASTLILRIDDLISAGKK--SEG---------KTGEKKESEKGKEED----- 553
giNP_376188     MNAIKAATEAATLILRIDDLIAAGKK--SES---------KGGESKSEEK-KEED----- 559
giCAA45326      MNAIKAATEAVTLVLRIDDIVAAGKKGGSEP---------GGKKEK--EEKSSED----- 552
giNP_341830     MNAVKAATEAVTLVLRIDDIVAAGKKSGSEP---------SGKKEKDKEEKSSED----- 557
giNP_148364     LNALKAATEVASLILRIDDVIAARKE----------------EEEKEEKRGGEEE----- 548
giAAL63957      INALKVAVEAASMILRIDEIIAASKLE--------------KEKEEKKEEKKEEFD----- 549
giO24734        AQVLKSAVEAATAILKIDDLIAAAPLKSGEK---------KGEKKEGGEEEKSSTPSSLE 559
giP50016        TQALASATEAAEMILRIDDVIAARELSKEEE----------EEE-----EEGGSSEF--- 545
giNP_275933     KQAIQSAAEAAEMILRIDDVIAASSSGSSEE----------GME-----EMGGMGGMPPM 538
giAAB99002      TQAIDSATEASVMLLRIDDVIAAEKVKGDEK----------GGEGG---DMGG-DEF--- 542
giBAA29085      KQAIKSASEAAIMILRIDDVIAASKLEKEKE---------GEKGGG-SEEFSGSSDLD-- 549
giNP_125709     KQAIKSASEAAIMILRIDDVIAAQKLEKEKE---------GEKGGGGSEDFSSSSDLD-- 550
giAAL82098      KQAIKSASEAAIMILRIDDVIAASKLEKEKEKE-------GEKGGG-SEDFS--SDLD-- 549
giO24730        KQAIKSASEAAIMILRIDDVIAASKLEKDKE---------GGKGGS--EDFG--SDLD-- 546
giAAP37564      KQAIKSASEAAIMILRIDDVIAASKLEKEKE---------GGKGPG--EEET---EF--- 544
giP61111        KQAIKSASEAAIMILRIDDVIAAKATK--PE---------GGQGGGMPGGMGG-MDMGM- 548
giNP_070280     TQAIGSATEVAVMILRIDDIIAAKGLEKEKG---------GGGEGG----MPEMPEF--- 545
giO28045        TQAITSATEVAIMILRIDDVIAAKGLEKEKG---------PEGESG----GEEDSEE--- 545
giNP_615060     TQVINAATESAVMILRIDDIIASTRAA-PG----------PEEMGGMPPGMGGMPPGMGG 546
giNP_633403     TQVINAATESAVMILRIDDIIASTRAAGPS----------PEEMGGMP-GMGGMP-GMGG 545
giAAZ70052      TQAINAATEAAIMVLRIDDVIAS-----SS----------PAKVG----GPGAIP---GG 537
giQ9HN70        TQAIESATEAATMILRIDDVIAAGDLAGGQVGDDDGDDGPAGGPGGMGGGMGG-MGGMGG 557
giO30561        TQAIESATEAAVMILRIDDVIAAGDLSGGQTGSDD-DDG--GAPGGMGGGMGG-MGGMGG 555
giYP_137342     TQAVESATEAAVMILRIDDVIAAGDLKGGQ-GDDDEDEGGPGGPGGAPGGMGGGMGGMGG 584
giYP_001689883EQAVTSASEAANLVLKIDDIISAGDLSTDK-GDDD------GGAGGMGGGMGG---GMGG 554
                :.:  * *    :*:**:::::

giBAB60294      ------
giCAC12109      ------
giAAT43320      ------
giBAB59649      ------
giAAY80050      ------
giNP_376188     ------
giCAA45326      ------
giNP_341830     ------
giNP_148364     ------
giAAL63957      ------
giO24734        ------
giP50016        ------
giNP_275933     ------
giAAB99002      ------
giBAA29085      ------
giNP_125709     ------
giAAL82098      ------
giO24730        ------
giAAP37564      ------
giP61111        ------
giNP_070280     ------
giO28045        ------
giNP_615060     MPPGMM 552
giNP_633403     MPPGMM 551
giAAZ70052      EMPEMM 543
giQ9HN70        -MGGAM 562
giO30561        -MGGAM 560
giYP_137342     GMGGMM 590
giYP_001689883----MM 556
```

Figure 3.132

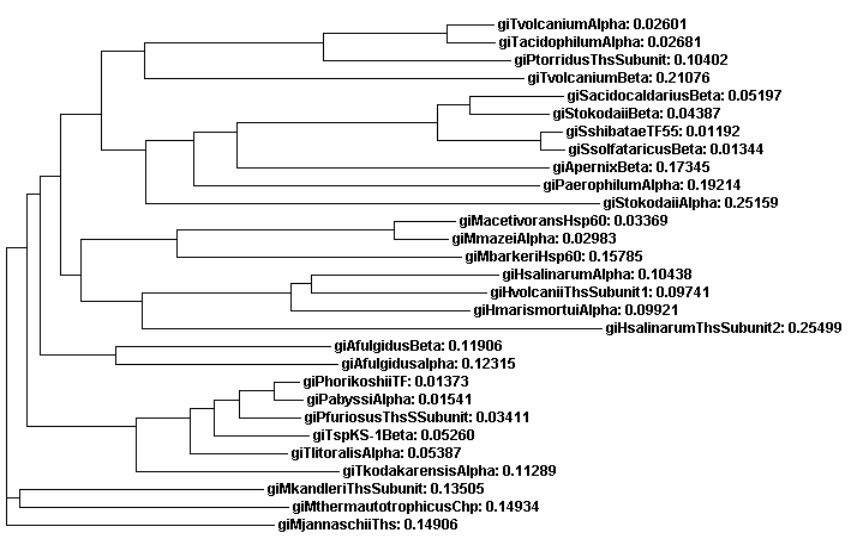

Figure 3.133: Phylogenetic tree constructed by clustal type multiple sequence alignments of amino acid sequence of *T. volcanium* Hsp60 α subunit protein with several archaeal Hsp60 proteins.

Phylogenetic tree has three branches: the first one for *Methanocaldococcus jannaschii* thermosome, the second one for *Methanopyrus kandleri* thermosome subunit and *Methanothermobacter thermautotrophicus* chaperonin, and the third one for Hsp60 proteins from other Archaea. In the third branch, hyperthermophilic archaeal Hsp60 proteins are clustered altogether, as a sub-branch. It is also possible to distinguish the distinct sub-branches including the members of the distinct Sulfolobales, Halobacteriales, and Thermoplasmatales. The clustering scheme is fairly consistent with the systematic classification of the Archaea Domain. The highest homology between Thermoplasma Hsp60 proteins and Picrophilus Hsp60 is also evident from this phylogenetic tree, since they are clustered altogether in the same group. Thermosome proteins of methanogenic species are clustered as three different groups. *Methanosarcina acetivorans* Hsp60 protein, *Methanosarcina mazei* thermosome alpha subunit and *Methanosarcina barkeri* thermosome alpha subunit are clustered as a sub-branch. These organisms belong to the class *Methanomicrobia* and their optimal growth temperatures is

37°C. *M. kandleri* thermosome subunit and *M. thermautotrophicus* chaperonin protein form the second branch. These organisms belong to the class *Methanopyri*. *M. jannaschii* thermosome forms a distinct branch. *M. jannaschii* belongs to the class *Methanococci* (Figure 3.133 and Table 3.10).

3.4.3 Sequence Alignments of *T. volcanium* Hsp60 β Subunit With Several Eukaryal, Archaeal and Bacterial Hsp60 Proteins

TVN0507 gene encodes Hsp60 β subunit protein of 544 aa length. This protein has a predicted molecular mass of 58482.50 Da and a theoretical pI of 4.7618. Multiple sequence alignments of amino acid sequence of *T. volcanium* Hsp60 β subunit protein with several eukaryal, archaeal and bacterial Hsp60 proteins were achieved by Clustal W 1.83 as described in Section 2.6. Protein sequences of Hsp60 subunits of organisms were derived from the online-database of NCBI (Figure 3.134). Scores of this alignment is given in Table 3.11 and 3.12. The highest homology was found between *T. volcanium* Hsp60 ß sequences and those of the *T. acidophilum* thermosome beta chain (P48425) (93%), and *Picrophilus torridus* thermosome subunit (YP_023973) (76%). The identity between *T. volcanium* Hsp60 β and Hsp60 β proteins from other Archaeabacteria is 50-60%. There was a 60% sequence similarity between *T. volcanium* Hsp60 α (BAB60294) and Hsp60 β. The identity between *T. volcanium* Hsp60 β and bacterial GroEL sequences differed between 20-23 %. Various eukaryotic organisms including human have Hsp60 proteins with aminoacid sequence identity of 36-38% to *T. volcanium* Hsp60 β protein (Table 3.12).

Hsp60 subunit proteins used in multiple sequence alignment are abbreviated in phylogenetic tree (Figure 3.135). Phylogenetic tree constructed by this alignment shows that bacterial and eukaryotic Hsp60 β and GroEL proteins are

Table 3.10: Scientific classification and optimal growth temperature information of archaeal organisms whose thermosome proteins were used in multiple sequence alignment.

Domain	Phylum	Class	Order	Family	Genus	Species	Optimal Growth Temperature
Archaea	Euryarchaeota	Thermoplasmata	Thermoplasmatales	Thermoplasmataceae	Thermoplasma	*Thermoplasma volcanium*	60°C
	Euryarchaeota	Thermoplasmata	Thermoplasmatales	Thermoplasmataceae	Thermoplasma	*Thermoplasma acidophilum*	59°C
	Euryarchaeota	Thermoplasmata	Thermoplasmatales	Picrophilaceae	Picrophilus	*Picrophilus torridus*	60°C
	Crenarchaeota	Thermoprotei	Sulfolobales	Sulfolobaceae	Sulfolobus	*Sulfolobus acidocaldarius*	75 to 80°C
	Crenarchaeota	Thermoprotei	Sulfolobales	Sulfolobaceae	Sulfolobus	*Sulfolobus tokodaii*	80°C
	Crenarchaeota	Thermoprotei	Sulfolobales	Sulfolobaceae	Sulfolobus	*Sulfolobus shibatae*	83°C
	Crenarchaeota	Thermoprotei	Sulfolobales	Sulfolobaceae	Sulfolobus	*Sulfolobus solfataricus*	80°C
	Crenarchaeota	Thermoprotei	Desulfurococcales	Desulfurococcaceae	Aeropyrum	*Aeropyrum pernix*	90 to 95°C
	Crenarchaeota	Thermoprotei	Thermoproteales	Thermoproteaceae	Pyrobaculum	*Pyrobaculum aerophilum*	100°C
	Euryarchaeota	Methanomicrobia	Methanosarcinales	Methanosarcinaceae	Methanosarcina	*Methanosarcina acetivorans*	35 to 40°C
	Euryarchaeota	Methanomicrobia	Methanosarcinales	Methanosarcinaceae	Methanosarcina	*Methanosarcina mazei*	37°C
	Euryarchaeota	Methanomicrobia	Methanosarcinales	Methanosarcinaceae	Methanosarcina	*Methanosarcina barkeri*	37°C
	Euryarchaeota	Halobacteria	Halobacteriales	Halobacteriaceae	Halobacterium	*Halobacterium salinarum*	37°C
	Euryarchaeota	Halobacteria	Halobacteriales	Halobacteriaceae	Haloferax	*Haloferax volcanii*	45°C
	Euryarchaeota	Halobacteria	Halobacteriales	Halobacteriaceae	Haloarcula	*Haloarcula marismortui*	40°C
	Euryarchaeota	Archaeoglobi	Archaeoglobales	Archaeoglobaceae	Archaeoglobus	*Archaeoglobus fulgidus*	83°C
	Euryarchaeota	Thermococci	Thermococcales	Thermococcaceae	Pyrococcus	*Pyrococcus horikoshii*	98°C
	Euryarchaeota	Thermococci	Thermococcales	Thermococcaceae	Pyrococcus	*Pyrococcus abyssi*	103°C
	Euryarchaeota	Thermococci	Thermococcales	Thermococcaceae	Pyrococcus	*Pyrococcus furiosus*	100°C
	Euryarchaeota	Thermococci	Thermococcales	Thermococcaceae	Thermococcus	Thermococcus sp.	85°C
	Euryarchaeota	Thermococci	Thermococcales	Thermococcaceae	Thermococcus	*Thermococcus litoralis*	85 to 88°C
	Euryarchaeota	Thermococci	Thermococcales	Thermococcaceae	Thermococcus	*Thermococcus kodakarensis*	85°C
	Euryarchaeota	Methanopyri	Methanopyrales	Methanopyraceae	Methanopyrus	*Methanopyrus kandleri*	100 to 110°C
	Euryarchaeota	Methanopyri	Methanobacteriales	Methanobacteriaceae	Methanothermobacter	*Methanothermobacter thermautotrophicus*	65°C
	Euryarchaeota	Methanococci	Methanococcales	Methanocaldococcaceae	Methanocaldococcus	*Methanocaldococcus jannaschii*	85°C

more closely related to one another then they are to archaeal proteins (Figure 3.135). Thermosome proteins of methanogenic species are clustered as two different groups. *Methanosarcina barkeri* Hsp60 protein, *Methanosarcina acetivorans* Hsp60 protein and *Methanosarcina mazei* thermosome alpha subunit are clustered as a sub-branch. These organisms belong to the class Methanomicrobia and genus Methanosarcina. They are mesophilic methanogens with optimal growth temperatures of 37°C. *M. kandleri* thermosome subunit, *Methanothermococcus thermolithotrophicus* chaperonin protein, *M. jannaschii* thermosome and *M. thermautotrophicus* chaperonin protein form a distinct branch. *M. kandleri* and *M. thermautotrophicus* belong to the class Methanopyri. *M. jannaschii* and *M. thermolithotrophicus* belong to the class Methanococci. These methanogens are either thermophilic or hyperthermophilic. Optimum growh temperature of the organisms in this distinct branch is higher than that of methanogens which belong to the class Methanomicrobia (Figure 3.135).

In Euryarchaeota, Hsp60 β proteins of mesophilic methanogens (*Methanosarcina*, optimum growth temperature 37°C) appeared to be more close to Halobacteria (optimum growth temperature 37-45°C) then thermophilic methanogens, and clustered together. Hsp60 β subunits of hyperthermophilic members of Euryarchaeota, other than hyperthermophilic methanogens (i.e. *Archaeoglobus*, *Pyrococcus*) are classified in the same group. These proteins seem to be more close to eukaryotic and bacterial orthologs and share the most recent ancestor. Hsp60 β proteins of hyperthermophilic archaea in Crenarchaeota (i.e. *Sulfolobus*, *Aeropyrum* and *Pyrobaculum* sp.) are clustered together. Eukaryotic and bacterial Hsp60 β proteins are clustered into two distinct, but phylogenetically related groups. Hsp60 β proteins of the archaea in phylum Euryarchaeota (i.e. *Thermoplasma* and *Picrophilus*) fall into same cluster, that is related to one which includes hyperthermophilic members of the same phylum.

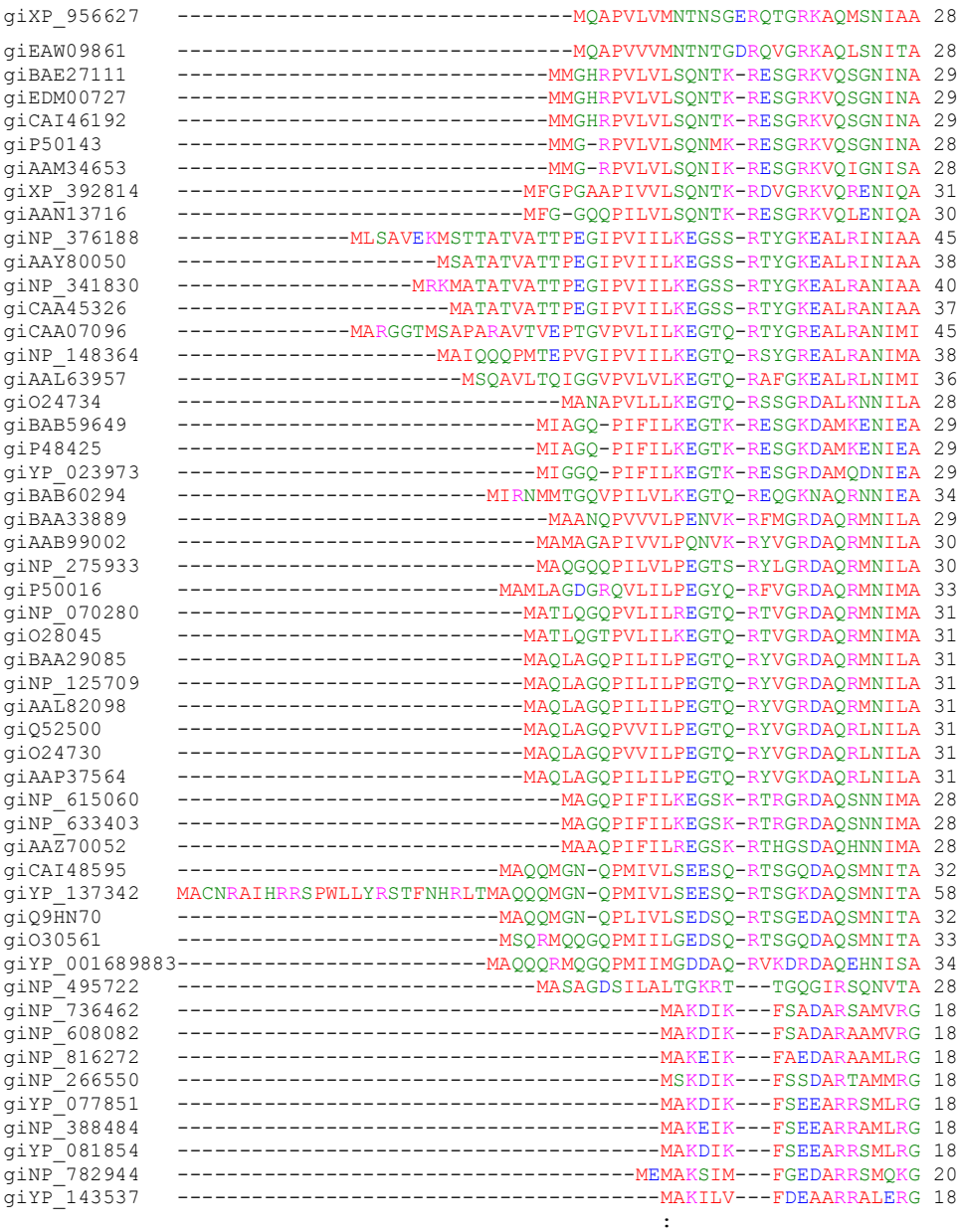

Figure 3.134: Clustal type multiple sequence alignments of amino acid sequence of *T. volcanium* Hsp60 β subunit protein with several eukaryal, archaeal and bacterial Hsp60 proteins.

Conserved sequences related to feature 1, feature 2 and feature 3 were indicated by #, #, and # symbols on the multiple sequence alignments, respectively.

```
                      ####
giXP_956627    AKTVADIIRSCLGPKAMLKMLLDPMGGIVLTNDGHAILREIEVSHP----AAKSMIELSR 84
giEAW09861     AKTVADIIRSCLGPKAMLKMLLDPMGGIVLTNDGHAILREIEVSHP----AAKSMIELSR 84
giBAE27111     AKTIADIIRTCLGPKSMMKMLLDPMGGIVMTNDGNAILREIQVQHP----AAKSMIEISR 85
giEDM00727     AKTIADIIRTCLGPKSMMKMLLDPMGGIVMTNDGNAILREIQVQHP----AAKSMIEISR 85
giCAI46192     AKTIADIIRTCLGPKSMMKMLLDPMGGIVMTNDGNAILREIQVQHP----AAKSMIEISR 85
giP50143       AKTIADIIRTCLGPRAMMKMLLDPMGGIVMTNDGNAILREIQVQHP----AAKSMIEISR 84
giAAM34653     AKTIADIIRTCLGPRAMMKMLLDPMGGIVMTNDGNAILREIQVQHP----AAKSMIEISR 84
giXP_392814    GKAIADVIRTCLGPQAMLKMLMDPMGGIVMTNDGNAILREITVQHP----AGKSMIEIAR 87
giAAN13716     GKAIADVIRTCLGPQAMLKMLMDPMGGIVMTNDGNAILREITVQHP----AAKSMIEIAR 86
giNP_376188    VKAVEEALKSTYGPRGMDKMLVDSLGDITITNDGATILDKMDLQHP----AAKLLVQIAK 101
giAAY80050     VKAVEEALKTTYGPRGMDKMLVDSLGDITITNDGATILDKMDLQHP----AAKLLVQIAK 94
giNP_341830    VKAIEEALKSTYGPRGMDKMLVDSLGDITITNDGATILDKMDLQHP----TGKLLVQIAK 96
giCAA45326     VKAIEEALKSTYGPRGMDKMFVDSLGDITITNDGATILDKMDLQHP----TGKLLVQIAK 93
giCAA07096     VRAIAETLRTTYGPKGMDKMLVDSLGDITITNDGATILDKMDVQHP----TAKLVVQIAK 101
giNP_148364    VRAIAQILKTTYGPKGMDKMLVDSLGDITITNNGATILDKMDVAHP----AAKMLVQISK 94
giAAL63957     ARAIAEVMRTTLGPKGMDKMLIDSLGDITITNDGATILDEMDVQHP----IAKLLVEISK 92
giO24734       AVTLAEMLKSSLGPRGLDKMLIDSFGDVTITNDGATIVKEMEIQHP----AAKLLVEAAK 84
giBAB59649     AIAISNSVRSSLGPRGMDKMLVDSLGDIVITNDGVTILKEMDVEHP----AAKMMVEVSK 85
giP48425       AIAISNSVRSSLGPRGMDKMLVDSLGDIVITNDGVTILKEMDVEHP----AAKMMVEVSK 85
giYP_023973    AKAIATSIRSTLGPRGMDKMLVDSLGDIVITNDGVTILKEMDIEHP----AAKMMVEVSK 85
giBAB60294     AKAIADAVRTTLGPKGMDKMLVDSIGDIIISNDGATILKEMDVEHP----TAKMIVEVSK 90
giBAA33889     GRIIGETVRSTLGPKGMDKMLVDDLGDIVVTNDGVTILKEMSVEHP----AAKMLIEVAK 85
giAAB99002     GRIIAETVRTTLGPKGMDKMLVDELGDIVVTNDGVTILKEMSVEHP----AAKMLIEVAK 86
giNP_275933    GKILAETVRTTLGPKGMDKMLVDSLGDIVVTNDGVTILKEMDIEHP----AAKMLVEVAK 86
giP50016       ARVVAETVRTTLGPMGMDKMLVDEMGDVVVTNDGVTILEEMDIEHP----AAKMVVEVAK 89
giNP_070280    ARVIAEAVRSTLGPKGMDKMLVDSLGDVVITNDGVTILKEIDVEHP----AAKMIIEVAK 87
giO28045       ARVIAEAVKSTLGPKGMDKMLVDSLGDVVITNDGVTILKEMDVEHP----AAKMIIEVAK 87
giBAA29085     ARIIAETVRTTLGPKGMDKMLVDSLGDIVITNDGATILDEMDIQHP----AAKMMVEVAK 87
giNP_125709    ARIIAETVRTTLGPKGMDKMLVDSLGDIVITNDGATILDEMDIQHP----AAKMMVEVAK 87
giAAL82098     ARIVAETIRTTLGPKGMDKMLVDSLGDIVITNDGATILDEMDIQHP----AAKMMVEVAK 87
giQ52500       ARIIAETVRTTLGPKGMDKMLVDSLGDIVITNDGATILDEMDIQHP----AAKMMVEVAK 87
giO24730       ARIIAETVRTTLGPKGMDKMLVDSLGDIVITNDGATILDEMDIQHP----AAKMMVEVAK 87
giAAP37564     ARIVAETVRTTLGPKGMDKMLVDSLGDIVITNDGATILDEMDIQHP----AAKMMVEVAK 87
giNP_615060    AKAVAEAVRTTLGPKGMDKMLVDSMGDVVITNDGATILKEMDIEHP----AAKMVVEVSK 84
giNP_633403    AKAVAEAVRTTLGPKGMDKMLVDSMGDVVITNDGATILKEMDIEHP----AAKMVVEVSK 84
giAAZ70052     AKAVAEAVRTTLGPKGMDKMLVDSMGDVVITNDGATILKEMDIEHP----GAKMIVEVAK 84
giCAI48595     GKAVAESVRTTLGPKGMDKMLVDSTGNVVVTNDGVTILGEMDIEHP----AANMIVEVAE 88
giYP_137342    GTAVAEAVRTTLGPKGMDKMLVDNSGSVVVTNDGVTILDEMDIEHP----AANMIVEVAQ 114
giQ9HN70       GKAVAESVRTTLGPKGMDKMLVDSSGEVVVTNDGVTILKEMDIEHP----AANMIVEVAE 88
giO30561       GKAVAEAVRTTLGPKGMDKMLVDSGGQVVVTNDGVTILKEMDIDHP----AANMIVEVSE 89
giYP_001689883ARAVADAVRSTLGPKGMDKMLVSSMGDVTVTNDGVTILQEMDIDNP----TAEMIVEVAE 90
giNP_495722    AVAIANIVKSSLGPVGLDKMLVDDVGDVIVTNDGATILKQLEVEHP----AGKVLVELAQ 84
giNP_736462    VDILADTVKVTLGPKGRNVVLEKAFGSPLITNDGVTIAKEIELEDHFENMGAKLVSEVAS 78
giNP_608082    VDMLADTVKVTLGPKGRNVVLEKAFGSPLITNDGVTIAKEIELEDHFENMGAKLVSEVAS 78
giNP_816272    VDVLADTVKVTLGPKGRNVVLEKSFGSPLITNDGVTIAKEIELEDHFENMGAKLVSEVAS 78
giNP_266550    IDILADTVKTTLGPKGRNVVLEKSYGSPLITNDGVTIAKEIELEDHFENMGAKLVSEVAS 78
giYP_077851    VDALADAVKVTLGPKGRNVVLEKKFGSPLITNDGVTIAKEIELEDAFENMGAKLVAEVAS 78
giNP_388484    VDALADAVKVTLGPKGRNVVLEKKFGSPLITNDGVTIAKEIELEDAFENMGAKLVAEVAS 78
giYP_081854    VDTLANAVKVTLGPKGRNVVLEKKFGSPLITNDGVTIAKEIELEDAFENMGAKLVAEVAS 78
giNP_782944    VDILADTVKVTMGPKGRNVVLDKKFGAPLITNDGVTIAREIELEDAYENMGAQLVKEVAT 80
giYP_143537    VNAVANAVKVTLGPRGRNVVLEKKFGSPTITKDGVTVAKEVELEDHLENIGAQLLKEVAS 78
                  :   ::   ** .   :: .  *   ::::* ::  :: : .      .: : : :
```

Figure 3.134: continued

```
                    #####
giXP_956627    TQDEEVGDGTTTVIILAGEILAQSLPQLERNIHPVVIISAFKRALKDALQIIE-DISLPI 143
giEAW09861     TQDEEVGDGTTTVIILAGEMLAQALPQLERNIHPVVIIQAFKRALADALAIVE-EVSLPV 143
giBAE27111     TQDEEVGDGTTSVIILAGEMLSVAEHFLEQQMHPTVVISAYRMALDDMISTLK-KISTPV 144
giEDM00727     TQDEEVGDGTTSVIILAGEMLSVAEHFLEQQMHPTVVISAYRMALDDMVSTLK-KISTPV 144
giCAI46192     TQDEEVGDGTTSVIILAGEMLSVAEHFLEQQMHPTVVISAYRKALDDMISTLK-KISIPV 144
giP50143       TQDEEVGDGTTSVIILAGEMLSVAEQFLEQQMHPTVIISAYRKALDDMVNTLK-EISTPV 143
giAAM34653     TQDEEVGDGTTSVIILAGEMLSVAEQFLEQQMHPTVVIGAYRQALDDMLNILK-DISTPV 143
giXP_392814    TQDEEVGDGTTSVIVLAGEILATAEPFLEQNMHPTVIIRAYRQALEDIVTILNEQVSIDL 147
giAAN13716     TQDEEVGDGTTSVIVLAGEMLAAAEPFLQQQIHPTVIIRAYREALEDIVGHLQSQLSIQL 146
giNP_376188    GQDEETADGTKTAVILAGELVKKAEELLYKEIHPTIIVSGFKKAEEQALKTIE-EIAQKV 160
giAAY80050     GQDEETADGTKTAVIFSGELVKKAEELLYKEIHPTIIVSGYKKAEEMAIKTIE-EISTKV 153
giNP_341830    GQDEETADGTKTAVILAGELAKKAEDLLYKEIHPTIIVSGYKKAEEIALKTIQ-EIAQPV 155
giCAA45326     GQDEETADGTKTAVILAGELAKKAEDLLYKEIHPTIIVSGYKKAEEIALKTIQ-DIAQPV 152
giCAA07096     GQDEEVGDGTKTAVILAGELLRVAEELLDKNVHPTIIVSGYKKAAEEAIKKLQ-ELAEPI 160
giNP_148364    GQEDEAGDGTKTTVIFAGELLKEAEKLLDINIHPTIIVEGYKEALRKASEVIE-SIAEPV 153
giAAL63957     SQEEEAGDGTTTAVVLAGALLEEAEKLLEKNIHPTVIVSGFKKALDVAAEHLR-KVAIPV 151
giO24734       AQDAEVGDGTTSAVVLAGLLLDKADDLLDQNIHPTIIIEGYKKALNKSLEIID-QLATKI 143
giBAB59649     TQDSFVGDGTTTAVIIAGGLLQQAEALINQNVHPTVISEGYRMASEEAKRIID-EISTKI 144
giP48425       TQDSFVGDGTTTAVIIAGGLLQQAQGLINQNVHPTVISEGYRMASEEAKRVID-EISTKI 144
giYP_023973    TQDSYVGDGTTTAVIIAGALLEQAQALVNQNVHPTVITEGYRMADEYARKVLD-EISIKI 144
giBAB60294     AQDTAVGDGTTTAVVLSGELLKQAETLLDQGVHPTVISNGYRLAVNEARKIID-EISVKS 149
giBAA33889     TQEKEVGDGTTTAVVIAGELLRKAEELLDQNVHPTIVIKGYQLAVQKAQEVLK-EIAMDV 144
giAAB99002     TQEKEVGDGTTTAVVIAGELLRKAEELLDQNIHPSVIINGYEMARNKAVEELK-SIAKEV 145
giNP_275933    TQEDEVGDGTTTAVIIAGELLKKAENLLEMEIHPTIIAMGYRQAAEKAQEILD-DIAIDA 145
giP50016       TQEDEVGDGTTTAVVLAGELLHKAEDLLQQDIHPTVIARGYRMAVEKAEEILE-EIAEEI 148
giNP_070280    TQDNEVGDGTTTAVVLAGELLKRAEELLDQEIHPAIIANGYRYAAEKALEILN-EIAIPI 146
giO28045       TQDNEVGDGTTTAVVLAGELLKKAEELLDQDIHPTVIARGYRMAANKAVEILE-SIAMDI 146
giBAA29085     TQDKEAGDGTTTAVVIAGELLKKAEELLDQNIHPSIIIKGYTLASQKAQEILD-SIAKEV 146
giNP_125709    TQDKEAGDGTTTAVVIAGELLKKAEELLDQNIHPSIVIKGYMLAAEKAQEILD-SIAKEV 146
giAAL82098     TQDKEAGDGTTTAVVIAGELLRKAEELLDQNIHPSIIIKGYTLAAQKAQEILE-NIAKEV 146
giQ52500       TQDKEAGDGTTTAVVIAGELLRKAEELLDQNIHPSIIIKGYALAAEKAQEILD-EIAKDV 146
giO24730       TQDKEAGDGTTTAVVIAGELLRKAEELLDQNIHPSIIIKGYALAAEKAQEILD-EIAKDV 146
giAAP37564     TQDKEAGDGTTTAVVIAGELLRKAEELLNQNIHPTIIVKGYTLAAEKAQEILE-SIAKDV 146
giNP_615060    TQDEQVGDGTTSAAVVAGELLKKAEDLIEQEIHPTIIASGYRLAAEKAVEVLN-SLAMNV 143
giNP_633403    TQDDEVGDGTTSAAVVAGELLNKAEDLIEQEIHPTIIASGYRLAAEKAIEVLN-SLAMSV 143
giAAZ70052     TQDAEVGDGTTTAAVLAGEFLTKAEDLLESGVHPTVIASGYRLAADQATKTID-TITISA 143
giCAI48595     TQEEEVGDGTTSSVVIAGELLSQAEDLLEQDIHATILAQGYRQAAAEAKAALE-EIAIEV 147
giYP_137342    TQEDEVGDGTTTAVVMAGELLSKAEELLDQDIHASILAQGYRQAAEKAKEILE-DNAIDV 173
giQ9HN70       TQETEVGDGTTTSVVVSGELLSEAETLLEQDIHATTLAQGYRQAAEKAKELLD-DAAIDV 147
giO30561       TQEDEVGDGTTTAVINAGELLDQAEDLLDSDVHATTIAQGYRQAAEKAKEVLE-DNAIEV 148
giYP_001689883TQEDEAGDGTTTAVAIAGELLKNAEDLLERDIHPTAIIKGYNLAAEQAREEVD-NVAVDV 149
giNP_495722    LQDEEVGDGTTSVVIVAAELLKRADELVKQKVHPTTIINGYRLACKEAVKYISENISFTS 144
giNP_736462    KTNDIAGDGTTTATVLTQAIVREGLKNVTAGANPIGIRRGIETAVSAAVEELK---EIAQ 135
giNP_608082    KTNDIAGDGTTTATVLTQAIVHEGLKNVTAGANPIGIRRGIETATATAVEALK---AIAQ 135
giNP_816272    KTNDIAGDGTTTATVLTQAIVREGLKNVTAGANPLGIRRGIELATKTAVEELH---NISS 135
giNP_266550    KTNDIAGDGTTTATVLTQAIVREGLKNVTAGANPVGIRRGIELAAETAVASIK---EMAI 135
giYP_077851    KTNDVAGDGTTTATVLAQAMIREGLKNVTAGANPVGVRKGIEQAVAVAVESLK---EISK 135
giNP_388484    KTNDVAGDGTTTATVLAQAMIREGLKNVTAGANPVGVRKGMEQAVAVAIENLK---EISK 135
giYP_081854    KTNDVAGDGTTTATVLAQAMIREGLKNVTAGANPMGLRKGIEKAVVAAVEELK---TISK 135
giNP_782944    KTNDVAGDGTTTATLLAQAIIREGLKNVTGGANPMLVRRGIQMAVEEAVKGIK---EISK 137
giYP_143537    KTNDVAGDGTTTATVLAQAIVREGLKNVAAGANPLALKRGIEKAVEAAVEKIK---ALAI 135
                 :  ..***.:    : :   .   :    :. :  .   *       :
```

Figure 3.134: continued

```
giXP_956627     DINDDQ------AMYKLISSSIGTKYVSRWS--ELMCGLALKAVRTVTWEQGNGKKEVDI 195
giEAW09861      DIDDDK------AMYTLIQSSIGTKFVSRWS--ELMCNLALKAVRTVSFDVGGGKREVDI 195
giBAE27111      DVNNRE------MMLSIINSSITTKVISRWS--SLACNIALDAVKTVQFEE-NGRKEIDI 195
giEDM00727      DVNNRD------MMLNIINSSITTKVISRWS--SLACNIALDAVKTVQFEE-NGRKEIDI 195
giCAI46192      DISDSD------MMLNIINSSITTKAISRWS--SLACNIALDAVKMVQFEE-NGRKEIDI 195
giP50143        DTNDRE------LMLKIINSAINTKAIKLWA--DMACGIALDAVKTVELEE-NGRKEIDI 194
giAAM34653      DVSNRD------MMLKIINSAINTKALSRWS--TLACNIALDAVRTVELDE-NGREEIDI 194
giXP_392814     DCNDKN------KMIQVINSCVRTKFIGRWC--ELACQIALDAVYTVLLEE-NGRREIDI 198
giAAN13716      DVKDKA------KMADVVKACVGTKFIGKWS--DLAVKIALDAVETVTLSE-NGRLEVDI 197
giNP_376188     SVNDM-------DILKKVAMTSLNSKAVAGAR--EYLADIVAKAVTQVAE-LRGDRWYVDL 211
giAAY80050      SVNDT------EILRKVALTSLSSKAVAGAR--EHLADIVVKAITQVAE-LRGDKWYVDL 204
giNP_341830     TINDT------DVLRKVALTSLGSKAVAGAR--EYLADLVVKAVAQVAE-LRGDKWYVDL 206
giCAA45326      SINDT------DVLRKVALTSLGSKAVAGAR--EYLADLVVKAVAQVAE-LRGDKWYVDL 203
giCAA07096      DINND------EILKKIARTSLTSKAVHGAR--DYLAEIVVKAVKQVTE-KRGDKWYIDL 211
giNP_148364     SYDDV------EKLKLIAKTSLNSKAVAEAR--DYFAELAVEAVRTVAE-RRGDRWYVDL 204
giAAL63957      NRTDV------DTLRKIAMTSMGGKISETVK--EYFADLAVKAVLQVAE-ERNGKWYVDL 202
giO24734        DVSNLNSLATRDQLKKIVYTTMSSKFIAGGEEMDKIMNMVIDAVSIVAEPLPEGGYNVPL 203
giBAB59649      GKDEKE------LLIKLAQTSLNSKSASVAK--DKLAEISYEAVKSVAELRDGK-YYVDF 195
giP48425        GADEKA------LLLKMAQTSLNSKSASVAK--DKLAEISYEAVKSVAELRDGK-YYVDF 195
giYP_023973     NPDDKD------KLIKMAMTSLNSKSAGVFK--DKLAELSYQAIKAIAEERDGK-YYVDF 195
giBAB60294      TDDET--------LRKIALTALSGKNTGLSN--TFLADLVVKAVNAVAEERDGK-IIVDT 198
giBAA33889      KADDKE------ILHKIAMTSITGKGAEKAK--EKLGEMIVEAVTAVVDES-G---KVDK 192
giAAB99002      KPEDTE------MLKKIAMTSITGKGAEKAR--EQLAEIVVEAVRAVVDEETG---KVDK 194
giNP_275933     S--DRD------TLMKVAMTAMTGKGTEKAR--EPLAELIVDAVKQVEEDG-----EVEK 190
giP50016        DPDDEE------TLKKIAKTAMTGKGVEKAR--DYLAELVVKAVKQVAEEEDGE-IVIDT 199
giNP_070280     SKDDDE------ILKKIATTAMTGKGAEVAI--DKLAEIAVNAVKMIAEESNGQ-VEVNT 197
giO28045        DVEDEE------TLKKIAATAITGKHSEYAL--DHLSSLVVEAVKRVAEKVDDR-YKVDE 197
giBAA29085      KPDDEE------VLLKAAMTAITGKAAEEER--EYLAKLAVEAVKLVAEEKDGK-LKVDI 197
giNP_125709     KPDDEE------VLLKAAMTAITGKAAEEER--EYLAKLAVEAVKLVAEEKDGK-FKVDI 197
giAAL82098      KPDDEE------ILLKAAMTSITGKAAEEER--EYLAKLAVEAVKLVAEKEDGK-YKVDI 197
giQ52500        DVEDRE------ILKKAAVTSITGKAAEEER--EYLAEIAVEAVKQVAEKVGET-YKVDL 197
giO24730        DVEDRE------ILKKAAVTSITGKAAEEER--EYLAEIAVEAVKQVAEKVGET-YKVDL 197
giAAP37564      SPMDEE------ILMKAATTAITGKAAEEER--EYLAKLAVDAVKLVAEEVDGK-YIVDI 197
giNP_615060     EMSNRE------LLVSIAETAMTGKGAEASK--KLLSGIAVDAVTSVVDTN--GKKTIDK 193
giNP_633403     DMGNRD------LLLSIAETAMTGKGAESSK--KLLAEIAVDAVTSVVDTN--GKMSVDK 193
giAAZ70052      SPEDTE------TLEKIAATAITGKGAEAQK--EHLSRLAVKAVKSVAEISEDGKITVDI 195
giCAI48595      DEDDAD------ILESIAATAMTGKGAEASK--DLLAELVVDSVQAVADD-GD----IDT 194
giYP_137342     DADDTE------TLEKVAATAMTGKGAESSK--DVLAELVVRAAQSVVDDDGS----VDT 221
giQ9HN70        SADDTE------TLEKIAATAMTGKGAENAK--GVLSDLVVRAVQSVADD-ND----VDT 194
giO30561        TEDDRE------TLTKIAATAMTGKGAESAK--DLLSELVVDAVLAVKDD-DG----IDT 195
giYP_001689883DPDDKD------LIRSVAETSMTGKGAELDK--ELLSSIIYDAVNQVAVETNDGGIVVDA 201
giNP_495722     DSIGRQ------SVVNAAKTSMSSKIIGPDA--DFFGELVVDAAEAVRVENNGK--VTYP 194
giNP_736462     PVSGKE------AIAQVAAVSSRSEKVGEYIS-EAMGRVGNDGVITIEESRGMETELEVV 188
giNP_608082     PVSGKE------AIAQVAAVSSRSEKVGEYIS-EAMERVGNDGVITIEESRGMETELEVV 188
giNP_816272     VVDSKE------AIAQVAAVSSGSEKVGQLIA-DAMEKVGNDGVITIEESKGIETELDVV 188
giNP_266550     PVHDKS------AIAQVATVSSRSEKVGEYIS-DAMERVGSDGVITIEESKGMQTELDVV 188
giYP_077851     PIEGKE------SIAQVASISAADEEVGSLIA-EAMERVGNDGVITIEESKGFTTELEVV 188
giNP_388484     PIEGKE------SIAQVAAISAADEEVGSLIA-EAMERVGNDGVITIEESKGFTTELEVV 188
giYP_081854     PIEGKS------SIAQVAAISAADEEVGQLIA-EAMERVGNDGVITLEESKGFTTELDVV 188
giNP_782944     PVEGKE------DIARVAAISADDKEIGKLIA-DAMEKVGNEGVITVEESNTMGTELDVV 190
giYP_143537     PVEDRK------AIEEVATISANDPEVGKLIA-DAMEKVGKEGIITVEESKSLETELKFV 188
                             :                       :   .   :
```

Figure 3.134: continued

```
giXP_956627    KRYARVEK--VPGGEIEDSRVLDGVMLNKDITHPKMRRRIENPRIILLDCPLEYKKGESQ 253
giEAW09861     KRYARIEK--IPGGQIEDSEVIDGVMINKDITHPKMRRRIENPRIILLDCPLEYKKGESQ 253
giBAE27111     KKYARVEK--IPGGIIEDSCVLRGVMINKDVTHPRMRRYIKNPRIVLLDSSLEYKKGESQ 253
giEDM00727     KKYARVEK--IPGGIIEDSCVLRGVMINKDVTHPRMRRYIKNPRIVLLDSSLEYKKGESQ 253
giCAI46192     KKYARVEK--IPGGIIEDSCVLRGVMINKDVTHPRMRRYIKNPRIVLLDSSLEYKKGESQ 253
giP50143       KKYAKVEK--IPGGIIEDSCVLRGVMVNKDVTHPKMRRLIKNPRIILLDCSLEYKKGESQ 252
giAAM34653     KKYAKVEK--VPGGIIEDSCVLRGVMVNKDVTHPRMRRLIKNPRIVLLDCSLEYKKGESQ 252
giXP_392814    KRYAKVEK--IPGGTIEDSTVLKGVMFNKDVTHPKMRRHIKNPRIVLLDCSLEYKKGESQ 256
giAAN13716     KRYAKVEK--IPGGAIEESCVLKGVMINKDVTHPKMRRLIENPRIVLLDCSLEYKKGESQ 255
giNP_376188    DN-IQIVK--KHGGSINDTQIIYGIVVDKEVVHPGMPKRVENAKIALLDASLEVEKPELD 268
giAAY80050     DN-VQIVK--KHGGSINDTQIVYGIIVDKEVVHPGMPKRVENAKIALLDASLEVEKPELD 261
giNP_341830    DN-VQIVK--KHGGSVNDTQLVYGIVVDKEVVHPGMPKRIENAKIALLDASLEVEKPELD 263
giCAA45326     DN-VQIVK--KHGGSINDTQLVYGIVVDKEVVHPGMPKRIENAKIALLDASLEVEKPELD 260
giCAA07096     DS-IQIIK--KHGGGLRDTQLVYGIVLDKEVVHPGMPKRVENAYIVLLDAPLEVEKPEID 268
giNP_148364    NN-IQIVK--KHGGSLRDTRLVRGIVLDKEVVHPDMPRRVENARIALLDTPLEIEKPEID 261
giAAL63957     DN-IQIVK--KHGGSLLDTQLVYGIVVDKEVVHAAMPKRVVNAKIALLDAPLEVEKPEID 259
giO24734       DL-IKIDK--KKGGSIEDSMLVHGLVLDKEVVHPGMPRRVEKAKIAVLDAALEVEKPEIS 260
giBAB59649     DN-IQVVK--KQGGAIDDTALINGIIVDKEKVHPGMPDVVKNAKIALLDAPLEIKKPEFD 252
giP48425       DN-IQVVK--KQGGAIDDTQLINGIIVDKEKVHPGMPDVVKDAKIALLDAPLEIKKPEFD 252
giYP_023973    DN-LQMVK--KQGGSVDETQLIDGIIIDKEKVHPGMPSTVENAKIALLDLALEVKKPEFD 252
giBAB60294     AN-IKVDK--KSGGSINDTQFISGIVVDKEKVHSKMPDVVKDAKIALIDSALEIKKTEIE 255
giBAA33889     DL-IKIEK--KEGASVDETELINGVLIDKERVSPQMPKKIENAKIALLNCPIEVKETETD 249
giAAB99002     DL-IKVEK--KEGAPIEETKLIRGVVIDKERVNPQMPKKVENAKIALLNCPIEVKETETD 251
giNP_275933    DH-IKIEK--KEGAAVDDSTLVQGVIIDKERVHPGMPKKVENAKIALLNCPIEVKETEVD 247
giP50016       DH-IKLEK--KEGGGLEDTELVKGMVIDKERVHPGMPRRVENAKIALLNCPIEVKETETD 256
giNP_070280    DY-IKIEK--RQGGSIEETELVDGIVLDKEVVHPGMPKRVENAKILLLDSALEVKETEID 254
giO28045       DN-IKLEK--RQGGSVADTKLVNGIVIDKEVVHPGMPKRVKNAKIAVLKAALEVKETETD 254
giBAA29085     DN-IKLEK--KEGGAVRDTRLIRGVVIDKEVVHPGMPKRIENAKIALINDALEVKETETD 254
giNP_125709    DN-IKFEK--KEGGAVSDTKLIRGVVIDKEVVHPGMPKRVEKAKIALINDALEVKETETD 254
giAAL82098     DN-IKLEK--KEGGSVRDTQLIRGVVIDKEVVHPGMPKRVEKAKIALINDALEVKETETD 254
giQ52500       DN-IKFEK--KEGGSVKDTQLIKGVVIDKEVVHPGMPKRVEGAKIALINEALEVKETETD 254
giO24730       DN-IKFEK--KEGGSVKDTQLIKGVVIDKEVVHPGMPKRVEGAKIALINEALEVKETETD 254
giAAP37564     DN-IKLEK--KEGGSVRDTQLIKGVVIDKERVHPGMPKKVENAKIALINEALEVKETETD 254
giNP_615060    DN-ISVVK--KVGGRIEDSELIPGMIIDKERVHTNMPEKVKDAKIALLNSAIELKDTEVD 250
giNP_633403    EN-ISVVK--KVGGKTEDSELIPGMIIDKERVHTNMPEKVKDAKIALLNTAIELKDTEVD 250
giAAZ70052     ED-IKVEK--RPGGSIKDSEIVDGVIVDKERVHPAMPEVVENAKILLLSVPIELKKTETK 252
giCAI48595     DN-IKVEK--VVGGAVDESELVEGVLVGKERVHDNMPALVEDADIALLDTPIEVKETEID 251
giYP_137342    DN-IQIET--VVGGATDESELVEGVIVDKERVHDNMPFAVEDADVALLDTAIEVPETELD 278
giQ9HN70       DN-VKVEK--VTGGAIENSELIEGVIVDKERVSENMPYAVEDANIALVDDGLEVQETEID 251
giO30561       NN-VSIEK--VVGGTIDNSELVEGVIVDKERVDENMPYAVEDANIAILDDALEVRETEID 252
giYP_001689883AN-INIET--QTGHGVNESQLLRGAAISKDPVHDQMPAAVEDADVLLLNEAIEVEEAEAD 258
giNP_495722    INAVNVLK--AHGKSARESVLVKGYALNCTVASQAMPLRVQNAKIACLDFSLMKAKMHLG 252
giNP_736462    EG-MQFDRGYLSQYMVTDNEKMVSELENPYILITDKKISNIQEILPLLEEVLKTNRPLLI 247
giNP_608082    EG-MQFDRGYLSQYMVTDNEKMVADLENPFILITDKKVSNIQDILPLLEEVLKTNRPLLI 247
giNP_816272    EG-MQFDRGYLSQYMVTDNDKMEAVLENPYILITDKKISNIQDILPLLEQILQQSRPLLI 247
giNP_266550    EG-MQFDRGYLSQYMVSNTEKMVAELDNPYILITDKKISNIQEILPLLEQILKTNRPLLI 247
giYP_077851    EG-MQFDRGYASPYMVTDSDKMEAVLENPYILVTDKKITNIQEILPVLEQVVQQGKPLLL 247
giNP_388484    EG-MQFDRGYASPYMVTDSDKMEAVLDNPYILITDKKITNIQEILPVLEQVVQQGKPLLL 247
giYP_081854    EG-MQFDRGYASPYMITDSDKMEAVLDNPYILITDKKISNIQEILPVLEQVVQQGKPLLI 247
giNP_782944    EG-MQFDRGYVSPYMVTDTEKMEASLDDAYILITDKKITNIQEILPVLEQIVQQGKRLLI 249
giYP_143537    EG-YQFDKGYISPYFVTNPETMEAVLEDAFILIVEKKVSNVRELLPILEQVAQTGKPLLI 247
                     .          :   : .   .              :   :.
```

Figure 3.134: continued

```
giXP_956627    TNIEITKEEDWNRILEIEEEQVKQMCEHILAFNPD--------------LVITEKGVSDL 299
giEAW09861     TNIEITKEDDWNRILEIEEEQVKHMCDAILALKPD--------------IVFTEKGVSDL 299
giBAE27111     TNIEITREEDFTQILQMEEEYIHQLCEDIIQLKPD--------------VVITEKGISDL 299
giEDM00727     TDIEITREEDFTRILQMEEEYIQQLCEDIIQLKPD--------------VVITEKGISDL 299
giCAI46192     TDIEITREEDFTRILQMEEEYIQQLCEDIIQLKPD--------------VVITEKGISDL 299
giP50143       TEIEITREEDFARILQMEEEYIQQVCEDIIRLKPD--------------VVITEKGISDL 298
giAAM34653     TDIEIAREEDFARILQMEEEYVQQICEDIIRLKPD--------------LIFTEKGISDL 298
giXP_392814    TNIEIMKDTDFTRILELEEEFVKKMCEDIISVKPD--------------VVITEKGVSDL 302
giAAN13716     TNVEIIGEQDFTRMLQIEEEFVQRICADIIAVKPD--------------LVFTEKGVSDL 301
giNP_376188    AEIRINDPTQMKKFLEEEENLLKEKVDKIAATGAN--------------VVICQKGIDEV 314
giAAY80050     AEIRINDPTQMKKFLDEEENILKEKVDKIAQTGAN--------------VVICQKGIDEV 307
giNP_341830    AEIRINDPTQMHKFLEEEENILKEKVDKIAATGAN--------------VVICQKGIDEV 309
giCAA45326     AEIRINDPTQMHKFLEEEENILKEKVDKIAATGAN--------------VVICQKGIDEV 306
giCAA07096     AEIRISDPTYLKKFLEEEERILEDMVEKIYNVAVERMKRDGMEPGKAGIVVITQKGIDEV 328
giNP_148364    LEISITSPEQIKALYEKQERILQEKIEKIAATGAN--------------VVITQKGIDDV 307
giAAL63957     AEIRINDPTQMRAFLEEEERILRGYVDKLKSLGVT--------------VLFTTKGIDDI 305
giO24734       AKISITSPEQIKAFLDEEAKYLKDMVDKLASIGAN--------------VVICQKGIDDV 306
giBAB59649     TNLRIEDPSMIQKFLAQEENMLREMVEKIKSVGAN--------------VVITQKGIDDM 298
giP48425       TNLRIEDPSMIQKFLAQEENMLREMVDKIKSVGAN--------------VVITQKGIDDM 298
giYP_023973    TNLQINDPRMIQKFLDQEEGILKEMVDKIQKTGAN--------------VVITQKGIDDM 298
giBAB60294     AKVQISDPSKIQDFLNQETSTFKEMVEKIKKSGAN--------------VVLCQKGIDDV 301
giBAA33889     AEIRITDPTKLMEFIEQEEKMLKDMVDTIKASGAN--------------VLFCQKGIDDL 295
giAAB99002     AEIRITDPAKLMEFIEQEEKMIKDMVEKIAATGAN--------------VVFCQKGIDDL 297
giNP_275933    AEIRITDPSQMQAFIEQEEQMIRDMVNSIVDTGAN--------------VLFCQKGIDDL 293
giP50016       AEIRITDPEQLQAFIEEEERMLSEMVDKIAETGAN--------------VVFCQKGIDDL 302
giNP_070280    AKIRITDPEKLQKFIEQEEAMLKEMVDKIVNAGAN--------------VVFCQKGIDDL 300
giO28045       AEIRITDPDQLMKFIEQEEKMLKEMVDRLAEAGAN--------------VVFCQKGIDDL 300
giBAA29085     AEIRITSPEQLQAFLEQEEKMLKEMVDKIKEVGAN--------------VVFVQKGIDDL 300
giNP_125709    AEIRITSPEQLQAFLEQEEKMLKEMVDKIKEVGAN--------------VVFVQKGIDDL 300
giAAL82098     AEIRITSPEQLQAFLEQEERMLREMVEKIKEVGAN--------------VVFVQKGIDDL 300
giQ52500       AEIRITSPEQLQAFLEQEEKMLREMVDKIKEVGAN--------------VVFVQKGIDDL 300
giO24730       AEIRITSPEQLQAFLEQEEKMLREMVDKIKEVGAN--------------VVFVQKGIDDL 300
giAAP37564     AEIRITSPEQLQAFLEQEEKMIKEMVDKIVATGAN--------------VVFCQKGIDDL 300
giNP_615060    AEISITSPDQLQSFLDQEEAMLKKIVQKVISSGAN--------------VVFCQKGVEDL 296
giNP_633403    AEISITSPDQLQSFLDQEEQMLKKIVQKVINSGAN--------------VVFCQKGVEDL 296
giAAZ70052     AEIKITNPDQMQLFLDQEEAMLKEIVDKVIKTGAN--------------VVFCQKGIDDL 298
giCAI48595     AEVNVTDPDQLEQFLEQEEKQLREMVDQLADAGAD--------------VVFCQKGIDDM 297
giYP_137342    TEVNVTDPDQLQQFLDQEEEQLKEMVDQLAEAGAD--------------VVFCQKGIDDM 324
giQ9HN70       TEVNVTDPDQLQNFLDQEEEQLKEMVDALKDAGAN--------------VVFADSGIDDM 297
giO30561       AEVNVTDPDQLQQFLDQEEKQLKEMVDQLVEVGAD--------------AVFVGDGIDDM 298
giYP_001689883TSVNIESPDQLQSFLDQEEKQLKEKVQQIADTGAN--------------VVFCQKGIDDM 304
giNP_495722    ISVVVEDPAKLEAIRREEFDITKRRIDKILKAGAN--------------VVLTTGGIDDL 298
giNP_736462    IADDVDGEALPTLVLNKIRGTFNVVAVKAPGFGDRR-------------KAMLEDIAILT 294
giNP_608082    IADDVDGEALPTLVLNKIRGTFNVVAVKAPGFGDRR-------------KAMLEDIAILT 294
giNP_816272    IADDVDGEALPTLVLNKIRGTFNVVAVKAPGFGDRR-------------KAMLEDIAILT 294
giNP_266550    VADDVDGEALPTLVLNKIKGVFNVVAVKAPGFGDRR-------------KAQLEDLAILT 294
giYP_077851    IAEDVEGEALATLVVNKLRGTFNAVAVKAPGFGDRR-------------KAMLEDISILT 294
giNP_388484    IAEDVEGEALATLVVNKLRGTFNAVAVKAPGFGDRR-------------KAMLEDIAVLT 294
giYP_081854    IAEDVEGEALATLVVNKLRGTFNVVAVKAPGFGDRR-------------KAMLEDIAILT 294
giNP_782944    ISEDIEGEALATLVVNKLRGTFTCVAVKAPGFGDRR-------------KEMLEDIATLT 296
giYP_143537    IAEDVEGEALATLVVNKLRGTLSVAAVKAPGFGDRR-------------KEMLKDIAAVT 294
                   :         .
```

Figure 3.134: continued

Figure 3.134: continued

```
giXP_956627    KIGDEYFTFLTK-CKDPKACTVLLRGP-SKDVLNEIERNLQDAMGVARNVMFHPRLSPGG 411
giEAW09861     KIGDEYFTFLRK-CQNPKACTILLRGP-SKDILNEIERNLQDAMSVARNVIFHPRLCPGG 411
giBAE27111     KIGDEYFTFITG-CKDPKACTILLRGA-SKEILSEVERNLQDAMQVCRNVLLDRQLVPGG 411
giEDM00727     KIGDEYFTFITD-CKDPKACTILLRGA-SKEILSEVERNLQDAMQVCRNVLLDPQLVPGG 411
giCAI46192     KIGDEYFTFITD-CKDPKACTILLRGA-SKEILSEVERNLQDAMQVCRNVLLDPQLVPGG 411
giP50143       KIGDEYFTFITD-CKDPKACTIVLRGA-SKEILAEVERNLQDAMQVCRNVVIDPYLVPGG 410
giAAM34653     KIGDEYFTFVTE-CKDPKACTILLRGA-SKEILAEVERNLQDAMQVCRNVLLDPYLLPGG 410
giXP_392814    KVGDEYFCFITE-CKDPKACTIILRGA-SKDVLNETERNLQDALHVARNLLIEPKLVPGG 414
giAAN13716     KIGDEYFTFVTE-CKEPKACTILLRGA-SKDILNETERNLQDALHVARNLVLEPRLVAGG 413
giNP_376188    KVGEDKMVFVEG-AKNPKAVSILIRGG-LERVVDETERALRDALGTVADVIRDGRAVAGG 425
giAAY80050     KIGEDKMVFIEG-AKNPKAVSILIRGG-LERVVDETERALRDALGTVADVVRDGRAIAGG 418
giNP_341830    KVGEDKMVFVEG-AKNPKSVSILIRGG-LERVVDETERALRDALGTVADVIRDGRAVAGG 420
giCAA45326     KVGEDKMVFVEG-AKNPKSVSILIRGG-LERVVDETERALRDALGTVADVIRDGRAVAGG 417
giCAA07096     KVGENKMVFIEG-CPNPKAVTIVIRGG-LERLVDEAERSIQDAMHAVADAIRDGKIFAGG 439
giNP_148364    KVGEDKMVFIEG-AKNPKSVTILLRGG-FERLVDEAERSLHDALSVVADAIMDGKIVAGG 418
giAAL63957     RVGDEKMVFVEQ-CKNPKAVSILVRGG-FERLVDEAERNLDDALSVVSDVVEDPYILPAG 416
giO24734       RVGNDKMVFIEG-AKNPKAVNILLRGS-NDMALDEAERSINDALHSLRNVLMKPMIVAGG 417
giBAB59649     KVGDDYMTFVTG-CKNPKAVSVLVRGE-TEHVVDEMERSITDSLHVVASALEDGAYTAGG 409
giP48425       KVGEDYMTFVTG-CKNPKAVSILVRGE-TEHVVDEMERSITDSLHVVASALEDGAYAAGG 409
giYP_023973    KIGDDYMTFVTG-AKNPKAVSILIRGE-TDHVVDEIERSITDSLHVVAAAVEDAAYVTGG 409
giBAB60294     KIGDDRMTFVTG-CKNPKAVSILIRGG-TEHVVSEVERALNDAIRVVAITKEDGKFLWGG 412
giBAA33889     KIAGDAMIFVEE-CKHPKAVTMLIRGT-TEHVIEEVARAVDDAIGVVACTIEDGKIVAGG 406
giAAB99002     KVAGDAMIFVEQ-CKHPKAVTILARGS-TEHVVEEVARAIDDAIGVVKCALEEGKIVAGG 408
giNP_275933    KISGEEMIFVEE-CKEPKAVTILVRGS-TEHVVSEVERAIEDAIGVVAATVEDGKVVAGG 404
giP50016       KVAGDKMIFVEG-CKDPKAVTILIRGG-TEHVVDEAERAIEDAIGVVAAALEDGKVVAGG 413
giNP_070280    KVGDEKMVFVTG-CKNPKAVTILVRGG-TEHVVEEIARGIEDAVRAVACAVEDGKVVVGA 411
giO28045       KVGDEKMVFIEG-CKNPKAVTILIRGG-SEHVVDEVERSLQDAIKVVKTALESGKVVAGG 411
giBAA29085     KVAGENMIFVEG-CKNPKAVTILIRGG-TEHVVDEVERALEDAIKVVKDILEDGKIIAGG 411
giNP_125709    KVAGENMIFVEG-CKNPKAVTILIRGG-TEHVVDEVERALEDAVKVVKDILEDGKIIAGG 411
giAAL82098     KVAGESMIFVEG-CQNPKAVTILIRGG-TEHVVDEVERALEDAIKVVKDILEDGKILAGG 411
giQ52500       KVAGENMIFVEG-CKNPKAVTILIRGG-TEHVVDEVERALEDAVKVVKDIVEDGKIVAAG 411
giO24730       KVAGENMIFVEG-CKNPKAVTILIRGG-TEHVVDEVERALEDAVKVVKDIVEDGKIVAAG 411
giAAP37564     KVAGENMVFVEG-CKNPKAVTILIRGG-TEHVVDEVERALEDAIKVVKDIVEDGKIVAGG 411
giNP_615060    KVGGDSMTFVTG-CDNPKAVTILLRGG-TEHVVDSVDSALEDALRVVGVAIEDEKLVSGG 407
giNP_633403    KVGGDSMTFVTG-CDNPKAVTILLRGG-TEHVVDSIDSALEDALRVVGVAIEDEKLVAGG 407
giAAZ70052     DVTGSRMTFVTG-CKDSKATSILLRGG-TEHVVEGIERALEDALRVVGVALEDQKIVVGG 409
giCAI48595     PIAGDEKIFVED-VDEAKAVTLILRGG-TEHVVDEIERAIEDSLGVVQTTLEDGQVLPGG 408
giYP_137342    DIAGDERIFVED-VEDARAVTMILRGG-TEHVVDEVERAIEDSLGVVAATLEDGKVLPGG 435
giQ9HN70       DIGGDERIFVED-VEEAKSVTLILRGG-TEHVVDEVERAIEDSLGVVRVTLEDGQVMPGG 408
giO30561       DVGGDERIFVED-VEDAKSVTLILRGG-TEHVVDELERAIEDSLGVVRTTLEDGKVLPGG 409
giYP_001689883--SDDELFYVEGESEQAHGVTLLLRGS-TDHVVDELERGVSDALDVSAQTLSDGRVLPGG 413
giNP_495722    RISDDELILIKG-PKSRTASSIILRGA-NDVMLDEMERSVHDSLCVVRRVLESKKLVAGG 415
giNP_736462    TSDFDREKLQERLAKLAGGVAVIKVGAATETELKEMKLRIEDALNATRAAVEEG-IVSGG 413
giNP_608082    TSDFDREKLQERLAKLAGGVAVIKVGAPTETALKEMKLRIEDALNATRAAVEEG-IVAGG 413
giNP_816272    TSDFDREKLQERLAKLAGGVAVVKVGAATETELKELKLRIEDALNATRAAVEEG-MVSGG 413
giNP_266550    TSDFDREKLQERLAKLAGGVAVVKVGAATETELKAMKLLIEDALNATRAAVEEG-IVSGG 413
giYP_077851    TSEFDKEKLQERLAKLAGGVAVIKVGAATETELKERKLRIEDALNSTRAAVEEG-IVSGG 413
giNP_388484    TSEFDREKLQERLAKLAGGVAVIKVGAATETELKERKLRIEDALNSTRAAVEEG-IVSGG 413
giYP_081854    TSEFDREKLQERLAKLAGGVAVIKVGAATETELKERKLRIEDALNSTRAAVEEG-IVAGG 413
giNP_782944    TSEFDREKLQERLAKLAGGVAVIKVGAATETELKERKLRIEDALAATKAAVEEG-IIPGG 415
giYP_143537    DSEYAREKLQERLAKLAGGVAVIRVGAATETELKEKKHRFEDALNATRAAVEEG-IVPGG 413
                                .  ::  *   .  :      . *::             ..
```

Figure 3.134: continued

```
                                                                  # ##  #
giXP_956627    GATEMAVSVRLTQLAKSIEGVQQWPYKAVAEALEVIPRTLVQNAGKSPVRVLTDLRAKHA 471
giEAW09861     GAIEMAVSVRLSQLAKSIEGVQQWPYKAVADAMEVIPRTLAQNAGASPIRVLTRLRAKHV 471
giBAE27111     GASEMAVAHALTEKSKAMTGVEQWPYRAVAQALEVIPRTLIQNCGASTIRLLTSLRAKHT 471
giEDM00727     GASEMAVAHALTEKSKAMTGVEQWPYRAVAQALEVIPRTLIQNCGASTIRLLTSLRAKHT 471
giCAI46192     GASEMAVAHALTEKSKAMTGVEQWPYRAVAQALEVIPRTLIQNCGASTIRLLTSLRAKHT 471
giP50143       GASEMSVAHILTEKSKTMTGVEQWPYRAVAQALEVIPRTLIQNCGASTIRILTSLRAKHT 470
giAAM34653     GAVEMEVSHRLTERSRAMTGVEQWPYRAVAQALEVVPRTLIQNCGASAIRVLTSLRAKHT 470
giXP_392814    GAVEMAVSRLLTEKAARLAGVEQWPYKAVAQALEIIPRTLAQNCGANTIRTLTALRAKHA 474
giAAN13716     GAVEMAASQLLTRKQVKG------PYTAVAHALEIIPRTLAQNCGANTIRALTALRAKHA 467
giNP_376188    GAVELEIAKRLRKYAPQIGGKEQLAIEAYASALENLVMILIENGGYDPIDLLVKLRSAHE 485
giAAY80050     GAVETEIAKRLRKYAPQVGGKEQLAIEAYANALESLVMILIENGGFDPIELLVKLRSAHE 478
giNP_341830    GAVEIEIAKRLRKYAPQVGGKEQLAIEAYANAIEGLIMILAENAGLDPIDKLMQLRSLHE 480
giCAA45326     GAVEIEIAKRLRKYAPQVGGKEQLAIEAYANAIEGLIMILAENAGLDPIDKLMQLRSLHE 477
giCAA07096     GAVEVELSKYLREIAPKIGGKEQLAVEAFARALEGLPMALAENAGLDPVEIMMKLRAAHS 499
giNP_148364    GAVEAEVAKVLYEYASKLPGKTQLAVEAFARAVEALPQALAHNAGHDPIEVLVKLRSAHE 478
giAAL63957     GAAEIEAAKAVRAFAPKVGGREQYAVEAFARALEVIPKALAENAGLDPIDILTELTHKHE 476
giO24734       GAVETELALRLREYARSVGGKEQLAIEKFAEALEEIPMILAETAGMEPIQTLMDLRAKHA 477
giBAB59649     GATAAEIAVRLRSYAQKIGGRQQLAIEKFADAIEEVPRALAENAGLDPIDILLKLRAEHA 469
giP48425       GATAAEIAFRLRSYAQKIGGRQQLAIEKFADAIEEIPRALAENAGLDPIDILLKLRAEHA 469
giYP_023973    GSAAEEIAFRLRTYASKVGGRQQLAIERFADALEEIPRALAENAGLDPIDILIKIRSEHA 469
giBAB60294     GAVEAELAMRLAKYANSVGGREQLAIEAFAKALEIIPRTLAENAGIDPINTLIKLKSEHE 472
giBAA33889     GAAEIELAMKLRDYAEGVSGREQLAVRAFADALEVVPRTLAENAGLDAIEMLVKLRAKHA 466
giAAB99002     GATEIELAKRLRKFAESVAGREQLAVKAFADALEVIPRTLAENSGLDPIDMLVKLRAAHE 468
giNP_275933    GAPEIEIAKRLKDYADSISGREQLAVSAFAEALEIVPKTLAENAGLDSIDVLVDLRAAHE 464
giP50016       GAPEVEVARQLRDFADGVEGREQLAVEAFADALEIIPRTLAENSGLDPIDVLVQLRAKHE 473
giNP_070280    GAPEIEVSLKLREWAPSLGGREQLAVEAFATALEIIPRTLAENAGLDPIDVLVELKAAHE 471
giO28045       GAPEIEVALKIRDWAPTLGGREQLAAEAFASALEVIPRALAENSGLDPIDILVELRKAHE 471
giBAA29085     GASEIELSIKLDEYAKEVGGKEQLAIEAFAEALKVIPRTLAENAGLDPIETLVKVIAAHK 471
giNP_125709    GAAEIELSIKLDEYAKEVGGKEQLAIEAFAEALKVIPRTLAENAGLDPIETLVKVIAAHK 471
giAAL82098     GAPEIELAIRLDEYAKEVGGKEQLAIEAFAEALKVIPRTLAENAGLDPIETLVKVIAAHK 471
giQ52500       GAPEIELAIRLDEYAKEVGGKEQLAIEAFAEALKVIPRTLAENAGLDPIETLVKVIAAHK 471
giO24730       GAPEIELSIRLDEYAKEVGGKEQLAIEAFAEALKVIPRTLAENAGLDPIETLVKVIAAHK 471
giAAP37564     GASEIELAIRLDEYAKEVGGKEQLAIEAFADALKVIPRTLAENAGLDPVDVLVKVTAAHK 471
giNP_615060    GSPEVEVALRLQEYAATLEGREQLAVKAYSEALEVIPRTLAENAGLDPIDMLMELRSQHE 467
giNP_633403    GSPEVEVALRLQEYAATLEGREQLAVKAYSEALEVIPRTLAENAGLDPIDMLMELRSQHE 467
giAAZ70052     GSPEIELSLRLKEYAATLKGREQLAVMKFAESLEIIPSTLAENAGLDPIDMLVEMRSQHE 469
giCAI48595     GAPEIALALALRDFADSVGGREQLAVEAFADAVDVIPRTLAENAGLDPIDSLVDLRSQHA 468
giYP_137342    GAPETQLALGLRDHADSVGGREQLAVEAFADAIDVIPRTLAENAGLDPIDSLVDLRSKHD 495
giQ9HN70       GAPETELAMQLRDFADSVGGREQLAVEAFADALEVIPRTLAENAGHDPIDSLVDLRSQHD 468
giO30561       GAPETELSLQLREFADSVGGREQLAVEAFAEALDIIPRTLAENAGLDPIDSLVDLRSRHD 469
giYP_001689883GATEVEVASRLRDFADSVSGREQLAVEAFADSLELVPRVLAENAGLDSIDTLVDLRSAHE 473
giNP_495722    GAVETSLSLFLETYAQTLSSREQLAVAEFASALLIIPKVLASNAARDSTDLVTKLRAYHS 475
giNP_736462    GTALVNVIEKVAALKLN--GDEETGRNIVLRALEEPVRQIAYNAGYEGSVIIERLKQSEI 471
giNP_608082    GTALITVIEKVAALELE--GDDATGRNIVLRALEEPVRQIALNAGYEGSVIIDKLKNSPA 471
giNP_816272    GTALVNVIGKVAALEAE--GDVATGIKIVVRALEEPIRQIAENAGYEGSVIVDKLKNVDL 471
giNP_266550    GTALVNAIAALDKLSEE--GDIQTGININIVRRALEEPVRQIAANAGYEGSVIIDKLRSEEV 471
giYP_077851    GTALVNVYNKVAALEAE--GDELTGININIVLRALEEPIRQIAHNAGLEGSVIVERLKNEEI 471
giNP_388484    GTALVNVYNKVAAVEAE--GDAQTGININIVLRALEEPIRQIAHNAGLEGSVIVERLKNEEI 471
giYP_081854    GTSLMNVYTKVASIVAE--GDEATGININIVLRALEEPVRQIAINAGLEGSVVVERLKGEKV 471
giNP_782944    GTAYAMVIKEVEKLNSET-HDIKLGIDIVKKSLEEPVRQIACNAGVEGSIVIEKVKHSEA 474
giYP_143537    GVTLLRAISAVEELIKKLEGDEATGAKIVRRALEEPARQIAENAGYEGSVIVQQILAETK 473
               *         :                    ::      :  . . .    :  :
```

Figure 3.134: continued

Figure 3.134: continued

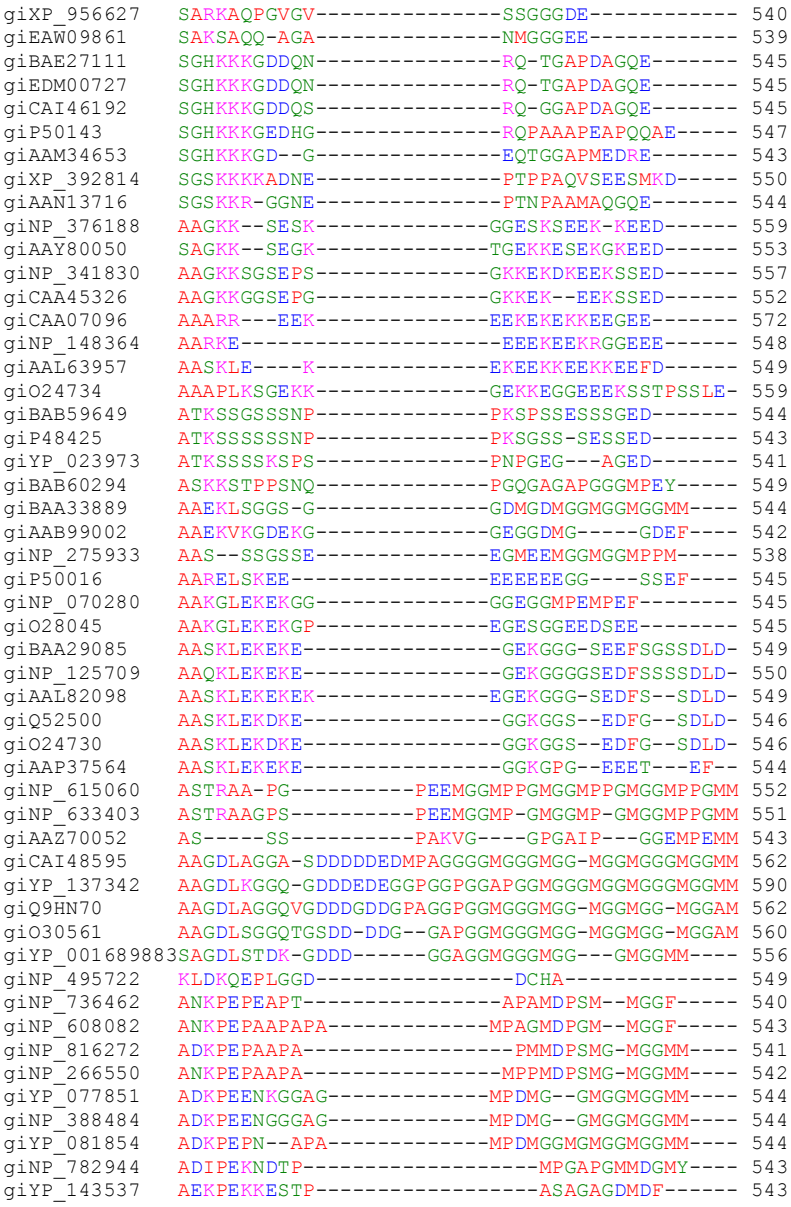

Figure 3.134

[giXP_956627: source organism= *Neurospora crassa* OR74A, product= t-complex protein 1 subunit gamma, length= 540 aa;
giEAW09861: source organism= *Aspergillus clavatus* NRRL 1, product=t-complex protein 1, gamma subunit, putative, length= 539 aa;
giBAE27111: source organism= Mus musculus, name= unnamed protein product, lenght= 545 aa;

giEDM00727: source organism= *Rattus norvegicus*, product= chaperonin subunit 3 (gamma), length= 545 aa;
giCAI46192: source organism= *Homo sapiens*, product= hypothetical protein (note="T-complex protein 1, gamma subunit), length= 545 aa;
giP50143: source organism=*Xenopus laevis*, product= t-complex protein 1 subunit gamma, length= 547 aa;
giAAM34653: organism= *Danio rerio*, product= chaperonin-containing TCP-1 complex gamma chain, length= 543 aa;
giXP_392814: source organism= *Apis mellifera*, product= similar to T-complex protein 1 subunit gamma (TCP-1-gamma) (CCT-gamma), length= 550 aa; giAAN13716: organism= *Drosophila melanogaster* product= CG8977-PB, isoform B gene= Cctgamma (name= CG8977 gene product from transcript CG8977-RB), length= 544 aa;
giNP_376188: source organism= *Sulfolobus tokodaii* str. 7, product= thermosome, beta subunit, length= 559 aa;
giAAY80050: source organism= *Sulfolobus acidocaldarius* DSM 639, product= thermosome beta subunit, length= 553 aa;
giNP_341830: organism= *Sulfolobus solfataricus* P2, product= thermosome subunit beta, length= 557 aa;
giCAA45326: source organism= *Sulfolobus shibatae*, product= thermophilic factor 55, length= 552 aa;
giCAA07096: source organism= *Pyrodictium occultum*, product= ThsB, length= 572 aa;
giNP_148364: source organism= *Aeropyrum pernix* K1, product= thermosome beta subunit, length= 548 aa;
giAAL63957: source organism= Pyrobaculum aerophilum str. IM2, product= thermosome (chaperonin) alpha subunit, length= 549 aa;
giO24734: source organism= *Sulfolobus tokodaii*, product= thermosome subunit alpha, length= 559 aa;
giBAB59649: source organism= *Thermoplasma volcanium* GSS1, product= archaeal chaperonin [group II], length= 544 aa;
giP48425: organism= *Thermoplasma acidophilum*, product= thermosome subunit beta, legth= 543 aa;
giYP_023973: source organism= *Picrophilus torridus* DSM 9790, product= thermosome subunit, length= 541 aa;
giBAB60294 organism= *Thermoplasma volcanium* GSS1, product= archaeal chaperonin [group II], length= 549 aa;
giBAA33889: source organism= *Methanothermococcus thermolithotrophicus* DSM 2095, product= chaperonin, length= 544 aa;
giAAB99002: source organism= *Methanocaldococcus jannaschii* DSM 2661, product= thermosome (ths), length= 542 aa;
giNP_275933: source organism= *Methanothermobacter thermautotrophicus* str.Delta H, product= chaperonin, length= 538 aa;
giP50016: source organism= *Methanopyrus kandleri*, product= thermosome subunit, length= 545 aa;
giNP_070280: source organism= *Archaeoglobus fulgidus* DSM 4304, product= thermosome, subunit beta (thsB), length= 545 aa;
giO28045: source organism=*Archaeoglobus fulgidus* , product=thermosome subunit alpha, length= 545 aa;

giBAA29085: source organism= *Pyrococcus horikoshii* OT3, product= 549aa long hypothetical thermophilic factor (motif=chaperonins TCP-1 signatures), length= 549 aa;
giNP_125709: source organism= *Pyrococcus abyssi* GE5, product= thermosome, subunit alpha, length= 550 aa;
giAAL82098: source organism= *Pyrococcus furiosus* DSM 3638 product= thermosome, single subunit, length= 549 aa;
giQ52500: source organism= *Thermococcus kodakarensis* KOD1, product=thermosome subunit beta, length= 546 aa;
giO24730: source organism= Thermococcus sp. KS-1, product= thermosome subunit beta, length= 546 aa;
giAAP37564: source organism= *Thermococcus litoralis*, product= thermosome alpha subunit, length= 544 aa;
giNP_615060: source organism= *Methanosarcina acetivorans* C2A, product= Hsp60, length= 552 aa;
giNP_633403: source organism= *Methanosarcina mazei* Go1, product= thermosome, alpha subunit, length= 551 aa;
giAAZ70052: source organism= *Methanosarcina barkeri* str. Fusaro, product= Hsp60, length= 543 aa;
giCAI48595: source organism= *Natronomonas pharaonis* DSM 2160, product= thermosome subunit 1 (alpha subunit), length= 562 aa;
giYP_137342: source organism= *Haloarcula marismortui* ATCC 43049, product= thermosome alpha subunit, length= 590 aa;
giQ9HN70: source organism= *Halobacterium salinarum*, product= thermosome subunit alpha, length= 562 aa;
giO30561: source organism= *Haloferax volcanii*, product= thermosome subunit 1, length= 560 aa;
giYP_001689883: source organism= *Halobacterium salinarum* R1, product= thermosome subunit 2, length= 556 aa;
giNP_495722: source organism= *Caenorhabditis elegans*, product= chaperonin containing TCP-1 family member (cct-1), length= 549 aa;
giNP_736462: source organism= *Streptococcus agalactiae* NEM316, product= chaperonin GroEL, length= 540 aa;
giNP_608082: source organism= *Streptococcus pyogenes* MGAS8232, product= chaperonin GroEL, length= 543 aa;
giNP_816272: source organism= *Enterococcus faecalis* V583, product= chaperonin, 60 kDa, length= 541 aa;
giNP_266550: source organism= *Lactococcus lactis* subsp. lactis Il1403, product= chaperonin GroEL, length= 542 aa;
giYP_077851: source organism= *Bacillus licheniformis* ATCC 14580, product= chaperonin GroEL, length= 544 aa;
giNP_388484: source organism= *Bacillus subtilis* subsp. subtilis str. 168, product= chaperonin GroEL, length= 544 aa;
giYP_081854: organism= *Bacillus cereus* E33L, product= chaperonin GroEL, length= 544 aa;
giNP_782944: source organism= *Clostridium tetani* E88, product= chaperonin GroEL, length= 543 aa;
giYP_143537: source organism= *Thermus thermophilus* HB8, product= chaperonin GroEL, length= 543 aa.]

Table 3.11: Scores of multiple sequence alignment of *T. volcanium* Hsp60 β subunit protein with several archaeal Hsp60 proteins.

Chaperonin source	Percent identity with chaperonin subunits from																														
	1	2	3	4	5	6	7	8	9	10	11	12	13	14	15	16	17	18	19	20	21	22	23	24	25	26	27	28	29	30	31	32
(1)TvolcaniumBeta	100	93	76	60	57	57	57	56	57	56	55	57	57	54	54	53	53	56	54	54	53	53	54	53	52	51	50	50	50	49	50	44
(2)TacidophilumBeta		100	78	60	57	57	58	57	57	58	56	58	58	54	54	53	55	55	56	54	55	54	55	53	52	51	51	50	50	49	50	44
(3)PtorridusThsSubunit			100	60	57	58	56	57	56	57	56	56	56	54	54	53	54	55	55	54	54	54	53	51	51	52	52	51	51	50	52	46
(4)TvolcaniumAlpha				100	59	60	59	59	57	59	57	58	58	54	57	55	54	56	52	57	52	52	52	50	52	51	52	52	50	50	51	45
(5)AfulgidusBeta					100	68	67	66	75	68	69	67	67	64	61	61	62	66	55	65	53	53	53	57	56	58	57	55	58	53	59	50
(6)TlitoralisAlpha						100	89	88	70	88	70	87	87	65	60	60	60	69	59	70	57	57	57	58	59	56	59	55	57	54	55	51
(7)PhorikoshiiTF							100	93	70	97	69	88	88	67	58	58	59	67	56	70	55	55	55	58	59	56	58	55	57	54	55	49
(8)PfuriosusThsSSubunit								100	69	92	70	91	90	66	58	59	59	67	56	70	55	55	54	59	58	56	58	54	57	54	55	50
(9)AfulgidusAlpha									100	70	69	70	69	61	59	58	58	62	56	66	54	54	54	57	57	56	57	56	58	55	56	49
(10)PabyssiAlpha										100	69	89	89	67	58	59	59	67	56	70	55	55	54	58	58	56	57	55	56	54	55	50
(11)MkandleriThsSubunit											100	67	67	65	61	61	61	71	55	70	54	54	54	57	58	63	57	60	63	53	62	53
(12)TkodakarensisBeta												100	99	66	57	58	59	67	58	69	56	55	55	59	58	56	58	54	56	55	54	50
(13)TspKS1Beta													100	66	57	58	59	66	57	69	56	55	55	59	58	56	57	54	56	55	54	49
(14)MthermolithotrophicusChp														100	55	57	58	71	52	78	50	51	50	52	50	61	51	59	60	46	58	50
(15)MbarkeriHsp60															100	69	68	59	50	57	49	49	50	47	46	56	50	56	56	46	57	48
(16)MacetivoransHsp60																100	93	60	49	60	48	48	48	48	49	59	50	57	58	47	59	49
(17)MmazeiAlpha																	100	61	50	59	49	49	49	49	50	60	50	57	60	47	59	50
(18)MthermautotrophicusChp																		100	53	69	52	52	52	53	52	62	54	60	61	50	59	52
(19)StokodaiiBeta																			100	54	90	86	87	66	65	46	59	44	46	52	46	44
(20)MjannaschiiThs																				100	52	52	52	54	54	60	54	56	59	50	56	50
(21)SacidocaldariusBeta																					100	85	86	65	64	46	58	46	47	52	47	43
(22)SsolfataricusBeta																						100	97	66	64	46	60	44	46	52	46	43
(23)SshibataeTF55																							100	66	64	46	60	45	46	52	47	43
(24)PoccultumThsB																								100	66	44	62	42	43	53	45	39
(25)ApernixBeta																									100	45	61	44	46	54	46	42
(26)NpharaonisAlpha																										100	49	79	81	43	78	56
(27)Paerophilum																											100	48	48	51	48	43
(28)HsalinarumAlpha																												100	78	43	79	53
(29)HmarismortuiAlpha																													100	44	79	57
(30) StokodaiiAlpha																														100	44	40
(31)HvolcaniiThsSubunit1																															100	55
(32)HsalinarumThsSubunit2																																100

Table 3.12: Scores of multiple sequence alignment of *T. volcanium* Hsp60 β subunit protein with several eukaryal Hsp60 proteins and bacterial GroEL proteins.

Chaperonin source	Percent identity with chaperonin subunits from																			
	1	33	34	35	36	37	38	39	40	41	42	43	44	45	46	47	48	49	50	51
(1)TvolcaniumBeta	100	38	37	38	37	37	36	36	36	38	36	23	22	21	22	22	21	21	21	20
(33)NcrassaTCP1gamma		100	63	62	62	83	63	63	63	31	60	19	18	17	20	19	18	16	17	18
(34)DrerioTCP1gamma			100	69	85	63	83	83	83	30	70	15	16	16	17	16	18	13	16	15
(35)AmelliferaTCP1gamma				100	72	62	70	71	71	33	76	21	20	17	19	19	20	20	18	19
(36)XlaevisTCP1gamma					100	63	85	86	86	32	69	18	17	16	17	16	19	14	16	16
(37)AclavatusTCP1gamma						100	63	64	64	30	61	19	19	18	20	18	19	15	16	17
(38)MmusculusChaperoninGamma							100	98	96	31	68	17	18	18	17	18	19	16	16	18
(39)RnorvegicusChaperoninGamma								100	97	32	69	17	18	19	17	18	19	13	16	16
(40)HsapiensTCP1gamma									100	31	69	16	16	18	17	16	19	14	15	16
(41)CelegansTCP1member										100	31	15	15	17	18	15	17	19	17	16
(42)DmelanogaterCCTgamma											100	16	16	18	18	17	18	17	15	17
(43)LlactisGroEL												100	82	71	80	80	72	61	64	72
(44)SagalactiaeGroEL													100	75	80	90	75	62	65	74
(45)BlicheniformisGroEL														100	77	73	95	64	70	87
(46)EfaecalisChaperonin60kd															100	81	78	64	66	77
(47)SpyogenesGroEL																100	73	63	64	74
(48)BsubtilisGroEL																	100	64	70	87
(49)TthermophilusGroEL																		100	62	67
(50CtetaniGroEL																			100	71
(51)BcereusGroEL																				100

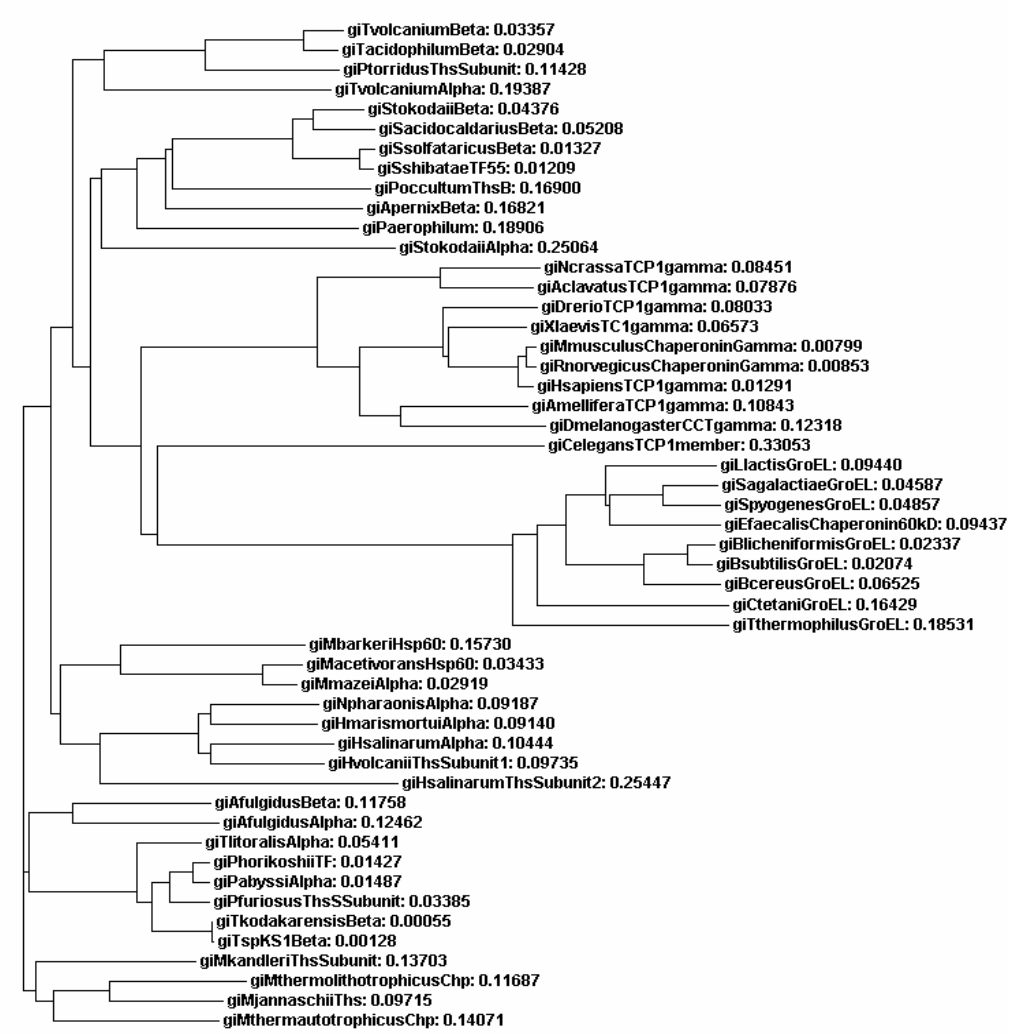

Figure 3.135: Phylogenetic tree constructed by clustal type multiple sequence alignments of amino acid sequence of *T. volcanium* Hsp60 β subunit protein with several eukaryal, archaeal and bacterial Hsp60 proteins.

3.4.4 Sequence Alignments of *T. volcanium* Hsp60 β Subunit With Several Archaeal Hsp60 Proteins

Multiple sequence alignments of amino acid sequence of *T. volcanium* Hsp60 β subunit protein with several archaeal Hsp60 proteins were performed by using Clustal W 1.83 as described in 2.6 Section (Figure 3.136). The archaeal Hsp60 subunit proteins are the same proteins used in 3.4.3 Section. Scores of this alignment is given in Table 3.11 Hsp60 subunit proteins used in multiple sequence alignment are abbreviated in score table and phylogenetic tree in order to make evaluation easier (Table 3.11 and Figure 3.137). Sequence identities were same as mentioned in Section 3.4.2.

```
giBAB59649     ----------------------------MIAGQ-PIFILKEGTKRESGKDAMKENIEAA 30
giP48425       ----------------------------MIAGQ-PIFILKEGTKRESGKDAMKENIEAA 30
giYP_023973    ----------------------------MIGGQ-PIFILKEGTKRESGRDAMQDNIEAA 30
giBAB60294     ------------------------MIRNMMTGQVPILVLKEGTQREQGKNAQRNNIEAA 35
giNP_376188    ----------MLSAVEKMSTTATVATTPEGIPVIILKEGSSRTYGKEALRINIAAV 46
giAAY80050     --------------------MSATATVATTPEGIPVIILKEGSSRTYGKEALRINIAAV 39
giNP_341830    ------------------MRKMATATVATTPEGIPVIILKEGSSRTYGKEALRANIAAV 41
giCAA45326     ----------------------MATATVATTPEGIPVIILKEGSSRTYGKEALRANIAAV 38
giCAA07096     ----------MARGGTMSAPARAVTVEPTGVPVLILKEGTQRTYGREALRANIMIV 46
giNP_148364    --------------------MAIQQQPMTEPVGIPVIILKEGTQRSYGREALRANIMAV 39
giAAL63957     ----------------------MSQAVLTQIGGVPVLVLKEGTQRAFGKEALRLNIMIA 37
giO24734       ------------------------------MANAPVLLLKEGTQRSSGRDALKNNILAA 29
giBAA33889     ------------------------------MAANQPVVVLPENVKRFMGRDAQRMNILAG 30
giAAB99002     ------------------------------MAMAGAPIVVLPQNVKRYVGRDAQRMNILAG 31
giNP_275933    ------------------------------MAQGQQPILVLPEGTSRYLGRDAQRMNILAG 31
giP50016       --------------------------MAMLAGDGRQVLILPEGYQRFVGRDAQRMNIMAA 34
giBAA29085     ----------------------------MAQLAGQPILILPEGTQRYVGRDAQRMNILAA 32
giNP_125709    ----------------------------MAQLAGQPILILPEGTQRYVGRDAQRMNILAA 32
giAAL82098     ----------------------------MAQLAGQPILILPEGTQRYVGRDAQRMNILAA 32
giQ52500       ----------------------------MAQLAGQPVVILPEGTQRYVGRDAQRLNILAA 32
giO24730       ----------------------------MAQLAGQPVVILPEGTQRYVGRDAQRLNILAA 32
giAAP37564     ----------------------------MAQLAGQPILILPEGTQRYVGKDAQRLNILAA 32
giNP_070280    ----------------------------MATLQGQPVLILREGTQRTVGRDAQRMNIMAA 32
giO28045       ----------------------------MATLQGTPVLILKEGTQRTVGRDAQRMNIMAA 32
giNP_615060    ------------------------------MAGQPIFILKEGSKRTRGRDAQSNNIMAA 29
giNP_633403    ------------------------------MAGQPIFILKEGSKRTRGRDAQSNNIMAA 29
giAAZ70052     ------------------------------MAAQPIFILREGSKRTHGSDAQHNNIMAA 29
giCAI48595     --------------------------MAQQMGN-QPMIVLSEESQRTSGQDAQSMNITAG 33
giYP_137342    MACNRAIHRRSPWLLYRSTFNHRLTMAQQQMGN-QPMIVLSEESQRTSGKDAQSMNITAG 59
giQ9HN70       --------------------------MAQQMGN-QPLIVLSEDSQRTSGEDAQSMNITAG 33
giO30561       --------------------------MSQRMQQGQPMIILGEDSQRTSGQDAQSMNITAG 34
giYP_001689883-------------------------MAQQQRMQGQPMIIMGDDAQRVKDRDAQEHNISAA 35
                                                :.:: :  .*  . :*   **
```

Figure 3.136: Clustal type multiple sequence alignments of amino acid sequence of *T. volcanium* Hsp60 β subunit protein with several archaeal Hsp60 proteins.

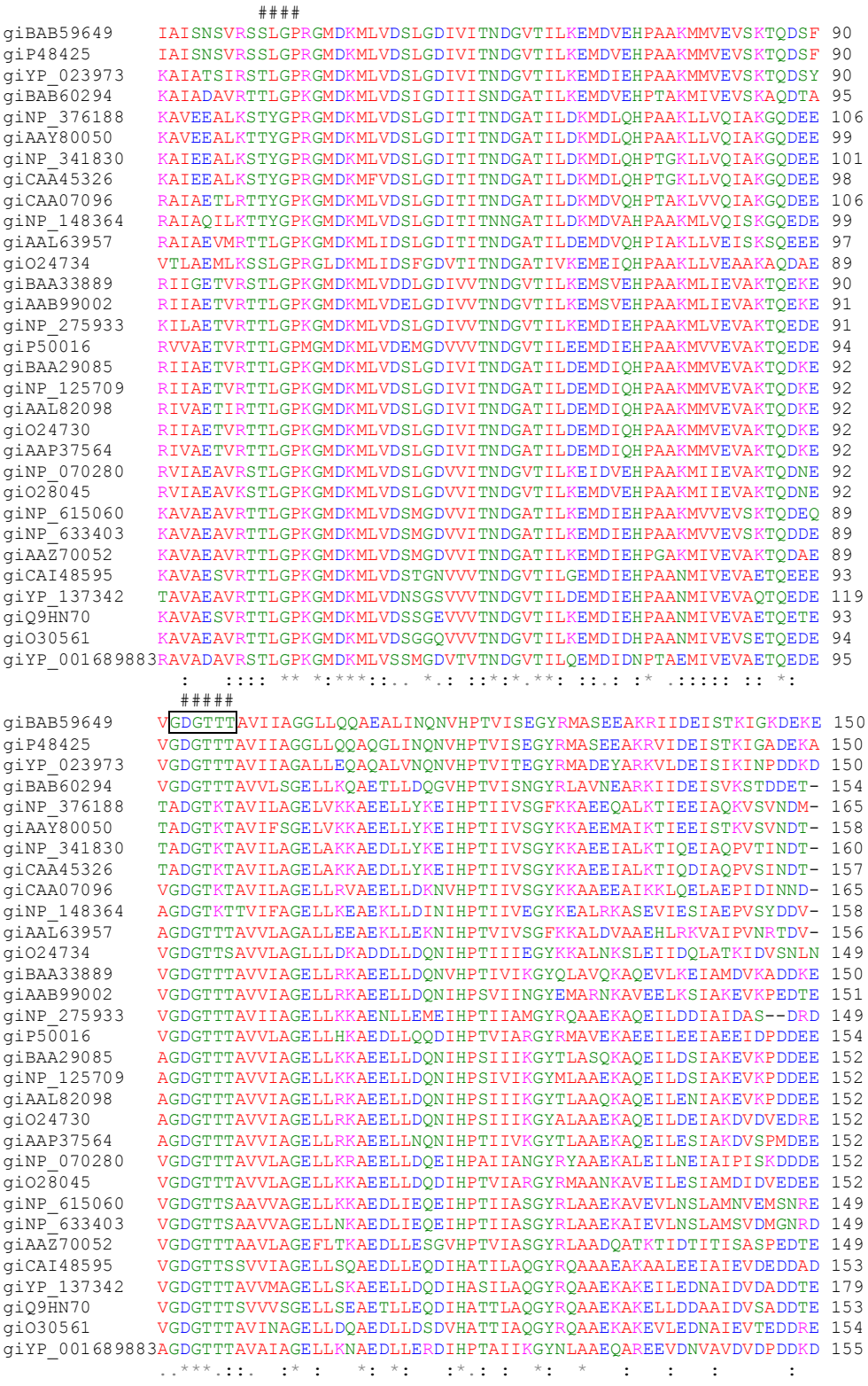
giBAB59649 IAISNSVRSSLGPRGMDKMLVDSLGDIVITNDGVTILKEMDVEHPAAKMMVEVSKTQDSF 90
giP48425 IAISNSVRSSLGPRGMDKMLVDSLGDIVITNDGVTILKEMDVEHPAAKMMVEVSKTQDSF 90
giYP_023973 KAIATSIRSTLGPRGMDKMLVDSLGDIVITNDGVTILKEMDIEHPAAKMMVEVSKTQDSY 90
giBAB60294 KAIADAVRTTLGPKGMDKMLVDSIGDIIISNDGATILKEMDVEHPTAKMIVEVSKAQDTA 95
giNP_376188 KAVEEALKSTYGPRGMDKMLVDSLGDITITNDGATILDKMDLQHPAAKLLVQIAKGQDEE 106
giAAY80050 KAVEEALKTTYGPRGMDKMLVDSLGDITITNDGATILDKMDLQHPAAKLLVQIAKGQDEE 99
giNP_341830 KAIEEALKSTYGPRGMDKMLVDSLGDITITNDGATILDKMDLQHPTGKLLVQIAKGQDEE 101
giCAA45326 KAIEEALKSTYGPRGMDKMFVDSLGDITITNDGATILDKMDLQHPTGKLLVQIAKGQDEE 98
giCAA07096 RAIAETLRTTYGPKGMDKMLVDSLGDITITNDGATILDKMDVQHPTAKLVVQIAKGQDEE 106
giNP_148364 RAIAQILKTTYGPKGMDKMLVDSLGDITITNNGATILDKMDVAHPAAKMLVQISKGQEDE 99
giAAL63957 RAIAEVMRTTLGPKGMDKMLIDSLGDITITNDGATILDEMDVQHPIAKLLVEISKSQEEE 97
giO24734 VTLAEMLKSSLGPRGLDKMLIDSFGDVTITNDGATIVKEMEIQHPAAKLLVEAAKAQDAE 89
giBAA33889 RIIGETVRSTLGPKGMDKMLVDDLGDIVVTNDGVTILKEMSVEHPAAKMLIEVAKTQEKE 90
giAAB99002 RIIAETVRTTLGPKGMDKMLVDELGDIVVTNDGVTILKEMSVEHPAAKMLIEVAKTQEKE 91
giNP_275933 KILAETVRTTLGPKGMDKMLVDSLGDIVVTNDGVTILKEMDIEHPAAKMLVEVAKTQEDE 91
giP50016 RVVAETVRTTLGPMGMDKMLVDEMGDVVVTNDGVTILEEMDIEHPAAKMVVEVAKTQEDE 94
giBAA29085 RIIAETVRTTLGPKGMDKMLVDSLGDIVITNDGATILDEMDIQHPAAKMMVEVAKTQDKE 92
giNP_125709 RIIAETVRTTLGPKGMDKMLVDSLGDIVITNDGATILDEMDIQHPAAKMMVEVAKTQDKE 92
giAAL82098 RIVAETIRTTLGPKGMDKMLVDSLGDIVITNDGATILDEMDIQHPAAKMMVEVAKTQDKE 92
giO24730 RIIAETVRTTLGPKGMDKMLVDSLGDIVITNDGATILDEMDIQHPAAKMMVEVAKTQDKE 92
giAAP37564 RIVAETVRTTLGPKGMDKMLVDSLGDIVITNDGATILDEMDIQHPAAKMMVEVAKTQDKE 92
giNP_070280 RVIAEAVRSTLGPKGMDKMLVDSLGDVVITNDGVTILKEIDVEHPAAKMIIEVAKTQDNE 92
giO28045 RVIAEAVKSTLGPKGMDKMLVDSLGDVVITNDGVTILKEMDVEHPAAKMIIEVAKTQDNE 92
giNP_615060 KAVAEAVRTTLGPKGMDKMLVDSMGDVVITNDGATILKEMDIEHPAAKMVVEVSKTQDEQ 89
giNP_633403 KAVAEAVRTTLGPKGMDKMLVDSMGDVVITNDGATILKEMDIEHPAAKMVVEVSKTQDDE 89
giAAZ70052 KAVAEAVRTTLGPKGMDKMLVDSMGDVVITNDGATILKEMDIEHPGAKMIVEVAKTQDAE 89
giCAI48595 KAVAESVRTTLGPKGMDKMLVDSTGNVVVTNDGVTILGEMDIEHPAANMIVEVAETQEEE 93
giYP_137342 TAVAEAVRTTLGPKGMDKMLVDNSGSVVVTNDGVTILDEMDIEHPAANMIVEVAQTQEDE 119
giQ9HN70 KAVAESVRTTLGPKGMDKMLVDSSGEVVVTNDGVTILKEMDIEHPAANMIVEVAETQETE 93
giO30561 KAVAEAVRTTLGPKGMDKMLVDSGGQVVVTNDGVTILKEMDIDHPAANMIVEVSETQEDE 94
giYP_001689883 RAVADAVRSTLGPKGMDKMLVSSMGDVTVTNDGVTILQEMDIDNPTAEMIVEVAETQEDE 95
giBAB59649 VGDGTTTAVIIAGGLLQQAEALINQNVHPTVISEGYRMASEEAKRIIDEISTKIGKDEKE 150
giP48425 VGDGTTTAVIIAGGLLQQAQGLINQNVHPTVISEGYRMASEEAKRVIDEISTKIGADEKA 150
giYP_023973 VGDGTTTAVIIAGALLEQAQALVNQNVHPTVITEGYRMADEYARKVLDEISIKINPDDKD 150
giBAB60294 VGDGTTTAVVLSGELLKQAETLLDQGVHPTVISNGYRLAVNEARKIIDEISVKSTDDET- 154
giNP_376188 TADGTKTAVILAGELVKKAEELLYKEIHPTIIVSGFKKAEEQALKTIEEIAQKVSVNDM- 165
giAAY80050 TADGTKTAVIFSGELVKKAEELLYKEIHPTIIVSGYKKAEEMAIKTIEEISTKVSVNDT- 158
giNP_341830 TADGTKTAVILAGELAKKAEDLLYKEIHPTIIVSGYKKAEEIALKTIQEIAQPVTINDT- 160
giCAA45326 TADGTKTAVILAGELAKKAEDLLYKEIHPTIIVSGYKKAEEIALKTIQDIAQPVSINDT- 157
giCAA07096 VGDGTKTAVILAGELLRVAEELLDKNVHPTIIVSGYKKAAEEAIKKLQELAEPIDINND- 165
giNP_148364 AGDGTKTTVIFAGELLKEAEKLLDINIHPTIIVEGYKEALRKASEVIESIAEPVSYDDV- 158
giAAL63957 AGDGTTTAVVLAGALLEEAEKLLEKNIHPTVIVSGFKKALDVAAEHLRKVAIPVNRTDV- 156
giO24734 VGDGTTSAVVLAGLLLDKADDLLDQNIHPTIIIEGYKKALNKSLEIIDQLATKIDVSNLN 149
giBAA33889 VGDGTTTAVVIAGELLRKAEELLDQNVHPTIVIKGYQLAVQKAQEVLKEIAMDVKADDKE 150
giAAB99002 VGDGTTTAVVIAGELLRKAEELLDQNIHPSVIINGYEMARNKAVEELKSIAKEVKPEDTE 151
giNP_275933 VGDGTTTAVIIAGELLKKAENLLEMEIHPTIIAMGYRQAAEKAQEILDDIAIDAS--DRD 149
giP50016 VGDGTTTAVVLAGELLHKAEDLLQQDIHPTVIARGYRMAVEKAEEILEEIAEEIDPDDEE 154
giBAA29085 AGDGTTTAVVIAGELLKKAEELLDQNIHPSIIIKGYTLASQKAQEILDSIAKEVKPDDEE 152
giNP_125709 AGDGTTTAVVIAGELLKKAEELLDQNIHPSIVIKGYMLAAEKAQEILDSIAKEVKPDDEE 152
giAAL82098 AGDGTTTAVVIAGELLRKAEELLDQNIHPSIIIKGYTLAAQKAQEILENIAKEVKPDDEE 152
giO24730 AGDGTTTAVVIAGELLRKAEELLDQNIHPSIIIKGYALAAEKAQEILDEIAKDVDVEDRE 152
giAAP37564 AGDGTTTAVVIAGELLRKAEELLNQNIHPTIIVKGYTLAAEKAQEILESIAKDVSPMDEE 152
giNP_070280 VGDGTTTAVVLAGELLKRAEELLDQEIHPAIIANGYRYAAEKALEILNEIAIPISKDDDE 152
giO28045 VGDGTTTAVVLAGELLKKAEELLDQDIHPTVIARGYRMAANKAVEILESIAMDIDVEDEE 152
giNP_615060 VGDGTTSAAVVAGELLKKAEDLIEQEIHPTIIASGYRLAAEKAVEVLNSLAMNVEMSNRE 149
giNP_633403 VGDGTTSAAVVAGELLNKAEDLIEQEIHPTIIASGYRLAAEKAIEVLNSLAMSVDMGNRD 149
giAAZ70052 VGDGTTTAAVLAGEFLTKAEDLLESGVHPTVIASGYRLAADQATKTIDTITISASPEDTE 149
giCAI48595 VGDGTTSSVVIAGELLSQAEDLLEQDIHATILAQGYRQAAAEAKAALEEIAIEVDEDDAD 153
giYP_137342 VGDGTTTAVVMAGELLSKAEELLDQDIHASILAQGYRQAAEKAKEILEDNAIDVDADDTE 179
giQ9HN70 VGDGTTTSVVVSGELLSEAETLLEQDIHATTLAQGYRQAAEKAKELLDDAAIDVSADDTE 153
giO30561 VGDGTTTAVINAGELLDQAEDLLDSDVHATTIAQGYRQAAEKAKEVLEDNAIEVTEDDRE 154
giYP_001689883 AGDGTTTAVAIAGELLKNAEDLLERDIHPTAIIKGYNLAAEQAREEVDNVAVDVDPDDKD 155

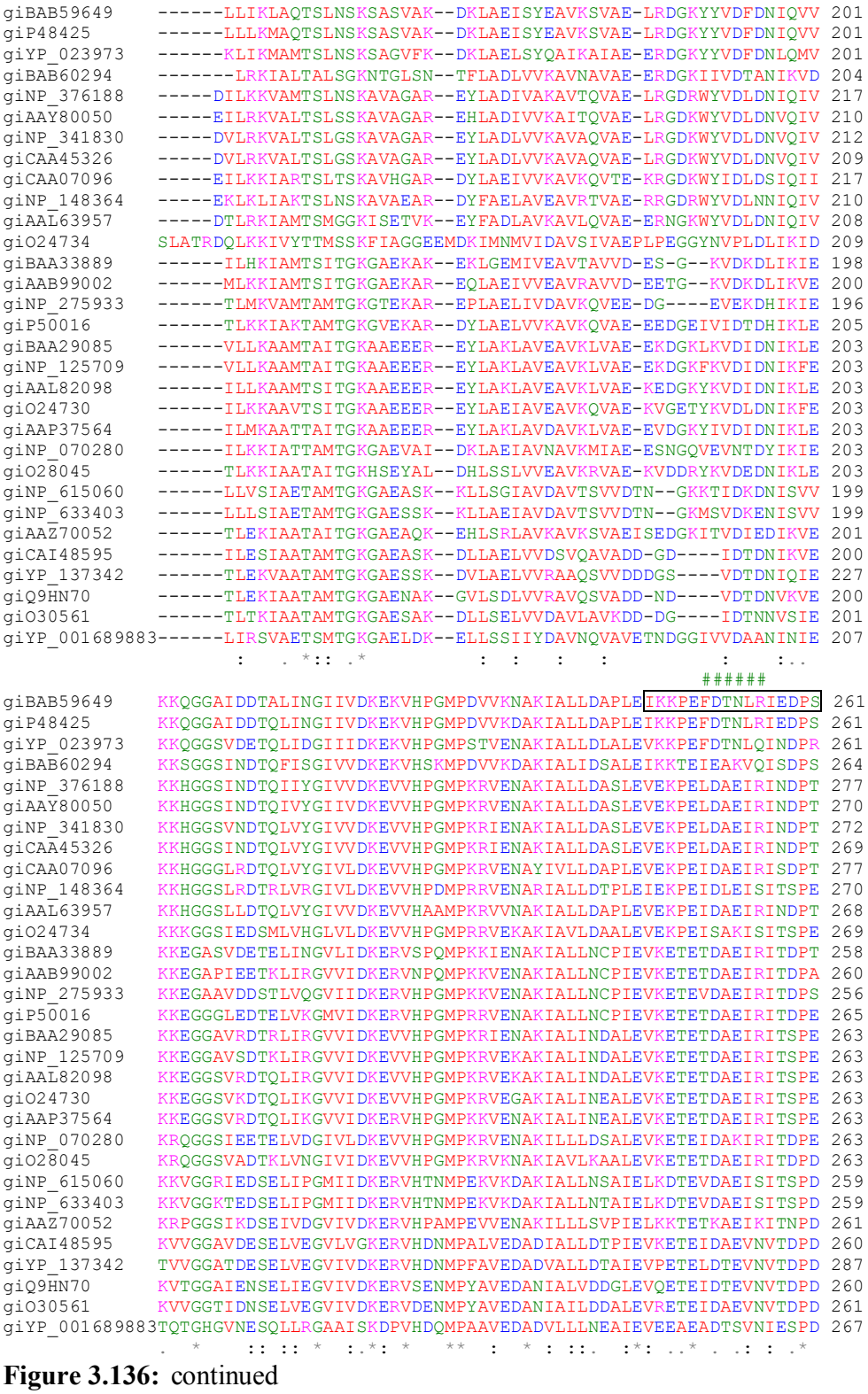

Figure 3.136: continued

```
giBAB59649      MIQKFLAQEENMLREMVEKIKSVGAN--------------VVITQKGIDDMAQHYLSKEG 307
giP48425        MIQKFLAQEENMLREMVDKIKSVGAN--------------VVITQKGIDDMAQHYLSRAG 307
giYP_023973     MIQKFLDQEEGILKEMVDKIQKTGAN--------------VVITQKGIDDMAQHYLAKAG 307
giBAB60294      KIQDFLNQETSTFKEMVEKIKKSGAN--------------VVLCQKGIDDVAQHYLAKEG 310
giNP_376188     QMKKFLEEEENLLKEKVDKIAATGAN--------------VVICQKGIDEVAQHYLAKKG 323
giAAY80050      QMKKFLDEEENILKEKVDKIAQTGAN--------------VVICQKGIDEVAQHYLAKKG 316
giNP_341830     QMHKFLEEEENILKEKVDKIAATGAN--------------VVICQKGIDEVAQHYLAKKG 318
giCAA45326      QMHKFLEEEENILKEKVDKIAATGAN--------------VVICQKGIDEVAQHYLAKKG 315
giCAA07096      YLKKFLEEEERILEDMVEKIYNVAVERMKRDGMEPGKAGIVVITQKGIDEVAQHFLAKKG 337
giNP_148364     QIKALYEKQERILQEKIEKIAATGAN--------------VVITQKGIDDVAQHFLAKKG 316
giAAL63957      QMRAFLEEEERILRGYVDKLKSLGVT--------------VLFTTKGIDDIAQYYLAKAG 314
giO24734        QIKAFLDEEAKYLKDMVDKLASIGAN--------------VVICQKGIDDVAQHFLAKKG 315
giBAA33889      KLMEFIEQEEKMLKDMVDTIKASGAN--------------VLFCQKGIDDLAQHYLAKEG 304
giAAB99002      KLMEFIEQEEKMIKDMVEKIAATGAN--------------VVFCQKGIDDLAQHYLAKKG 306
giNP_275933     QMQAFIEQEEQMIRDMVNSIVDTGAN--------------VLFCQKGIDDLAQHYLAKAG 302
giP50016        QLQAFIEEEERMLSEMVDKIAETGAN--------------VVFCQKGIDDLAQHYLAKKG 311
giBAA29085      QLQAFLEQEEKMLKEMVDKIKEVGAN--------------VVFVQKGIDDLAQHYLAKYG 309
giNP_125709     QLQAFLEQEEKMLKEMVDKIKEVGAN--------------VVFVQKGIDDLAQHYLAKYG 309
giAAL82098      QLQAFLEQEERMLREMVEKIKEVGAN--------------VVFVQKGIDDLAQHYLAKYG 309
giQ52500        QLQAFLEQEEKMLREMVDKIKEVGAN--------------VVFVQKGIDDLAQHYLAKYG 309
giO24730        QLQAFLEQEEKMLREMVDKIKEVGAN--------------VVFVQKGIDDLAQHYLAKYG 309
giAAP37564      QLQAFLEQEEKMIKEMVDKIVATGAN--------------VVFCQKGIDDLAQHYLAKAG 309
giNP_070280     KLQKFIEQEEAMLKEMVDKIVNAGAN--------------VVFCQKGIDDLAQYYLAKAG 309
giO28045        QLMKFIEQEEKMLKEMVDRLAEAGAN--------------VVFCQKGIDDLAQYYLAKAG 309
giNP_615060     QLQSFLDQEEAMLKKIVQKVISSGAN--------------VVFCQKGVEDLAQHYLAKAG 305
giNP_633403     QLQSFLDQEEQMLKKIVQKVINSGAN--------------VVFCQKGVEDLAQHYLAKAG 305
giAAZ70052      QMQLFLDQEEAMLKEIVDKVIKTGAN--------------VVFCQKGIDDLAQYYMTKAG 307
giCAI48595      QLEQFLEQEEKQLREMVDQLADAGAD--------------VVFCQKGIDDMAQHYLAQEG 306
giYP_137342     QLQQFLDQEEEQLKEMVDQLAEAGAD--------------VVFCQKGIDDMAQHYLAQEG 333
giQ9HN70        QLQNFLDQEEEQLKEMVDALKDAGAN--------------VVFADSGIDDMAQHYLAKEG 306
giO30561        QLQQFLDQEEKQLKEMVDQLVEVGAD--------------AVFVGDGIDDMAQHYLAKEG 307
giYP_001689883QLQSFLDQEEKQLKEKVQQIADTGAN--------------VVFCQKGIDDMAQHYLAKEG 313
                 :  :  ::   :   :: :   ..               .::  .*::::**::::: *

giBAB59649      IYAVRRVKKSDMDKLAKATGATVVSTIDEISASDLGSADRVEQVKVGDDYMTFVTG-CKN 366
giP48425        IYAVRRVKKSDMDKLAKATGASIVSTIDEISSSDLGTAERVEQVKVGEDYMTFVTG-CKN 366
giYP_023973     IYAVRRVKKSDVDKLAKATGAAIVSSLDEMTEADLGKADKVEQVKIGDDYMTFVTG-AKN 366
giBAB60294      IYAVRRVKKSDMEKLAKATGAKIVTDLDDLTPSVLGEAEKVEERKIGDDRMTFVTG-CKN 369
giNP_376188     ILAVRRAKKSDLEKLARATGGRVVSNIDELTPQDLGYAALVEERKVGEDKMVFVEG-AKN 382
giAAY80050      ILAVRRAKKSDLEKLARATGGRVVSNIDELTSQDLGYATLVEERKIGEDKMVFIEG-AKN 375
giNP_341830     ILAVRRAKKSDLEKLARATGGRVISNIDELTSQDLGYAALVEERKVGEDKMVFVEG-AKN 377
giCAA45326      ILAVRRAKKSDLEKLARATGGRVISNIDELTSQDLGYAALVEERKVGEDKMVFVEG-AKN 374
giCAA07096      IMAVRRVKRSDIEKISKATGAKIVSNIEDLTPEDLGFAKLVEERKVGENKMVFIEG-CPN 396
giNP_148364     ILAVRRVKRSDIEKIARATGARIVTDIEDLRPEDLGYAELVEERKVGEDKMVFIEG-AKN 375
giAAL63957      ILAVRRVKRSDIEKLVRATGARLVTSIEDLTEADLGFAGLVEERRVGDEKMVFVEQ-CKN 373
giO24734        ILAVRRVKRSDIEKLEKALGARIISSIKDATPEDLGYAELVEERRVGNDKMVFIEG-AKN 374
giBAA33889      ILAVRRVKKSDMEKLSKATGANVVTNIKDLKAEDLGEAGIVEERKIAGDAMIFVEE-CKH 363
giAAB99002      ILAVRRVKKSDMEKLAKATGARIVTKIDDLTPEDLGEAGLVEERKVAGDAMIFVEQ-CKH 365
giNP_275933     VLAVRRVKKSDMEKLSKATGANIVTNIEDLSPEDLGEAGVVSEKKISGEEMIFVEE-CKE 361
giP50016        ILAVRRVKKSDMQKLARATGARIVTNIDDLSEEDLGEAEVVEEKKVAGDKMIFVEG-CKD 370
giBAA29085      ILAVRRVKKSDMEKLAKATGAKIVTNIRDLTPEDLGEAELVEERKVAGENMIFVEG-CKN 368
giNP_125709     ILAVRRVKKSDMEKLAKATGAKIVTNIRDLTPEDLGEAELVEERKVAGENMIFVEG-CKN 368
giAAL82098      IMAVRRVKKSDMEKLAKATGAKIVTNIRDLTPEDLGYAELVEERKVAGESMIFVEG-CQN 368
giQ52500        IMAVRRVKKSDMEKLAKATGAKIVTNVRDLTPEDLGEAELVEQRKVAGENMIFVEG-CKN 368
giO24730        IMAVRRVKKSDMEKLAKATGAKIVTNVRDLTPEDLGEAELVEQRKVAGENMIFVEG-CKN 368
giAAP37564      ILAVRRVKKSDMEKLAKATGAKIVTNVRDLTPDDLGYAELVEERKVAGENMVFVEG-CKN 368
giNP_070280     VLAVRRVKKSDMEKLAKATGAKVLTDLRDISSEDLGEAALVEERKVGDEKMVFVTG-CKN 368
giO28045        ILAVRRVKQSDIEKIAKACGAKIITDLREITSADLGEAELVEERKVGDEKMVFIEG-CKN 368
giNP_615060     IFAIRRVKKSDMEKLARATGGKLITNLDEITPEDLGFAKLVEEKKVGGDSMTFVTG-CDN 364
giNP_633403     IFAVRRVKKSDMEKLARATGGKLITNLDEIVPEDLGFAKLVEEKKVGGDSMTFVTG-CDN 364
giAAZ70052      IFGMRRVKKSDMDKLSRATGAKIITSLDEIEESDLGHAGLVEEKDVTGSRMTFVTG-CKD 366
giCAI48595      ILAVRRAKKSDMKALARATGGRVVSNIDDITADDLGFAGSVSQKPIAGDEKIFVED-VDE 365
giYP_137342     ILAVRRAKKSDIEALSRSTGARIISNIDDIEADDLGFAGSVAQKDIAGDERIFVED-VED 392
giQ9HN70        ILAVRRAKSDDFTRLSRATGATPVSNVNDIEAADLGAAGSVAQKDIGGDERIFVED-VEE 365
giO30561        ILAVRRAKSSDLKRLARATGGRVVSSLDDIEADDLGFAGSVGQKDVGGDERIFVED-VED 366
giYP_001689883ILAVRRTKKSDIEFLTNVLDASVVTDLDAASEADV-VAGSVTRD--SDDELFYVEGESEQ 370
               : .:**.* .*.  : .  ..  :: :       :  *  * .     .   ::     .
```

```
giBAB59649      PKAVSVLVRGETEHVVDEMERSITDSLHVVASALEDGAYTAGGGATAAEIAVRLRSYAQK 426
giP48425        PKAVSILVRGETEHVVDEMERSITDSLHVVASALEDGAYAAGGGATAAEIAFRLRSYAQK 426
giYP_023973     PKAVSILIRGETDHVVDEIERSITDSLHVVAAAVEDAAYVTGGGSAAEEIAFRLRTYASK 426
giBAB60294      PKAVSILIRGGTEHVVSEVERALNDAIRVVAITKEDGKFLWGGGAVEAELAMRLAKYANS 429
giNP_376188     PKAVSILIRGGLERVVDETERALRDALGTVADVIRDGRAVAGGGAVELEIAKRLRKYAPQ 442
giAAY80050      PKAVSILIRGGLERVVDETERALRDALGTVADVVRDGRAIAGGGAVETEIAKRLRKYAPQ 435
giNP_341830     PKSVSILIRGGLERVVDETERALRDALGTVADVIRDGRAVAGGGAVEIEIAKRLRKYAPQ 437
giCAA45326      PKSVSILIRGGLERVVDETERALRDALGTVADVIRDGRAVAGGGAVEIEIAKRLRKYAPQ 434
giCAA07096      PKAVTIVIRGGLERLVDEAERSIQDAMHAVADAIRDGKIFAGGGAVEVELSKYLREIAPK 456
giNP_148364     PKSVTILLRGGFERLVDEAERSLHDALSVVADAIMDGKIVAGGGAVEAEVAKVLYEYASK 435
giAAL63957      PKAVSILVRGGFERLVDEAERNLDDALSVVSDVVEDPYILPAGGAAEIEAAKAVRAFAPK 433
giO24734        PKAVNILLRGSNDMALDEAERSINDALHSLRNVLMKPMIVAGGGAVETELALRLREYARS 434
giBAA33889      PKAVTMLIRGTTEHVIEEVARAVDDAIGVVACTIEDGKIVAGGGAAEIELAMKLRDYAEG 423
giAAB99002      PKAVTILARGSTEHVVEEVARAIDDAIGVVKCALEEGKIVAGGGATEIELAKRLRKFAES 425
giNP_275933     PKAVTILVRGSTEHVVSEVERAIEDAIGVVAATVEDGKVVAGGGAPEIEIAKRLKDYADS 421
giP50016        PKAVTILIRGGTEHVVDEAERAIEDAIGVVAAALEDGKVVAGGGAPEVEVARQLRDFADG 430
giBAA29085      PKAVTILIRGGTEHVVDEVERALEDAIKVVKDILEDGKIIAGGGASEIELSIKLDEYAKE 428
giNP_125709     PKAVTILIRGGTEHVVDEVERALEDAVKVVKDILEDGKIIAGGGAAEIELSIKLDEYAKE 428
giAAL82098      PKAVTILIRGGTEHVVDEVERALEDAIKVVKDILEDGKILAGGGAPEIELAIRLDEYAKE 428
giO24730        PKAVTILIRGGTEHVVDEVERALEDAVKVVKDIVEDGKIVAAGGAPEIELSIRLDEYAKE 428
giAAP37564      PKAVTILIRGGTEHVVDEVERALEDAIKVVKDIVEDGKIVAGGGASEIELAIRLDEYAKE 428
giNP_070280     PKAVTILVRGGTEHVVEEIARGIEDAVRAVACAVEDGKVVVGAGAPEIEVSLKLREWAPS 428
giO28045        PKAVTILIRGGSEHVVDEVERSLQDAIKVVKTALESGKVVAGGGAPEIEVALKIRDWAPT 428
giNP_615060     PKAVTILLRGGTEHVVDSVDSALEDALRVVGVAIEDEKLVSGGGSPEVEVALRLQEYAAT 424
giNP_633403     PKAVTILLRGGTEHVVDSIDSALEDALRVVGVAIEDEKLVAGGGSPEVEVALRLQEYAAT 424
giAAZ70052      SKATSILLRGGTEHVVEGIERALEDALRVVGVALEDQKIVVGGGSPEIELSLRLKEYAAT 426
giCAI48595      AKAVTLILRGGTEHVVDEIERAIEDSLGVVQTTLEDGQVLPGGGAPEIALALALRDFADS 425
giYP_137342     ARAVTMILRGGTEHVVDEVERAIEDSLGVVAATLEDGKVLPGGGAPETQLALGLRDHADS 452
giQ9HN70        AKSVTLILRGGTEHVVDEVERAIEDSLGVVRVTLEDGQVMPGGGAPETELAMQLRDFADS 425
giO30561        AKSVTLILRGGTEHVVDELERAIEDSLGVVRTTLEDGKVLPGGGAPETELSLQLREFADS 426
giYP_001689883AHGVTLLLRGSTDHVVDELERGVSDALDVSAQTLSDGRVLPGGGATEVEVASRLRDFADS 430
               .:...:: **  :  :.     : *::        .     ..*:     :  :   *
                                              # ##   #
giBAB59649      IGGRQQLAIEKFADAIEEVPRALAENAGLDPIDIILKLRAEHAKG-NKYAGVNVFSGEIE 485
giP48425        IGGRQQLAIEKFADAIEEIPRALAENAGLDPIDILLKLRAEHAKG-NKTYGINVFTGEIE 485
giYP_023973     VGGRQQLAIERFADALEEIPRALAENAGLDPIDILIKIRSEHAAG-HTKYGLNVFTGEVE 485
giBAB60294      VGGREQLAIEAFAKALEIIPRTLAENAGIDPINTLIKLKSEHEKG-KISMGVDLDSNGAG 488
giNP_376188     IGGKEQLAIEAYASALENLVMILIENGGYDPIDLLVKLRSAHENEANKWYGINVFTGQVE 502
giAAY80050      VGGKEQLAIEAYANALESLVMILIENGGFDPIELLVKLRSAHENETNKWHGINVYTGQIQ 495
giNP_341830     VGGKEQLAIEAYANAIEGLIMILAENAGLDPIDKLMQLRSLHENETNKWYGLNLFTGNPE 497
giCAA45326      VGGKEQLAIEAYANAIEGLIMILAENAGLDPIDKLMQLRSLHENETNKWYGLNLFTGNPE 494
giCAA07096      IGGKEQLAVEAFARALEGLPMALAENAGLDPVEIMMKLRAAHSKPDGKWYGINVFNGNVE 516
giNP_148364     LPGKTQLAVEAFARAVEALPQALAHNAGHDPIEVLVKLRSAHEKPENKWYGVDLDTGEIV 495
giAAL63957      VGGREQYAVEAFARALEVIPKALAENAGLDPIDILTELTHKHEQTDGWKYGLDVYQGKVV 493
giO24734        VGGKEQLAIEKFAEALEEIPMILAETAGMEPIQTLMDLRAKHAKG-LINAGVDVMNGKIA 493
giBAA33889      VSGREQLAVRAFADALEVVPRTLAENAGLDAIEMLVKLRAKHAEGNNAYYGLNVFTGDVE 483
giAAB99002      VAGREQLAVKAFADALEVIPRTLAENSGLDPIDMLVKLRAAHEKEGGEVYGLDVFEGEVV 485
giNP_275933     ISGREQLAVSAFAEALEIVPKTLAENAGLDSIDVLVDLRAAHEES--TYMGIDVFDGKIV 479
giP50016        VEGREQLAVEAFADALEIIPRTLAENSGLDPIDVLVQLRAKHEDGQ-VTAGIDVYDGDVK 489
giBAA29085      VGGKEQLAIEAFAEALKVIPRTLAENAGLDPIETLVKVIAAHKEKG-QTIGIDVYEGEPA 487
giNP_125709     VGGKEQLAIEAFAEALKVIPRTLAENAGLDPIETLVKVIAAHKEKG-PTIGIDVYEGEPA 487
giAAL82098      VGGKEQLAIEAFAEALKVIPRTLAENAGLDPIETLVKVIAAHKEKG-PTIGVDVYEGEPA 487
giO24730        VGGKEQLAIEAFAEALKVIPRTLAENAGLDPIETLVKVIAAHKEKG-PTIGVDVFEGEPA 487
giAAP37564      VGGKEQLAIEAFADALKVIPRTLAENAGLDPVDVLVKVTAAHKDKG-ATIGVDVFAGEPA 487
giNP_070280     LGGREQLAVEAFATALEIIPRTLAENAGLDPIDVLVELKAAHEKGQ-KYAGVDVDTGKVV 487
giO28045        LGGREQLAAEAFASALEVIPRALAENSGLDPIDILVELRKAHEEGK-TTYGVDVFSGEVA 487
giNP_615060     LEGREQLAVKAYSEALEVIPRTLAENAGLDPIDMLMELRSQHEKGMK-TAGLDVYEGKVV 483
giNP_633403     LEGREQLAVKAYSEALEVIPRTLAENAGLDPIDMLMELRSQHEKGMK-TAGLNVYEGKVV 483
giAAZ70052      LKGREQLAVMKFAESLEIIPSTLAENAGLDPIDMLVEMRSQHEKGNK-RAGLNVYTGKIE 485
giCAI48595      VGGREQLAVEAFADAVDVIPRTLAENAGLDPIDSLVDLRSQHAEGDD-AAGLDAYTGDVI 484
giYP_137342     VGGREQLAVEAFADAIDVIPRTLAENAGLDPIDSLVDLRSKHDGGAV-TSGLDAYTGEVV 511
giQ9HN70        VGGREQLAVEAFADALEVIPRTLAENAGHDPIDSLVDLRSQHDGGDT-EAGLDAYNGDVI 484
giO30561        VGGREQLAVEAFAEALDIIPRTLAENAGLDPIDSLVDLRSRHDGGEF-AAGLDAYTGEVI 485
giYP_001689883VSGREQLAVEAFADSLELVPRVLAENAGLDSIDTLVDLRSAHENDDDEHIGLNVLSGDLE 490
               : *: * *   :: ::. :   * ...* :.:: : .:   *        *::   .
```

Figure 3.136: continued

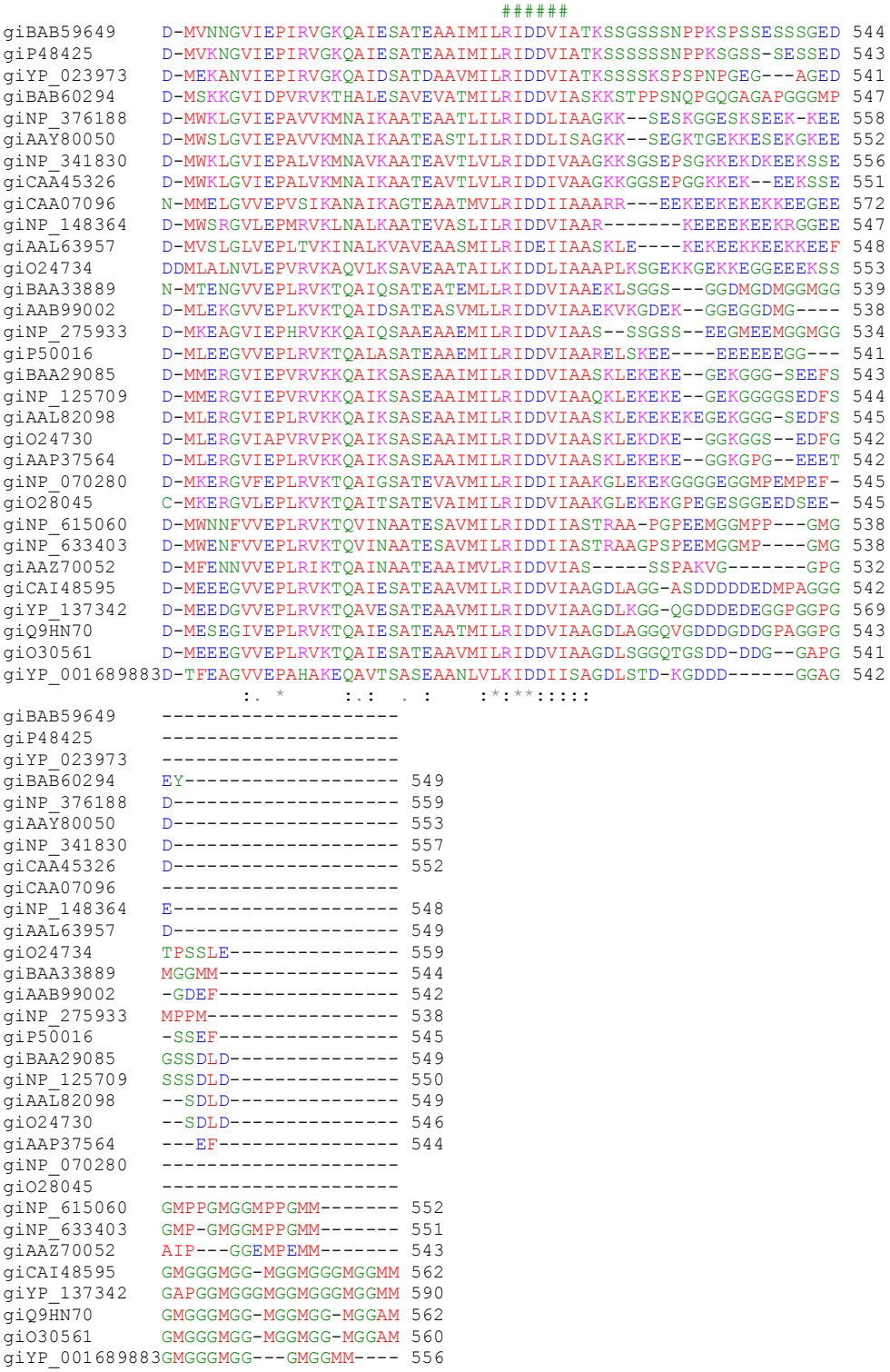
######
giBAB59649 D-MVNNGVIEPIRVGKQAIESATEAAIMILRIDDVIATKSSGSSSNPPKSPSSESSSGED 544
giP48425 D-MVKNGVIEPIRVGKQAIESATEAAIMILRIDDVIATKSSSSSSNPPKSGSS-SESSED 543
giYP_023973 D-MEKANVIEPIRVGKQAIDSATDAAVMILRIDDVIATKSSSSKSPSPNPGEG---AGED 541
giBAB60294 D-MSKKGVIDPVRVKTHALESAVEVATMILRIDDVIASKKSTPPSNQPGQGAGAPGGGMP 547
giNP_376188 D-MWKLGVIEPAVVKMNAIKAATEAATLILRIDDLIAAGKK--SESKGGESKSEEK-KEE 558
giAAY80050 D-MWSLGVIEPAVVKMNAIKAATEASTLILRIDDLISAGKK--SEGKTGEKKESEKGKEE 552
giNP_341830 D-MWKLGVIEPALVKMNAVKAATEAVTLVLRIDDIVAAGKKSGSEPSGKKEKDKEEKSSE 556
giCAA45326 D-MWKLGVIEPALVKMNAIKAATEAVTLVLRIDDIVAAGKKGGSEPGGKKEK--EEKSSE 551
giCAA07096 N-MMELGVVEPVSIKANAIKAGTEAATMVLRIDDIIAAARR---EEKEEKEKEKKEEGEE 572
giNP_148364 D-MWSRGVLEPMRVKLNALKAATEVASLILRIDDVIAAR-------KEEEEKEEKRGGEE 547
giAAL63957 D-MVSLGLVEPLTVKINALKVAVEAASMILRIDEIIAASKLE----KEKEEKKEEKKEEF 548
giO24734 DDMLALNVLEPVRVKAQVLKSAVEAATAILKIDDLIAAAPLKSGEKKGEKKEGGEEEKSS 553
giBAA33889 N-MTENGVVEPLRVKTQAIQSATEATEMLLRIDDVIAAEKLSGGS---GGDMGDMGGMGG 539
giAAB99002 D-MLEKGVVEPLKVKTQAIDSATEASVMLLRIDDVIAAEKVKGDEK--GGEGGDMG---- 538
giNP_275933 D-MKEAGVIEPHRVKKQAIQSAAEAAEMILRIDDVIAAS--SSGSS--EEGMEEMGGMGG 534
giP50016 D-MLEEGVVEPLRVKTQALASATEAAEMILRIDDVIAARELSKEE----EEEEEEGG--- 541
giBAA29085 D-MMERGVIEPVRVKKQAIKSASEAAIMILRIDDVIAASKLEKEKE--GEKGGG-SEEFS 543
giNP_125709 D-MMERGVIEPVRVKKQAIKSASEAAIMILRIDDVIAAQKLEKEKE--GEKGGGGSEDFS 544
giAAL82098 D-MLERGVIEPLRVKKQAIKSASEAAIMILRIDDVIAASKLEKEKEKEGEKGGG-SEDFS 545
giO24730 D-MLERGVIAPVRVPKQAIKSASEAAIMILRIDDVIAASKLEKDKE--GGKGGS--EDFG 542
giAAP37564 D-MLERGVIEPLRVKKQAIKSASEAAIMILRIDDVIAASKLEKEKE--GGKGPG--EEET 542
giNP_070280 D-MKERGVFEPLRVKTQAIGSATEVAVMILRIDDIIAAKGLEKEKGGGGEGGMPEMPEF- 545
giO28045 C-MKERGVLEPLKVKTQAITSATEVAIMILRIDDVIAAKGLEKEKGPEGESGGEEDSEE- 545
giNP_615060 D-MWNNFVVEPLRVKTQVINAATESAVMILRIDDIIASTRAA-PGPEEMGGMPP---GMG 538
giNP_633403 D-MWENFVVEPLRVKTQVINAATESAVMILRIDDIIASTRAAGPSPEEMGGMP----GMG 538
giAAZ70052 D-MFENNVVEPLRIKTQAINAATEAAIMVLRIDDVIAS-----SSPAKVG-------GPG 532
giCAI48595 D-MEEEGVVEPLRVKTQAIESATEAAVMILRIDDVIAAGDLAGG-ASDDDDDEDMPAGGG 542
giYP_137342 D-MEEDGVVEPLRVKTQAVESATEAAVMILRIDDVIAAGDLKGG-QGDDDEDEGGPGGPG 569
giQ9HN70 D-MESEGIVEPLRVKTQAIESATEAATMILRIDDVIAAGDLAGGQVGDDDGDDGPAGGPG 543
giO30561 D-MEEEGVVEPLRVKTQAIESATEAAVMILRIDDVIAAGDLSGGQTGSDD-DDG--GAPG 541
giYP_001689883 D-TFEAGVVEPAHAKEQAVTSASEAANLVLKIDDIISAGDLSTD-KGDDD------GGAG 542
:. * :.: . : :*:**:::::
giBAB59649 ----------
giP48425 ----------
giYP_023973 ----------
giBAB60294 EY---------- 549
giNP_376188 D---------- 559
giAAY80050 D---------- 553
giNP_341830 D---------- 557
giCAA45326 D---------- 552
giCAA07096 ----------
giNP_148364 E---------- 548
giAAL63957 D---------- 549
giO24734 TPSSLE---------- 559
giBAA33889 MGGMM---------- 544
giAAB99002 -GDEF---------- 542
giNP_275933 MPPM---------- 538
giP50016 -SSEF---------- 545
giBAA29085 GSSDLD---------- 549
giNP_125709 SSSDLD---------- 550
giAAL82098 --SDLD---------- 549
giO24730 --SDLD---------- 546
giAAP37564 ---EF---------- 544
giNP_070280 ----------
giO28045 ----------
giNP_615060 GMPPGMGGMPPGMM------- 552
giNP_633403 GMP-GMGGMPPGMM------- 551
giAAZ70052 AIP---GGEMPEMM------- 543
giCAI48595 GMGGGMGG-MGGMGGGMGGMM 562
giYP_137342 GAPGGMGGGMGGMGGGMGGMM 590
giQ9HN70 GMGGGMGG-MGGMGG-MGGAM 562
giO30561 GMGGGMGG-MGGMGG-MGGAM 560
giYP_001689883 GMGGGMGG---GMGGMM---- 556

Figure 3.136

Conserved sequences related to feature 1, feature 2 and feature 3 were indicated by #, #, and # symbols on the multiple sequence alignments, respectively.

Phylogenetic tree has three branches: one of the branches includes thermosome subunits of hyperthermophilic methanogenic archea in phylum Euryarchaeota, one of the branches includes thermosome subunits of other hyperthermophilic archaea (i.e. *Thermococci*) of the same phylum and the last one includes subclusters of *Thermoplasma*, *Sulfolobus*, *Methanosarcina* and *Halobacterium* thermosome subunits. Since *Thermoplasma* and *Picrophilus* thermosome subunit sequences showed the highest sequence identity, they were all clustered together in the phylogenetic tree (Figure 3.137).

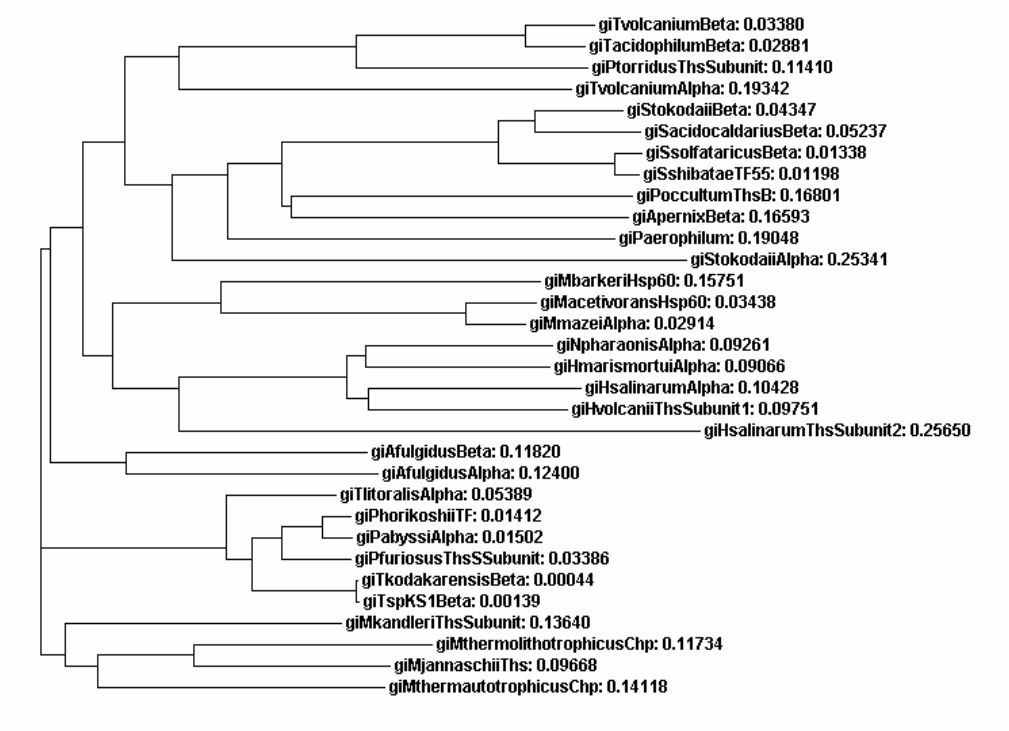

Figure 3.137: Phylogenetic tree constructed by clustal type multiple sequence alignments of amino acid sequence of *T. volcanium* Hsp60 β subunit protein with several archaeal Hsp60 proteins.

3.5 Conserved Domain Search For *T. volcanium* Hsp60 α and Hsp60 β Subunit Proteins

Conserved domain search for *T. volcanium* Hsp60 α and Hsp60 β subunit proteins gives the schematic representation in Figure 3.138. Both subunit proteins belong to the same clusters of orthologous groups (COG) classification class i.e., COG0459.

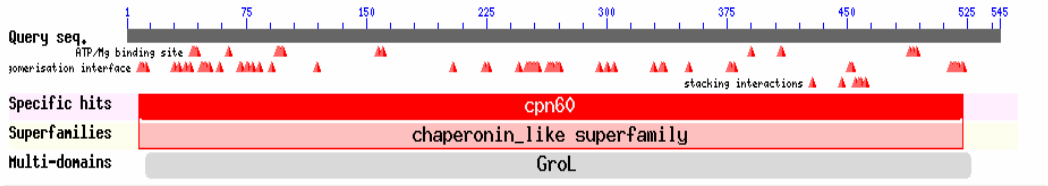

Figure 3.138: Schematic representation of conserved domains for *T. volcanium* Hsp60 α and Hsp60 β subunit proteins.

NCBI protein search showed that Hsp60 α and β subunit proteins are classified in COG0459 class called chaperonin GroEL (Hsp60 family). This COG class includes 122 proteins with functional roles in post translational modification, protein turnover and chaperoning.

The conserved domains shared by the proteins in this class are cpn 60, which is a characteristic motif of cpn60 chaperonin family (archaeal ortholog, thermosome) and GroL, which is the common motif of chaperonin GroEL (Hsp60 family). Sub-family hierarchy of cpn60 family is shown in Figure 3.139. Cpn60 family (cd03343) chaperonins are involved in productive folding of proteins. They share a common general morphology, a double toroid of 2 stacked rings. Archaeal cpn60 (thermosome), together with TF55 from thermophilic bacteria and the eukaryotic cytosol chaperonin (CTT), belong to the group II chaperonins. Cpn60 consists of two stacked octameric rings, which are composed of one or two different subunits. Their common function is to sequester nonnative proteins inside their central

cavity and promote folding by using energy derived from ATP hydrolysis. There are three structural motifs common to features cpn60 family are: ATP/Mg binding site (Figure 3.140), ring oligomerisation interface (Figure 3.141) and stacking interactions (Figure 3.142). Multiple sequence alignments which are derived from NCBI Data Base demonstrating conserved sequences related to these three features are given as Appendix D.

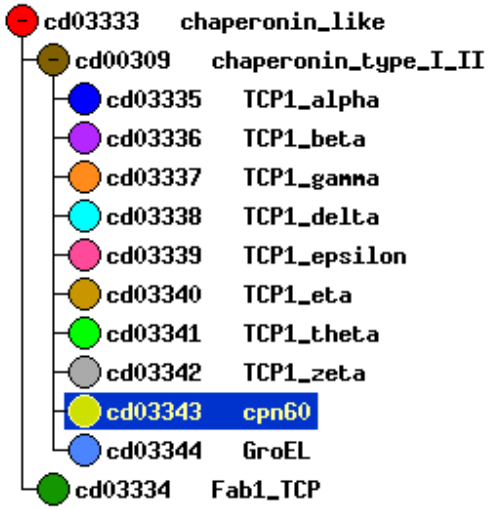

Figure 3.139: Subfamily hierarchy for cpn60 family

Figure 3.140: 3-D Illustration for ATP/Mg Binding Site

Feature 1 for Cpn60 Chaperonin Family is ATP/Mg Binding Site**.**

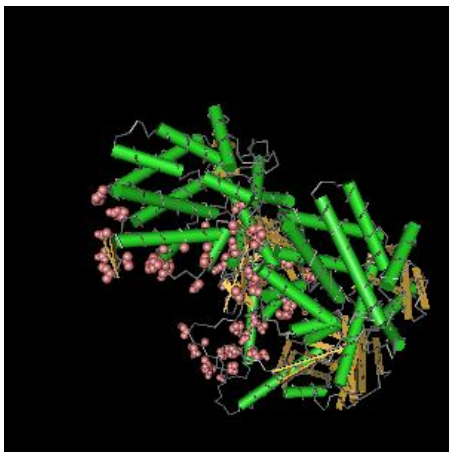

Figure 3.141: Illustration for ring oligomerisation interface

Feature 2 for Cpn60 Chaperonin Family is ring oligomerisation interface.

Figure 3.142: Illustration for stacking interactions

Feature 3 for Cpn60 Chaperonin Family is stacking interactions.

Chaperonin-like superfamily: Chaperonins are involved in productive folding of proteins. They share a common general morphology, a double toroid of 2 stacked rings, each composed of 7-9 subunits. There are 2 main chaperonin groups.

The symmetry of group I is seven-fold and they are found in eubacteria (GroEL) and in organelles of eubacterial descent (hsp60 and RBP). The symmetry of group II is eight- or nine-fold and they are found in archea (thermosome), thermophilic bacteria (TF55) and in the eukaryotic cytosol (CTT). Their common function is to sequester nonnative proteins inside their central cavity and promote folding by using energy derived from ATP hydrolysis. This superfamily also contains related domains from Fab1-like phosphatidylinositol 3-phosphate (PtdIns3P) 5-kinases that only contain the intermediate and apical domains.

Chaperonin GroEL (HSP60 family) are chaperones that are involved in posttranslational modification and protein turnover.

CHAPTER 4

DISCUSSION

Molecular chaperones are essential proteins for organisms from the three phylogenetic domains. They are essential components of a cell's ability to respond to environmental challenges (Ruepp, *et al*, 2001). Molecular chaperones are comprised of several chaperone families. Among which chaperonins (Hsp60 protein family) are large ring assemblies that differ from other molecular chaperones by providing nonnative proteins a sequestered cavity to fold in. Chaperonins are required both in cellular activities and under stress conditions (Spiess, *et al*, 2004). They have been shown to be induced under stress conditions (Lund, *et al*, 2003, Phipps, *et al*, 1993, Emmerhoff, *et al*, 1998 and Rohlin, *et al*, 2005). They may contribute to thermotolerance of cells.

In this research, we have cloned and overexpressed Hsp60 subunit proteins of thermoacidophilic archaeon *Thermoplasma volcanium*. In addition, changes in the expression profiles of the subunit genes as a response to heat and oxidative stress have been investigated by Real Time PCR. Archaea are more closely related to eukaryotes than to bacteria (Yan, *et al*, 1997). Archaeal chaperones have a considerably lower degree of complexity as compared to eukaryotic counterparts (Ruepp, *et al*, 2001). In this view, serving as ideal model systems, studies on archaeal chaperonins provide invaluable information to uncover the protein folding mechanisms in eukaryotes and also the related evolutionary pathways (Ruepp, *et al*, 2001).

We have successfully cloned two genes encoding α and β subunit proteins of the Hsp60 protein (thermosome) of *T. volcanium* in *E.coli* as 1939 bp and 1920 bp fragments, respectively. Open reading frame derived from the sequence information of the cloned Hsp60 α and β subunit genes was same with the sequence given in genome databases. Two genes, then subcloned to pUC18 vector in order to construct a co-expression vector. We have achieved to express the subunit genes from their own promoter. This finding is consistent with our previous experience which showed that archaeal promoters are functional in *E. coli* (Erduran and Kocabıyık, 1998). Recombinant *T. volcanium* Hsp60 in the cell free extract of the *E. coli* pUC18-α/β 19 bearing co-expression vector, showed a chaperone activity by refolding citrate synthase from pig heart at 50°C. We have found out that the recovery of citrate synthase activity at 50°C in the presence of the *Thermoplasma volcanium* thermosome was higher than that of spontaneous refolding. Under this condition, citrate synthase activities associated with control and test were ΔmA_{412}/min:19.0 and ΔmA_{412}/min:24.0 respectively. This is a promising result, since a chaperonin of archaeal origin could induce folding of a eukaryotic protein, and might be of relevance chaperonotherapy and several biotechnological applications (Walter and Buchner, 2002, Macario and Conway de Macario, 2007). This study is the first report of cloning and expression of Hsp60 protein subunits from *T. volcanium*. Our research on purification and folding activity of recombinant *T. volcanium* Hsp60 chaperonin using a number of model substrates is still going on. There are several studies which report chaperone activities of Hsp60 protein subunits from other archaea on different substrate proteins. The chaperonin of *S. solfataricus* was reported to possess protein refolding activity. Aggregation of the heat denatured chicken egg white lysozyme (one 14.4-kDa chain), yeast α-glucosidase (one 68.5-kDa chain), chicken liver malic enzyme (four 65-kDa subunits), and yeast alcohol dehydrogenase (four 37.5-kDa subunits), was prevented in the presence of an equimolar amount of the

chaperonin (Guagliardi *et al.*, 1995). Nakamura, *et al.* (1997) reported the effect of recombinant chaperonin from *Sulfolobus* sp. strain 7 on the refolding of the chemically denatured lactate dehydrogenase (LDH). The recovery of LDH activity was found significantly lower than that of spontaneous refolding in the presence of the *Sulfolobus* chaperonin. Yoshida, *et al* (1997) reported the cloning and sequencing of two genes coding chaperonin subunits from the hyperthermophilic archaeum *Thermococcus* strain KS-1. The recombinant α and ß subunits of chaperonin assembled to generate homo-oligomeric double-ring complexes. This complex was found induce spontaneous refolding of a chemically denatured thermophilic isopropylmalate dehydrogenase (IPMDH) enzyme when ATP exists. The yield of spontaneous refolding of the chemically denatured IPMDH was nearly 16,7 % in this study. The yield of the refolding of IPMDH by assistance of aggregate of the β subunit complexes was about 19,0 %. However, the recovery ratio with assistance of the α subunit single complex was 3,6 % (Yoshida, *et al,* 1997). Prevention of thermal aggregation of the denatured rhodanese by the group II chaperonin α from the aerobic hyperthermophilic crenarchaeon *Aeropyrum pernix* K1 (*Ap*cpnA) was examined by Jang, *et al.* (2007). Yan *et al.* (1997) reported that the recombinant chaperonin β subunit of *Pyrococcus* sp. strain KOD1 (CpkB) repressed the thermal denaturation and increased thermostability of *Saccharomyces cerevisiae* alcohol dehydrogenase (Yan, *et al*, 1997). Three recombinant complex species of *Pyrococcus* chaperonin, namely recombinant all-α, recombinant all-β, and recombinant αβ slowed down the aggregation of citrate synthase, alcohol dehydrogenase, and insulin. Therefore, it was concluded that the recombinant protein complexes possess a chaperone-like activity, interacting with non-native proteins. They exhibit this chaperone-like activity at temperatures below the lower physiological limit of growth (Minuth, *et al*, 1998). In our study, we have determined the chaperone activity of thermosome from *T. volcanium* at 50°C. This temperature is within the temperature range for growth of the organism (33ºC-67ºC) (Segerer, *et al*, 1988). Recombinant CpkA was investigated for

chaperonin functions in comparison with CpkB (β subunit). Results suggested that both CpkA and CpkB, two subunits of the chaperonin from *Pyrococcus kodakaraensis* KOD1, could assist protein folding in *E. coli* without requiring energy from ATP hydrolysis (Izumi, *et al*, 1999). Furutani *et al.* (1998) reported that the recombinant *Methanococcus thermolithotrophicus* thermosome (the MTTS) complex assisted the refolding of chemically denatured thermophilic archaeal citrate synthase and glucose dehydrogenase at 50°C in an ATP-dependent manner (Furutani, *et al*, 1998). The recombinant chaperonin from *Methanococcus maripaludis* (Mm-cpn) was found to be fully functional and assisted refolding of guanidinium-chloride-denatured rhodanese and it can prevent the aggregation of citrate synthase in a nucleotide-dependent manner under physiological conditions of 37°C. ATP binding is adequate to effect folding, but ATP hydrolysis is not necessary (Kusmierczyk, *et al.* 2003). Bergeron *et al.* showed that recombinat thermosome from *Methanocaldococcus jannaschii* is much more stable as compared to GroEL from *E.coli* (Bergeron, *et al.,* 2008).

We have shown that thermosome from *T. volcanium* is a stress protein by showing its induction under heat shock and oxidative stress conditions. Heat shock at 65°C, 70°C and 75°C induced growth of cultures after 2 hours of application. However, heat shock application at 78°C caused retardation of cell growth. New cultures initiated by the inocula from heat shocked cell culture at 75°C and that from control culture showed nearly the same growth rates. However, the new culture initiated by inoculation of fresh medium with 2h heat-shocked (at 78°C) culture of *T. volcanium* did not grow. Induction of expressions of Hsp60 subunit proteins were studied by using Real-Time PCR technique. Expression of Hsp60 α and β subunit genes were shown to be induced by heat shock applications at 65°C and 70°C in a time dependent manner. These results are consistent with the results from the heat shock experiments on growth of cultures at the same temperatures. Heat shock at 75°C for 2 hours did not induce expressions of both subunit genes.

There are reports of induction of expressions of thermosome proteins under heat shock conditions in other archaea (Shockley, *et al*, 2003, Rohlin, *et al*, 2005, Kagawa, *et al*, 2003 and Emmerhoff, *et al*, 1998). Shockley *et al*. performed heat shock by shifting the temperature from 90°C to 105°C for 1 h. They showed induction of genes by northern analyses in conjunction with a targeted cDNA microarray. The effects of thermal stress on growth and the induction of known and putative stress genes existing in *P. furiosus* was obvious. The genes which encode the major Hsp60-like chaperonin (thermosome) in *P. furiosus,* the Hsp20-like small heat shock protein and two other molecular chaperones (VAT) belonging to the CDC48/p97 branch of the AAA^+ family were found to be strongly induced (Shockley, *et al*, 2003). Rohlin *et al.* observed induction of genes under heat shock condition by employing whole-genome microarrays for *Archaeoglobus fulgidus* strain VC-16. Heat shock was applied by shifting temperature from 78°C to 89°C for 60 min. Generally, the *A. fulgidus* genes that were strongly induced at 5 minutes stayed induced for the 60 minutes duration of the heat shock exposure. Of the 11 genes that were strongly induced at 5 minutes (5- to 10-fold), 5 were previously explained as heat shock genes. Two were not known to be induced by heat shock (AF1813 and AF1323), and four encode hypothetical proteins (AF1298, AF0172, AF1526, and AF1835). Of the remaining annotated HSPs in *A. fulgidus*, genes for the HSP60s (thermosomes) and the genes for the small heat shock protein (sHSP20) (AF1296 and AF1971) were also monitored to be induced by heat (Rohlin, *et al*, 2005). The chaperonin complex from *Sulfolobus shibatae* (also called as rosettasome or TF55) is made up of three subunits. Kagawa, *et al* (2003) reported about rosettasome that alpha and beta gene expression was induced by heat shock by using Northern blot analyses. Expression of the gamma gene was reported to be undetectable at heat shock temperatures and low at normal growth temperatures (Kagawa, *et al*, 2003). Emmerhoff, *et al.* (1998) reported that they cloned and sequenced the genes encoding two chaperonin subunits (Cpn-α and Cpn-ß), from *Archaeoglobus fulgidus*, a sulfate-

reducing hyperthermophilic archaeon. The chaperonin genes seem to be induced under heat shock, as both proteins accumulate following temperature shift-up as shown by SDS-PAGE and western blot analysis. This observation indicates a role for the chaperonin in thermoadaptation (Emmerhoff, *et al*, 1998). In our study, two subunit genes encoding thermosome protein of *Thermoplasma volcanium* were found to be induced by heat shock.

Different concentrations of H_2O_2 were added to *T. volcanium* cultures at the time of inoculation and concentrations ≥ 0,025 mM were found to be toxic for the cell growth. Growth of the culture, supplemented with 0,01 mM H_2O_2 concentration, was retarded about 48-72 hours and then there was a sharp increase in growth. The same absorbance value was reached as the control. Culture supplemented with 0,005 mM H_2O_2 concentration showed a slightly lower growth rate as compared to the control culture. 0,01 mM H_2O_2 concentration may be a threshold concentration for *T. volcanium* cells for toxicity. When different concentrations of H_2O_2 were added to *T. volcanium* culture in mid-log phase in different experiments, growth inhibition was observed in a concentration dependent manner. 0,02 mM and 0,03 mM concentrations of H_2O_2 caused retardation of growth of cultures and 0,05 mM concentration of H_2O_2 was found to inhibit the growth. Induction of expressions of Hsp60 α and ß subunits of *T. volcanium* were studied by using Real-Time PCR technique. Expression of Hsp60 α subunit gene was induced by 0,008 mM H_2O_2 starting from the 60th minute of application. Addition of 0,01 mM H_2O_2 to mid-log culture increasingly induced expression of Hsp60 α subunit gene during first 90 minutes. Exposure of the mid-log phase cultures to 0,02 mM H_2O_2 increasingly induced expression of Hsp60α subunit gene during 2 hours. Addition of 0,03 mM H_2O_2 to mid-log culture did not induce expression of Hsp60 α subunit gene for the first 30 minutes but induced transcription between 30th min and 90th min of the H_2O_2 application. Oxidative stress imposed by 0,05 mM H_2O_2 application induced expression of Hsp60 α subunit gene for the first 30 minutes.

Exposure of mid-log culture to 0,008 mM H_2O_2 did not induce expression of Hsp60 β subunit gene during first 1 hour. Addition of 0,01 mM H_2O_2 to mid-log phase culture induced expression of Hsp60 β subunit gene during first 90 minutes. Oxidative stress generated by 0,02 mM H_2O_2 did not induce expression of Hsp60 β subunit gene for first 30 minutes but induction was observed between 30th min and 60th min of the application. Application of 0,02 mM H_2O_2 did not induce expression of Hsp60 β subunit gene after 90th min. Addition of 0,03 mM H_2O_2 did not induce expression of Hsp60 β subunit gene for first 60 minutes but induction was obvious at 90th min and 120th min of the H_2O_2 application. H_2O_2 at 0,05 mM induced expression of Hsp60 β subunit gene for the first 30 minutes. At 0,02 mM and 0,03 mM concentrations, H_2O_2 were found to cause retardation of growth of cultures and at 0,05 mM concentration was found to inhibit the growth. As a result, expression of *T. volcanium* Hsp60 α and β subunit genes are induced in the H_2O_2 supplemented mid-log cultures, even at its toxic concentrations, as a stress response. Mid-log cultures when supplemented with 0,02 mM and 0,03 mM H_2O_2, induction of expression of subunit proteins starts 30 min or 60 min after H_2O_2 application. Our results show expression of Hsp60 α subunit gene is induced faster than that of Hsp60 β subunit gene. Limauro, *et al.* reported that they grew the *S. solfataricus* P2 strain until the early exponential phase and they set oxidative stress by adding 0,05 mM H_2O_2, 0,1 mM paraquat or 0,05 mM tert-butyl hydroperoxide. Addition of these oxidant agents to the cultures although inhibited growth, did not kill the cells (Limauro, *et al*, 2006). This result is consistent with our result from the gene expression experiment under stress induced by 0,05 mM H_2O_2. Kawakami, et al (2004) reported that they cloned and expressed the gene encoding a hyperthermostable peroxiredoxin from an anaerobic hyperthermophilic archaeon *Pyrococcus horikoshii*. Results of this study suggest that peroxiredoxin plays an important role in the peroxide-scavenging system in an anaerobic archaeon *P. horikoshii* (Kawakami, *et al.*, 2004). Jeon and Ishikawa (2002) reported to identify and characterize a thermostable thioredoxin system in the aerobic

hyperthermophilic archaeon *Aeropyrum pernix*. Authors suggest that results of the study indicated a lower redox potential of thioredoxin is not necessary for keeping catalytic disulfide bonds reduced and coping with oxidative stress in an aerobic hyperthermophilic archaea (Jeon and Ishikawa, 2002). It is tempting to see whether any orthologs of these stress genes play role in stress response in *T. volcanium*, as well. Our research on this subject stil is in progress.

Results of multiple sequence alignments of the Hsp60 and GroEL subunit proteins were generally parallel with the systematic hierarchy of organisms. Interestingly, the differentiation of archaeal thermosome subunits seems to have occurred fairly recently in evolution and independently in most archaeal lineages. It is proposed that some archaea may be on an evolutionary path leading to a similar subunit complexity as seen in eukaryotes (Archibald *et al.,* 1999). A phylogenetic analysis using all the available archaeal chaperonin sequences, suggests that the α and β chaperonin subunits from *Archaeoglobus fulgidus* are the results of late gene duplications. High degree of homology between the Hsp60 α and β subunit sequences (60% in *T. volcanium*, 75% in *A. fulgidus*, 50% in *S. tokodaii*, 52% in *H. salinarum*) supports this notion (Table 3.12). These duplications might have occured after the establishment of the main archaeal evolutionary lines (Emmerhoff, *et al*, 1998).

Hsp60 α subunit protein of *T. volcanium* (BAB60294) includes the highly conserved, putative ATP binding site (97–GDGTTT-102) (Figure 3.130). Same sequence (92–GDGTTT-97) was identified in the Hsp60 β subunit protein (BAB59649) sequence of *T. volcanium* (Andrä, *et al*, 1996).

As suggested for α subunit of *T. acidophilum* thermosome, 249-IKKTEIEAKVQISDPSKIQDFLNQETSTF-277 sequence of Hsp60 α subunit protein of *T. volcanium* (BAB60294) may be responsible for helical protrusion

(Figure 3.130). As suggested for β subunit of *T. acidophilum* thermosome, 246-IKKPEFDTNLRIEDPSMIQKFLAQEENML-274 sequence may be responsible for helical protrusion of Hsp60 β subunit protein of *T. volcanium* (BAB59649) (Figure 3.134) (Klumpp, *et al*, 1997).

In conclusion, in this study we have cloned and expressed Hsp60 α and β subunit genes of *T. volcanium* in *E.coli* for the first time. Our results show that recombinant *T. volcanium* Hsp60 chaperonin promoted the refolding of the chemically denatured citrate synthase from pig heart. Purification and biochemical characterization of the recombinant Hsp60 is in progress in our laboratory. Also, in this study, differential expressions of Hsp60 subunit genes under heat-shock and oxidative stress were analyzed by Real time quantitative PCR. The results indicated that both subunit genes are induced in a temperature and H_2O_2 concentration dependent manner.

REFERENCES

Andrä, S., Frey, G., Nitsch, M., Baumeister, W., Stetter, K. O., 1996, Purification and structural characterization of the thermosome from the hyperthermophilic archeum *Methanopyrus kandleri*, FEBS Letters, 379, 127-131.

Anfinsen, C. B., 1973, Principles that govern the folding of protein chains, Science, New Series, 181, 223-230.

Archibald, J. M., Logsdon Jr. J. M., Doolittle, W. F., 1999, Recurrent paralogy in the evolution of archaeal chaperonins, Current Biology, 9 (18), 1053-1056.

Archibald, J. M., Blouin, C., and Doolittle, W. F., 2001, Gene duplication and the evolution of group II chaperonins: implications for structure and function, Journal of Structural Biology, 135, 157-169.

Arrigo, A-P., 2001, Hsp-27: novel regulator of intracellular redox state, IUBMB *Life*, 52, 303-307.

Barral, J. M., Broadley, S. A., Schaffar, G., Hartl, F. U., 2004, Roles of molecular chaperones in protein misfolding diseases, Seminars in Cell & Developmental Biology, 15, 17-29.

Becker, J., and Craig, E. A., 1994, Heat-shock proteins as molecular chaperones, Eur. J. Biochem., 219, 11-23.

Bergeron, L. M., Lee, C., Tokatlian, T., Höllrigl, V., Clark, D. S., 2008, Chaperone function in organic co-solvents: experimental characterization and modelling of a hyperthermophilic chaperone subunit from *Methanocaldococcus jannaschii*, Biochimica et Biophysica Acta, 1784, 368-378.

Bova, M. P., Huang, Q., Ding, L., and Horwitz, J., 2002, Subunit exchange, conformational stability, and chaperone-like function of the small heat shock protein 16.5 from *Methanococcus jannaschi*, The Journal of Biological Chemistry, 277, 38468-38475.

Braig, K., 1998, Chaperonins, Current Opinion in Structural Biology, 8, 159-165.

Bree, R. T., Stenson-Cox, C., Grealy, M., Byrnes, L., Gorman, A. M., and Samali, A., 2002, Cellular longevity: role of apoptosis and replicative senescence, Biogerontology, 3, 195-206.

Brocchieri, L., de Macario, E. C., Macario, A. J. L., 2007, Chaperonomics, a new tool to study ageing and associated diseases, Mechanisms of Ageing and Development, 128, 125-136.

Brown, M. A., Zhu, L., Schmidt, C., Tucker, P. W., 2007, Hsp90-from signal transduction to cell transformation, Biochemical and Biophysical Research Communications, 363, 241-246.

Bustin, S. A., 2000, Absolute quantification of mRNA using real-time reverse transcription polymerase chain reaction assays, Journal of Molecular Endocrinology, 25, 169-193.

Carrascosa, J. L., Llorca, O., Valpuesta, J. M., 2001, Structural comparison of prokaryotic and eukaryotic chaperonins, Micron, 32, 43-50.

Chung, C.T., Niemela, S.L., and Miller, R.H., 1989, One-step preparation of competent *Escherichia coli*: transformation and storage of bacterial cells in the same solution, Proc. Nat. Acad. Sci. U.S.A., 86, 2172.

Conway de Macario, E. C., and Macario, A. J. L., 2000, Stressors, stress and survival; overview, Frontiers in Bioscience 5, 780-786.

Conway de Macario, E. C., Maeder, D. L., and Macario, A. J. L., 2003, Breaking the mould: archaea with all four chaperoning systems, Biochemical and Biophysical Research Communications, 301, 811-812.

Ditzel, L., Löwe, J., Stock, D., Stetter, K.-O., Huber, H., Huber, R., and Steinbacher, S., 1998, Crystal structure of the thermosome, the archaeal chaperonin, and homolog of CCT, Cell, 93, 125-138.

Ellis, R. J., 1993, The general concept of molecular chaperones, *Philosophical Transactions*: *Biological Sciences*, 339, 257-261.

Emmerhoff, O. J., Klenk, H-P., Birkeland, N-K., 1998, Characterization and sequence comparison of temperature-regulated chaperonins from the hyperthermophilic archaeon *Archaeoglobus fulgidus*, Gene, 215, 431-438.

Erbse, A., Mayer, M. P., and Bukau, B., 2004, Mechanism of substrate recognition by Hsp70 chaperones, Biochemical Society Transactions, 32, 617-621.
Erduran, İ., and Kocabıyık, S., 1998, Amino acid substitutions in the subunit interface enhancing thermostability of *Thermoplasma acidophilum* citrate synthase, Biochemical and Biophysical Research Communications, 249, 566-571.

Evstigneeva, Z. G., Solov'eva, N. A., and Sidel'nikova, L. I., 2001, Structures and functions of chaperones and chaperonins (review), Applied Biochemistry and Microbiology, Vol. 37, 1-13.

Furutani, M., Iida, T., Yoshida, T., and Maruyama, T., 1998, Group II chaperonin in a thermophilic methanogen, *Methanococcus thermolithotrophicus*, The Journal of Biological Chemistry, 273, 28399-28407.

Gaasterland, T., 1999, Archaeal genomics, Current Opinion in Microbiology, 2, 542-547.

Gabai, V. L., Meriin A. B., Mosser, D. D., Caron, A. W., Rits, S., Shifrin, V. I., and Sherman, M. Y., 1997, Hsp70 prevents activation of stress kinases, The Journal of Biological Chemistry, 272, 18033-18037.

Gabai, V. L., Mabuchi, K., Mosser, D. D., Sherman, M. Y., 2002, Hsp72 and stress kinase c-jun N-terminal kinase regulate the bid-dependent pathway in tumor necrosis factor-induced apoptosis, Molecular and Cellular Biology, 22, 3415-3424.

Galea-Lauri, J., Richardson A. J., Latchman D. S., Katz, D. R., 1996, Increased heat shock protein 90 (Hsp90) expression leads to increased apoptosis in the monoblastoid cell line U937 following induction with TNF-alpha and cycloheximide: a possible role in immunopathology, Journal of Immunology, 157 (9), 4109-4118.

Gómez-Puertas, P., Martín-Benito, J., Carrascosa, J. L., Willison, K. R., and Valpuesta, J. M., 2004, The substrate recognition mechanisms in chaperonins, Journal of Molecular Recognition, 17, 85-94.

Guagliardi, A., Cerchia, L.,Rossi, M., 1995, Prevention of *in vitro* protein thermal aggregation by the *Sulfolobus solfataricus* chaperonin, The Journal of Biological Chemistry, 270, 28126-28132.

Gutsche, I., Mihalache, O., and Baumeister, W., 2000b, ATPase cycle of an archaeal chaperonin, *J. Mol. Biol*., 300, 187-196.

Gutsche, I., Holzinger, J., Rauh, N., Baumeister, W., and May, R. P., 2001, ATP-induced structural change of the thermosome is temperature-dependent, Journal of Structural Biology, 135, 139-146.
Hartl, F. U., 1996, Molecular chaperones in cellular protein folding, Nature, 381, 571-580.

Hartl, F. U., and Hayer-Hartl, M., 2002, Molecular chaperones in the cytosol: from nascent chain to folded protein, Science, 295, 1852-1858.

Haslbeck, M., Walke, S., Stromer, T., Ehrnsperger, M., White, H. E., Chen, S., Saibil, H. R., and Buchner, J., 1999, Hsp26: a temperature-regulated chaperone, The EMBO Journal, 18, 6744-6751.

Haslbeck, M., Franzmann, T., Weinfurtner, D., and Buchner, J., 2005, Some like it hot: the structure and function of small heat-shock proteins, Nature Structural & Molecular Biology, 12, 842-846.

Hemmingsen S. M., Woolford, C., Van Der Vies, S. M., Tilly, K., Dennis D. T., Georgopoulos, C. P., Hendrix, R. W., Ellis, R. J., 1988, Homologous plant and bacterial proteins chaperone oligomeric protein assembly, Nature, 333, 330-334.

Horwich, A. L., Fenton, W. A., Chapman, E., Farr, G. W., 2007, Two families of chaperonin: physiology and mechanism, Annu. Rev. Cell Dev. Biol., 23, 115-145.

Housley, P. R., Sanchez, E. R., Westphal, H. M., Beato, M., and Pratt W.B., 1985, The molybdate-stabilized L-cell glucocorticoid receptor isolated by affinity chromatography or with a monoclonal antibody is associated with a 90-92-kDa nonsteroid-binding phosphoprotein, The Journal of Biological Chemistry, 260, 13810-13817.

Iizuka, R., Yoshida, T., Shomura, Y., Miki, K., Maruyama, T., Odaka, M., Yohda, M., 2003, ATP binding is critical for the conformational change from an open to closed state in archaeal group II chaperonin, The Journal of Biological Chemistry, 278, 44959-44965.

Izumi, M., Fujiwara, S., Takagi, M., Kanaya, S., Imanaka, T., 1999, Isolation and characterization of a second subunit of molecular chaperonin from *Pyrococcus kodakaraensis* KOD1: analysis of an ATPase-deficient mutant enzyme, Applied and Environmental Microbiology, 65, 1801-1805.

Jang, K. J., Bae, Y-J., Jeon, S-J., Kim, K., Lee, J-H., Yea, S. S., Oh, S., Jeong, Y-J., Kim, D-E., 2007, Nucleotide and manganese ion is required for chaperonin function of the hyperthermostable group II chaperonin α from *Aeropyrum pernix* K1, *Bull. Korean Chem. Soc.*, 28, 2261- 2265.

Jeon, S-J., and Ishikawa, K., 2002, Identification and characterization of thioredoxin and thioredoxin reductase from Aeropyrum pernix K1, *Eur. J. Biochem.*, 269, 5423-5430.

Kagawa, H. K., Yaoi, T., Brocchieri, L., McMillan, R. A., Alton, T., and Trent, J. D., 2003, The composition, structure, and stability of a group II chaperonin are temperature regulated in a hyperthermophilic archaeon, Molecular Microbiology, 48 (1), 143-156.

Kapatai, G., Large, A., Benesch, J. L. P., Robinson, C.V., Carrascosa, J. L., Valpuesta, J. M., Gowrinathan, P., and Lund, P. A., 2006, All three chaperonin genes in the archaeon *Haloferax volcanii* are individually dispensable, Molecular Microbiology, 61(6), 1583-1597.

Kawakami, R., Sakuraba, H., Kamohara, S., Goda, S., Kawarabayasi, Y., Ohshima, T., 2004, Oxidative stress response in an anaerobic hyperthermophilic archaeon: presence of a functional peroxiredoxin in *Pyrococcus horikoshii*, J. Biochem., 136, 541-547.

Kawashima, T., Amano, N., Koike, H., Makino, S-i., Higuchi, S., Kawashima-Ohya, Y., Watanabe, K., Yamazaki, M., Kanehori, K., Kawamoto, T., Nunoshiba, T., Yamamoto, Y., Aramaki, H., Makino, K., and Suzuki, M., 2000, Archaeal adaptation to higher temperatures revealed by genomic sequence of *Thermoplasma volcanium*, PNAS, 97, 14257-14262.

Kawashima, T., Yokoyama, K., Higuchi, S., Suzuki, M., 2005, Identification of proteins present in the archaeon *Thermoplasma volcanium* cultured in aerobic and anaerobic conditions, Proc. Japan Acad., 81(B), 204-219.

Kim, S-J., Jeong, D-G., Chi, S-W., Lee, J-S., Ryu, S-E., 2001, Crystal structure of proteolytic fragments of the redox-sensitive Hsp33 with constitutive chaperone activity, Nature Structural Biology, 8, 459-466.

Klumpp, M., Baumeister, W., and Essen, L-O., 1997, Structure of the substrate binding domain of the thermosome, an archaeal group II chaperonin, Cell, 91, 263-270.

Klumpp, M., Baumeister, W., 1998, The thermosome: archetype of group II chaperonins, FEBS Letters, 430, 73-77.

Klunker, D., Haas, B., Hirtreiter, A., Figueiredo, L., Naylor, D. J., Pfeifer, G., Müller, V., Deppenmeier, U., Gottschalk, G., Hartl, F. U., Hayer-Hartl, M., 2003, Coexistence of group I and group II chaperonins in the archaeon *Methanosarcina mazei*, The Journal of Biological Chemistry, 278, 33256-33267.

Kregel, K. C., 2002, Heat-shock proteins: modifying factors in physiological stress responses and acquired thermotolerance, *J. Appl. Physiol*., 92, 2177-2186
Kubota, H., Matsumoto, S., Yokota, S-i., Yanagi, H., Yura, T., 1999, Transcriptional activation of mouse cytosolic chaperonin CCT subunit genes by heat shock factors HSF1 and HSF2, FEBS Letters, 461, 125-129.

Kusmierczyk, A. R., and Martin, J., 2003, Nucleotide-dependent protein folding in the type-II chaperonin from the mesophilic archaeon *Methanococcus maripaludis*, Biochem. J., 371, 669-673.

Laksanalamai, P., Whitehead, T. A., and Robb, F. T., 2004, Minimal protein-folding systems in hyperthemophilic archaea, Nature Reviews, 2, 315-324.

Laskey, R. A., Honda, B. M, Mills, A. D., and Finch, J. T., 1978, Nucleosomes are assembled by an acidic protein which binds histones and transfers them to DNA, *Nature,* 275, 416-420.

Leroux, M. R., Fändrich, M., Klunker, D., Siegers, K., Lupas, A. N., Brown, J. R., Schiebel, E., Dobson, C. M., Hartl, F. U., 1999, MtGimC, a novel archaeal chaperone related to the eukaryotic chaperonin cofactor GimC/prefoldin, The EMBO Journal, 18, 6730-6743.

Limauro, D., Pedone, E., Pirone, L., and Bartolucci, S., 2006, Identification and characterization of 1-cys peroxiredoxin from *Sulfolobus solfataricus* and its involvement in the response to oxidative stress, FEBS Journal, 273, 721-731.

Liou, A. K. F., and Willison, K. R., 1997, Elucidation of the subunit orientation in CCT (chaperonin containing TCP1) from the subunit composition of CCT micro-complexes, The EMBO Journal, 16, 4311-4316.

Lund, P. A., Large, A. T., and Kapatai, G., 2003, The chaperonin: perspectives from the archaea, Biochemical Society Transactions, 31, 681-685.

Macario, A. J. L., and de Macario, E. C., 2004, The pathology of cellular anti-stress mechanisms: a new frontier, Stress, 7:4, 243-249.

Macario A. J. L., de Macario, E. C., 2007, Molecular chaperones: multiple functions, pathologies, and potential applications, Frontiers in Bioscience, 12, 2588-2600.

Maeder, D. L., Macario A. J. L., de Macario, E. C., 2005, Novel chaperonins in a prokaryote, Journal of Molecular Evolution, 60, 409-416.

Margulis, L., 1996, Archaeal-eubacterial mergers in the origin of Eukarya: phylogenetic classification of life, Proceedings of the National Academy of Sciences of the United States of America, 93, 1071-1076.

Maurizi, M. R., and Xia, D., 2004, Protein binding and disruption by Clp/Hsp100 chaperones, Structure, 12, 175-183.

Meyer, A. S., Gillespie, J. R., Walther, D., Millet, I. S., Doniach, S., Frydman, J., 2003, Closing the folding chamber of the eukaryotic chaperonin requires the transition state of ATP hydrolysis, Cell, 113, 369-381.

Minuth, T., Frey, G., Lindner, P., Rachel, R., Stetter, K. O., Jaenicke, R., 1998, Recombinant homo- and hetero-oligomers of an ultrastable chaperonin from the archaeon *Pyrodictium occultum* show chaperone activity *in vitro*, *Eur. J. Biochem*, 258, 837-845.

Morel, Y., and Barouki, R., 1999, Repression of gene expression by oxidative stress, Biochem J., 342, 481-496.

Nakamura, N., Taguchi, H., Ishii, N., Yoshida, M., Suzuki, M., Endo, I., Miura, K-i., Yohda, M., 1997, Purification and molecular cloning of the group II chaperonin from the acidothermophilic archaeon, *Sulfolobus* sp. strain 7, Biochemical and Biophysical Research Communications, 236, 727-732.

Nitsch, M., Klumpp, M., Lupas, A., and Baumeister, W., 1997, The thermosome: alternating α and β-subunits within the chaperonin of the archaeon *Thermoplasma acidophilum*, *J. Mol. Biol.*, 267, 142-149.

Nixon, B., Asquith K. L., Aitken, R. J., 2005, The role of molecular chaperones in mouse sperm-egg interactions, Molecular and Cellular Endocrinology, 240, 1-10.

Nylansted, J., Rohde, M., Brand, K., Bastholm, L., Elling, F. and Jäättelä, M., 2000, Selective depletion of heat shock protein 70 (Hsp70) activates a tumor-specific death program that is independent of caspases and bypasses Bcl-2, PNAS, 97, 7871-7876.

Okochi, M., Matsuzaki, H., Nomura, T., Ishii, N., Yohda, M., 2005, Molecular characterization of the group II chaperonin from the hyperthermophilic archaeum *Pyrococcus horikoshii* OT3, Extremophiles, 9, 127-134.

Phipps, B. M., Hoffmann, A., Stetter, K. O., and Baumeister, W., 1991, A novel ATPase complex selectively accumulated upon heat-shock is a major cellular component of thermophilic archaebacteria, The EMBO Journal, 10, 1711-1722.

Phipps, B. M., Typke, D., Hegerl, R., Volker, S., Hoffmann, A., Stetter, K.O., and Baumeister, W., 1993, Structure of a molecular chaperone from a thermophilic archaebacterium, Nature, 361, 475-477.

Proctor, C. J., Sóti, C., Boys, R. J., Gillespie, C. S., Shanley, D. P., Wilkinson, D. J., Kirkwood, T. B. L., 2005, Modelling the actions of chaperones and their role in ageing, Mechanisms of Ageing and Development, 126, 119-131.

Quaite-Randall, E., Trent, J. D., Josephs, R., Joachimiak, A., 1995, Conformational cycle of the archaeosome, a TCP1-like chaperonin from *Sulfolobus shibatae*, The Journal of Biological Chemistry, 270, 28818-28823.

Reysenbach, A-L., Liu, Y., Banta, A. B., Beveridge, T. J., Kirshtein, J. D., Schouten, S., Tivey, M. K., Von Damm, K. L., Voytek, M. A., 2006, A ubiquitous thermoacidophilic archaeon from deep-sea hydrothermal vents, Nature, 442, 444-447.

Robb, F.T., and Place, A.R., 1995, Archaea: a laboratory manual, Cold Spring Harbor Laboratory Press.

Rohlin, L., Trent, J. D., Salmon, K., Kim, U., Gunsalus, R. P., Liao, J. C., 2005, Heat shock response of *Archaeoglobus fulgidus*, Journal of Bacteriology, 187, 6046-6057.

Roseman, A. M., Chen, S., White, H., Braig, K., Saibil, H. R., 1996, The chaperonin ATPase cycle: mechanism of allosteric switching and movements of substrate-binding domains in GroEL, Cell, 87, 241-251.

Ruepp, A., Rockel, B., Gutsche, I., Baumeister, W., and Lupas, A. N., 2001, The chaperones of the archaeon *Thermoplasma acidophilum*, Journal of Structural Biology, 135, 126-138.

Samali, A., Cai, J., Zhivotovsky, B., Jones, D. P., and Orrenius, S., 1999, Presence of a pre-apoptotic complex of pro-caspase-3, Hsp60 and Hsp10 in the mitochondrial fraction of Jurkat cells, The EMBO Journal, 18, 2040-2048.

Schäfer, G., Engelhard, M., and Müller, V., 1999, Bioenergetics of the archaea, Microbiology and Molecular Biology Reviews, 63, 570-620.

Schoehn, G., Hayes, M., Cliff, M., Clarke, A. R., Saibil, H. R., 2000, Domain rotations between open, closed and bullet-shaped forms of the thermosome, an archaeal chaperonin, *J. Mol. Biol*., 301, 323-332.

Segerer, A., Langworthy, T. A., and Stetter, K. O., 1988, *Thermoplasma acidophilum* and *Thermoplasma volcanium* sp. nov. from solfatara fields, System. Appl. Microbiol., 10, 161-171.

Shockley, K. R., Ward, D. E., Chhabra, S. R., Conners, S. B., Montero, C. I., and Kelly, R. M., 2003, Heat shock response by the hyperthermophilic archaeon *Pyrococcus furiosus*, Applied and Environmental Microbiology, 69, 2365-2371.

Siegers, K., Waldmann, T., Leroux, M. R., Grein, K., Shevchenko, A., Schiebel, E., Hartl, F. U., 1999, Compartmentation of protein folding *in vivo*: sequestration of non-native polypeptide by the chaperonin-GimC system, The EMBO Journal, 18, 75-84.

Siegert, R., Leroux, M. R., Scheufler, C., Hartl, F. U., Moarefi, I., 2000, Structure of the moleculer chaperone prefoldin: unique interaction of multiple coiled coil tentacles with unfolded proteins, Cell, 103, 621-632.

Sóti, C., Csermely, P., 2003, Aging and molecular chaperones, Experimental Gerontology, 38, 1037-1040.

Sóti, C., Sreedhar, A. S., and Csermely, P., 2003, Apoptosis, necrosis and cellular senescence: chaperone occupancy as a potential switch, Aging Cell, 2, 39-45.

Spiess, C., Meyer, A. S., Reissmann, S., and Frydman, J., 2004, Mechanism of the eukaryotic chaperonin: protein folding in the chamber of secrets, *TRENDS in Cell Biology*, 14, 598-604.

Srere, P. A., Brasil, H., and Gonen, L., 1963, The citrate condensing enzyme of pigeon breast muscle and moth flight muscle, Acta Chem. Scand., 17, S129-S143.

Steinbacher, S., and Ditzel, L., 2001, Review: nucleotide binding to the *Thermoplasma* thermosome: implications for the functional cycle of group II chaperonins, Journal of Structural Biology, 135, 147-156.

Su, C-Y., Chong, K-Y., Chen, J., Ryter, S., Khardori, R., and Lai, C-C., 1999, A Physiologically relevant hyperthermia selectively activates constitutive hsp70 in H9c2 cardiac myoblasts and confers oxidative protection, J Mol Cell Cardiol, 31, 845-855.

Sutherland, K.J., Henneke, C.M., Towner, P., Hough, D.W., and Danson, M.J., 1990, Citrate synthase from the thermophilic *Archaebacteria Thermoplasma acidophilum*: Cloning and sequencing of the gene, Europ. Jour. Biochem., 194, 839-844.

Trent, J. D., Osipiuk, J., Pinkau, T., 1990, Acquired thermotolerance and heat shock in the exteremely thermophilic archaebacterium *Sulfolobus* sp. strain B12, Journal of Bacteriology, 172, 1478-1484.

Trent, J. D., Nimmesgern, E., Wall, J. S., Hartl, F. U., Horwich, A. L., 1991, A molecular chaperone from a thermophilic archaebacterium is related to the eukaryotic protein t-complex polypeptide-1, Nature, 354, 490-493.

Trent, J. D., Gabrielsen, M., Jensen, B., Neuhard, J., and Olsen, J., 1994, Acquired thermotolerance and heat shock proteins in thermophiles from the three phylogenetic domains, Journal of Bacteriology, 176, 6148-6152.

Trent, J. D., 1996, A review of acquired thermotolerance, heat-shock proteins, and molecular chaperones in archaea, FEMS Microbiology Reviews, 18, 249-258.

Trent, J. D., Kagawa, H. K., Yaoi, T., Olle, E., Zaluzec, N. J., 1997, Chaperonin filaments: the archaeal cytoskeleton?, Proc. Natl. Acad. Sci. USA, 94, 5383-5388.

Trent, J. D., Kagawa, H. K., Paavola, C. D., McMillan, R.A., Howard, J., Jahnke, L., Lavin, C., Embaye, T., Henze, C. E., 2003, Intracellular localization of a group II chaperonin indicates a membrane-related function, PNAS, 100, 15589-15594.

Uhl, J. R., Bell, C. A., Sloan, L. M., Espy, M. J., Smith, T. F., Rosenblatt, J. E., Cockerill, F. R., 2002, Application of rapid-cycle real-time polymerase chain reaction for the detection of microbial pathogens: the mayo-roche rapid anthrax test, Mayo Clin. Proc., 77, 673-680.

Van Montfort, R. L. M., Basha, E., Friedrich, K. L., Slingsby, C., Vierling, E., 2001, Crystal structure and assembly of a eukaryotic small heat shock protein, Nature Structural Biology, 8, 1025-1030.

Verbeke, P., Fanoger, J., Clark, B. F. C. and Rattan, S. I. S., 2001, Heat shock response and ageing: mechanisms and applications, *Cell Biology International,* 25, 845-857.

Waldmann, T., Nitsch, M., Klumpp, M., Baumeister, W., 1995, Expression of an archaeal chaperonin in *E. coli*: formation of homo- (α, β) and hetero-oligomeric (α + β) thermosome complexes, FEBS Letters, 376, 67-73.

Walter, S. and Buchner, J., 2002, Molecular chaperones-cellular machines for protein folding, Angew. Chem. *Int. Ed.*, *41*, 1098-1113.

Winter, J., and Jakop, U., 2004, Beyond transcription-new mechanisms for the regulation of molecular chaperones, Critical Reviews in Biochemistry and Molecular Biology, 39, 297-317.

Xanthoudakis, S., Roy, S., Rasper, D., Hennessey, T., Aubin, Y., Cassady, R., Tawa, P., Ruel, R., Rosen, A., and Nicholson, D. W., 1999, Hsp60 accelerates the maturation of pro-caspase-3 by upstream activator proteases during apoptosis, The EMBO Journal, 18, 2049- 2056.

Xu, Z., Horwich, A. L., and Sigler, P. B., 1997, The crystal structure of the asymmetric GroEL-GroES-$(ADP)_7$ chaperonin complex, Nature, 388, 741-750.

Yan, Z., Fujiwara, S., Kohda, K., Takagi, M., and Imanaka, T., 1997, *In vitro* stabilization and *in vivo* solubilization of foreign proteins by the β subunit of a chaperonin from the hyperthermophilic archaeon *Pyrococcus* sp strain KOD1, Applied and Environmental Microbiology, 63, 785-789.

Yoshida, T., Yohda, M., Iida, T., Maruyama, T., Taguchi, H., Yazaki, K., Ohta, T., Odaka, M., Endo, I., and Kagawa, Y., 1997, Structural and functional characterization of homooligomeric complexes of α and β chaperonin subunits from the hyperthermophilic archaeum *Thermococcus* strain KS-1, *J. Mol. Biol.,* 273, 635-645.

Young, J. C., Moarefi, I., and Hartl, F. U., 2001, Hsp90: a specialized but essential protein-folding tool, The Journal of Cell Biology, 154, 267-273.

Zhang, X., Beuron, F., and Freemont, P. S., 2002, Machinery of protein folding and unfolding, Current Opinion in Structural Biology, 12, 231-238.

APPENDIX A

BUFFERS AND SOLUTIONS

TE Buffer pH: 8.0

- TrisHCl ..... 10 mM
- EDTA ..... 1 mM

TAE Buffer pH: 8.0

- Tris acetate ..... 0.04 M
- EDTA ..... 0.001 M

LB Medium (1 L) pH:7.4

- Tryptone ..... 10 g
- Yeast extract ..... 5 g
- NaOH .....10 g

10x FA Gel Buffer pH:7

- MOPS .....200 mM
- Sodium acetate ($NaCH_3COO$)……...50 mM
- EDTA……10 mM

1,2% FA Gel

- Agarose .....0,48 g
- 10xFA gel buffer……..……4 ml
- RNase free water……..to 40 ml
- Melt and cool to 65°C
- 37% Formaldehyde…….720 µl
- Ethidium bromide……...5 µl

APPENDIX B

CLONING VECTORS

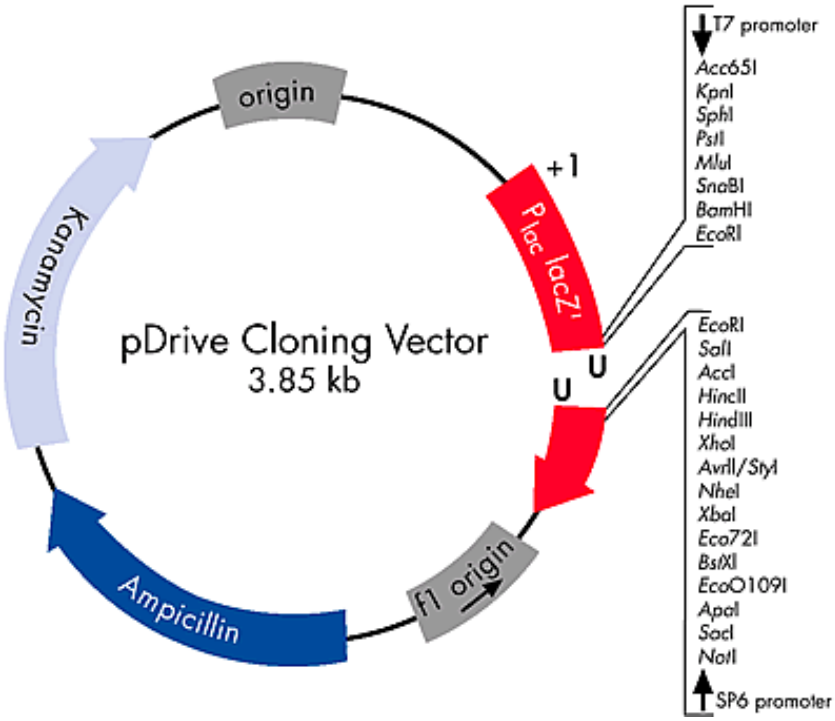

Figure B.1: pDrive Cloning Vector (QIAGEN)

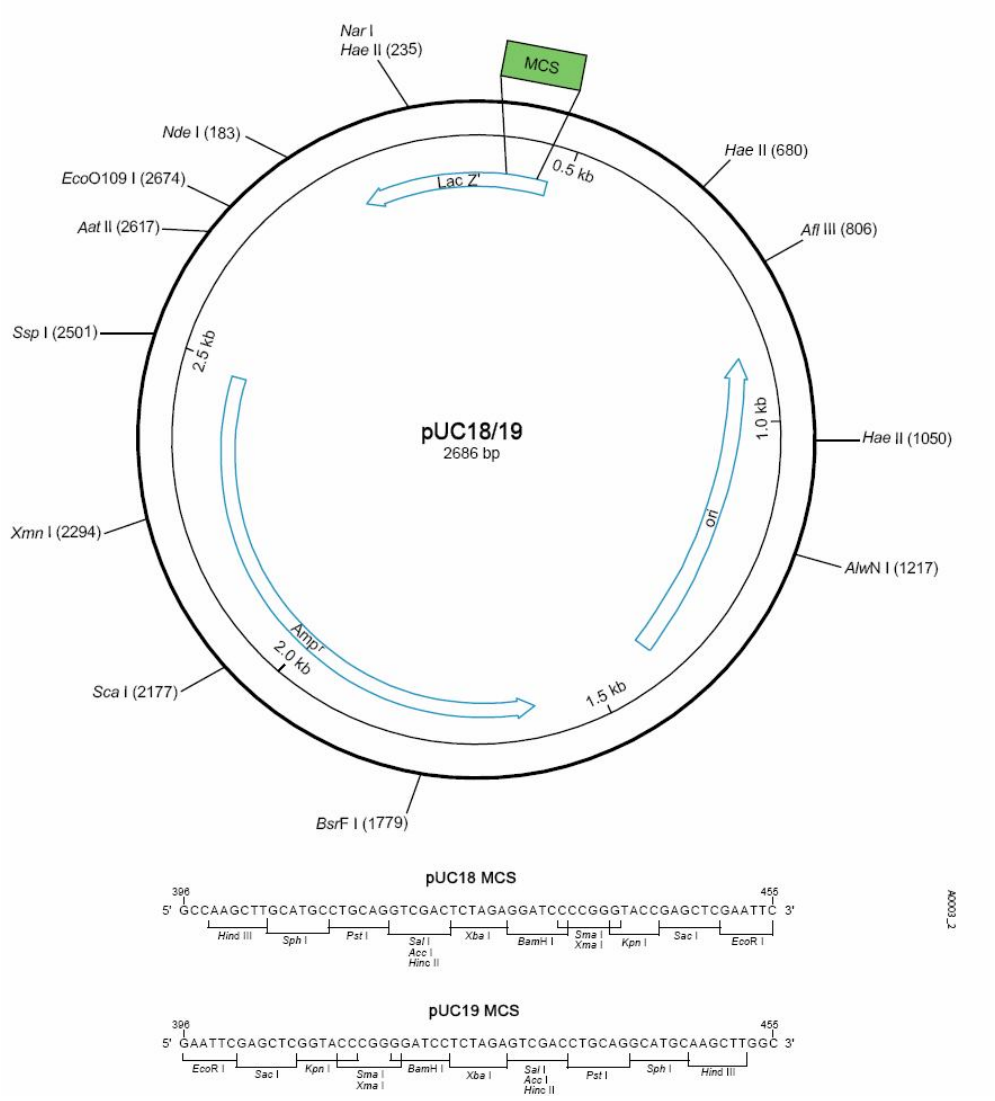

Figure B.2: pUC18 Cloning Vector (MBI Fermentas AB, Vilnius, Lithuania)

APPENDIX C

MOLECULER SIZE MARKERS

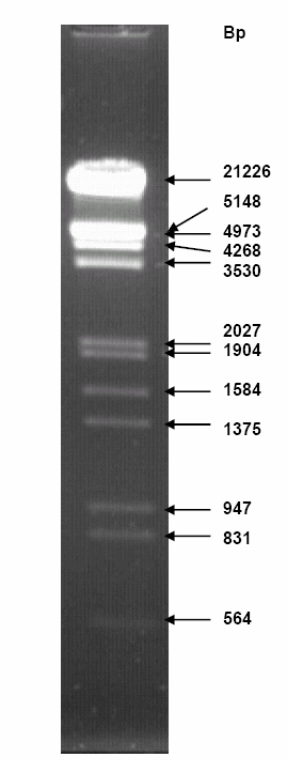

Figure C.1: *EcoRI*+HindIII cut Lambda DNA (MBI Fermentas AB, Vilnius, Lithuania)

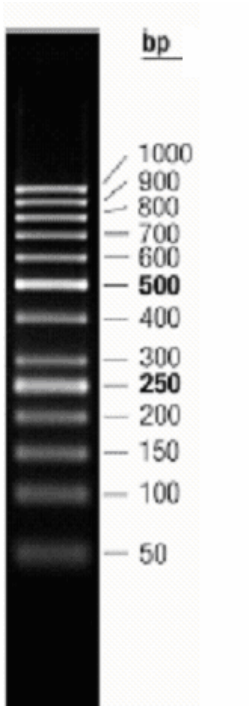

Figure C.2: Gene Ruler, 1 kb DNA Ladder (MBI Fermentas AB, Vilnius, Lithuania)

APPENDIX D

MULTIPLE SEQUENCE ALIGNMENTS REGARDING THREE STRUCTURAL MOTIFS COMMON TO FEATURES CPN60 FAMILY

Figure D.1: Alignment for Feature 1 (derived from NCBI Data Base).

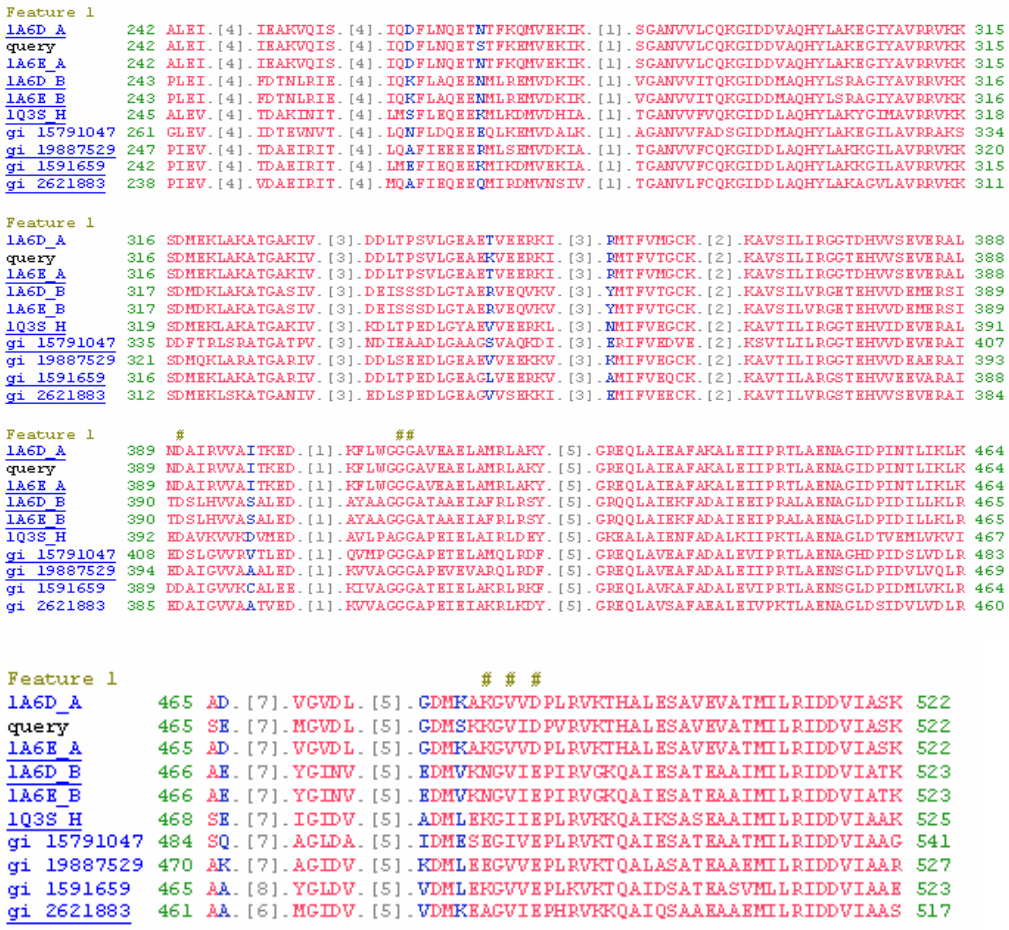
Feature 1
1A6D_A 242 ALEI.[4].IEAKVQIS.[4].IQDFLNQETNTFKQMVEKIK.[1].SGANVVLCQKGIDDVAQHYLAKEGIYAVRRVKK 315
query 242 ALEI.[4].IEAKVQIS.[4].IQDFLNQETSTFKEMVEKIK.[1].SGANVVLCQKGIDDVAQHYLAKEGIYAVRRVKK 315
1A6E_A 242 ALEI.[4].IEAKVQIS.[4].IQDFLNQETNTFKQMVEKIK.[1].SGANVVLCQKGIDDVAQHYLAKEGIYAVRRVKK 315
1A6D_B 243 PLEI.[4].FDTNLRIE.[4].IQKFLAQEENMLREMVDKIK.[1].VGANVVITQKGIDDMAQHYLSRAGIYAVRRVKK 316
1A6E_B 243 PLEI.[4].FDTNLRIE.[4].IQKFLAQEENMLREMVDKIK.[1].VGANVVITQKGIDDMAQHYLSRAGIYAVRRVKK 316
1Q3S_H 245 ALEV.[4].TDAKINIT.[4].LMSFLEQEEKMLKDMVDHIA.[1].TGANVVFVQKGIDDLAQHYLAKYGIMAVRRVKK 318
gi 15791047 261 GLEV.[4].IDTEVNVT.[4].LQNFLDQEEQLKEMVDALK.[1].AGANVVFADSGIDDMAQHYLAKEGILAVRRAKS 334
gi 19887529 247 PIEV.[4].TDAEIRIT.[4].LQAFIEEEERMLSEMVDKIA.[1].TGANVVFCQKGIDDLAQHYLAKKGILAVRRVKK 320
gi 1591659 242 PIEV.[4].TDAEIRIT.[4].LMEFIEQEEKMIKDMVEKIA.[1].TGANVVFCQKGIDDLAQHYLAKKGILAVRRVKK 315
gi 2621883 238 PIEV.[4].VDAEIRIT.[4].MQAFIEQEEQMIRDMVNSIV.[1].TGANVLFCQKGIDDLAQHYLAKAGVLAVRRVKK 311
Feature 1
1A6D_A 316 SDMEKLAKATGAKIV.[3].DDLTPSVLGEAETVEERKI.[3].RMTFVMGCK.[2].KAVSILIRGGTDHVVSEVERAL 388
query 316 SDMEKLAKATGAKIV.[3].DDLTPSVLGEAEKVEERKI.[3].RMTFVTGCK.[2].KAVSILIRGGTEHVVSEVERAL 388
1A6E_A 316 SDMEKLAKATGAKIV.[3].DDLTPSVLGEAETVEERKI.[3].RMTFVMGCK.[2].KAVSILIRGGTDHVVSEVERAL 388
1A6D_B 317 SDMDKLAKATGASIV.[3].DEISSSDLGTAERVEQVKV.[3].YMTFVTGCK.[2].KAVSILVRGETEHVVDEMERSI 389
1A6E_B 317 SDMDKLAKATGASIV.[3].DEISSSDLGTAERVEQVKV.[3].YMTFVTGCK.[2].KAVSILVRGETEHVVDEMERSI 389
1Q3S_H 319 SDMEKLAKATGAKIV.[3].KDLTPEDLGYAEVVEERKL.[3].NMIFVEGCK.[2].KAVTILIRGGTEHVIDEVERAL 391
gi 15791047 335 DDFTRLSRATGATPV.[3].NDIEAADLGAACSVAQKDI.[3].ERIFVEDVE.[2].KSVTLILRGGTEHVVDEVERAI 407
gi 19887529 321 SDMQKLARATGARIV.[3].DDLSEEDLGEAEVVEEKKV.[3].KMIFVEGCK.[2].KAVTILIRGGTEHVVDEAERAI 393
gi 1591659 316 SDMEKLAKATGARIV.[3].DDLTPEDLGEACLVEERKV.[3].AMIFVEQCK.[2].KAVTILARGSTEHVVEEVARAI 388
gi 2621883 312 SDMEKLSKATGANIV.[3].EDLSPEDLGEACVVSEKKI.[3].EMIFVEECK.[2].KAVTILVRGSTEHVVSEVERAI 384
Feature 1 # ##
1A6D_A 389 NDAIRVVAITKED.[1].KFLWGGGAVEAELAMRLAKY.[5].GREQLAIEAFAKALEIIPRTLAENAGIDPINTLIKLK 464
query 389 NDAIRVVAITKED.[1].KFLWGGGAVEAELAMRLAKY.[5].GREQLAIEAFAKALEIIPRTLAENAGIDPINTLIKLK 464
1A6E_A 389 NDAIRVVAITKED.[1].KFLWGGGAVEAELAMRLAKY.[5].GREQLAIEAFAKALEIIPRTLAENAGIDPINTLIKLK 464
1A6D_B 390 TDSLHVVASALED.[1].AYAAGGGATAAEIAFRLRSY.[5].GRQQLAIEKFADAIEEIPRALAENAGLDPIDILLKLR 465
1A6E_B 390 TDSLHVVASALED.[1].AYAAGGGATAAEIAFRLRSY.[5].GRQQLAIEKFADAIEEIPRALAENAGLDPIDILLKLR 465
1Q3S_H 392 EDAVKVVKDVMED.[1].AVLPAGGAPEIELAIRLDEY.[5].GKEALAIENFADALKIIPKTLAENAGLDTVEMLVKVI 467
gi 15791047 408 EDSLGVVRVTLED.[1].QVMPGGGAPETELAMQLRDF.[5].GREQLAVEAFADALEVIPRTLAENAGHDPIDSLVDLR 483
gi 19887529 394 EDAIGVVAAALED.[1].KVVAGGGAPEVEVARQLRDF.[5].GREQLAVEAFADALEIIPRTLAENSGLDPIDVLVQLR 469
gi 1591659 389 DDAIGVVKCALEE.[1].KIVAGGGATEIELAKRLRKF.[5].GREQLAVKAFADALEVIPRTLAENSGLDPIDMLVKLR 464
gi 2621883 385 EDAIGVVAATVED.[1].KVVAGGGAPEIEIAKRLKDY.[5].GREQLAVSAFAEALEIVPKTLAENAGLDSIDVLVDLR 460
Feature 1 # # #
1A6D_A 465 AD.[7].VGVDL.[5].GDMKAKGVVDPLRVKTHALESAVEVATMILRIDDVIASK 522
query 465 SE.[7].MGVDL.[5].GDMSKKGVIDPVRVKTHALESAVEVATMILRIDDVIASK 522
1A6E_A 465 AD.[7].VGVDL.[5].GDMKAKGVVDPLRVKTHALESAVEVATMILRIDDVIASK 522
1A6D_B 466 AE.[7].YGINV.[5].EDMVKNGVIEPIRVGKQAIESATEAAIMILRIDDVIATK 523
1A6E_B 466 AE.[7].YGINV.[5].EDMVKNGVIEPIRVGKQAIESATEAAIMILRIDDVIATK 523
1Q3S_H 468 SE.[7].IGIDV.[5].ADMLEKGIIEPLRVKKQAIKSASEAAIMILRIDDVIAAK 525
gi 15791047 484 SQ.[7].AGLDA.[5].IDMESEGIVEPLRVKTQAIESATEAATMILRIDDVIAAG 541
gi 19887529 470 AK.[7].AGIDV.[5].KDMLEEGVVEPLRVKTQALASATEAAEMILRIDDVIAAR 527
gi 1591659 465 AA.[8].YGLDV.[5].VDMLEKGVVEPLKVKTQAIDSATEASVMLLRIDDVIAAE 523
gi 2621883 461 AA.[6].MGIDV.[5].VDMKEAGVIEPHRVKKQAIQSAAEAAEMILRIDDVIAAS 517

Figure D.1

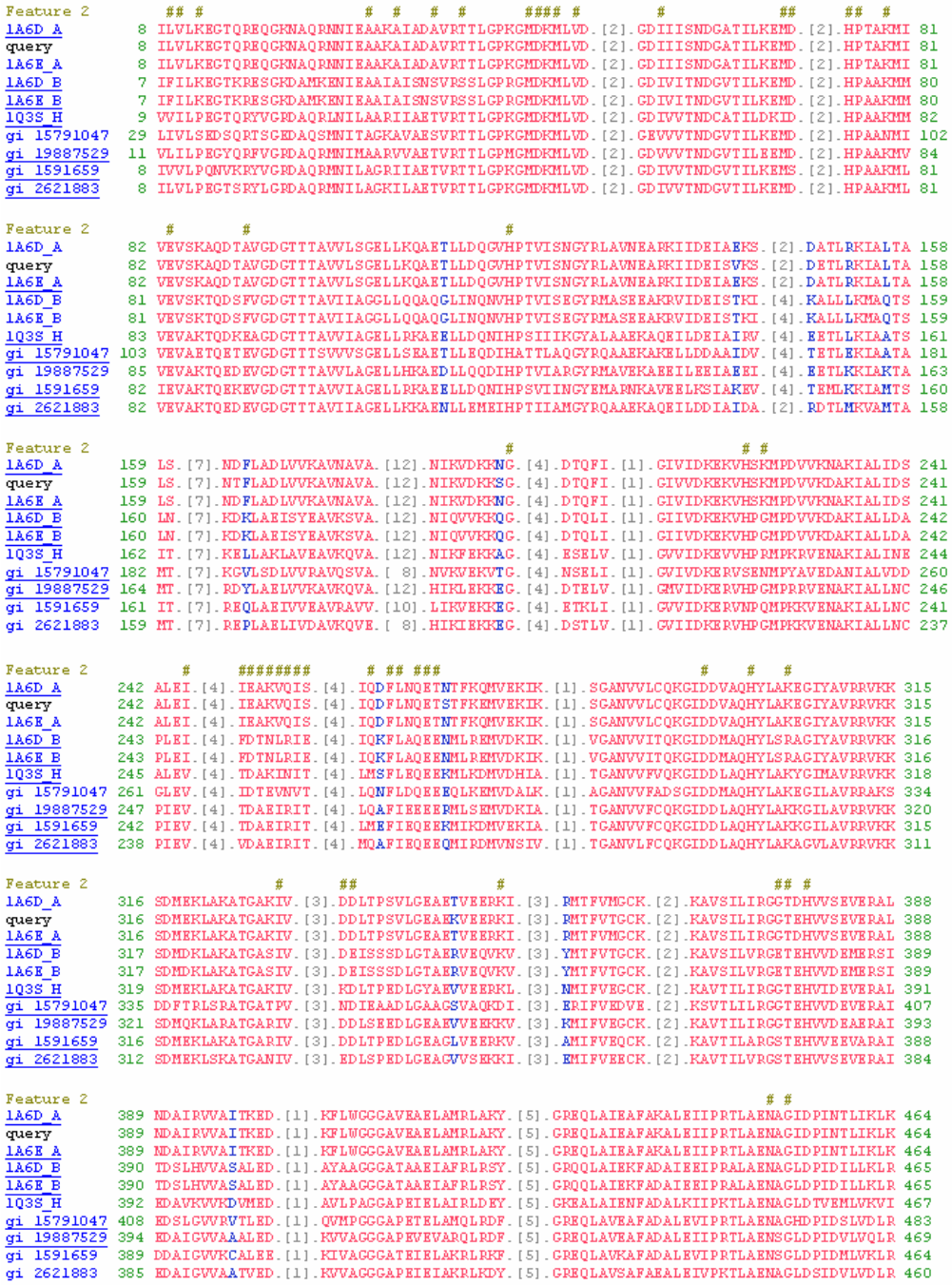

Figure D.2: Alignment for Feature 2 (derived from NCBI Data Base).

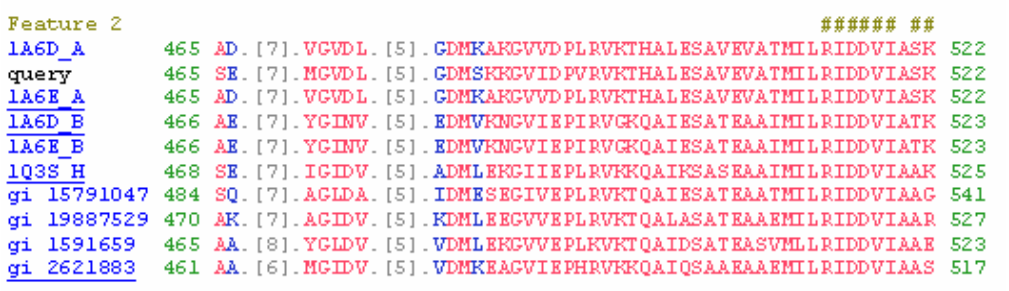

Figure D.2

Figure D.3: Alignment for Feature 3 (derived from NCBI Data Base).

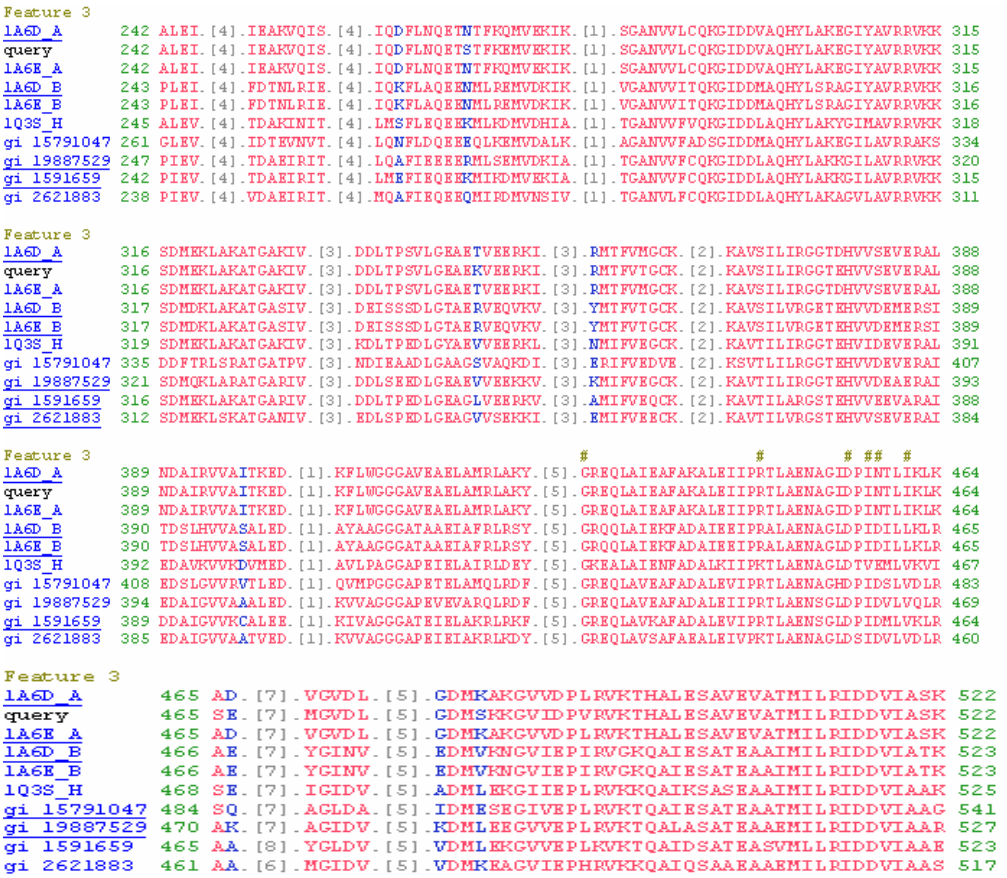

Figure D.3

1A6D_A: Chain A, thermosome from *T. Acidophilum*, length: 545 aa.
1A6E_A: Chain A, thermosome-Mg-Adp-Alf3 Complex, source: *Thermoplasma acidophilum*, length: 545 aa.
1A6D_B: Chain B, thermosome from *T. Acidophilum*, length: 543 aa.
1A6E_B: Chain B, thermosome-Mg-Adp-Alf3 complex, Source: *Thermoplasma acidophilum*, length: 543 aa.
1Q3S_H: Chain H, crystal structure of the chaperonin from *Thermococcus* strain Ks-1 (Formiii Crystal Complexed With Adp), length: 548 aa.
gi 15791047: CctA from *Halobacterium* sp. NRC-1, length: 581 aa.
gi 19887529: HSP60 family chaperonin from *Methanopyrus kandleri* AV19, length: 545 aa.
gi 1591659: thermosome (ths) from *Methanocaldococcus jannaschii* DSM 2661, length: 542 aa.
gi 2621883: chaperonin from *Methanothermobacter thermautotrophicus* str. Delta H, length: 538 aa.